

**Consequences of CTL-mediated Immune Pressure for
HIV-1 Capsid Stability and Innate Sensing**

Dissertation

with the aim of achieving a doctoral degree
at the Faculty of Mathematics, Informatics and Natural Sciences
Department of Chemistry, University of Hamburg
submitted by

Christopher Thomas Ford

M.Sc.R, B.Sc. (Hons)

From Edinburgh, Scotland

August 2019

Dissertationsgutachter / Dissertation reviewer:

1. Gutachter / First reviewer: Prof. Dr. Marcus Altfeld,

Department of Virus Immunology, Heinrich Pette Institute (HPI), Leibniz-Institute for Experimental Virology, Hamburg, Germany.

2. Gutachter / Second reviewer: Prof. Dr. Kay Grünewald,

Department of Viral Structural Biology, Institute for Biochemistry and Molecular Biology, Centre for Structural Systems Biology (CSSB), Hamburg, Germany.

vorgelegt von / submitted by: Christopher Thomas Ford

vorgelegt am / submitted on: 14th of August, 2019

This work was conducted in the period from 23rd of June 2016 until 7th of June 2019 in the research department of Virus Immunology under the direction of Prof. Dr. med. Marcus Altfeld at the Heinrich Pette Institute, Leibniz Institute for Experimental Virology, Hamburg.

Diese Arbeit wurde im Zeitraum vom 23. Juni 2016 bis zum 7. Juni 2019 am Heinrich-Pette Institut Hamburg in der Arbeitsgruppe Virus Immunologie von Prof. Dr. med Marcus Altfeld angefertigt.

Christopher T. Ford was supported by a Doctoral Fellowship from the German Research Foundation priority programme SPP1923.

Christopher T. Ford wurde durch ein Promotionsstipendium des Schwerpunktprogramms der Deutschen Forschungsgemeinschaft SPP1923 unterstützt.

Day of the Defence: 18th October 2019

Tag der Disputation: 18. Oktober. 2019



HPI

Leibniz
Leibniz
Association

Publications List

van Stigt Thans, T., Akko, J., A. Niehrs, W. Garcia Bertran, L. Richert, C. Stuerzel, **C. T. Ford**, H. Li, C. Ochsenbauer, J. Kappes, B. Hahn, F. Kirchhoff, G. Martrus, D. Sauter, M. Altfeld and A Hölzemer. (2019) "Primary HIV-1 strains use Nef to downmodulate HLA-E surface expression." *J Virol*, JVI.00719-00719.

Oberle, A., A. Brandt, M. Voigtlaender, B. Thiele, J. Radloff, A. Schulenkorf, M. Alawi, N. Akyuz, M. Marz, **C. T. Ford**, A. Krohn-Grimberghe and M. Binder (2017). "Monitoring multiple myeloma by next-generation sequencing of V(D)J rearrangements from circulating myeloma cells and cell-free myeloma DNA." *Haematologica* 102(6): 1105-1111.

Akyuz, N., A. Brandt, A. Stein, S. Schliffke, T. Mahrle, J. Quidde, E. Goekkurt, S. Loges, T. Haalck, **C. T. Ford**, A. M. Asemissen, B. Thiele, J. Radloff, T. Thenhausen, A. Krohn-Grimberghe, C. Bokemeyer and M. Binder (2017). "T-cell diversification reflects antigen selection in the blood of patients on immune checkpoint inhibition and may be exploited as liquid biopsy biomarker." *Int J Cancer* 140(11): 2535-2544.

Schliffke, S., N. Akyüz, **C. T. Ford**, T. Mährle, T. Thenhausen, A. Krohn-Grimberghe, S. Knop, C. Bokemeyer and M. Binder (2016). "Clinical response to ibrutinib is accompanied by normalization of the T-cell environment in CLL-related autoimmune cytopenia." *Leukemia* 30(11): 2232-2234.

Hatch, V. L., M. Marin-Barba, S. Moxon, **C. T. Ford**, N. J. Ward, M. L. Tomlinson, I. Desanlis, A. E. Hendry, S. Hontelez, I. van Kruijsbergen, G. J. Veenstra, A. E. Munsterberg and G. N. Wheeler (2016). "The positive transcriptional elongation factor (P-TEFb) is required for neural crest specification." *Dev Biol* 416(2): 361-372.

Brown, S. B., C. S. Tucker, **C. T. Ford**, Y. Lee, D. R. Dunbar and J. J. Mullins (2007). "Class III antiarrhythmic methanesulfonanilides inhibit leukocyte recruitment in zebrafish." *J Leukoc Biol* 82(1): 79-84.

Table of Contents

Abbreviations	1
Zusammenfassung	3
Abstract	4
1. Introduction	5
1.1 HIV-1 Epidemiology and Routes of Transmission	5
1.1.1 HIV-1 structure and function	6
1.1.1.1 Genome	6
1.1.1.2 Structure.....	8
1.1.1.3 Biomolecular structure of p24 Gag.....	8
1.1.1.4 HIV-1 entry and early events during infection	10
1.1.2 Models of capsid uncoating.....	14
1.1.2.1 Rapid uncoating	17
1.1.2.2 Gradual/biphasic uncoating	17
1.1.2.3 Uncoating at the nuclear pore.....	17
1.1.3 Innate Sensing of HIV-1	18
1.2 Adaptive Immune Response to HIV-1	19
1.2.1 HLA Class I.....	19
1.2.2 CD8 ⁺ T cell response	21
1.2.3 Viral Mutations in Response to CTL Immune Control.....	23
1.2.3.1 Escape mutation.....	23
1.2.3.2 Compensatory mutation.....	25
1.3 Aim and Hypotheses of this dissertation	26
2. Results	27
2.1 Investigations into producing gag/pol and gag protease clinical isolate derived lentiviral constructs	27
2.1.1 Viral systems used to test <i>gag/pol</i> clinical isolates efficiencies in vitro	27
2.1.2 Methods for the construction of HIV-1-GFP clinical isolate derived particles	28
2.1.3 Identification of pNL4-3 Δ env-eGFP and pMDLg/pRRE expression constructs containing respective clinical isolate <i>gag/pol</i> sequence	31
2.1.4 Validation of in vitro production of infectious proviral particles	32
2.1.5 Titration of 3rd generation LV particles containing gag/pol derived from clinical isolates to yield infectious particles and washout assay	34
2.1.6 Titration of NL4-3 <i>gag/pol</i> chimeric particles from clinical isolates.....	38
2.1.7 High through-put production of gag-protease pNL4-3 chimera	38
2.2 Investigations into innate sensing and restriction of HIV-1 capsid mutants	41
2.2.1 Viral fitness is highly affected by p24 escape mutations	41
2.2.2 p24 escape mutations R264K and R264K plus L268M do not increase the number of infected MDM cells.....	45
2.2.3 MDM cells respond to HIV-1 infection/LPS activation	52
2.2.4 Mutations in HIV-1 are dependent on CypA.....	53
2.2.5 Jurkat cells respond to IFN α 2a-stimulation and regulate a stronger transcriptional upregulation of IFN α 2a-regulated genes compared to Jurkat CypA-/-	56
2.2.6 Transcriptional analysis of Jurkat and Jurkat CypA-/- reveals differential regulation	58
2.2.7 Proteins are specifically affected upon IFN α 2a stimulation and PBAP may provide a mechanism for the observed CypA-/- (<i>Ppia</i> -/-) phenotype.....	60
3. Research Materials and Methods	70
3.1 Material	70
3.1.1 Reagents.....	70

3.1.2 Buffers and Solutions	71
3.1.3 Equipment.....	71
3.1.4 Kits.....	72
3.1.5 Bacterial cell lines.....	73
3.1.6 Cell lines	73
3.1.7 Reporter cell lines.....	73
3.1.8 Media.....	74
3.1.9 Antibodies	74
3.1.10 Plasmids	74
3.1.11 Primer Oligonucleotides.....	77
3.1.12 Software	82
3.2 Methods.....	83
3.2.1 Transformation of bacteria.....	83
3.2.1.1 Transformation of lab adapted constructs.....	83
3.2.1.2 Transformation of proviral HIV-1 constructs	83
3.2.1.3 Transformation of ligated gag/pol into pMDLg pRRE Δgag/pol	84
3.2.1.4 Transformation of mutagenesis products	84
3.2.2 DNA preparations.....	84
3.2.2.1 Minipreparation.....	84
3.2.2.2 Midi preparation of constructs.....	85
3.2.2.3 Maxi preparation	85
3.2.3 Mutagenesis.....	86
3.2.3.1 Mutagenesis – Deletion of internal restriction sites	86
3.2.4 Cloning.....	87
3.2.4.1 gag-pol gene segment PCR-out.....	87
3.2.4.2 Digestion of XhoI and XmaI containing constructs	87
3.2.4.3 Agarose gel electrophoresis.....	87
3.2.4.4 QIAquick Gel Extraction Kit	88
3.2.4.5 Gel dissolution and Gene Clean	88
3.2.4.6 Digestion of the pMDLg pRRE vector.....	88
3.2.4.7 Ligation	89
3.2.4.8 Digestion of ligated cloned gag/pol into pMDLg pRRE Δgag-pol	89
3.2.4.9 DNA sequencing of clones.....	89
3.2.4.10 Quantitative determination of nucleic acid concentrations.....	89
3.2.4.11 nested PCR amplification of gag-protease from proviral vectors.....	90
3.2.5 Cell Culture	90
3.2.5.1 Cell lines.....	90
3.2.5.2 Cryopreservation of cell lines	91
3.2.5.3 Cell thawing	91
3.2.6 Methods for the production of virus particles and reporter cell lines.....	92
3.2.6.1 Lipofectamine Transfection of Plasmid DNA	92
3.2.6.2 Production of gag-prot chimeric HIV-1 by gene electrotransfer in MT4 cells.....	92
3.2.6.3 Production of CRISPR/Cas9 reporter Jurkat cells.....	93
3.2.6.4 Concentration of viral stocks.....	93
3.2.6.5 Titration of Viral Stocks.....	94
3.2.7 Preparation of RNA and Real-time PCR	95
3.2.7.1 RNA Extraction	95
3.2.7.2 DNase treatment	96
3.2.7.3 cDNA transcription.....	96
3.2.7.4 RT-PCR	96
3.2.8 Proteomic techniques	98
3.2.8.1 SILAC labelling of Jurkat and Jurkat CypA ^{-/-} cells.....	98
3.2.8.2 Preparation of whole cell lysates for MS analysis	98
3.2.8.3 Preparation of whole cell lysates.....	99
3.2.8.4 SDS – Polyacrylamide gel electrophoresis.....	99
3.2.8.5 Western blotting	100
3.2.9 PBMC Acquisition.....	100
3.2.9.1 Peripheral blood sample acquisition	100
3.2.9.2 PBMC isolation through density gradient centrifugation	101
3.2.10 Functional Experiments	101

3.2.10.1 The IFN sensitivity assay	101
3.2.10.2 The MDM infection assay.....	103
3.2.10.2.1 Isolation of monocyte-derived macrophages (MDM) from EDTA tubes.....	103
3.2.10.2.2 Preparation of MDMs for RNA extraction, antibody staining and supernatant ELISA	104
3.2.10.2.3 MDM staining for flow cytometry analysis	105
3.2.10.3 ELISA assays.....	105
3.2.10.3.1 Determination of cytokine and HIV-1 production by ELISA	105
3.2.10.4 Fluidigm	106
3.2.10.4.1 Single cell capture and cDNA synthesis.....	106
3.2.10.4.2 Quantitative PCR (qPCR) using 96.96 Dynamic Array Integrated Fluidic Circuits...	106
3.2.10.4.3 Preamplification.....	107
3.2.10.4.4 Quantitative PCR assay and sample master mix preparation.....	107
3.2.10.4.5 Chip priming.....	107
3.2.10.4.6 Chip loading.....	108
3.2.10.4.7 qPCR and data analysis.....	108
3.2.10.5 The Cyclosporine washout assay	108
4. Discussion.....	110
4.1 HLA and Capsid mutants	110
4.2 Oligonucleotide Innate sensing	115
5. Outlook	117
6. Conclusions.....	118
7. References	119
8. Appendix.....	134
8.1 Risk and safety statements/List of hazards substances utilised according to GSH	134
8.2 Plasmid Maps	135
8.3 Sequence Alignments	139
9. Curriculum Vitae.....	142
10. Acknowledgements.....	143
11. Declaration on oath.....	144

List of Figures

Figure 1 HIV-1 genome schematic, reference sequence annotated HXB2 (Genbank accession K03455).....	6
Figure 2 Structure and assembly of the HIV-1 p24 Gag protein.....	9
Figure 3 Capsid interaction domains.	10
Figure 4 HIV-1 replicative cycle.....	12
Figure 5 Stages of HIV-1 infection and the associated immunopathogenesis.....	13
Figure 6 Course of HIV-1 infection.	14
Figure 7 Principal models of HIV-1 capsid uncoating.	16
Figure 8 CsA washout assay.....	19
Figure 9 Cartoon of the CA functional domains and two major protective CTL alleles.....	22
Figure 10 Construction of HIV-1-GFP patient-derived <i>gag/pol</i> LV particles.	29
Figure 11 Construction of HIV-1-GFP patient-derived <i>gag/pol</i> LV particles.	30
Figure 12 Sequencing strategy for confirming cloned <i>gag</i> and <i>pol</i> genes into lenti-viral vector backbones.	31
Figure 13 FACs gating and titration of viral vector constructs for optimal infectivity range.....	34
Figure 14 Construction and titration of HIV-1-GFP clinical isolate-derived <i>gag/pol</i> 3 rd generation lenti-viral particles.	36
Figure 15 CsA washout assay to determine capsid stability and uncoating kinetics.....	37
Figure 16 Titration of clinical isolate-derived <i>gag/pol</i> gene segments cloned into the pNL4-3-eGFP construct.....	38
Figure 17 Methodology to develop a high through-put production of <i>gag</i> -protease NL4-3 chimeric viruses.....	41
Figure 18 Viral fitness is highly affected by p24 escape mutations.....	44
Figure 19 MDM cells can achieve high infection rates.	45
Figure 20 Percentage of infected MDM cells overtime.....	46
Figure 21 Real-time PCR reveals infection kinetics at 48 and 72 hours.	47
Figure 22 TNF- α produced upon HIV-1 viral infection.....	48
Figure 23 IL-10 ELISA reporting donor variation in detection overtime.	50
Figure 24 IL-1 β ELISA reporting donor variation in detection overtime.	51
Figure 25 Activation and stimulation of MDM cells overtime.	52
Figure 26 Activation and stimulation of MDM cells overtime.	53
Figure 27 Immuno blot analysis of CypA, MX2, TRIM5 and MX2 plus CypA CRISPR targeted Jurkat T cells.....	54
Figure 28 CTL escape mutations render HIV to be more sensitive to INF α mediated.....	56
Figure 29 Immunoblots of CypA and MX2 and real-time PCR of ISG's.	57
Figure 30 Violin plots and hierarchical clustering of a T cell gene panel comparing Jurkat cells and Jurkat CypA cells.....	59
Figure 31 Confirming the incorporation of stable isotope labelling in Jurkat wt and Jurkat CypA-/- (<i>Ppia</i> -/-) cells.	61
Figure 32 Lysine-Arginine isotope label incorporation into peptides extracted from Jurkat and Jurkat CypA-/- (<i>Ppia</i> -/-).....	62
Figure 33 Gene ontology analysis.....	64
Figure 34 Down Regulated proteins in Jurkat CypA vs WT.	65
Figure 35 After stimulation differential expression (down-regulated genes).	66
Figure 36 Up-Regulated proteins in Jurkat CypA vs WT.....	67
Figure 37 After stimulation differential expression (up-regulated genes).	68
Figure 38 Cartoon of pre-treated cells under increasing IFN α 2a concentrations with the addition of viral suspension.....	103
Figure 39 Representative workflow of the MDM assay.	104
Figure 40 Plate set-up for the infection of MDMs.....	104
Figure 41 Mechanism of the CsA washout assay	109
Figure 42 Alignment of <i>Gag</i> sequences from transmitted founder (TF) viruses and the corresponding 6-month (6mo) virus sequences	140
Figure 43 <i>Gag</i> chronic virus sequences	141

List of Tables

Table 1 Based on LANL HIV-1 Sequence Database. [45]	7
Table 2 Based on LANL HIV-1 Sequence Database. [46]	8
Table 3 General laboratory consumables of reagents used.	71
Table 4 Buffer and solutions	71
Table 5 Equipment	72
Table 6 Commercial kits	73
Table 7 Bacterial cell lines provided within the commercial kits	73
Table 8 Commercially available cell lines	73
Table 9 Reporter cell lines generated to address the aim 2 of this dissertation.	73
Table 10 Commercially available media	74
Table 11 Flow cytometry antibodies	74
Table 12 Immunoblotting antibodies	74
Table 13 Lab adapted and proviral constructs	75
Table 14 Lab adapted constructs	76
Table 15 Constructs required for Lenti-viral vector systems	77
Table 16 CRISPR/Cas9 gRNA constructs generated to establish reporter cell lines.	77
Table 17 Oligonucleotides for cloning gag-pol.	77
Table 18 Oligonucleotides for 2-step cloning of gag-protease.	78
Table 19 Oligonucleotides for removal of XhoI restriction site in CH058 transmitted founder and 6 month chronic pro-virus and removal in CH166_ZM3576F pro-virus.	78
Table 20 Oligonucleotides for sequencing gag-pol cloned into vector backbones.	78
Table 21 Oligonucleotides used for real-time PCR	79
Table 22 Oligonucleotides use for the amplification of cDNA transcripts using Fluidigm technology. T cell panel primers listed.	82
Table 23 Software packages	82
Table 24 PCR conditions for Real-time PCR	97
Table 25 Plate layout used for the correct pipetting strategy	103
Table 26 Antibody master mix	105

Abbreviations

Acquired immunodeficiency virus	AIDS
Antigen-presenting cells	APCs
C terminal domain	CTD
C-C chemokine receptor type 5	CCR5
C-X-C chemokine receptor type 4	CXCR4
Capsid	CA
Cyclophilin A	CypA
Cytotoxic T-lymphocyte	CTL
danger-associated molecular patterns	DAMPs
Elite controllers	EC
Endoplasmic reticulum	ER
Envelope	Env
Genome-wide association study	GWAS
Group specific antigen	Gag
Heterosexual	HSX
Heterosexual-female	HSX-female
Highly active anti-retroviral therapy	HAART
Human Immunodeficiency Virus	HIV-1
Human leukocyte antigen	HLA
Integrase	IN
Interferon	IFN
Interferon-stimulated gene	ISG
Long term non progressors	LNTPs
Major histocompatibility complex	MHC
Matrix	MA
Men who have Sex with Men	MSM
Monocyte-derived macrophages	MDMs
N terminal domain	NTD
Nuclear pore complex	NPC
Nucleocapsid	NC
Nucleoporins	Nups
Open reading frames	ORFs
Pathogen associated molecular patterns	PAMPs
pathogen recognition receptors	PRRs
Polymerase	Pol
Pre-integration complex	PIC
Protease	PR
Rev response element	RRE
Rev-binding element	RBE
Reverse transcription complexes	RTC
RNA polymerase II	RNAP2

Simian Immunodeficiency Virus	SIV
Simian Immunodeficiency Virus Chimpanzees	SIVcpz
Simian Immunodeficiency Virus Gorillas	SIVgor
Simian Immunodeficiency Virus Macaques	SIVmac
Single nucleotide polymorphisms	SNPs
Transporter for antigen processing	TAP
Vesicular-Stomatitis-Virus-G-Protein	VSV-g
Viral nucleoprotein complex	VNC
Viral replicative capacity	VRC

Zusammenfassung

HIV-1 ist ein Retrovirus der Gattung der *Lentiviren*, welches sich bei Menschen durch eine persistierende Infektion auszeichnet. In der ersten Hälfte des 20[1, 2]. Jahrhunderts entstand HIV-1 durch die Übertragung von SIV von Schimpansen und Gorillas auf den Menschen. HIV-1 entgeht der antiviralen Immunantwort von CD8⁺ T-Zellen und NK-Zellen durch die Selektion von spezifischen Sequenzvarianten im viralen Genom. Individuen, welche schützende/vorteilhafte humane Leukozyten-Antigen (HLA) Klasse 1 Allele wie *HLA-B*27* und *-B*57* tragen, können eine Immunantwort gegen Epitope in konservierten Regionen des Kapsid-Proteins p24 entwickeln. Jedoch ist auch in diesen Individuen ein Entkommen des Virus vor dem Immunsystem durch Veränderungen in der Kapsidsequenz häufig. In manchen Fällen sind diese Sequenz-Veränderungen mit einer reduzierten viralen Replikation verbunden. Über die molekularen Mechanismen, die zu einer reduzierten viralen Replikation führen, ist noch wenig bekannt[3]. Basierend auf kürzlich veröffentlichten Daten soll die Hypothese untersucht werden, dass immun-induzierte Fluchtmutationen die im HIV-1 Kapsid auftreten, die Stabilität des Kapsids modulieren. Dieses führt zu einer verbesserten Erkennung von viralen Nukleotiden durch Mustererkennungsrezeptoren (PRRs), welches normalerweise durch das Kapsid vor der Erkennung durch das angeborene Immunsystem geschützt sind. Ziel dieser Arbeit ist es, den Einfluss von Virus-Fluchtmutationen in HIV-1-Kapsiden auf die Kapsid-Stabilität und deren Erkennung durch das angeborene Immunsystem zu untersuchen.

Die hier präsentierten Daten verknüpfen das bisherige Wissen über die virale Immunevasion von HIV-1 in Bezug auf die intrazelluläre Erkennung des Kapsids und die gewärtigen Erkenntnisse über die virale Suppression durch Restriktionsfaktoren des menschlichen Wirts. Die in dieser Arbeit erbrachten Erkenntnisse tragen zur Entwicklung eines neuen Modells bei, in welchem der zelluläre Immundruck die Erkennung von Infektionen durch Rezeptoren des angeborenen Immunsystems fördert. Die exakten Mechanismen dieses Prozesses sind jedoch noch nicht vollständig aufgeklärt und bedürfen weiterer Untersuchungen.

Abstract

HIV-1 is a retrovirus of the genus *Lentivirus* that causes persistent infection of humans and arose from the cross-species transmissions of SIV of chimpanzees and gorillas in the first half of the 20th century[1, 2]. HIV-1 evades antiviral CD8⁺ T cell and natural killer (NK) cell responses through the selection of region-specific sequence variants within the viral genome. Individuals that encode protective human leukocyte antigen (HLA) class I alleles like HLA-B27 and –B57 can orchestrate an immune response targeting epitopes within the conserved regions of the p24 capsid. However, virus escape is common in individuals that encode for protective HLA class I alleles, resulting in alteration of the capsid sequence and in some cases reduced viral replication capacity. The molecular mechanisms governing the reduced viral replication in these individuals that develops over the course of persistent infection are poorly understood. Based on recently published data[3], the aim of the thesis is to test the hypothesis that immune-driven escape mutations arising within the HIV-1 capsid can modulate capsid stability and, therefore, enhance innate immune sensing of viral nucleotides that are normally cloaked by the capsid from the recognition by pattern recognition receptors (PRRs). The specific objective of this PhD thesis aims to determine the impact of cytotoxic T-lymphocyte (CTL)-driven viral escape mutations within HIV-1 capsids on capsid stability and innate immune sensing.

The data herein serves to connect our understanding of viral escape within the capsid from intracellular detection by the heightened innate sensing of viral escape variants and our knowledge of viral suppression through host restriction factors. Meeting these proposed objectives have served our aim of further developing the novel model that cellular immune pressure heightens the sensing of infection by innate immune receptors although the exact mechanism remains elusive, and therefore, requires further investigation.

1. Introduction

1.1 *HIV-1 Epidemiology and Routes of Transmission*

Human immunodeficiency virus type 1 (HIV-1) is a lentivirus and the causative agent of the Acquired Immunodeficiency Syndrome (AIDS), the most advanced stage of disease with severe loss of immunocompetence in individuals. It is estimated that the virus entered the human species during the early 20th century as revealed by phylogenetic analyses[4]. Subsequently, HIV-1 to date has infected more than 77 million individuals and taken the lives of more than 35 million[5]. Annually, 1.8 million individuals are infected with the HIV-1 virus despite widespread efforts in preventative strategies to reduce transmission[5].

There are four groups in which HIV-1 is stratified – M (main), N (non-M, non-O), O (outlier) and P (pending the identification of further human cases)[6]. These groups are defined by 4 independent zoonotic transmissions of the Simian Immunodeficiency Virus (SIV) to humans, with groups M and N originating from an SIV infecting chimpanzees (SIVcpz) and groups O and P derived from an SIV infecting gorillas (SIVgor)[2, 6, 7]. The major group accounting for 99% of all worldwide HIV-1 infections is M and is further characterised on genetic differences resulting in further classification defined by subtypes A, B, C, D, F, G, H, J, K and recombinants circulating within[6, 8, 9]. Of these subtypes, namely B and C are the most predominant of group M-infected individuals identifiable by geographic location[10]. Predominant in Western Europe and Northern America is subtype B, however, accounting for half of all HIV-1 infections worldwide is subtype C. This subtype C is predominant in sub-Saharan Africa and India[11].

The transmission of HIV-1 occurs through various avenues of exposure, namely mucosal, perinatal and parenteral routes. Nowadays, mucosal transmission accounts for around 90% of HIV-1 naïve individuals becoming infected[8, 12]. Heterosexual (HSX) exposure is the predominant route of transmission, responsible for 70% of infections, however, men who have sex with men (MSM) account for 20% of the total number of infections globally. Sexual intercourse is a very inefficient route of HIV-1 transmission with probability of transmission per sexual exposure are to be 1 in 20 to 1 in 3000[8, 12-16]. Estimating probability of exposure during sexual intercourse must take into account criteria such as donor viral load, concomitant sexually transmitted diseases with ulceration and inflammation as well as sex-gender

differences and various other factors[16-34]. Typically, HIV-1 infection leads to a decline in CD4⁺ T cell counts, a T cell subset crucial in their role to form a functioning immune system[35]. AIDS is defined as a declining CD4⁺ T cell count below 200 cells/ μ L resulting in opportunistic infection, cancers, for example, Kaposi's sarcoma and extreme immunodeficiency leading to death if not treated[36-38]. Even though currently AIDS and progression to AIDS can be prevented and reverted by highly active antiretroviral therapy (HAART), an effective vaccine remains elusive.

1.1.1 HIV-1 structure and function

1.1.1.1 Genome

The HIV-1 genome is 9.7 kB comprising of nine genes and encoding fifteen proteins. HIV-1 contains three essential components: *gag*, *pol* and *env* (figure 1, table 1 & 2). The *gag* gene encodes p17 matrix, p24 capsid, p7 nucleocapsid, adjacent to the p2 'spacer' peptide and p6, which is essential for viral assembly and budding, separated by peptide p1 directing the translational frameshift into the overlap regions of the *pol* gene[39-42]. Encoded within the *pol* gene is viral protease, reverse transcriptase, integrase and RNase. The protease processes the precursor *gag-pol* polyprotein into Group-specific antigen (Gag) and Polymerase (Pol)[43]. The precursor Env glycoprotein gp160 is cleaved to become the surface proteins gp120 and the transmembrane protein gp41 to form the virion particle. Genomic structural elements are encoded by HIV-1 to integrate viral reverse transcribed RNA product. Identical long terminal repeats at the 5'LTR and 3'LTR are required for integration in the human genome. Integrated 5'LTR is a promoter element for viral replication and the 3'LTR is essential for nascent RNA polyadenylation and encodes part of the *nef* gene.

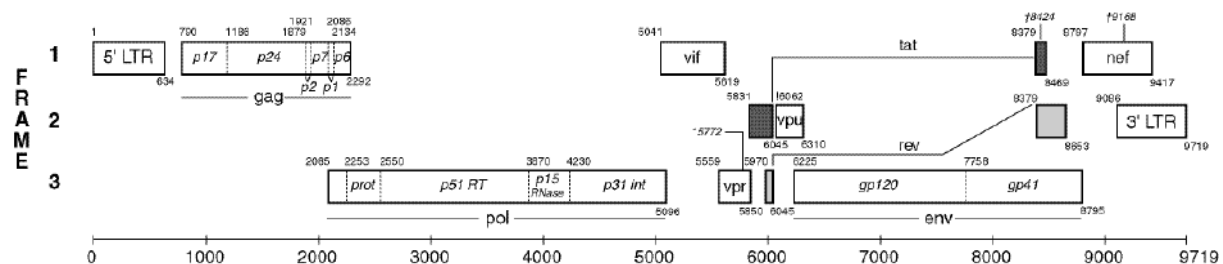


Figure 1 HIV-1 genome schematic, reference sequence annotated HXB2 (Genbank accession K03455).

All open reading frames (ORF's) are shown as rectangles. Derived from [44]

Gene		Function/Gene Product	
<i>gag</i>	Group-specific antigen	p17, Matrix (MA)	Forms viral matrix layer, targeting of Gag polyprotein to lipid rafts. Required for nuclear import of the provirus.
		p24, Capsid (CA)	NTD binds to the innate sensor CypA for the timely uncoating of the capsid. CTD is required for particle assembly and core formation.
		p7, Nucleocapsid (NC)	Essential for specific packaging the two copies of viral RNA into the virion particle.
		p6	Binds Vpu. Unique to HIV-1, variable in length and sequence and can promote release of assembled virions from the cell.
<i>pol</i>	Polymerase	p10, Protease (PR)	Required for Gag/Pol cleavage and maturation of the virion.
		p66, RT, RNase H	Required for reverse transcription of ssRNA into dsDNA.
		p31, Integrase (IN)	Essential for integration of the provirus into the host genome.
<i>env</i>	Envelope	gp120	Binds to CD4 and chemokine receptors CCR5 and CXCR4.
		gp41	Mediator of cell fusion.
<i>tat</i>	Transactivator	p16/14	Activates viral gene expression.
<i>rev</i>	Regulator of viral expression	p19	Inhibits viral RNA splicing and promotes nuclear export of incompletely spliced, stabilised viral mRNAs. Binds to retroviral response element (RRE).
<i>vif</i>	Viral infectivity factor	p23	Accelerates virion maturation and infectivity; inhibits host derived restriction factor APOBEC3G.
<i>vpr</i>	Viral protein R	p15	Nuclear import of provirus; increase virus production; promotes cell-cycle arrest.
<i>vpu</i>	Viral protein U	p23	Promotes CD4 degradation in the ER and viral budding.
<i>nef</i>	Negative-regulation factor	p27	Downregulation of CD4 and HLA-A/B. Increases T-cell activation. Increases infectivity.

Table 1 Based on LANL HIV-1 Sequence Database. [45]

Element		Function
LTR	Long terminal repeat	634 nucleotides. Contains important regulatory regions, especially for transcription initiation and polyadenylation.
TAR	Target sequence for viral transactivation	45 nucleotides of viral mRNAs. TAR RNA forms a hairpin structure with a side bulge that is the Tat and cellular proteins binding site.
RRE	Rev responsive element	Approximately 200 nucleotides, located in <i>env</i> region. Contains 7 binding sites for Rev.
PE	Psi element Ψ	Presence only in unspliced genomic transcripts. A set of 4 stem-loop structures, preceding and overlapping the Gag start codon. Recognised by a conserved motif called the cysteine histidine box, present in the Gag p7 protein.
SLIP	TTTTTT slippery site	Followed by a stem-loop structure. Responsible for regulating ribosomal frameshift out of the Gag reading frame into the Pol reading frame.
CRS	Cis-acting repressive sequences	Located in <i>pol</i> . Inhibit structural protein expression in the absence of Rev.
INS	Inhibitory/Instability RNA sequence	Multiple INSS exist within the genome. Inhibit expression post transcriptionally. Mutation of the RNA elements was shown to lead to INS inactivation and up-regulation of gene expression.

Table 2 Based on LANL HIV-1 Sequence Database. [46]

1.1.1.2 Structure

HIV-1 virus is composed of two copies of positive sense and single-stranded RNA. HIV-1 RNA binds p7 nucleocapsid and late-assembly p6 protein[47, 48]. The RNA genome is encapsulated by a conical nucleocapsid protein p24 incorporating accessory proteins Vif, Vpu, Vpr and Nef and regulatory proteins Tat and Rev alongside protease, integrase and reverse transcriptase. The nucleocapsid is further surrounded by matrix protein p17 and with lipid membrane-anchoring envelope glycoprotein complexes and cell derived proteins[47, 49] (figure 2a).

1.1.1.3 Biomolecular structure of p24 Gag

Gag is the genetic component that encodes core structural proteins of retroviruses. Within HIV-1 Gag, p24 is highly conserved and serves to protect the viral genome from innate immune sensors. Contained within its structure are many immunodominant epitopes targeted by T cells [50]. Approximately 1500 p24 subunits self-assemble into hexameric units, with very few pentamers that serve to facilitate the curvature of the capsid core creating a closed structure[51-

53] (figure 2a & b). Each monomer contains two domains: the 150 aa-amino-terminal-domain (NTD -NH₂-terminus; CA 1 – 145, HXB2 133-277) and the 80 aa-amino-acid carboxy-terminal domain (CTD -COOH-terminus; CA 151 – 231, HXB2 Gag 283-363). After self-assembly of the capsid core, the NTD faces the external surface and the CTD domain faces the inward surface (figure 2c & d).

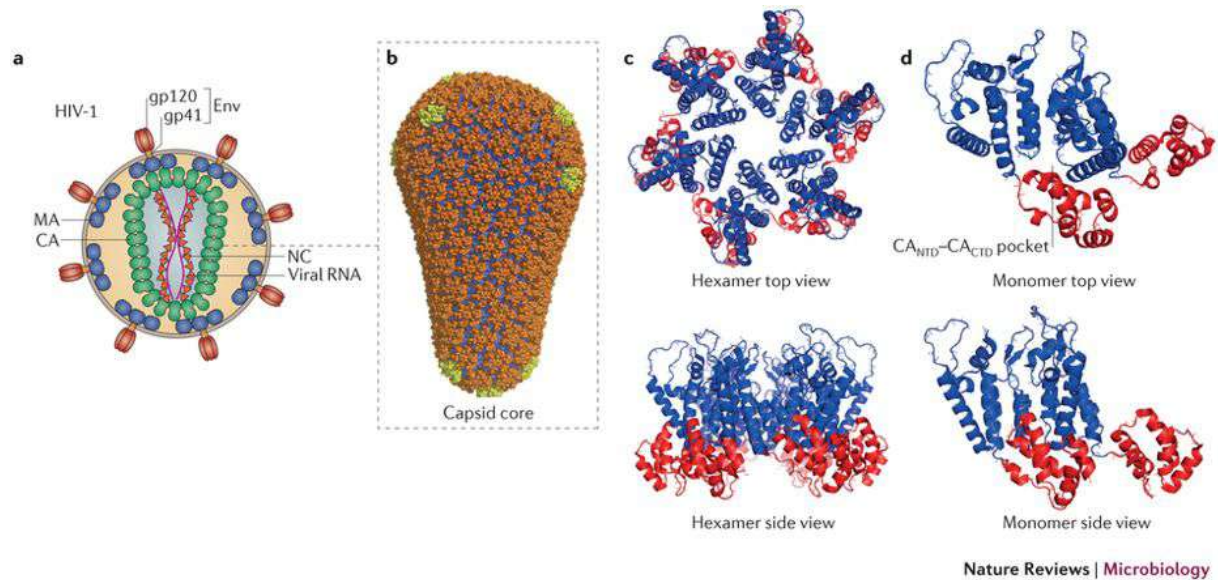


Figure 2 Structure and assembly of the HIV-1 p24 Gag protein.

(a) Cartoon of the mature HIV-1 virion, presenting the viral glycoprotein envelope (Env, composed of glycoprotein 120 (gp120) and gp41 subunits), and the Gag polypeptide-derived proteins matrix (MA), capsid (CA) and nucleocapsid (NC). CA hexamers and pentamers assemble to construct the capsid core. The capsid core protects the viral RNA genome that associates with NC. (b) The conical capsid core assembles into a fullerene cone, containing hexameric (orange) and pentameric (yellow) CA subunits. (c) Top view and side view of the hexameric subunits forming the HIV-1 virion capsid core. (Protein Data Bank (PDB) identifier: 3GV2). The interactions between the p24 Gag amino-terminal domain (NTD; blue) and the p24 Gag carboxy-terminal domain (CTD; red) of adjacent monomers stabilise the assembled hexamer are depicted. (d) Here, the structure of two p24 Gag monomers of a hexamer, demonstrating the CA_{NTD}-CA_{CTD} pocket that mediates interactions between p24 Gag and host cell proteins and proteins restricting infection. Derived from [51].

NTD domains of the CA core are made up of one β -hairpin and seven α -helices orientated to form an arrowhead with an extended loop structure that connects helices 4 and 5. This structure creates the binding loop for prolyl isomerase cyclophilin A (CypA) to interact with the CA core. The proline rich binding loop for CypA interacts with host cell innate sensors to promote the timely disassembly of the CA core during infection[54-56] (figure 3a & b).

The CTD domain is made up of 3₁₀ helices, an extended strand and four α -helices (CA helices 8-11) that correspond to its symmetry-related unit[54, 57]. This domain contains the conserved 20aa-long major homology region (MHR; CA 153-172, Gag 285-304) commonly found in onco- and lenti-virus particles, a structure essential for virion assembly, maturation and early

events of infection[58-62]. The MHR has a critical role in recruiting innate sensors and binding them with high affinities in order to serve different roles during restriction events upon CA release[54]. The flexible linker between the two domains – NTD-CTD contacts (CA 145-151, HXB2 278-282) further stabilises the hexameric or pentameric subunits within the core structure essential for viral genome packaging and inclusion of enzymes and accessory proteins for particle infectivity[63, 64] (figure 3b).

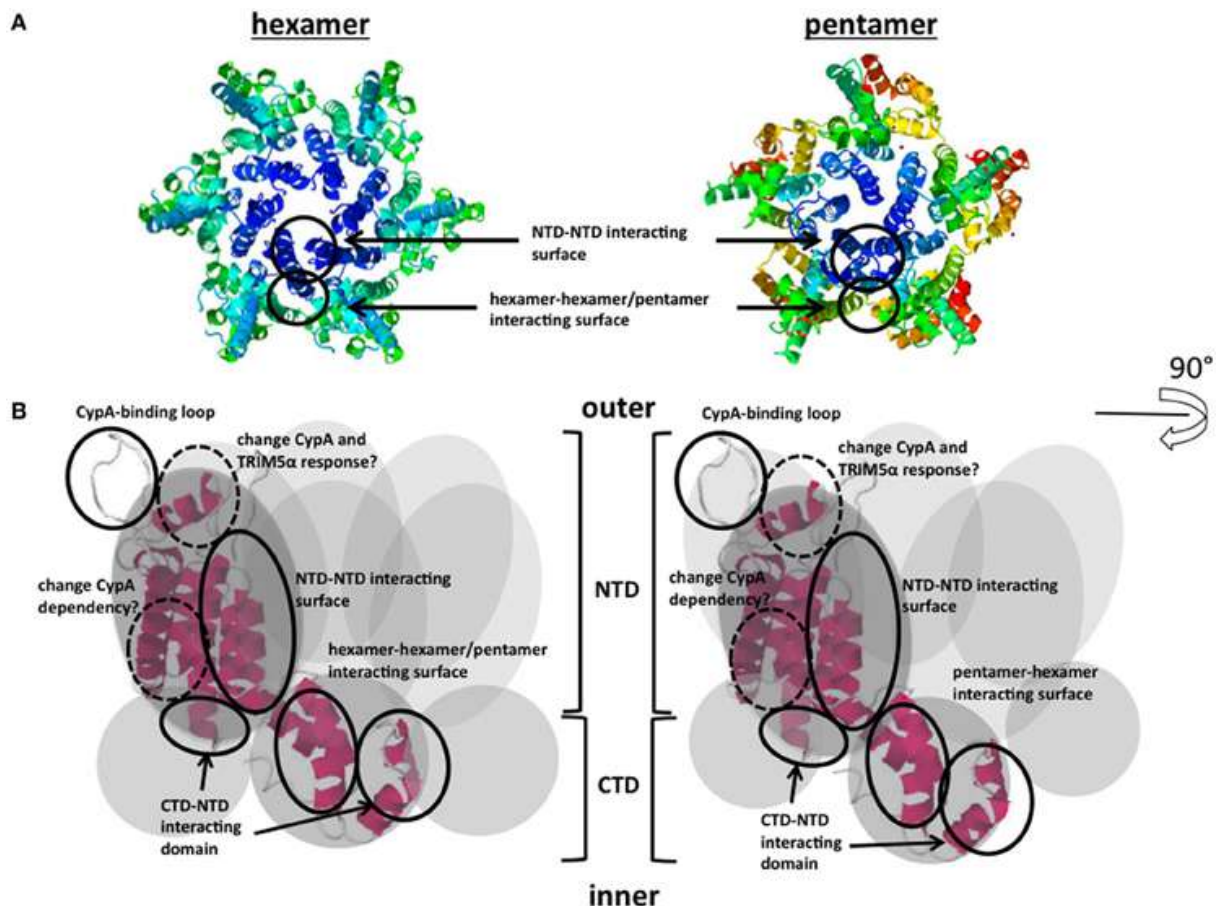


Figure 3 Capsid interaction domains.

(a) Hexameric and pentameric models suggested from structural analysis of the HIV-1 core. Cores comprise approximately 250 hexamers and exactly 12 pentamers. The accession numbers of protein Databases are 3H47, 3P05. (B) Functional surfaces in the CA protein. Shown in the grey circles indicate monomers of CA. NTD-NTD or CTD-NTD interacting surfaces, CypA-binding loops, and hexamer-hexamer/pentamer interacting surfaces. CA; viral capsid; NTD; N-terminal domain, CTD; C-terminal domain. The accession numbers of protein database are 3DIK. Derived from [65]

1.1.1.4 HIV-1 entry and early events during infection

Successful entry of HIV-1 to establish infection requires the interaction of the viral envelope glycoprotein (Env) with the CD4 receptor on the host cell and co-receptor binding for viral entry and subsequent CA release[66] (figure 4). As co-receptors, HIV-1 requires either C-C chemokine receptor type 5 (CCR5) or C-X-C chemokine receptor type 4 (CXCR4) co-10

receptors. Usage of CXCR4 is limited to T cells and is mainly observed in the chronic stage of infection in certain individuals[67, 68], whilst CCR5 is predominantly favoured in acute infections and facilitates the infection of macrophages and T cells[69-71] [72-75]. Most strains enter through CCR5 (R5 viruses), while CXCR4-tropic strains (X4 viruses) are associated with poorer disease progression[67].

Upon infection, viral RNA is reverse-transcribed into double stranded cDNA by reverse transcriptase (RT) and integrated into the host cell genome by IN and can continue its life cycle or persist in a state of latency[76, 77]. Upregulated transcription factors NF- κ B and NFAT bind to the LTR on the integrated viral sequence and initiate transcription[78-80]. The LTR provides the suitable template for RNA polymerase II (RNAP2) to bind[81]. Upon recruitment of p-TEFb and viral Tat binding to TAR productive elongation is initiated by RNAP2-transcription[82-84]. HIV-1 viral RNA is composed of multiple splicing variants, which are not fully understood: 9kb-unsliced mRNA encoding *gag-pol* precursors and viral ssRNA, and several splicing variants such as 4.5kb single sliced mRNA encoding *env*, *vif*, *vpu* and *vpr*; and 2kb multiple sliced mRNA encoding *tat*, *rev* and *nef*[85, 86]. Export of viral mRNAs and transcripts that are incomplete and un-spliced for structural genes are highly dependent upon the level of Rev[87].The transcripts are exported from the nucleus to the cytoplasm upon binding of Rev to the Rev-binding Element (RBE), a sequence present within the Rev response element (RRE) (table 2) in encoded in *env* [88, 89]. As the transcripts are translated, HIV-1 proteins translocate to the plasma membrane of the virally infected cell to assemble into mature virions by incorporating envelope proteins and lipids (figure 4) [90]. The process of budding is assisted by p6 gag and Vpu is downmodulated by BST2 to avoid tethering of BST2 to the virus to enhance the release of virus. Late domains in group-specific antigen (Gag) recruit components of multivesicular bodies to the site of budding, so that virus is released from the infected cell [91, 92]. Completing virion budding of the immature viral particle, the viral protease cleaves Gag-Pol polyprotein creating the mature virion and, thereby, completing the life cycle to continue infecting other cells[92] (figure 4).

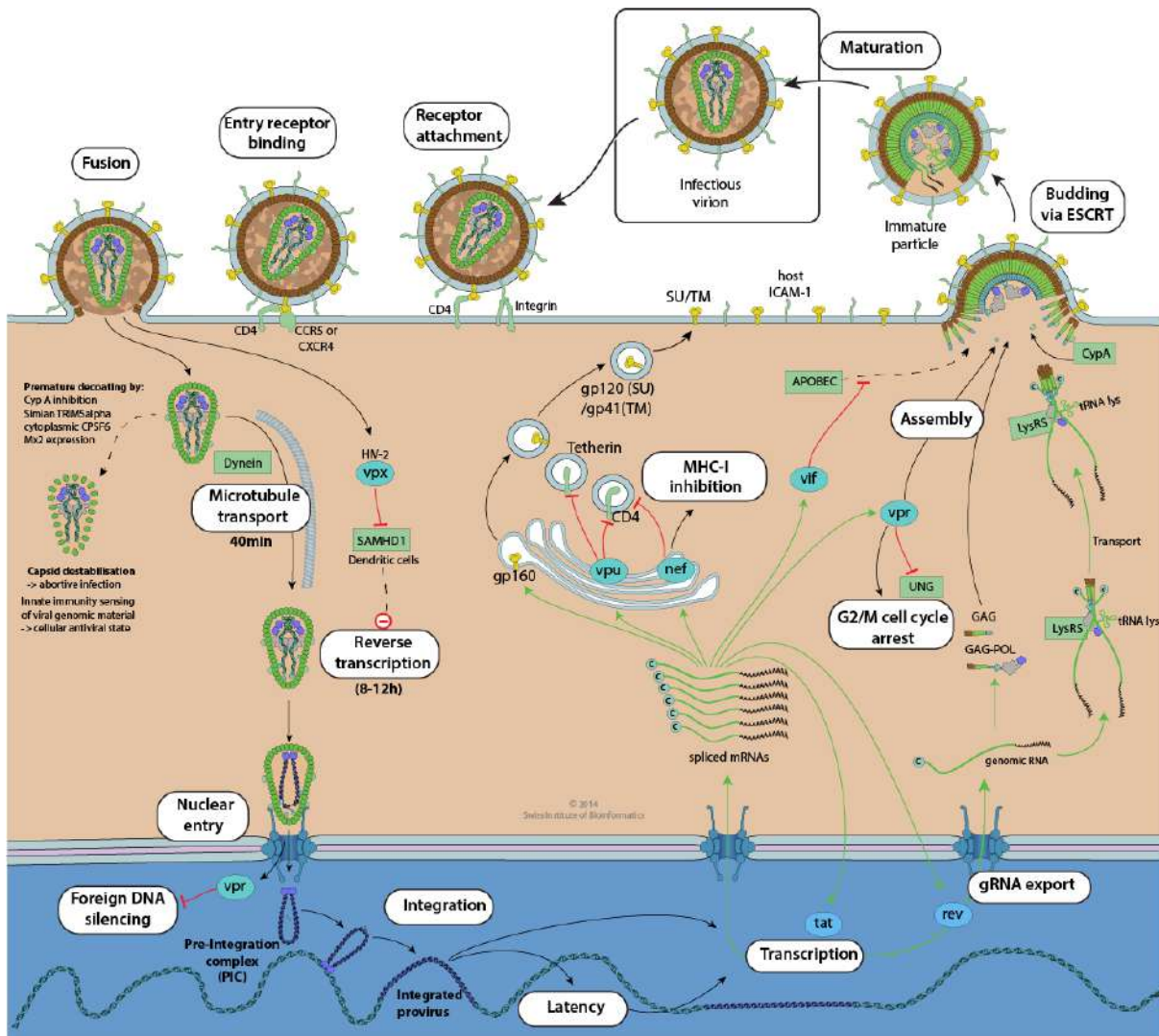


Figure 4 HIV-1 replicative cycle.

Envelope protein binds to the CD4 receptor and either CCR5 or CXCR4 receptor to allow the virus to enter the cell through the fusion of viral and cellular membranes. The viral capsid is uncoated and viral genome is reverse transcribed into double-strand cDNA that is further transported into the nucleus and integrated into the host genome (provirus). Upon cellular activation, proviral DNA produces spliced transcripts and the encoded accessory and structural proteins. These components are then exported from the nucleus and assemble into a new virion, finally budding out from the cell as an immature particle. Upon protease cleavage, HIV-1 particle matures and becomes an infectious virion, ready to enter a novel round of infection. Derived from [93]

Studying early stages in the transmission of HIV-1 in individuals is challenging and, therefore, animal models, such as Rhesus macaques and Simian immunodeficiency virus (SIV_{mac}) have immensely helped to understand this infection phase[94]. Numerous locations in the female genital tract including the ectocervix, transitional zone, endocervix and the epithelial tissue in the vagina are susceptible to SIV and HIV-1 entry [95-102]. Equally, in males, the foreskin, penile tissue and rectum are prone to infection from SIV and HIV-1[97, 103-107]. Subsequently following transmission, a succession of host and viral immune markers are expressed

reproducibly across individuals independent of the HIV-1 subtype or transmission path. This set of markers were first defined by Fiebig and associates and is used to stage individuals during acute infection[108]. Following transmission, a period of approximately 10 days known as the eclipse phase between infection and the detection of viral RNA occurs is clinically silent. The period is followed by the detection of viral RNA (Fiebig I), p24 antigen (Fiebig II), virus specific antibodies detected initially by ELISA (Fiebig III), followed by immunoblotting by western (Fiebig IV-VI)[108] (figure 5). Soon after the clinically silent period or eclipse phase, an exponential increase in viral RNA levels is observed in the blood, as a consequence of an exponential HIV-1 replication [109]. This period of exponential replicating virus is characterised by an elevated reproductive ratio (R_0) of 8[110]. R_0 is a numerical descriptor to indicate the number of cells that are infected by virus from a singly infected cell. $R_0 > 1$ values represent propagating virus and opposing $R_0 < 1$ indicated clearance of infected cells[111].

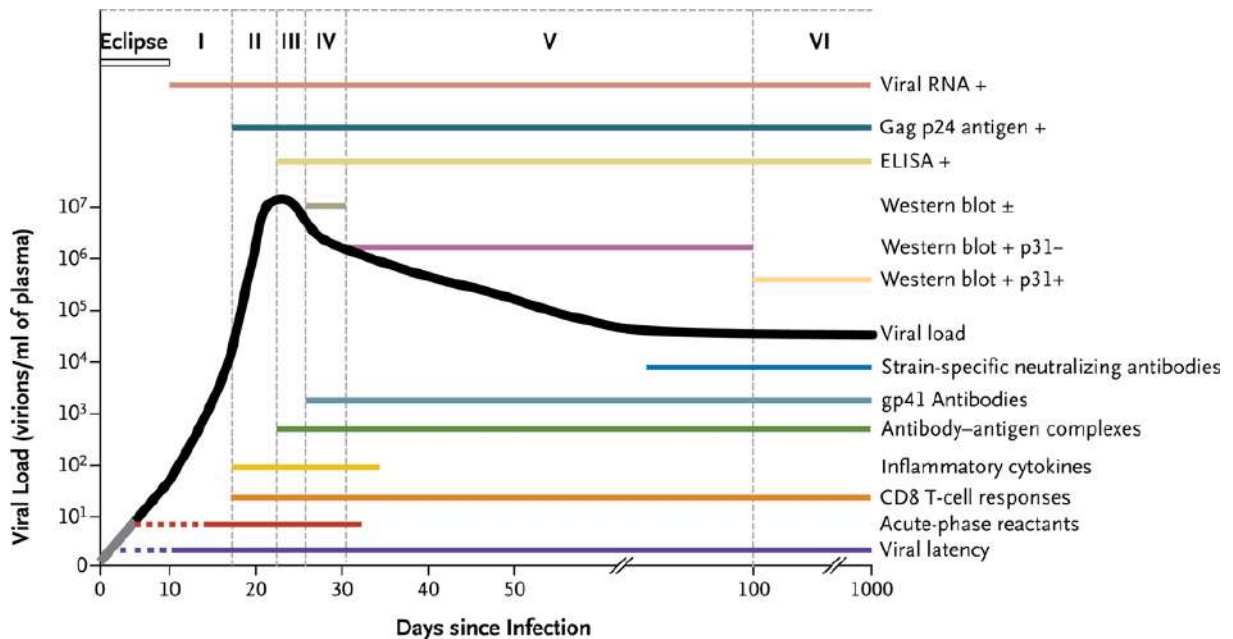


Figure 5 Stages of HIV-1 infection and the associated immunopathogenesis.

HIV-1 infection can be divided into six distinct stages based on the detection of viral RNA, the Gag protein and antibodies against HIV-1 proteins, first detectable by ELISA and western blot, indicated above the viral load curve. The lines beneath the viral load curve indicate early events and immune responses in the host, starting with the establishment of viral latency, and the development of CD8⁺ T-cell responses and binding and neutralizing antibodies. Derived from [30]

HIV-1 infection during the acute phase is defined as a period of approximately 4 weeks spanning from the acquisition to establishment of the viral set point following a decrease in the viral load from the peak of viral set-point of the viremia[112]. The viral set-point has been defined as a predictor of disease progression to AIDS in absence of highly active antiretroviral

therapy (HAART) [113-115] (figure 5), in which HIV-1 enters a latent phase ranging from 5 years to greater than 10 years (median progression to AIDS is in the range of 8-10 years)[116, 117]. A small percentage of HIV-1⁺ individuals naturally control HIV-1 and are divided in two groups, the long term non progressors (LNTPs) and elite controllers (EC). The individuals who have not received HAART that are asymptomatic for a long period of time (over 10 years) with normal CD4 cell counts (over 500 cells/mm³) are LTNPs[118-120]. Individuals whose viral loads remain undetectable over a greater period of time are further defined EC[121, 122]. Ultimately, AIDS is defined as the period with low CD4 cell count, by below 200 cells/mm³, with an impaired immune system response, leading to opportunistic infections and AIDS-related cancers[123, 124] (figure 6).

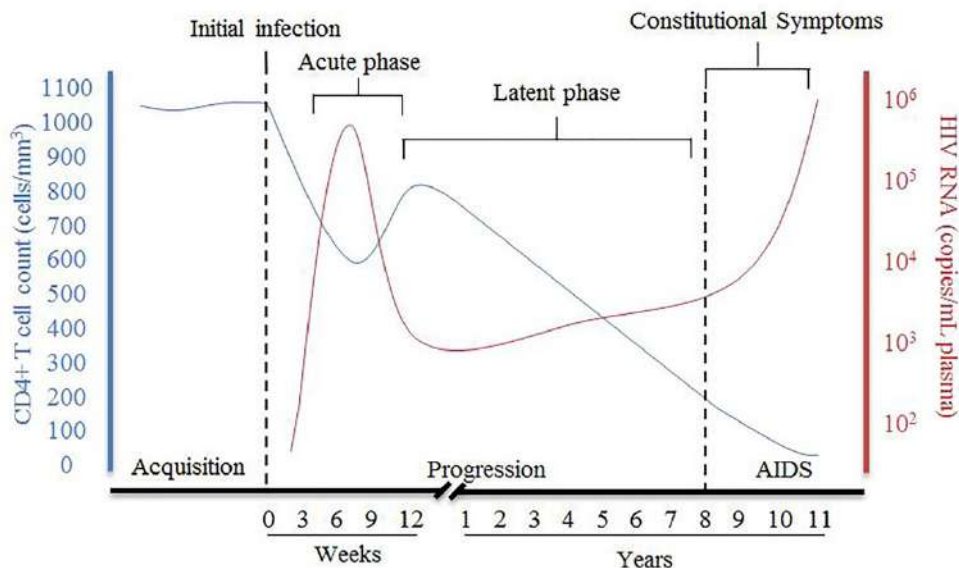


Figure 6 Course of HIV-1 infection.

Primary infection begins from the acquisition of HIV-1 with a short period until seroconversion, followed by the peak of viraemia and the decline of CD4 count. The symptoms of the acute infection show during this phase as virus spreads throughout the infected individual. Establishment of chronic infection is after the viral set-point when the viral load decreases and stabilises, whereas CD4 count is at a gradual decline rate for around 10 years. The final stage of the infection is the development of AIDS with opportunistic infection and/or CD4 count <200 cell/mm³, resulting in untimely death. Derived from [125].

1.1.2 Models of capsid uncoating

Capsid uncoating from the view point of structural virology has until recently only been considered in the context of its structural properties and is defined as the specific dissociation of the capsid shell from the viral core upon entry into the host cytoplasm[126]. However, based on recent evidence, HIV-1 capsid can influence late infection events including nuclear import

and integration[127-133], and has been visualised to colocalise with IN within the nucleus[134, 135]. It is unlikely that CA loss from the reverse transcription complex (RTC) is a single, discrete event, therefore, re-evaluation of the traditional definition of uncoating is needed[136].

Widely accepted is that uncoating occurs after fusion-dependent entry into the cytoplasm and before nuclear entry. However, there is a conflicting evidence as to the precise moment and location within the host cell at which this occurs and the extent that capsid disassembly from the viral nucleoprotein complex (VNC) before nuclear translocation. One of the defining features of HIV-1 infection is its ability to infect non-dividing cells that necessitates the translocation of the pre-integration complex (PIC) from the cellular cytoplasm into the nucleus through the nuclear pore complex (NPC)[137]. Studies have revealed that the upper size limit for passage within the NPC to be ~39 nm, which is considerably smaller than the 50-60 nm diameter of the wide end of the capsid cone, supporting the model of cytoplasmic capsid uncoating in the host cell[138-140].

Three main models of uncoating have been proposed (figure 7):

- 1) A rapid core disassembly following cellular entry (a).
- 2) A more gradual uncoating as the virus traverses the cytoplasm towards the nucleus (b).
- 3) Uncoating at the nuclear pore (c).

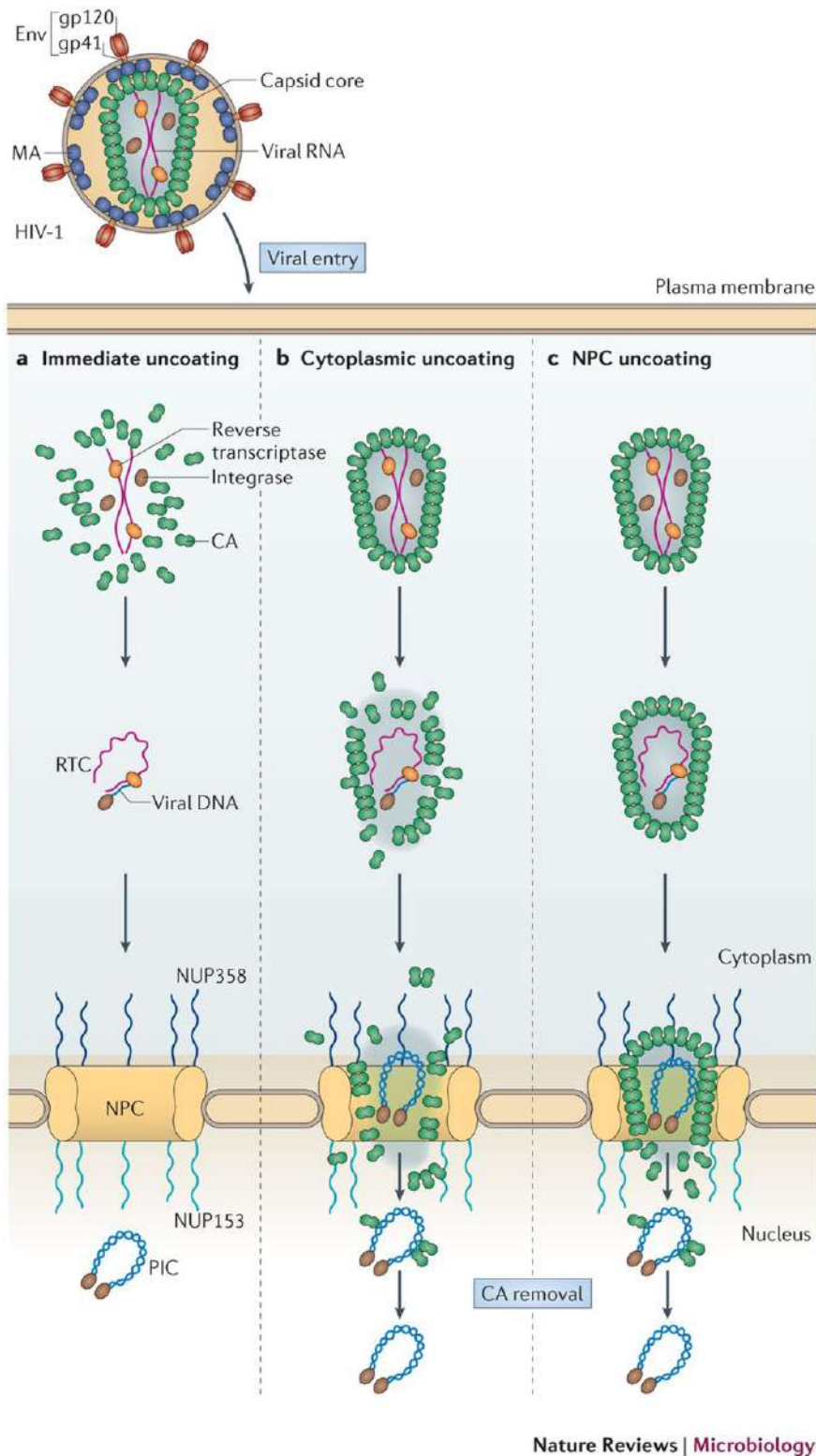


Figure 7 Principal models of HIV-1 capsid uncoating.

Proposed are three models of uncoating (a) Immediate uncoating of the entire capsid core directly after viral fusion with the cellular membrane (b) Gradual/biphasic uncoating, in which a measurable amount of capsid disassembly occurs as the VNC traffics through the cytoplasm, with a portion of the capsid remaining to mediate nuclear docking and translocation. (c) Uncoating at the NPC, in which the capsid core remains intact up until mooring at the nuclear pore, whereby uncoating is facilitated through interaction with nucleoporins (Nups). Derived from [136].

1.1.2.1 Rapid uncoating

In this first model, it is proposed that the capsid core disassembles close to the cellular membrane soon after viral fusion (figure 7a). Whilst most of the capsid is described to disassociate from the VNC, this does not rule out the presence of a residual amount of CA remaining with the RTC/PIC after uncoating[141-144]. This model was proposed due to the absence of detectable CA when using biochemical means to study the content of the RTC[145, 146]. This model fails to account for the cytosolic innate sensors that would be activated in the presence of viral RNA/cDNA pathogen associated molecular patterns (PAMPs) upon quick core disassembly[147-149], or the loss of a closed environment to facilitate reverse transcription of the RNA genome.

1.1.2.2 Gradual/biphasic uncoating

The second model proposes that the viral core remains intact for some time post-fusion, and that uncoating takes place gradually during passage towards the nucleus through interaction with cytoplasmic host cell factors and reverse transcription (figure 7b)[150, 151]. This is supported by studies using the intact capsid core targeting properties of TRIM-CypA, and immunofluorescent imaging[150, 152]. Loss of sensitivity to TRIM-CypA binding was observed 3-4 h post-infection, and approximately two thirds of RTCs still contained detectable amounts of CA 4 h post-infection. It has been suggested that CA-CA interactions, creating the delicate lattice of the viral core, would not tolerate a gradual disassembly of CA and, like the rapid uncoating model, the cDNA would be exposed to cytosolic sensors[136, 153]. However, cellular factors recruited to the RTC/PIC during capsid uncoating may be able to mask the nascent viral cDNA from antiviral innate immune detection[136].

1.1.2.3 Uncoating at the nuclear pore

The last model proposes that the capsid core remains intact during transport towards the nucleus, and uncoating takes place at the nuclear pore (figure 7c)[153]. Untimely uncoating is suppressed through the interaction of CypA and CPSF6. Upon docking at the NPC the capsid core binds to Nup358 and uncoating is triggered with the assistance of CA-associating factors (CypA, CPSF6, TNPO3), upon which the PIC is released and is translocated through the nuclear pore into the nucleus[153]. In this model, the viral genome is protected by the capsid core, thereby, excluding the upregulation of the innate DNA sensor of cyclic GMP-AMP synthase

(cGAS). This working model is supported by work performed in monocyte-derived macrophages (MDMs) that have been shown to be infected with WT HIV-1 without triggering an innate immune response[147]. Capsid mutations, however, and HIV-1 infection in CPSF6 and CypA-depleted macrophages, which potentially generate the premature release of cDNA, activate an antiviral state within the cell.

1.1.3 Innate Sensing of HIV-1

A major role of the viral capsid is to shield nascent viral DNA from innate immune sensors[154, 155]. Sensing of reverse transcribed RNA into DNA in the cytoplasm results in recognition of viral DNA by DNA sensors, thereby, triggering an innate immune response[148]. Capsid stability and uncoating are regulated by cellular restriction factors, for example, TRIM5 α , MX2 and CypA (as reviewed in [156]). CA interactions can be perturbed by CypA and CPSF6 in order to generate an interferon (IFN) response as demonstrated in macrophages [147]. The role of CypA in innate sensing has also been shown in monocyte-derived dendritic cells[149]. Capsid stability is the major intrinsic property regulating disassembly and release of viral DNA.

The Cyclosporine A (CsA) washout assay exploits the properties of HIV-1 restriction by TRIM-CypA (TRIM-CypA) fusion protein first described in Owl Monkeys[157]. The binding of the CypA component of the TRIM-CypA fusion protein to intact capsid cores can initiate timely uncoating and can also affect restriction of the capsid from innate sensors leading to premature uncoating[158, 159]. Interaction through TRIM-CypA can be blocked by the addition of CsA to allow the capsid core to go through the process of uncoating and genome release. At defined intervals, CsA is washed out of the cells, thereby, allowing restriction to take place (figure 8). TRIM-CypA-mediated restriction is a good indicator for the initiation of uncoating of intact capsid cores. The half-life of uncoating can be determined by the time post-infection of CsA washout. HIV-1 GFP-labelled viruses are employed and GFP is the final readout for flow cytometry. Dissimilar to other methods that determine the uncoating of bulk virus samples[160-163], many of which may not be infectious, the CsA-washout assay measures the uncoating of infective viruses that have escaped TRIM-CypA mediated restriction[136]. The caveat within this assay is that by directly measuring capsid uncoating using a single capsid binding restriction factor, it is plausible that other host restriction factors compete with TRIM-CypA for a limited number of binding sites within the capsid core structure[153].

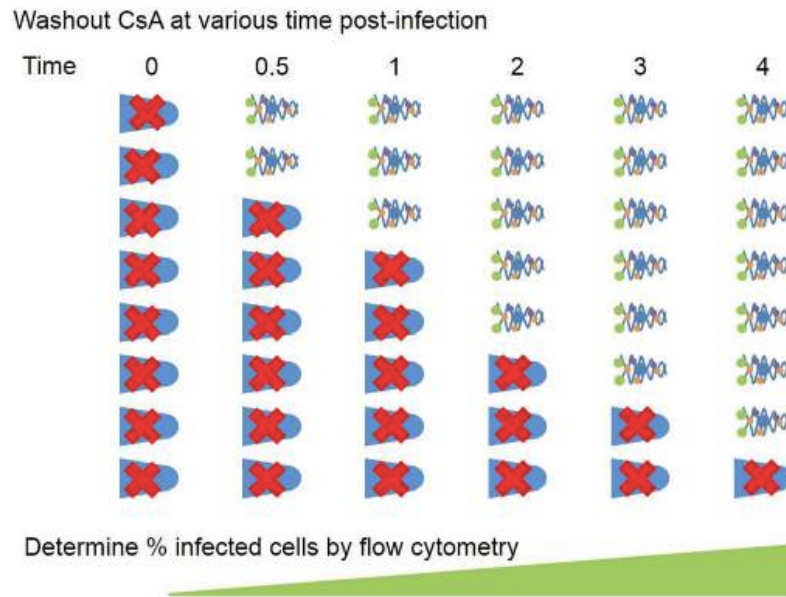


Figure 8 CsA washout assay.

The HIV-1-GFP reporter virus in the presence of CsA infects OMK cells. CsA can be washed out post-infection at different times that causes viral complexes to be restricted by TRIM-CypA. Uncoated particles are able to continue through their replicative cycle to infect cells. The sum of infected cells (%) at intervals were CsA is washed out can be determined by flow cytometry analysis. Derived from [3].

1.2 Adaptive Immune Response to HIV-1

1.2.1 HLA Class I

The adaptive immune response is initiated through presentation of antigen. Antigen presentation is conducted by professional antigen-presenting cell (APCs) such as macrophages and dendritic cells, two cell subsets that process endogenous and exogenous antigens. The antigens are then loaded on major histocompatibility complex (MHC) I and II molecules[49]. Human Leukocyte Antigen (HLA) class I, or HLA is expressed on the surface of nucleated cells in order to present antigen to CD8⁺ T cells and is encoded from a highly polymorphic region in the genome[164]. Located in the short arm of human chromosome 6 (6p21.3), classical HLA contains 12375 alleles of the HLA-A, -B and -C loci as well as 107 alleles of the non-classical HLA-E,-F,-G [164, 165]. HLA polymorphism of class I molecules is the outcome of competitive pressure to eradicate invading pathogens that evolve evasion mechanisms to avoid detection.

HLA presentation starts with the cleavage of pathogen proteins by proteosomal degradation in the cytosol by targeted polyubiquitination. Ubiquitinated proteins are then bound to the

proteasome enabling their degradation through proteolytic cleavage otherwise called proteolysis by β -subunits of the proteasome 20S core particle[166]. Peptides ranging in size from 4 to 20 amino acids are then transported by transporter for antigen processing (TAP) to the endoplasmic reticulum body (ER) through ATP hydrolysis[167, 168]. TAP is also important for facilitating peptide loading through recruitment of chaperone proteins such as tapasin, calreticulin, and ERp60 to form MHC-1 loading complex[169-171]. HLA class I-restricted peptides have typically 9 residues but can range from 8 – 11 residues in length, which, therefore, means peptides of only a certain length can occupy the MHC molecule peptide-binding groove[171]. Residues exceeding the size of the groove are processed further by aminopeptidase or the ER[172, 173]. Following peptide loading, the MHC-1 complex exits the ER to undergo post-translational modification in the Golgi network. Adequately modified, the complex enters the cell membrane to present its loaded peptide for antigen recognition by CD8⁺ T cells to initiate cytotoxic T-lymphocyte (CTL) signalling [174].

HLA-1 consists of three α domains and a soluble β 2- macroglobulin with the peptide binding groove formed by α 1 and α 2 domains comprising a sheet of eight β -pleated strands with two neighbouring walls comprised by an α -helix domain [175-177] . The transmembrane α 3 domain, together alongside the β 2-microglobulin, maintains the peptide-binding site[177]. The peptide-binding groove forms six pockets, named A-F. However, not all pockets are inevitably occupied, depending upon the different HLA types, pocket B (position 2) and pocket F (carboxy-terminus) are the most selective positions for HLA-A, -B and -C allotypes[177, 178]. HLA-1 molecules can also express very common allotypes, or public allotypes such as Bw4 and Bw6 epitopes. Epitopes are present on a single HLA (private epitope) or shared by multiple antigens (public epitope). Bw4 public epitopes are ligands for KIR3DL1 and an association between a slower HIV-1 disease progression and the presence of high expressing KIR3DL1 allotypes in combination with Bw4-80I HLA-B alleles was described[179, 180]. These results illustrate the crucial role that HLA-I has in moulding the natural killer cell (NK) response [181]. This thesis focuses on the significance of the cytotoxic T cell (CTL) response and, therefore, NK cells will not be further discussed.

During the course of HIV-1 infection, the most important single nucleotide polymorphisms (SNPs) associated with slower disease progression are located in HLA class I coding regions, as shown by genome-wide association studies (GWAS)[181-183]. HLA-B alleles have been stronger associate with worse or better disease outcomes[183, 184]. Well-described and

characterised alleles such as HLA-B*27 (HLA-B*27:05) and HLA-B*57:01 are termed “protective” and found enriched in clade B–infected long term non-progressors (LTNPs) from northern hemisphere cohorts [183, 185-187]. The protective allele HLA-B*81:01 is found in clade C–infected individuals, mainly located in Sub-Saharan Africa[188-190]. HLA-B*35 (HLA-B*35:01) is, in contrast, associated with more rapid disease progression[183, 191]. The specific mechanistic attributes governing how different motifs can accommodate numerous viral peptides and how peptide-MHC stabilities contributes towards control of HIV-1 during infection remains to be revealed[181]. Emerging from our current knowledge on HIV-1 viremia control is the significance of HIV-1-specific response directed towards multiple conserved epitopes. Therefore, viral escape from immune control directly has a consequence on viral replicative capacity, resulting in a fitness cost. In broad terms, Gag-specific CD8⁺ T cell responses can control viremia. A plethora of factors other than CD8⁺ T cell responses govern the control of viremia and further investigations are required to understand and identify epitope specific effects and the availability of T cell receptors for MHC loaded peptide recognition[181, 192-197].

1.2.2 CD8⁺ T cell response

Following presentation of viral peptide by HLA class I molecule, CD8⁺ T cells are assisted by CD4⁺ T cells and APCs with their co-stimulatory signals in order to become primed[198]. Priming of CD8⁺ T cells give rise to clonal expansion of HLA-restricted CD8⁺ effector T cells that secrete cytokines,(IFN- γ and TNF- α) and cytotoxic molecules (perforin, granzymes and granzymes) in order to induce apoptosis of virally infected cells[49, 199]. This reaction is termed the CTL response and is key to orchestrate the suppression of HIV-1 infection[193, 200, 201]. In the run up to peak viraemia during the acute phase, HIV-1 specific T cell responses play an important role in determining the viral set-point and, therefore, the rate of progression towards individuals developing AIDS[115, 202]. During chronic infection, there are distinctive characteristics qualifying CTL responses in EC versus those disease-progressors.

Phenotypically, HIV-1–specific CD8⁺ T cells in EC display to a lesser extent exhaustion and senescent markers, while maintaining a high proliferative state and cytotoxic response[203-205], by eliciting a higher IFN- γ or cytotoxic granule production[206]. Characteristically, HLA class-I restricted CTLs are resilient towards T regulatory (Tregs) cell–mediated inhibition and display polyfunctionality in EC[207, 208]. Furthermore, distinctive features of T cell receptors

(TCRs) in ECs are: 1) the affinity of TCRs to their ligands and 2) the ability of recognising the diversity of viral mutations reflecting the pool of viral quasi-species in circulation[197, 209].

CTLs specifically target susceptible parts of the viral proteome, for example, Gag and Pol, to slower the progression to AIDS through specific CTL responses towards Gag residues[193, 210]. A possible explanation for Gag-specific CTL responses may be due to the high amount of Gag production as well as the rapid proteolytic digestion of Gag within the cytosol in infected cells [197, 211]. A further tangible explanation would be that there is an increased fitness cost for the virus to mutate within conserved regions of its genome[212, 213]. Nonetheless, epitopes outside of Gag are also targeted in order for the immune system overall to mount an effective and prolonged suppression of viral production and provide effective immune control of viremia[214, 215] (figure 9).

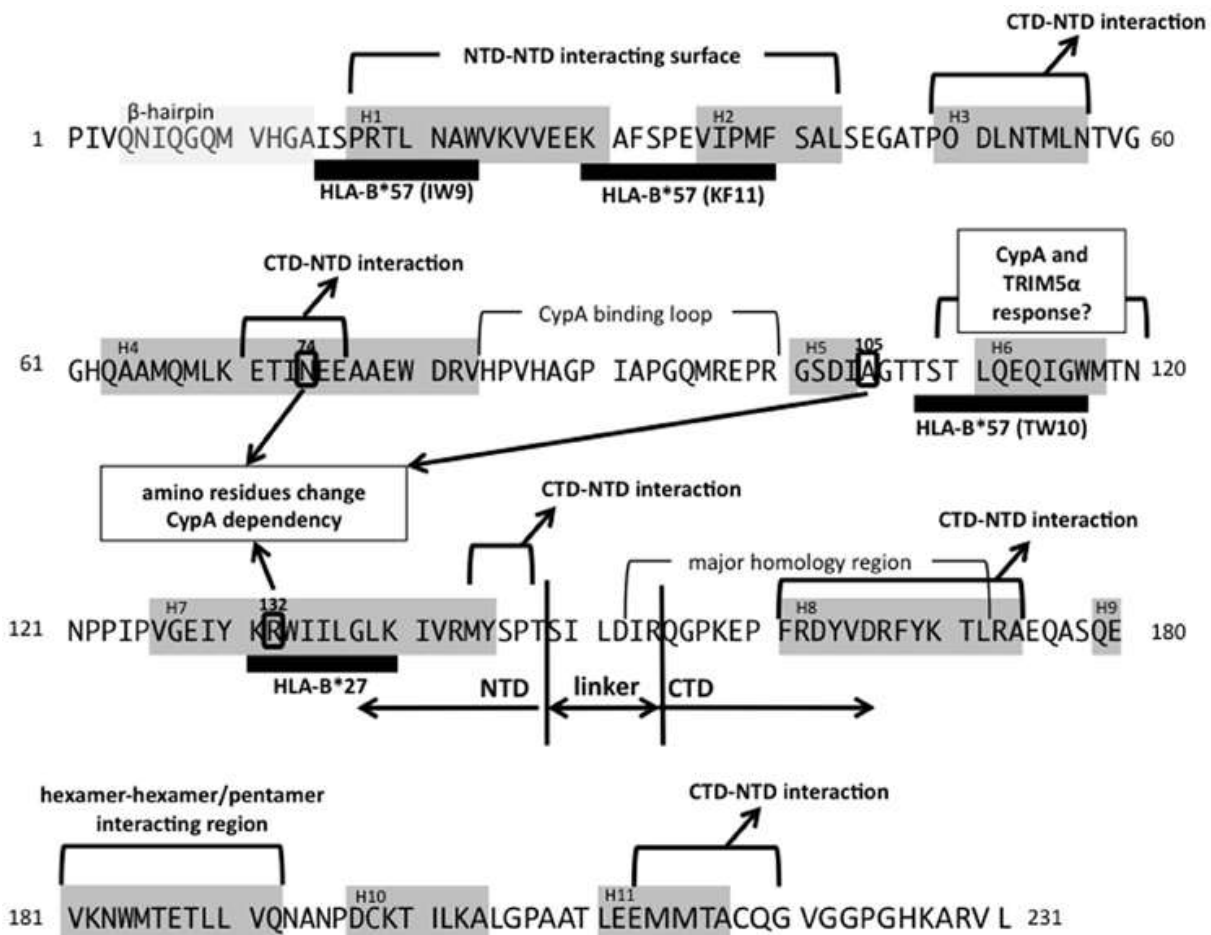


Figure 9 Cartoon of the CA functional domains and two major protective CTL alleles.

Grey boxes indicates the β -hairpin (amino acids 4–14) and helix structures (H1–H11). The black bars highlight the CTL epitopes restricted by each allele. The NTD-NTD, CTD-NTD, or hexamer-hexamer/pentamer interacting regions are illustrated. The 3 amino residues (N74, A105, and R132) that change CypA dependency, are encircled. Reference amino acids sequences are from HXB2 (accession number; AB50258.1). Derived from [216]

1.2.3 Viral Mutations in Response to CTL Immune Control

1.2.3.1 *Escape mutation*

As explained previously, CTL strongly mediate immune control of HIV-1, particularly in viraemic controllers, whom express protective HLA class I alleles. CTLs apply a strong selection pressure upon the virus, however, a population of HIV-1 containing mutations allowing escape from CTL control rises[217]. Soon after sero-conversion, escape mutations from CTL arise as the HIV-1 rapidly mutates in order to prevent restriction[218-221]. Individuals expressing protective HLA-I molecules are more likely to give rise to virus that undergoes more frequent mutations generating escape mutants[222, 223]. The mechanisms that govern the selection of escape mutations between individuals is conceivably due to the potency of the response by CTLs[220, 221].

Escape mutations are classified into three categories depending upon the mechanistic route through which the acquired mutation facilitates evasion of viral recognition by the immune system. Classifying escape mutations aids our understanding of viral evasion events for which targeted therapies may be appropriately applied in the clinical setting to benefit patients. Firstly, escape mutations can impair proteosomal processing directly affecting the binding of TAP on either the C- or N- Terminus and may also prevent the cleavage from the ER aminopeptidase[224-227]. However, mutations of this aetiology are normally located outside of the epitope rarely occurring within it[219, 228]. Secondly, escape mutations can result in altered peptide-MHC binding. Mutation(s) arising at peptide position 2 and within the C-terminus, corresponding to the HLA-I B and/or F pocket, respectively, reduce binding of the peptide to the MHC. Nonetheless, if other residues of the peptide are mutated, principally within P1, P3 and in exceptional cases P5 and P7, considerable significant effects upon peptide-MHC binding through the interaction with A, D, C and E pockets are observed, respectively. Cumulatively, these alterations result in the third mechanism, by which altered peptide to MHC binding affects the interactions of the presented peptide with the TCR on the CD8⁺ T cell, by altering the secondary structure of the epitope peptide[229].

Amongst all the HLA-driven mutations possible, the second mechanism of escape accounts for approximately 20% of all mutations reported, resulting in a greater than 10-fold decrease in peptide binding affinity to HLA-1 [190, 230, 231]. Reported most in the literature are R264K mutant of HLA-B*27-restricted Gag KK10 epitope (263-272, KRWILGLNK) and A163X of

HLA-B*5703- restricted KF11 epitope (162-172, KAFSPEVIPMF)[232, 233]. Our laboratory has reported altered capsid stability of the R264K mutation [3, 234-238].

The third mechanistic route of escape does not impact peptide loading; however, it significantly diminishes and abrogates TCR recognition. Therefore, advantageously for the virus, viral peptide would still be presented by HLA-I on the cell surface to lessen the extent of CTL recognition. This is a chink in the virus that can be the Achilles heel to develop a *de novo* CTL clone capable of recognising this variant and, thereby, reverse the cloak that lessens CTL recognition[239-241]. Taken together, mutations that arise within the epitope disrupting antigen presentation and TCR recognition are the main means by which CTL surveillance is evaded by HIV-1. On the other hand, without HLA-restricted CTL immune pressure, the mutant can reverse back to wild-type and regain viral fitness, which has been observed in transmission pair analysis[242-244].

During HIV-1 infection, the consequence of acquiring an escape mutation can alter viral replicative capacity (VRC). Viral fitness as the capability of an organism to adapt in order to reproduce in a given environment under a selection pressure i.e. viral activity and stability [245]. Escape mutations that arise can simultaneously reduce VRC but increase viral fitness of the virus. The redundancy of CTL responses targeting Gag, one of the most conserved regions, are associated with viral control of HIV-1[246]. Consequently, escape mutations in Gag epitopes may result in a significant fitness cost.

Reduction in VRC has been reported in several individual cases and cohorts[189, 247-249]. Mutated HIV-1 virions can persist as attenuated viruses due to their lower VRC[249]. EC harbouring escape mutations elicit a reduction in their VRC, thereby, allowing control of viraemia by the host immune system and consequently slowing the disease progression towards AIDS[212, 250, 251]. However, escape mutations resulting in a limited or modest impact on VRC sees the possibility of CTL control being lost as reflected by high viral load and progression towards AIDS[232, 234, 241]. Notably, there is no absolute direct correlation between reduced VRC and a high CD4 cell count or low viral load. Strikingly, HIV-1 is able to balance evasion of CTL recognition and lessening its own viral replicative capacity. Several considerations besides viral fitness must be kept in mind when understanding the factors maintaining immune control, for example, timing of CTL targeting, T cell efficacy, immunodominance and TCR usage[238].

1.2.3.2 Compensatory mutation

Reduced VRC resulting from acquisition of an escape mutation(s) can be restored towards that of the wild-type virus through the emergence of a compensatory mutation[46, 248, 252], allowing the evasion of immune surveillance and still curbing competent replicative capacity. Interestingly, the number of escape and compensatory mutations are correlative[253]. Taking the association of HLA alleles with the frequency by which these compensatory mutations arise, these mutations can be found upstream or downstream in close proximity to the escape epitope when seen in the secondary structure[252, 254, 255].

Compensatory mutations alone are able to reduce VRC in the absence of an escape mutation[248, 255, 256] although some, reported exceptions have an influence upon viral fitness[221]. Procurement of two simultaneous and effective mutations may be in the range of years to decades depending upon host cell factors and HLA control[181, 257]. Loss of control in LTNPs and ECs who have protective HLA-B alleles such as HLA-B*27 may be in part explained by the time it takes to obtain a compensatory mutation[46, 248]. During the course of immune pressure, naturally occurring mutations can accumulate and it may be likely that compensatory mutation(s) arise before the corresponding escape mutation allowing CTL recognition to be evaded[221, 258].

1.3 Aim and Hypotheses of this dissertation

Determine the impact of CTL-driven viral escape mutations within HIV-1 capsids on capsid stability and innate sensing.

Hypothesis: CTL-driven escape mutations within capsid epitopes restricted by protective HLA class I alleles will result in reduced capsid stability and increased immune activation.

Motivation: In HIV-1–infected individuals, virus-specific CD8⁺ T cell responses that are restricted by the protective HLA class I alleles B27 and B57, which are specifically targeting epitopes positioned within conserved regions of the HIV-1 p24 Gag sequence. Evasion of robust CD8⁺ T cell responses by HIV-1 is through selection of escape mutants that possess variations within their capsid epitopes. The extent to which these capsid mutations have an impact on capsid stability remains elusive and requires further investigation. The aim of this thesis is to determine the effect of CTL-driven viral escape mutations within the capsid and to further extend the study to examine *in vitro* the *in vivo* compensatory mutations selected in patients for capsid stability and innate sensing.

Meeting this proposed objective will serve as a novel model that links cellular immune pressure to the heightened sensing of infection by innate immune receptors to better design and execute patient care.

2. Results

2.1 Investigations into producing gag/pol and gag protease clinical isolate derived lentiviral constructs

2.1.1 Viral systems used to test gag/pol clinical isolates efficiencies in vitro

To determine the consequences of CTL-driven escape mutations within HIV-1 p24 Gag for capsid stability, clinical isolate derived gag-containing particles were generated. The aim was to use *gag* sequences from primary isolates with known consequences for immune activation and disease progression and to subsequently construct additional viruses with specific CTL- and NK cell-induced escape mutations within Gag. These additional viruses are outlined in section 3.1.10. It has been reported that HIV-1 viruses with higher replicative capacity cause more immune activation and CD4⁺ T cell decline, independent of viral load[259].

The main hypothesis of this thesis is that differences in capsid stability might represent a link between the observed association between VRC and immune activation and CD4 decline. Here, clinical isolates were tested in the CsA washout assay to measure the uncoating kinetics, thereby, observed differences in this assay will provide insights into capsid stability and might help to understand the clinical consequences.

To do so, I used three different technical approaches to generate the viruses. The first one focused on a 3rd generation lentiviral packaging system, which is shown in figures 10 and 14. A and consists of the lentiviral transfer plasmid pSH0-GFP that becomes self-inactivated (SIN) after integration due to a deletion in the 3'LTR; the packaging plasmid pMDLg/pRRE that contains the *gag/pol* clinical isolate gene segments and pRSV-Rev required for viral protein expression. These particles can then be pseudotyped with the packaging plasmid pCMV-VSV-G. The second approach was based on cloning *gag/pol* sequences from the clinical isolates into pNL4-3Δenv-eGFP and produce pseudotyped viruses with VSVg envelope. The third approach was a modification from the second one, where gag protease was cloned into pNL4-3ΔgagprotΔenv-eGFP[260, 261].

2.1.2 Methods for the construction of HIV-1-GFP clinical isolate derived particles

The first system, the 3rd generation packaging system, does not express Tat, but expresses Gag and Pol in one packaging plasmid (pMDLg/pRRE) and Rev in another plasmid (pRSV Rev). The second system consists of a full-length replication incompetent, infectious HIV-1 subtype B NL4-3 molecular clone, whereby the *gag/pol* from clinical isolates replaced that of the endogenous *gag/pol* sequence. The 3rd generation lenti-viral packaging system does not express the HIV-1 accessory genes Vif, Vpr, Vpu, Nef compared to the replication incompetent HIV-1 NL4-3 strain that does encode these accessory proteins. To generate pNL4-3 Δ env-eGFP and pMDLg/pRRE expression constructs containing *gag/pol* clinical isolate derived sequences, a novel approach was employed (figure 10).

The pNL4-3 Δ env-eGFP and pMDLg/pRRE expression constructs had XhoI and XmaI restriction sites introduced by site directed mutagenesis flanking the *gag/pol* segments, respectively (figure 10.A). Primer-specific PCR amplification of *gag/pol* fragments from the clinical isolates (figure 11) was performed with the designed primers, that introduced overhangs of Kozak sequence and XhoI flanking the start of *gag* and XmaI flanking the end of the *pol*. In parallel, pNL4-3 Δ env-eGFP and pMDLg/pRRE expression constructs were digested with *XmaI* and *XhoI* to i) cut out *gag/pol* and ii) achieve linearisation. The resulting PCR product was introduced by ligation into the XhoI/XmaI linearised vectors (figure 10. B-E).

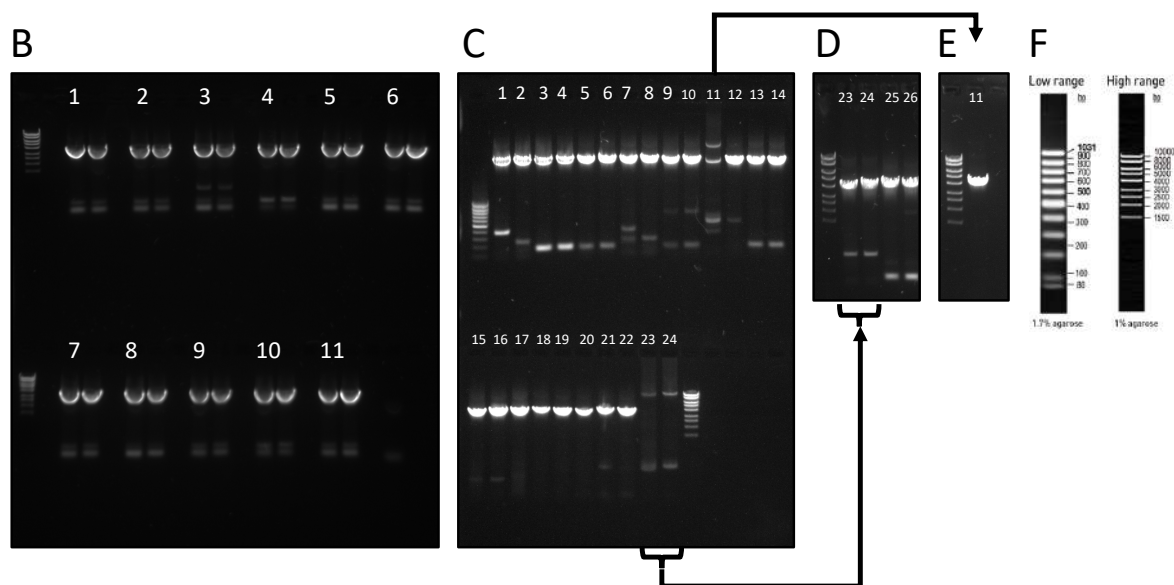
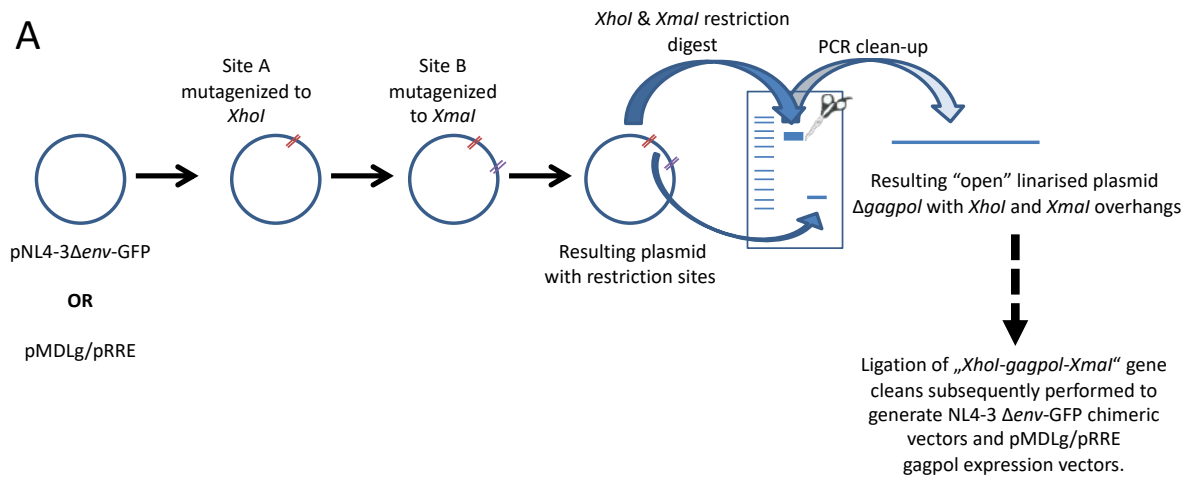


Figure 10 Construction of HIV-1-GFP patient-derived *gag/pol* LV particles.

(A) The pNL4-3 Δenv -eGFP and pMDLg/pRRE expression constructs were mutagenised at the 5' *gag* start and 3' *pol* end to introduce *XhoI* and *XmaI* restriction sites, respectively. These modifications were used for restriction site cloning. Resulting open vectors were used for ligation reactions after gel electrophoresis and PCR clean-up. Ligation of PCR-generated *gag/pol* fragments amplified from clinical-isolates *gag/pol* with complementary sticky ends was performed. (B) PCR products were run in duplicate. Note that L=Lane: L1, Z1008M; L2, MJ4 WT; L3, Z2013F; L4, Z1781M; L5, Z1515M; L6, Z2003M; L7, Z3576F; L8, Z2063M; L9, Z3681F; L10, Z1123M; L11, Z3863F. (C) L1, CH058 TF; L2, CH058 6mo; L3, CH164 TF; L4, CH164 6mo; L5, CH264 TF; L6, CH264 6mo; L7, CH470 TF; L8, CH470 6mo; L9, CH569 TF; L10, CH569 6mo; L11, CH850 TF; L12, CH850 6mo; L13, CH042 TF; L14, CH042 6mo; L15, CH162 TF; L16, CH162 6mo; L17, CH185 TF; L18, CH185 6mo; L19, CH236 TF; L20, CH236 6mo; L21, CH040 TF; L22, CH040 6mo; L23, CH077 TF; L24, CH077 6mo. (D) L1 sample 23, CH077 TF; L2 sample 24, CH077 6mo; L3 sample 25, CH107 TF; L4 sample 26, CH107 6mo. (E) L1 sample 11, CH850 TF. (F) DNA ladders low and high range.

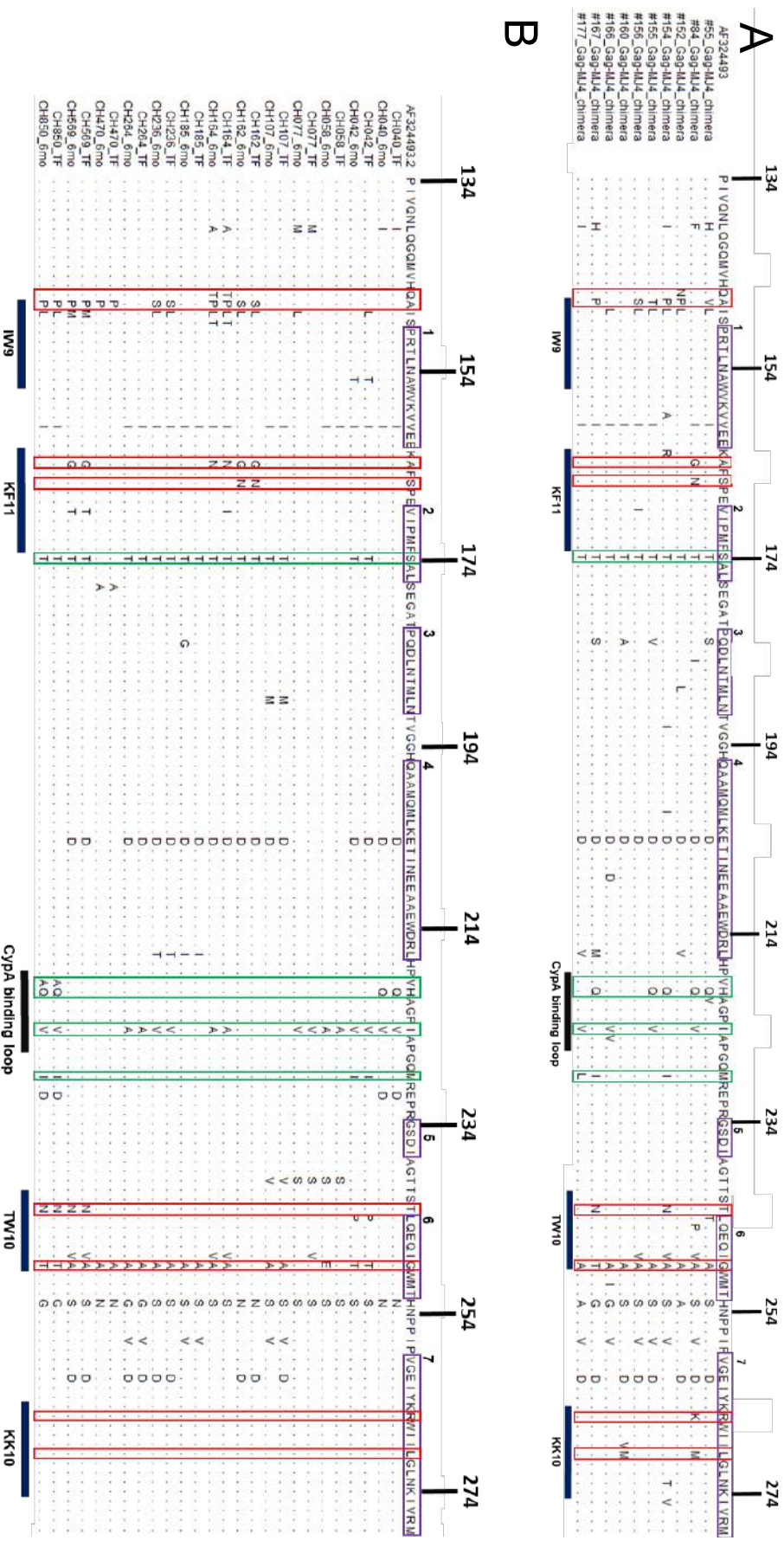


Figure 11 Construction of HIV-1-GFP patient-derived gag/pol LV particles.

Annotated sequence of the amino-terminal domain of HIV-1 capsid aligned to NL4-3 AF324493. The seven helical regions are boxed and numbered (numbers in bold). The CTL epitopes IW9, KF11, TW10 and KK10 are indicated, with the exception of QW9, which is located in the C-terminal CA domain. Amino acids are commonly mutated to induce resistance to CTLs recognising these epitopes (red) or to compensate for impaired replication resulting from CTL resistance mutations (green). (A) Gag-MJ4 Chimera amino acid sequences of the constructs gifted by Professor Eric Hunter. (B) Proviral transmitted and 6-month amino acid sequences of the constructs gifted by Professor Beatrice Hahn.

2.1.3 Identification of pNL4-3Δenv-eGFP and pMDLg/pRRE expression constructs containing respective clinical isolate gag/pol sequence

A DNA sequencing strategy was developed on the basis of approximate spacing of consensus gene sequence within the clinical isolate sequence. This approach allowed the overlap of amplicon retrieved sequences to reconstitute the full-length *gag/pol* gene segment introduced by ligation into the NL4-3Δenv-eGFP and pMDLg/pRRE expression constructs (figure 12). A primer set of 7 consensus primers with additional degenerate primers that have a substitution of different bases sequences allowed for the sequencing of the entire length of the introduced *gag/pol* gene segment. (figure 12. A). This also allowed to exclude any errors in ligation and also to confirm the introduction of the kozak sequence and restriction sites (figure 12. B & C). Restriction digest of clones allowed a quick identification of clones containing *gag/pol* inserts.

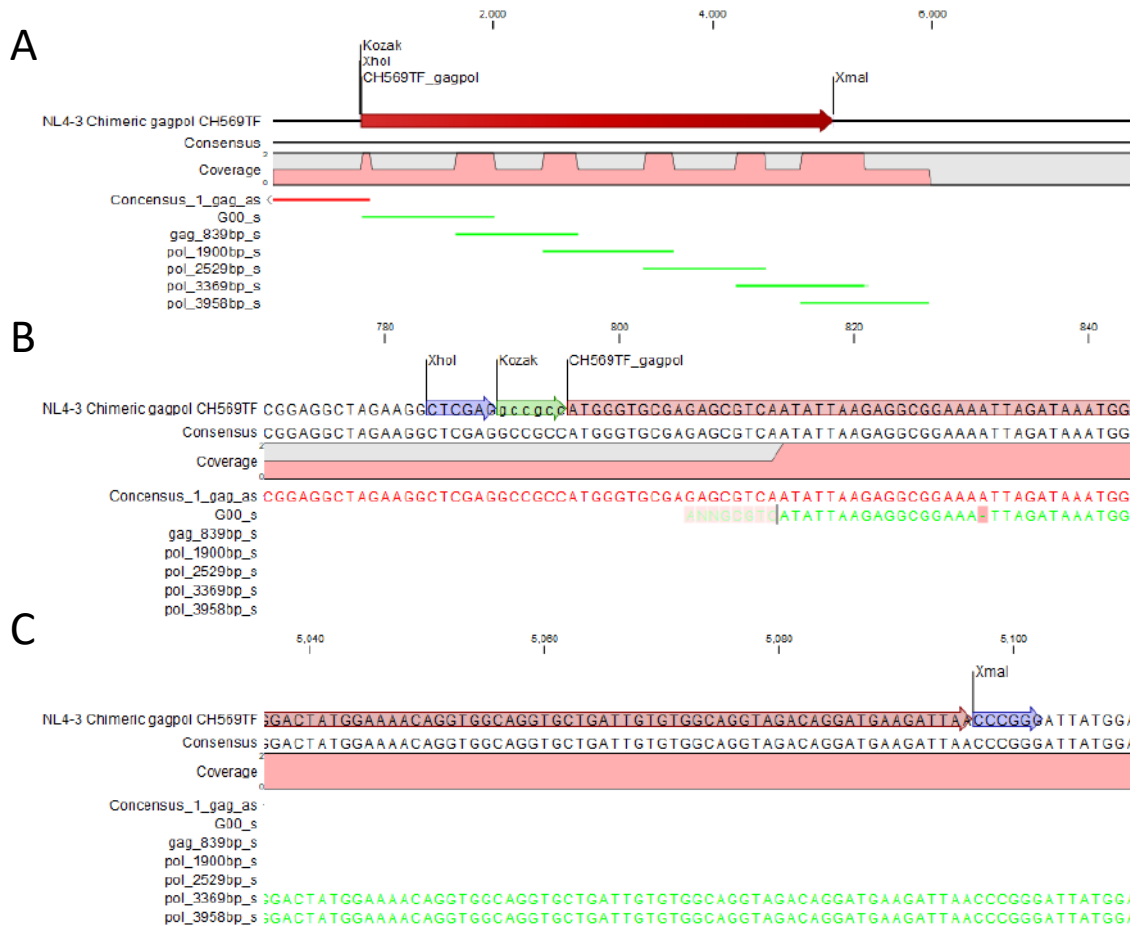


Figure 12 Sequencing strategy for confirming cloned gag and pol genes into lenti-viral vector backbones.

Degenerate sequencing primers suitable for sanger sequencing were designed for regions of high sequence similarity where amplicon sequences overlap after trimming and aligning to the reference vector sequence. (A) Representation of amplicon sequences aligned to the *gag/pol* sequence that was cloned. Red sequencing amplicon represents the antisense direction of sequencing and green represents the sense direction of sequencing. (B) The 5' *gag* sequence the kozak sequence and the XhoI restriction site were confirmed. (C) The 3' *pol* sequence and the XmaI restriction site were confirmed. Figure Arrows: Blue: restriction sites; Green: kozak sequence; Red: *gag/pol* gene clean insert.

2.1.4 Validation of in vitro production of infectious proviral particles

To address the effect of p24 gag mutations upon innate sensing, point mutations were previously introduced into *gag* of the pNL4-3 Δ env-eGFP lab-adapted proviral strain of HIV-1. Gag forms the structural component that encapsulates the HIV-1 negative-sense RNA genome made up of p24 subunits. R264K, L268M mutations identified in clinical isolates within the KK10 epitope and the compensatory S173A mutation located adjacent to the KF11 epitope were introduced to measure differences in capsid stability. This investigation is further studied in the context of innate immune sensing of these capsid mutants.

In order to reveal differences in heightened immune sensing, IFN α 2a stimulation and a monocyte derived macrophage (MDM) infection assay were performed. To determine the number virally infected cells, flow cytometry was performed to calculate the percentage of HIV-1-GFP⁺ cells (figure 13). High virus titre stocks were frozen and stored at -80 °C until required. High titres of infectious particles were needed and were determined by titration in OMK cells under restricted and unrestricted sensing where TRIM-CypA was washed out using Cyclosporin A (CsA) (figure 13. B). To assess if unrestricted sensing by TRIM-CypA was achieved, viral particles were titrated under control conditions where ethanol was substituted for CsA. The particles were also titrated in a monocyte derived cell line, THP-1 cells, for comparison (figure 13. C). The restriction pattern seen in the THP-1 cell line shows that the R264K and R264K plus L268M had 5-fold reduced infectivity compared to the WT and the compensatory mutant S173A plus R264K plus L268M. These data show in the THP-1 cell line the R264K and R264K plus L268M escape mutants to have less GFP⁺ cells compared to the S173A plus R264K plus L268M compensatory mutant.

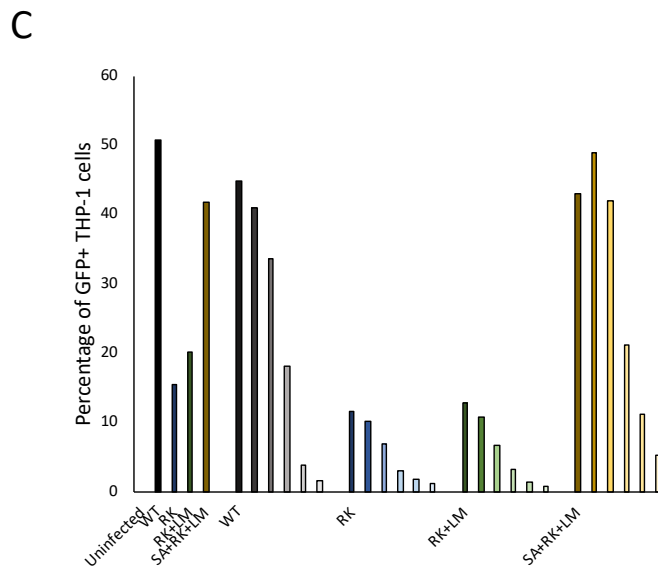
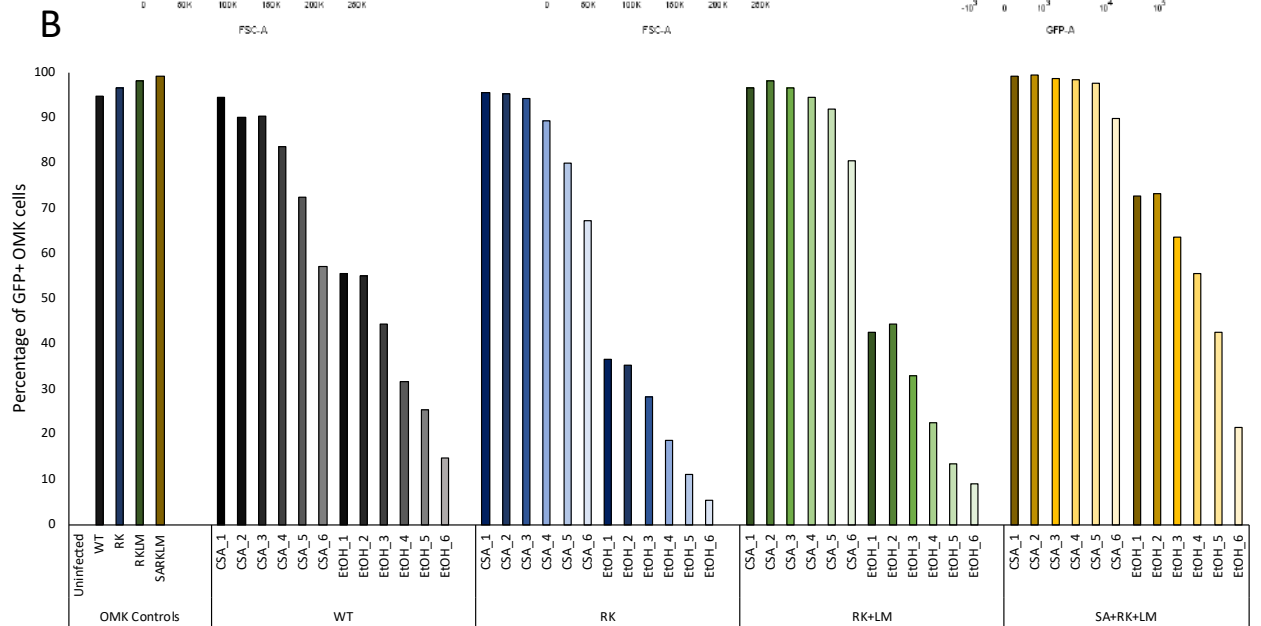
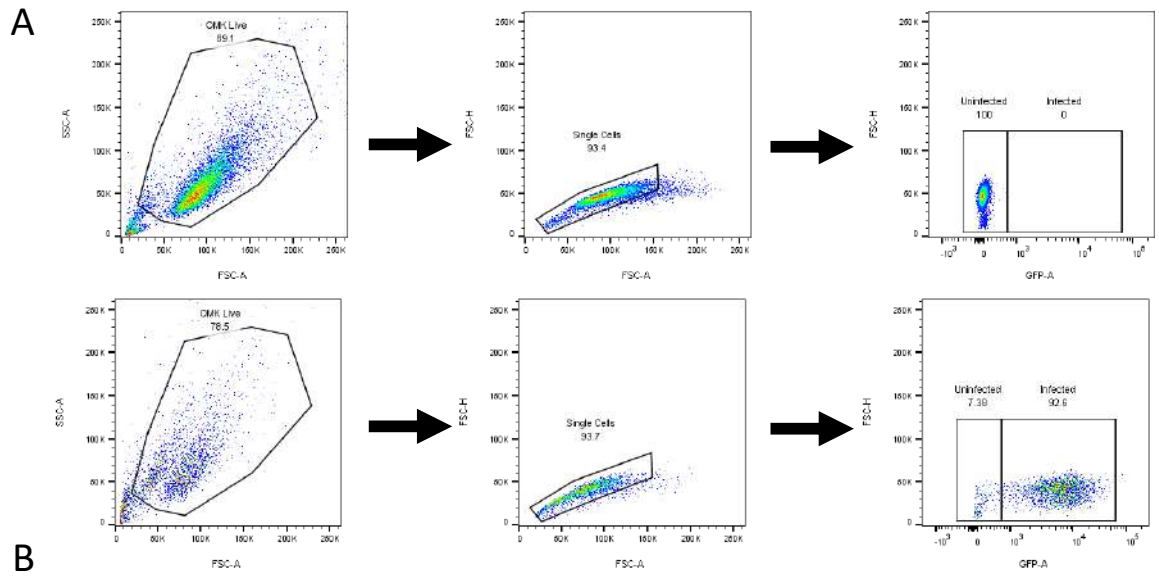


Figure 13 FACs gating and titration of viral vector constructs for optimal infectivity range.

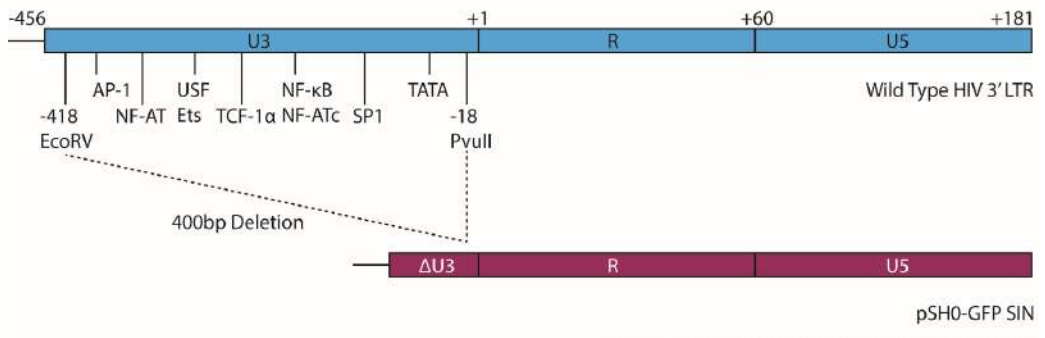
(A) Schematic representation of the gating strategy that was used to identify transduced OMK cells and THP-1 cells that expressed GFP representing virally infected cells. Each dot represents one cell. The cell density is represented by a colour code. Blue dots show low density, whereas red dots illustrate a high cell density. The gate that defines the selected population is highlighted with by a black coloured frame. OMK and THP-1 cells were gated using forward and side scatter areas (FSC-A/SSC-A). The cell population was then sub-analysed by area and height of the forward scatter (FSC-A/FSC-H) defining single cells. Infected cell subsets were sub-gated for the expression of GFP. (B) Titration curves of OMK cells treated with CsA and EtOH to determine the maximum and minimum percentage of lenti-virally transduced cells. The NL4-3 viral gag mutants shown are WT, R264K R264K plus L268M and S173A plus R264K plus L268M. OMK controls represent the maximum level of virally-infected cells. (C). Titration curves of THP-1 cells untreated with CsA (unrestricted infection) and EtOH (restricted infection) to determine the maximum and minimum percentage of lenti-virally transduced cells. The NL4-3 viral gag mutants shown are WT, R264K R264K plus L268M and S173A plus R264K plus L268M. OMK controls represent the maximum level of virally-infected cells. Titrations determined at 48 hours following spinoculation.

2.1.5 Titration of 3rd generation LV particles containing gag/pol derived from clinical isolates to yield infectious particles and washout assay

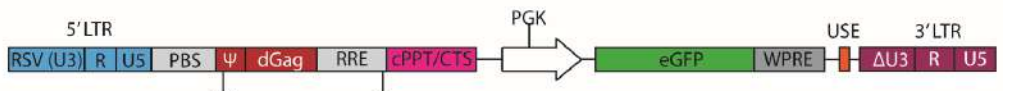
To determine if the 3rd generation lentiviral packaging system was suitable (figure 14. A), the lentiviral particles were transduced in OMK cells and the titre was determined by the percentage of GFP⁺ cells, indicating successful infection (figure 14. B). A variability in the maximal infectivity rate was observed for the different viruses produced, as shown by the titres (figure 14. B). The LV-particles ZM1008M (45%), ZM2013F(60%), ZM1781M (40%), ZM1515M (55%), ZM2003M (44%), ZM2063M (35%), ZM1123M (49%), ZM3863F (80%) and the NL4-3 (83%) showed a suitable titre for the CsA washout assay. The two isolates ZM3576F (4%) and ZM3681F (7%) titres were too low and were not appropriate for the CsA washout assay as greater than 40% infectious titre was required.

A

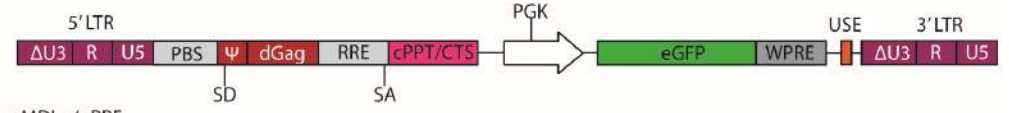
Modification of the 3' LTR "Self-Inactivating"



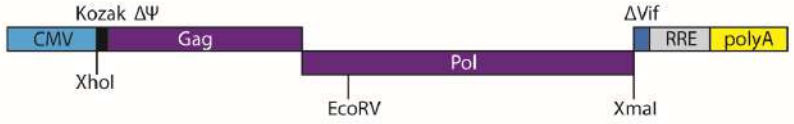
pSH0-GFP SIN



The deletion is transferred to the 5' LTR after reverse transcription and integration in infected cells



pMDLg/pRRE



pRSV-Rev



pCMV-VSV-G



B

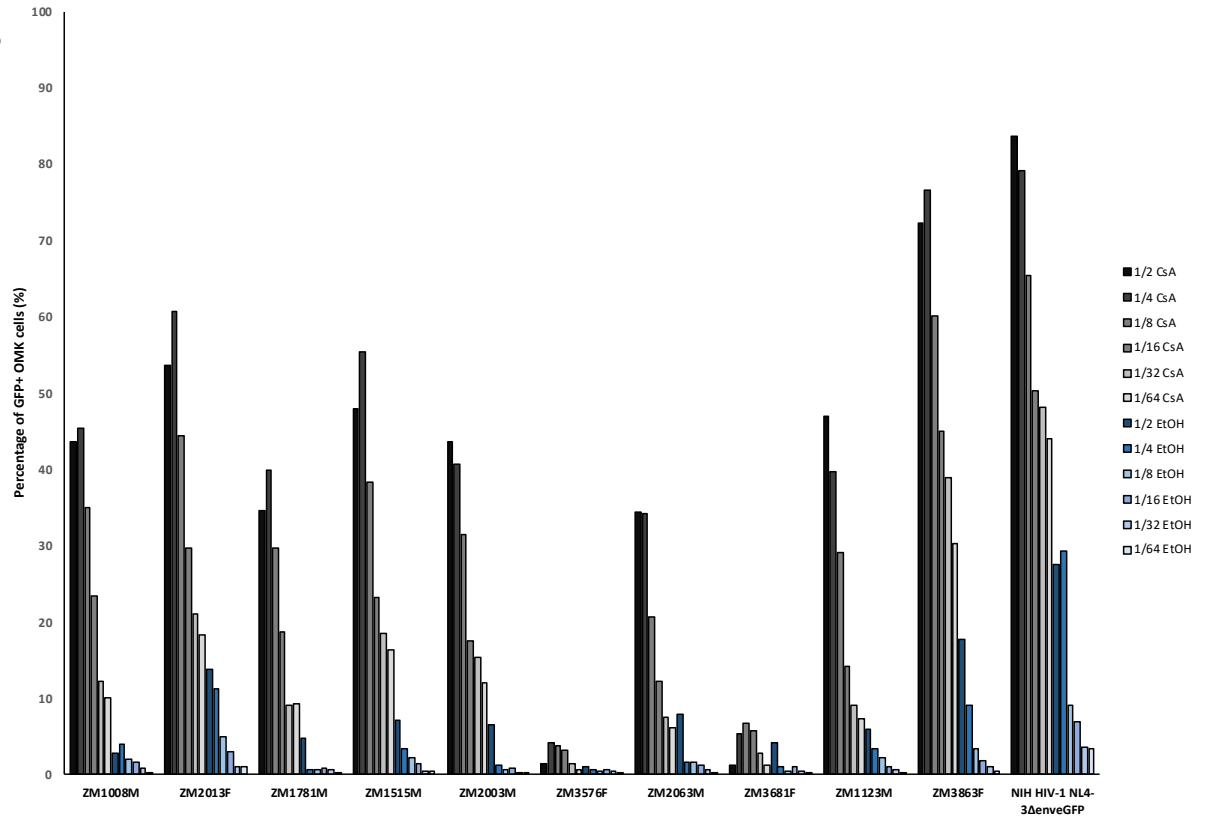


Figure 14 Construction and titration of HIV-1-GFP clinical isolate-derived *gag/pol* 3rd generation lenti-viral particles.

(A) Schematic drawing of the four constructs used to make a lentivirus vector of the 3rd generation classification. The viral LTRs, the reading frames of the viral genes, the major 5' splice donor site (SD), the packaging sequence (Ψ), and the RRE are shown. The conditional packaging construct, pMDLg/pRRE, expresses the *gag* and *pol* genes from the CMV promoter and intervening sequences and polyadenylation site of the human β -globin gene. As the transcripts of the *gag* and *pol* genes contain *cis*-repressive sequences, they are expressed only if Rev promotes their nuclear export by binding to the RRE. All *tat* and *rev* exons have been deleted, and the viral sequences upstream of the *gag* gene have been replaced. A non-overlapping construct, RSV-Rev, expresses the *rev* cDNA. The transfer construct, pSH0-GFP SIN, contains HIV-1 *cis*-acting sequences and an expression cassette for the GFP transgene (reporter). This is the only portion transferred to the target cells (OMK, THP-1 or MDM's) and does not contain wild-type copies of the HIV LTR. The 5' LTR is chimeric, with the enhancer/promoter of RSV replacing the U3 region (RRL) to rescue the transcriptional necessity of Tat. The 3' LTR has an almost complete deletion of the U3 region, which includes the TATA box (from nucleotides -418 to -18 relative to the U3/R border). As the latter is the template used to generate both copies of the LTR in the integrated provirus, transduction of this vector results in transcriptional inactivation of both LTRs; thus, it is a self-inactivating vector (SIN-18). The fourth construct, pCMV-VSV-G encodes a heterologous envelope to pseudotype the vector, here shown coding for Vesicular-Stomatitis-Virus-G-Protein (VSV G). (B) Successful generation of *gag/pol* lenti-viral vectors using the 3rd generation system were confirmed by titration to determine infectivity and titre in OMK target cells under CsA (unrestricted infection) and EtOH (restricted) infection. GFP expression in OMK cells following infection with viruses containing escape mutations and compensatory mutations. Shown is an assessment of the infectivity of clinical isolate derived *gag/pol* ZM1008M, ZM2013F, ZM1781M, ZM1515M, ZM2003M, ZM3576F, ZM2063M, ZM3681F, ZM1123M, ZM3863F and the NL4-3 harbouring mutations in p24 Gag. Titrations determined at 48 hours on day 4 following spinoculation on day 1.

During the course of these washout assays on the particles, including the positive control NL4-3, the capsids were found to be unstable and had already prematurely uncoated at time point 0, as shown by the high expression of GFP at baseline (figure 15). Therefore, the 3rd generation lentiviral packaging system was determined as unsuitable for the CsA washout assay.

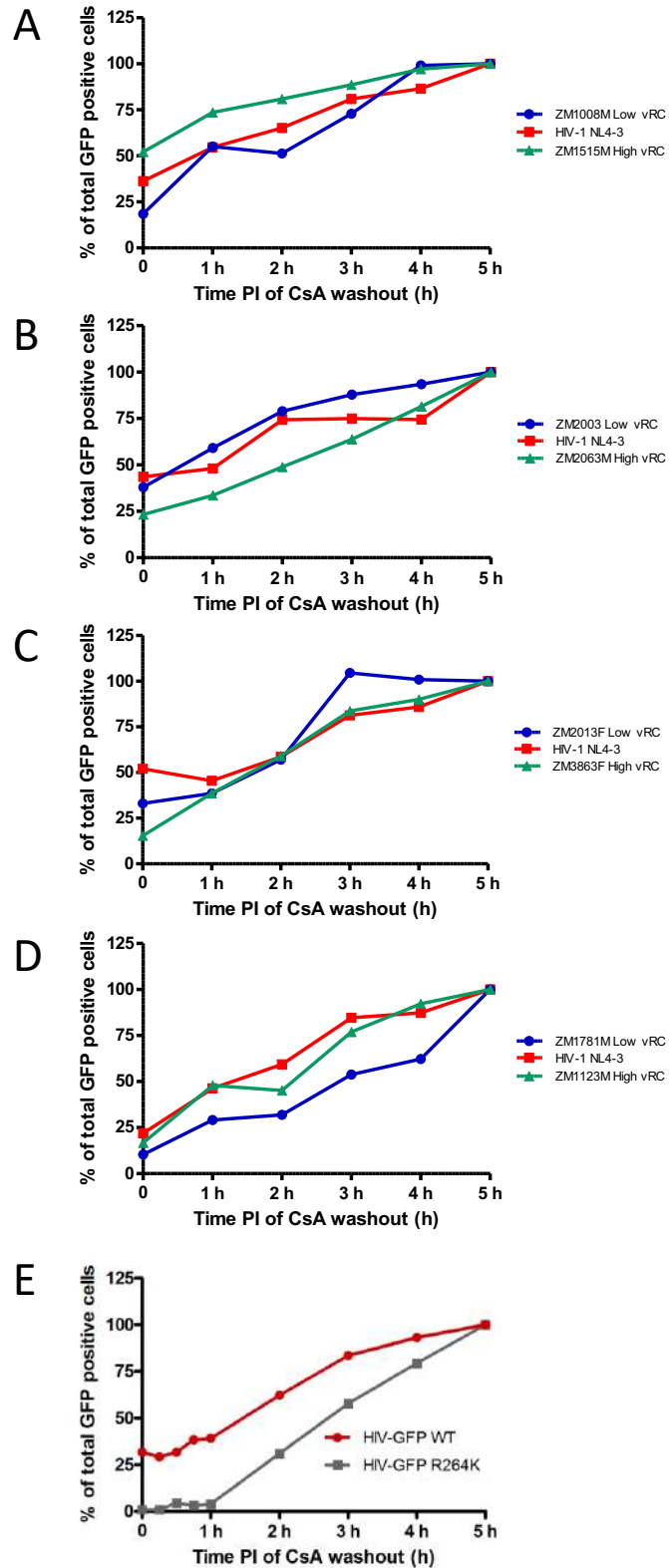


Figure 15 CsA washout assay to determine capsid stability and uncoating kinetics.

GFP⁺ OMK cells following infection with viruses containing escape mutations and compensatory mutations after CsA washout in a time-dependent manner. CsA washout of viruses with increasing amounts of GFP⁺ OMK cells over time. Titrations determined at 48 hours on day 4 following spinoculation on day 1. (A) ZM1008M low VRC vs NL4-3 vs ZM1515M high VRC (B) ZM2003 low VRC vs NL4-3 vs ZM2063M high VRC (C) ZM2013F low VRC vs NL4-3 vs ZM3863F high VRC (D) ZM1781M low VRC vs NL4-3 vs ZM1123M high VRC (E) NL4-3 HIV-1 GFP WT vs NL4-3 HIV-1 GFP R264K.

2.1.6 Titration of NL4-3 *gag/pol* chimeric particles from clinical isolates

Taking in account the results with the 3rd generation lentiviral system, a new approach was necessary to generate LV particles apt for the CsA washout assay. Here, ligation of the *gag/pol* cleans into the pNL4-3 Δ env-eGFP was performed. As described, particle infectivity was determined by titration in the OMK cells. The highest and lowest percentage of GFP⁺ cells corresponded to the highest and lowest viral infectivity rate, respectively (figure 16). Nonetheless, none of the viral clinical isolate's stocks produced reached the required threshold of 40% of GFP⁺ cells (figure 16). These results indicated that the *gag/pol* generated chimeras were extremely attenuated, as the transfection of the all plasmids was performed under exactly the same conditions as the controls and the R264K, R264K plus L268M, S173A plus R264K plus L268Mmutants.

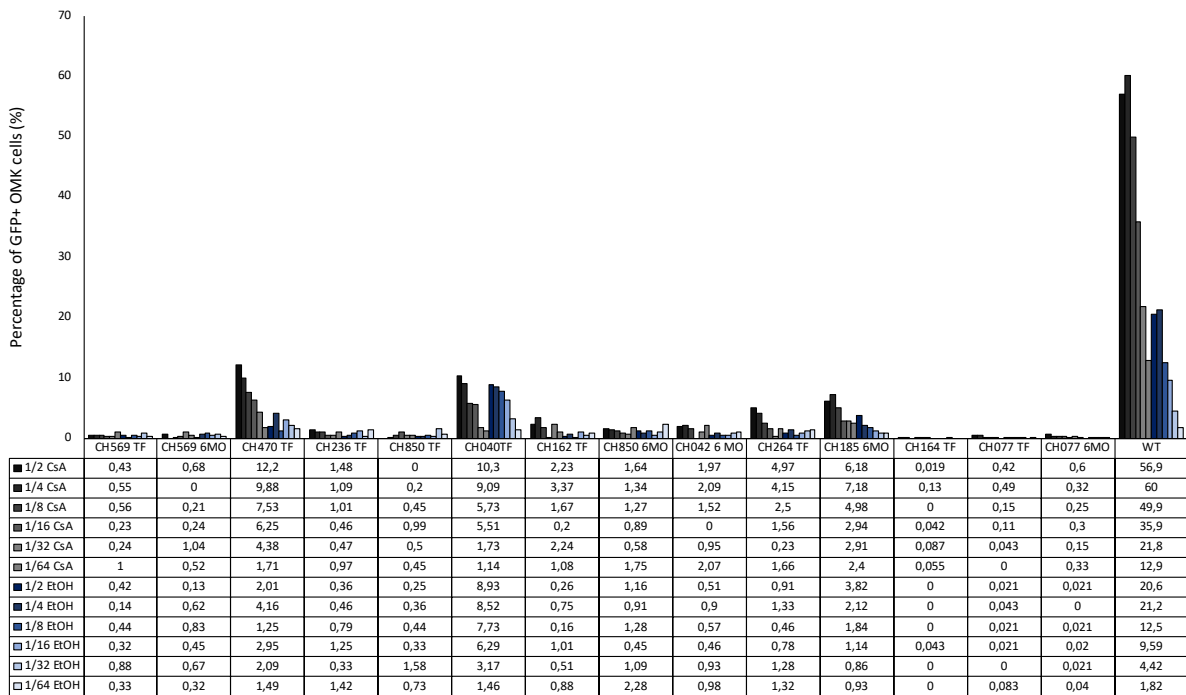


Figure 16 Titration of clinical isolate-derived *gag/pol* gene segments cloned into the pNL4-3-eGFP construct.

Generation of NL4-3 *gag/pol* chimeric particles from clinical isolates were confirmed by titration to determine infectivity and titre in OMK target cells under CsA (unrestricted infection) and EtOH (restricted) infection. Shown is an assessment of the infectivity of clinical isolate derived *gag/pol* CH569TF, CH569 6mo, CH460TF, CH236TF, CH850TF, CH040TF, CH162TF, CH850 6mo, CH042 6mo, CH264 TF, CH185 6mo, CH164TF, CH077TF, CH077 6mo and the NL4-3 harbouring mutations in p24 Gag. Titrations determined at 48 hours on day 4 following spinoculation on day 1.

2.1.7 High through-put production of gag-protease pNL4-3 chimera

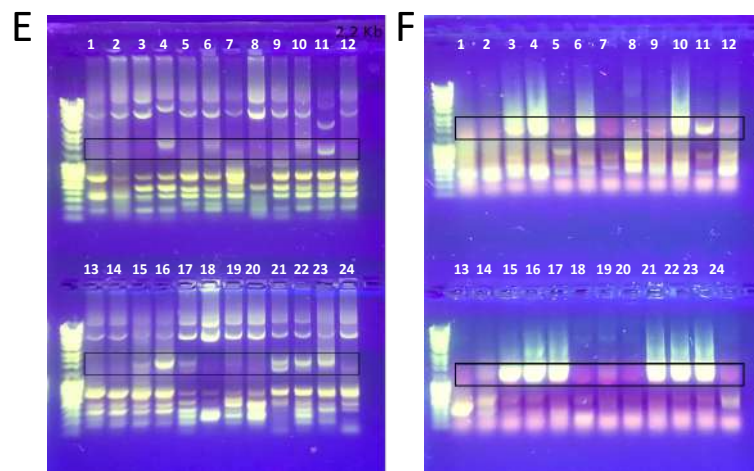
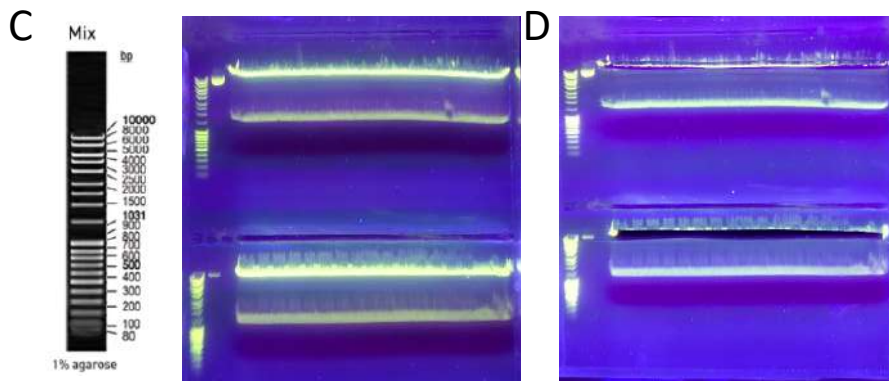
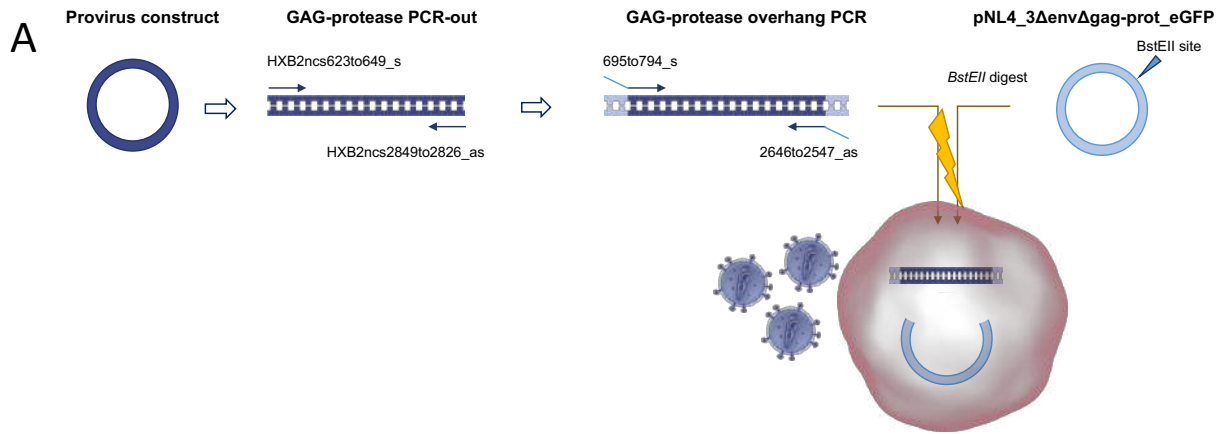
Having established that the 3rd generation lentiviral packaging system was unable to produce suitable viruses for the CsA washout assay and that the second method, where clinical isolate

gag/pol was substituted into an NL4-3 backbone produced very low or no detectable titre's in OMK cells, another approach was required (figure 17. A).

To generate chimeric viruses containing *gag-protease* sequences from clinical isolates, Δ *gag-protease* pNL4-3 was used as a backbone. The plasmid pNL4-3 Δ *gag-protease* is based on the wt plasmid pNL4-3, where the *gag/protease* region was deleted and replaced by a *BstEII* target sequence (described in [257]). First, the plasmid was linearised using the *BstEII* enzyme (figure 17. C & D). A two-step PCR approach was used: i) the first PCR, or PCR out, generated the clinical isolates *gag/protease* inserts from the template proviral DNAs (figure 17. E); ii) the second subsequent nested PCR then generated amplicons with overhangs complementary to the pNL4-3 construct sequence (figure 17. F).

The expected size of the PCR-generated *gag/protease* amplicons was of 2-2.2 kB (figure 17. E & F). Of all 24 clinical isolates that were tested in the first nested PCR reaction to obtain *gag-protease*, only 10 isolates had amplicons within this defined size (L4, CH185 6mo, L6, CH569 6mo, L10, CH264 6mo; L11, CH162 TF, L15, CH058 TF; L16, CH040 TF; L17, CH040 6mo, L21, CH470 TF; L22, CH470 6mo; L23, CH077 TF). On the nested PCR, only 11 isolates had amplicons matching the expected 2kb size (L3, CH185 TF, L4, CH185 6mo, L6, CH569 6mo, L10, CH264 6mo; L11, CH162 TF, L15, CH058 TF; L16, CH040 TF; L17, CH040 6mo, L21, CH470 TF; L22, CH470 6mo; L23, CH077 TF). Of note, since CH185 TF was not amplified in the first PCR reaction and, therefore, was excluded from further analysis. Of the 11 amplicons that were produced in the second nested PCR, only 3 were tested due to the amount of DNA determined by Qubit measurements being too low (L7 CH164 TF, L10, CH264 6mo, L15, CH058 TF).

CH236 TF, CH164 TF, CH164 6mo, CH264 TF, CH 264 6mo and CH058 TF viruses were produced by electroporation of *gag-protease* amplicons and the linearised pNL4-3 Δ *gag-protease* in MT-4 cells, Viral production was measured by determination of the amount of p24 capsid in the supernatant by ELISA from day 2 to 6 (figure 17. G). Only two constructs tested positive for p24 on the ELISA: CH236 TF and CH264 6mo at day 5 post-transfection (figure 17. G). Taken together, it can be concluded by p24 ELISA that virus particles were not produced. In conclusion, further optimisation and development of this assay is required.



G

Days	HIV-1 p24 (pg/mL)					
	CH236 TF CS909	CH164 TF CS914	CH164 6 mo CS915	CH264 TF CS916	CH264 6 mo CS917	CH058 TF CS922
2	0,00	0,00	0,00	0,00	20,05	0,00
3	0,00	0,00	0,00	0,00	21,72	23,80
4	0,00	0,00	0,00	16,20	21,75	0,00
5	48,43	0,00	0,00	0,00	338,42	37,33
6	236,30	50,03	0,00	33,73	0,00	0,00

Dilution	HIV-1 p24 (pg/mL)	
	CH236 TF CS909	CH264 6 mo CS917
1:10	0,00	0,00
1:100	0,00	0,00
1:1000	0,00	0,00
1:10000	0,00	0,00

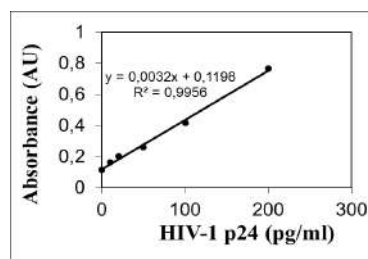


Figure 17 Methodology to develop a high through-put production of gag-protease NL4-3 chimeric viruses.

(A) Schematic drawing of the methodology to produce gag-protease NL4-3 chimeric viruses from proviral clinical isolate constructs using a PCR based amplification protocol. (C) DNA ladder. (C + D) Gel electrophoresis of *BstEII* digested Δ Gag-protease pNL4-3. (E + F) Gel electrophoresis of the PCR using clinical isolate construct and 2nd PCR to produce overhang PCR product of the 1st PCR amplicon. Clinical isolates are labelled as L1, CH236 6mo; L2, CH236 TF; L3, CH185 TF; L4, CH185 6mo; L5, CH569 TF; L6, CH569 6mo; L7, CH164 TF; L8, CH164 6mo; L9, CH264 TF; L10, CH264 6mo; L11, CH162 TF; L12, CH162 6mo; L13, CH042 TF; L14, CH042 6mo; L15, CH058 TF; L16, CH040 TF; L17, CH040 6mo; L18, CH107 TF; L19, CH850 TF; L20, CH850 6mo; L21, CH470 TF; L22, CH470 6mo; L23, CH077 TF; L24, CH077 6mo. (G) p24 ELISA results of selected isolates, in bold are transmission pairs. All p24 ELISAs were normalised to the standard curve of HIV-1 p24. Colour key: Red – negative for p24; Yellow – low amount of detectable p24; Green – p24 detectable above the limit of detection (out of range).

2.2 Investigations into innate sensing and restriction of HIV-1 capsid mutants

The second objective in this study was to determine whether the two HLA-B27-restricted CTL escape mutations R264K (RK) and R264K plus L268M (RK plus LM) in p24 Gag and the compensatory mutation S173A (SA plus RK plus LM) influence the sensitivity of HIV-1 to IFN α 2a-induced restriction. HLA-B27⁺ “Elite Controllers” have been suggested to control HIV-1 through specific cytotoxic T-cells (CTL), which exert immune selection pressure on HIV-1 resulting in CTL-escape mutations. Better control of viremia in these patients is associated with mutations in p24 capsid. Type1 interferons (IFNs), including IFN α 2a, upregulate cellular innate sensors, with some acting as host restriction factors in CD4⁺ T cells, such as Cyclophilin A (Cyp A)[262]. HIV-1 strains have shown to differ in their sensitivity to IFN α 2a-mediated restriction, although viral replication is impaired[263]. CypA has been shown to affect intracellular HIV-1 with opposing effects: although CypA facilitates infection by mediating timely uncoating of the capsid acting as an intracellular sensor and cofactor for restriction factors[264]. The interactions of HIV-1 carrying CTL-escape mutations and CypA were further investigated in this thesis.

To achieve the goal, the mutations naturally occurring in p24 gag were studied by introducing point mutations in p24 gag of the NL4-3 laboratory strain. These mutations were R264K, R264K plus L268M and S173A R264K plus L268M.

2.2.1 Viral fitness is highly affected by p24 escape mutations

As already shown previously for other mutations[265], the viral fitness of HIV-1 might be highly affected by the CTL escape mutations R264K, R264K plus L268M and S173A plus R264K plus L268M in p24 gag. I infected MDMs with the different produced viruses in one donor and measured the rate of infection and the production of Gag, TNF- α and IL-10 mRNA

transcripts. The WT virus induced infection rates of MDMs at 11% for and reduced infection rates for R264K and R264K plus L268M at 1.83% and 3.77%, respectively (figure 18. A). The compensatory mutation S173A plus R264K plus L268M rescued the effect of the R264K and R264K plus L268M escape mutations and increased infection levels higher than the WT to 18.3% (figure 18. A). Next, I sought to confirm these results by measuring by real-time PCR the levels of p24 gag transcript and the levels of antiviral factors of TNF- α and IL-10 transcripts at 48 hours and 72 hours post-infection. At 48 hours, gag transcripts for the WT mutant were approximately 1000-fold greater than the escape mutants R264K and R264K plus L268M. The level of gag transcript was approximately 70,000-fold greater than these escape mutants and 69,000 fold greater than the WT in MDMs at 48 hours. At 72 hours, the transcript levels of gag on the escape mutations increased for the R264K and R264K plus L268M mutants at 500 and 1500-fold, respectively while it decreased slightly for WT and the compensatory mutant. Taken together these results suggest that the escape mutants R264K and R264K plus L268M are less fit in avoiding host immunity compared to WT and the compensatory mutants S173A plus R264K plus L268M. However, further experiments are needed to determine the viral fitness of these escape mutants.

The pro-inflammatory gene TNF- α was measured at 48 hours and 72 hours. The R264K and the R264K plus L268M mutants increased TNF- α gene expression 40 and 10-fold greater than the WT, respectively. The compensatory mutant increased transcript levels only slightly to 4-fold induction of gene expression. At 72 hours, the levels of transcript decreased as anti-viral effector genes were upregulated as seen for the fold induction of anti-inflammatory IL-10 gene. At 48 hours, the WT and viral mutants induced a low level of IL-10 transcript, however, at 72 hours the greatest effect was measured. The WT induced gene expression approximately 5-fold greater than basal levels. The escape mutants R264K and R264K plus L268M increased transcript levels 15- and 17-fold greater than basal levels, respectively. Interestingly, the compensatory mutant increased transcript levels 10-fold.

Repeated measurements were made with two more donors x (D anon x) and z (D anon z), for the change in the rate of infection of the p24 capsid mutants. Infection levels varied between donors and the maximum infection rate achieved was 53.5% (figure 19). The infection rate was tested in this one donor, donor z using only the WT virus was measured against unstained and LPS stimulated MDMs at 0 and 24 hours post-infection and stimulation. The basal level of uninfected cells that are the LPS stimulated and uninfected MDMs was approximately 10%.

Upon virus infection an approximate level of 6% infection occurred and at 24 hours an estimated number of totally infected cells subtracting background was 37.1%. Altogether, these data show high infection levels can be achieved, however, donor variation plays an important role in sensing and restriction. In order to further establish the MDM infection, p24 escape mutations R264K and R264K plus L268M were tested for their ability to induce Gag, TNF- α and IL-10 mRNA transcripts and for the production of TNF- α , IL-10 and IL-1 β protein.

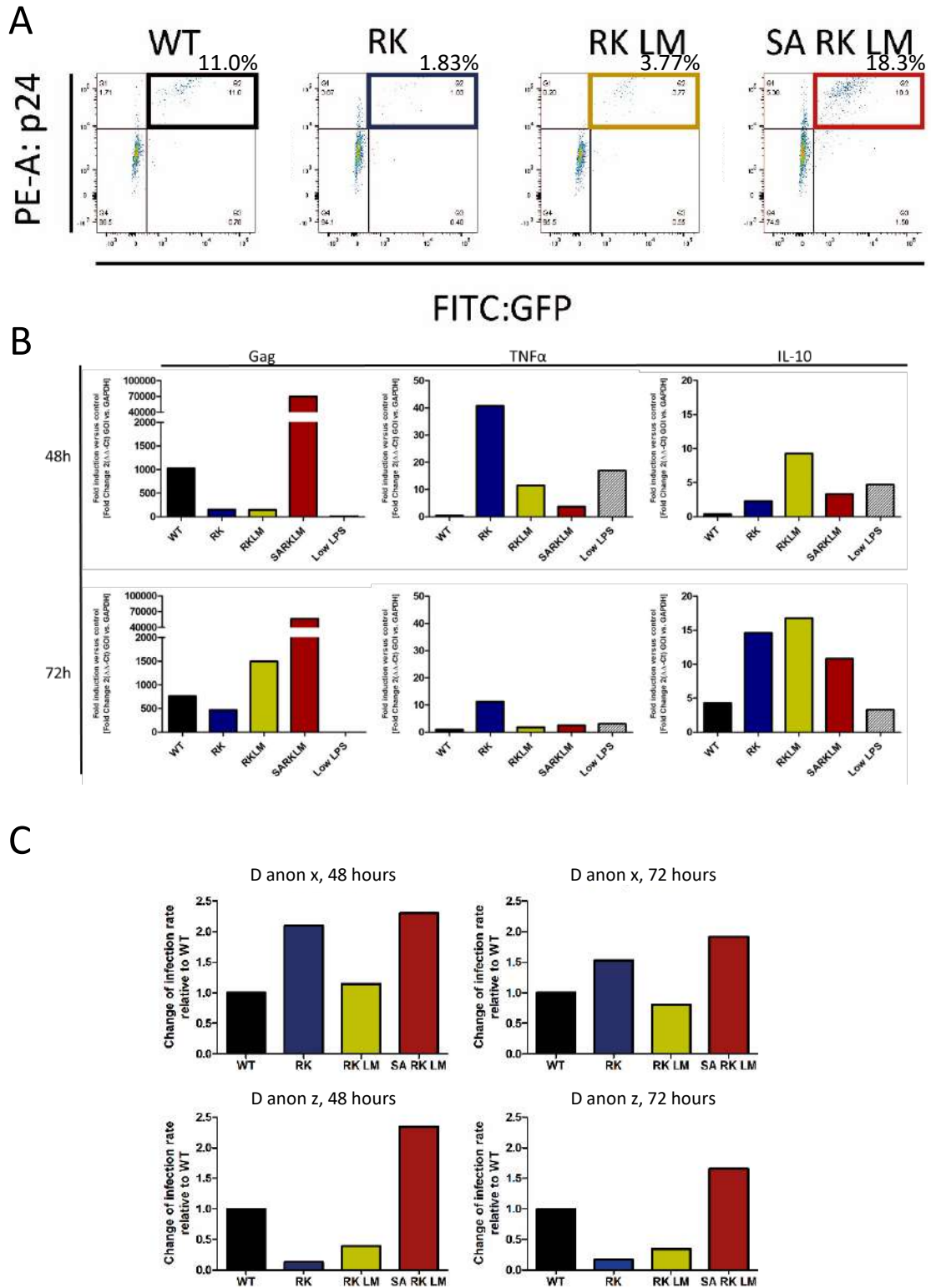


Figure 18 Viral fitness is highly affected by p24 escape mutations.

Infection rates of the wildtype HIV-1 (WT) and the respective mutations as seen in HLA B27+ individuals in human MDMs (n=3). CTL escape mutations (R264K and R264K plus L268M) have a huge impact on viral fitness, which is ameliorated by the compensatory mutation (S173A plus R264K plus L268M) A) Infectious titre of HIV-1 capsid mutants determined by p24 staining in MDM's using flow cytometry. B) Gene expression data showing the fold change in Gag, TNF- α and IL-10 RNA transcript determined by real time PCR at 48h and 72h post-infection. C) D anon represents anonymised donor x and z. Plotted is the fold change of the rate of infection of the capsid mutants R264K, R264K plus L268M and S173A plus R264K plus L268M relative to WT.

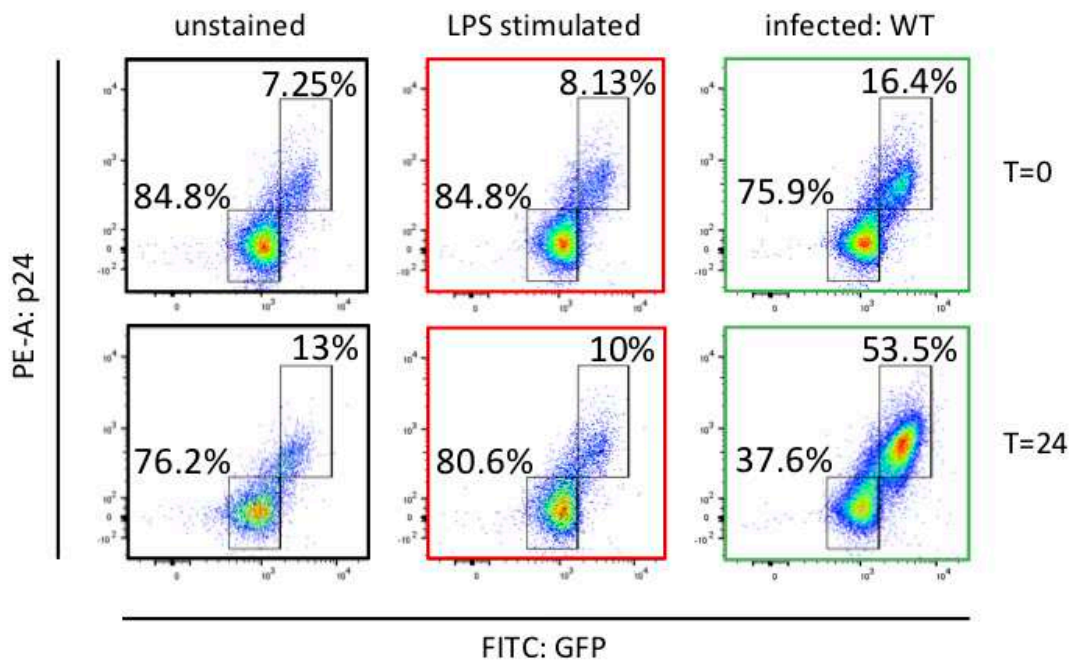


Figure 19 MDM cells can achieve high infection rates.

Each dot represents one cell. The cell density is represented by a colour code. Blue dots show low density, whereas red dots illustrate a high cell density. The gate that defines the selected population is highlighted with by a black coloured frame. Infected populations are represented by a shift to the top right quadrant. Uninfected cells are represented in the bottom left quadrant. FACs plot key: Black outline – unstained MDM cells; Red outline – LPS stimulated MDMs; Green – infected with WT NL4-3 strain.

2.2.2 p24 escape mutations R264K and R264K plus L268M do not increase the number of infected MDM cells

Isolated monocytes from 6 different donors were stimulated with GM-CSF, to induce polarization towards M2-type MDMs, and were infected with WT, R264K, R264K plus L268M and S173A plus R264K plus L268M HIV-1 viruses. Spinfection was not performed to allow a more natural infection to take place, recapitulating the normal human host environment. Infection rates were determined by FACs analysis and overall for all donors tested the infection rates remained below 10% (figure 20). As a control for TNF- α production, MDMs were stimulated with LPS and measured alongside untransduced MDM cells.

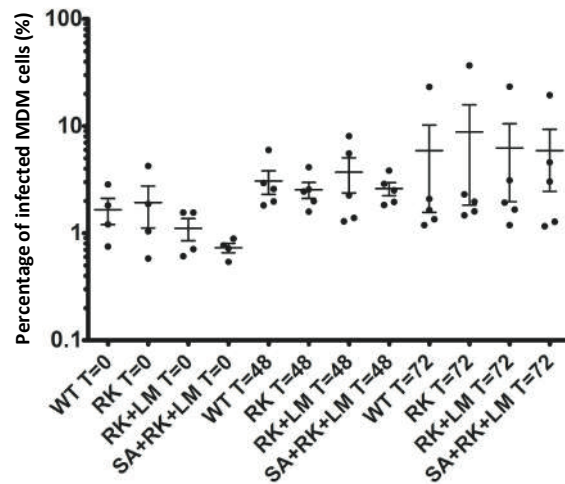


Figure 20 Percentage of infected MDM cells overtime.

The percentage of infected MDM cells (%) are plotted against the NL4-3 WT, escape mutants R264K and R264K plus L268M and the compensatory mutant S173A plus R264K plus L268M at time points during infection of 0, 48 and 72 hours. Donors plotted at 0 hours equals 4 and at 48 and 72 hours equals 5.

The mRNA expression levels of gag, IL-1 β , TNF- α and IL-10 were measured by real-time PCR and the protein expression of secreted TNF- α , IL-10 and IL-1 β by ELISA. At 48 and 72 hours, for the escape mutations R264K and R264K plus L268M a lower gag transcript was detected compared to the wild type and on the contrary the compensatory mutant S173A plus R264K plus L268M had a higher level of transcript compared to the wild type (figure 21. A & B). However, the difference did not reach statistical significance. At 72 hours post-infection, the compensatory S173A plus R264K plus L268M mutant induced the production of IL-1 β mRNA transcript (figure 21. C & D). Interestingly, at 48 and 72 hours, the escape mutants caused a decreased induction of TNF- α transcript (figure 21. E & F). All viruses except for the R264K mutant were able to induce high levels of IL-10 mRNA transcript production, similar to the ones induced by LPS stimulation (figure 21. G & F).

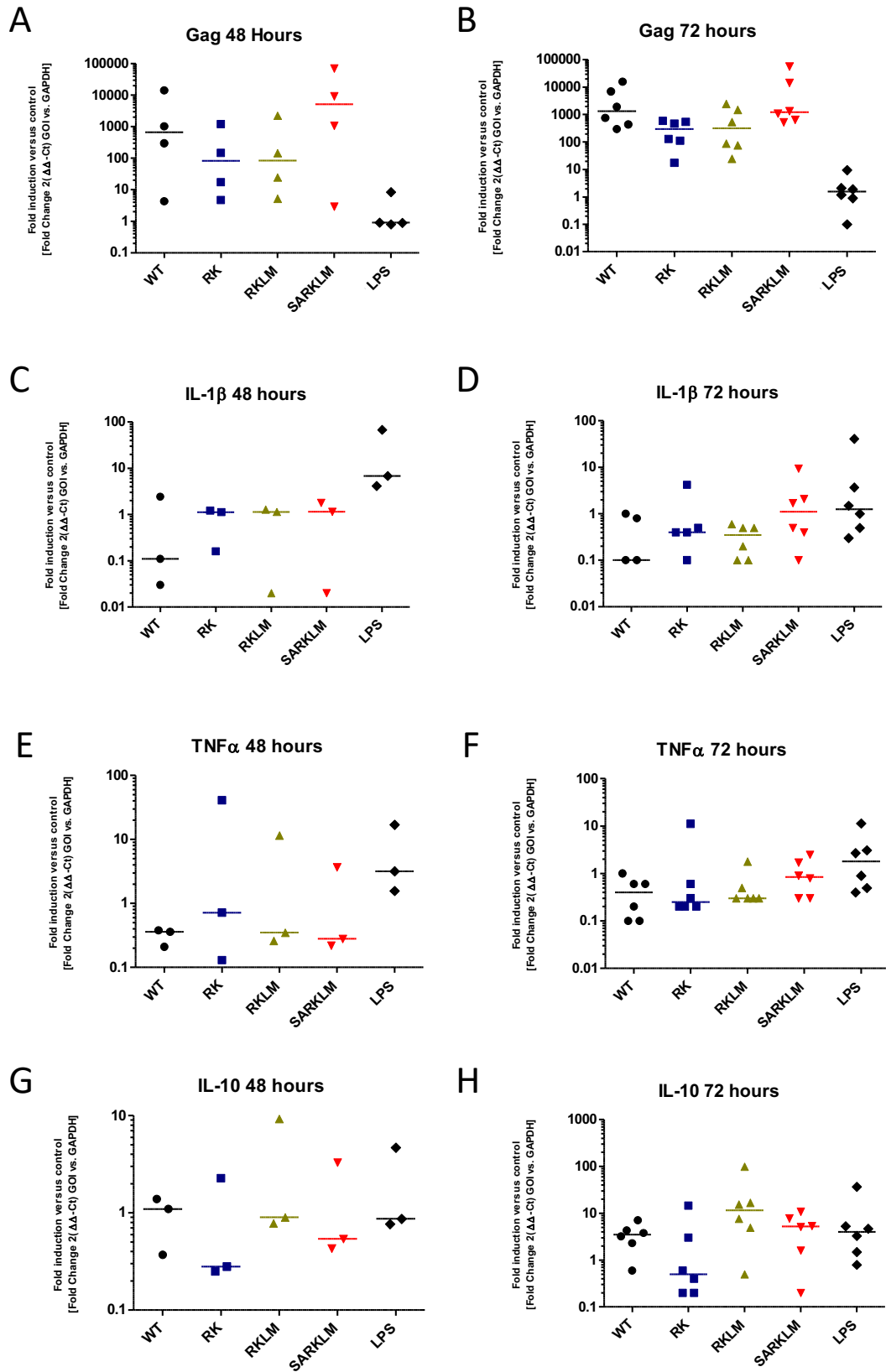


Figure 21 Real-time PCR reveals infection kinetics at 48 and 72 hours.

(A + B) Gag transcript at 48 and 72 hours. (C+D) IL-1 β transcript at 48 and 72 hours. (E+F) TNF- α transcript at 48 and 72 hours. (G+H) IL-10 at 48 and 72 hours. Fold induction was normalised to the 0-hour time point. Shown are the median values.

TNF- α production was measured from the supernatants of 3 donors for which enough media was retrieved to obtain reliable measurements. At time point 0 hours, the MDM cells for each donor were already producing TNF- α , indicating activation (figure 22. A). The levels of TNF- α production reduced during the course of time from 0 hours to 72 hours (figure 22. A). Once values were normalized to time point 0, the production of TNF- α was reduced at 48h and 72h by 15 to 20% for the escape mutations R264K and R264K plus L268M, respectively (figure 22. B & C).

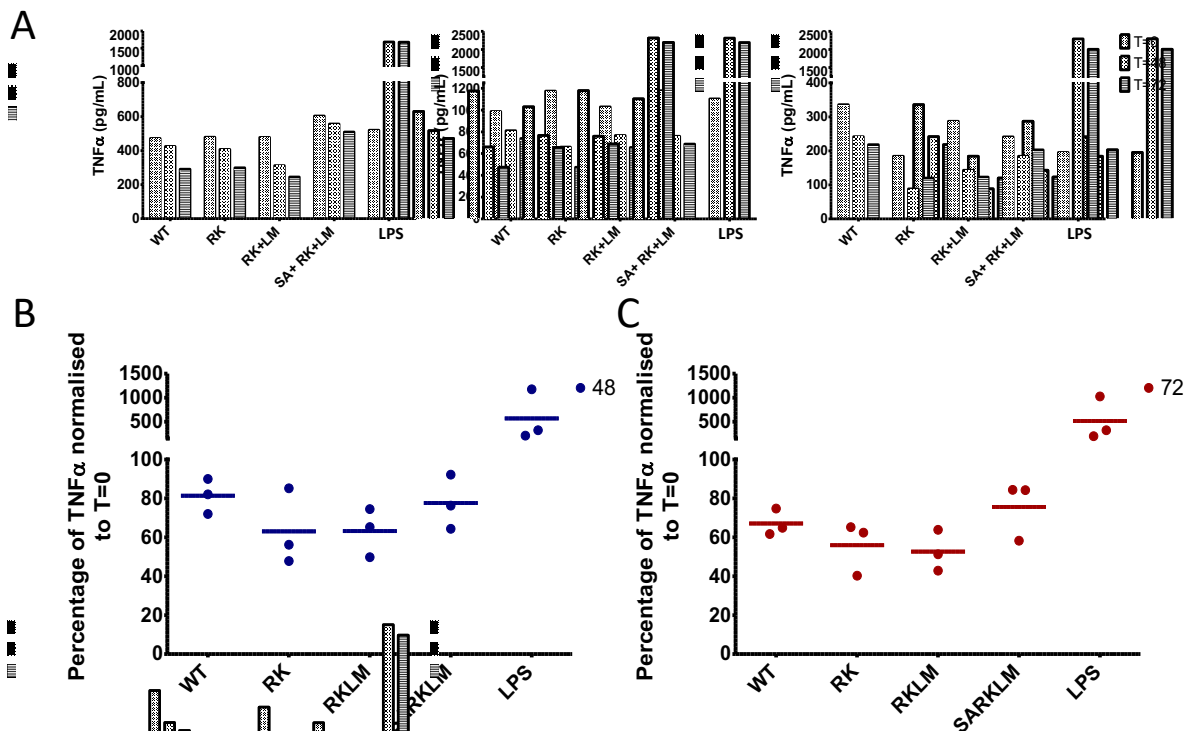


Figure 22 TNF- α produced upon HIV-1 viral infection.

ELISA for TNF- α production upon infection of NL4-3, escape mutants R264K and R264K plus L268M and compensatory mutant S173A plus R264K plus L268M. (A) represents donor MDM variation (n=3) and (B+C) donor MDM production of TNF- α at 48 (blue) and 72 (red) hours normalised to time point 0.

The quantification of secreted IL-10 and IL-1 β in the cell supernatant was performed by specific ELISAs (figure 23 and 24). At 48 hours post-infection, a tendency towards an increased IL-10 production in the S173A plus R264K plus L268M virus was observed for 4 out of 7 donors (figure 23). Except for one donor, the WT, R264K, R264K plus L268M viruses had a decreased IL-10 production compared to the S173A plus R264K plus L268M virus (figure 23). The pattern for IL-1 β protein secretion was variable among the 7 donors: 2 donors (A and B) had no detectable IL-1 β in any of the viral infection conditions (figure 24); S173A plus R264K plus L268M had a lower production of IL-1 β in 2 donors C and D; no differences were observed in the rest of the donors. As a control, LPS stimulation donor resulted in IL-10 production in 6 out

of 7 donors, (figure 24) and all 7 donors produced IL-1 β (figure 24). Altogether, escape mutations do not increase the sensitivity of IFN α 2a induced restriction as the level of TNF- α transcript and TNF- α protein is not increased more than the WT and compensatory S173A plus R264K plus L268M mutant. These data suggest that the escape mutants do not increase innate immune sensing upon infection in MDM cells.

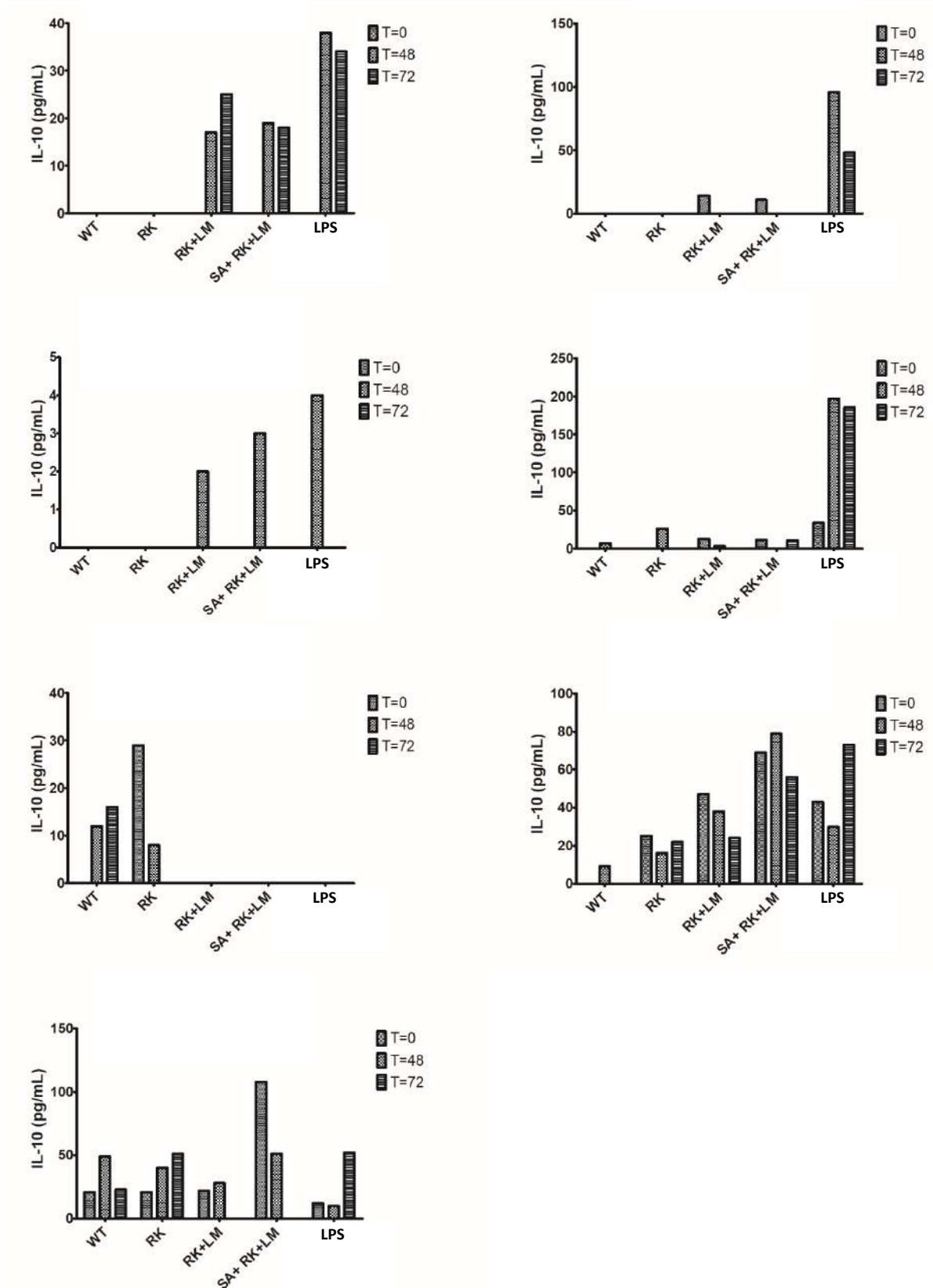


Figure 23 IL-10 ELISA reporting donor variation in detection overtime.

Supernatant collected at 0, 48- and 72-hours intervals for the validation of IL-10 production from 5 donor MDM experiments.

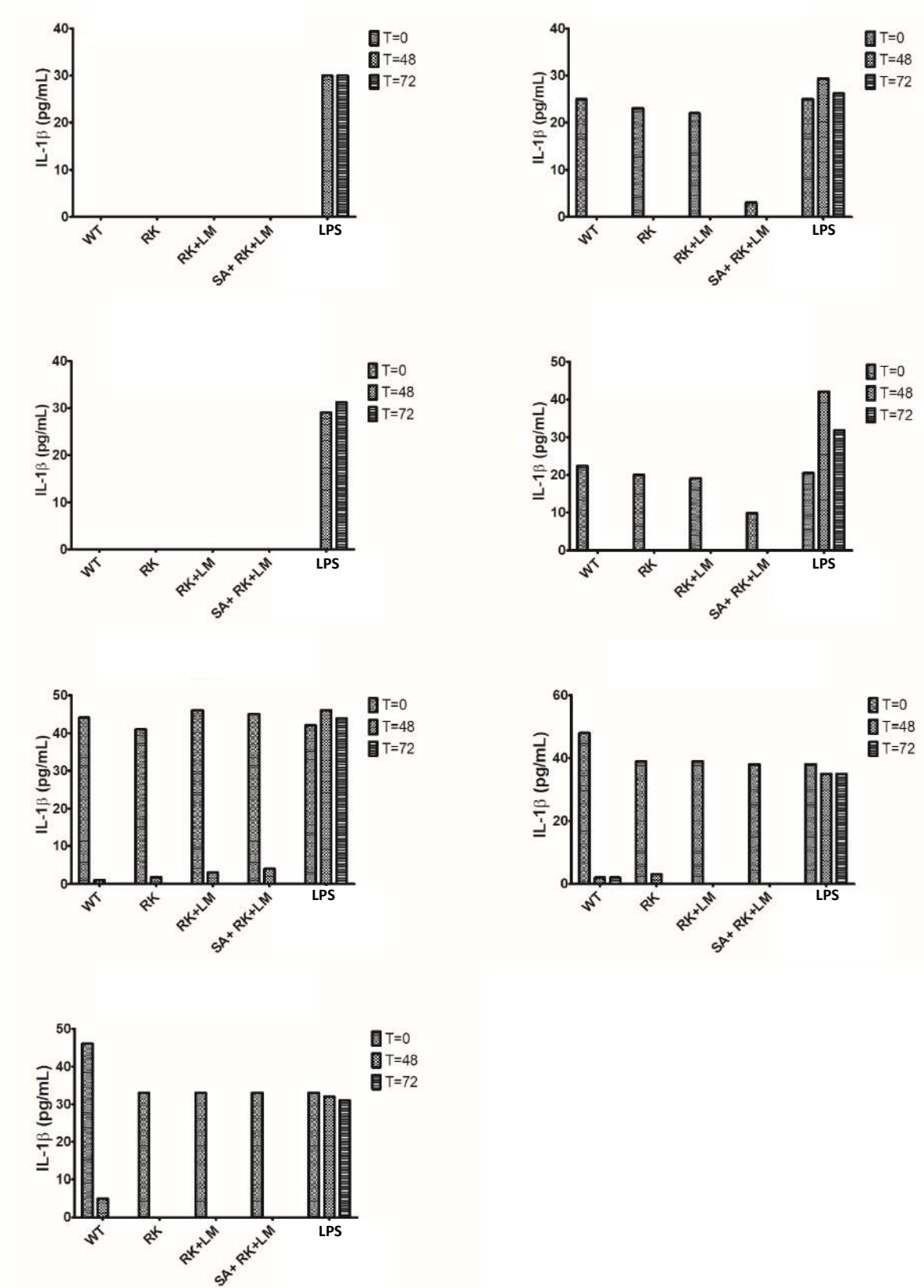


Figure 24 IL-1 β ELISA reporting donor variation in detection overtime.

Supernatant collected at 0, 48- and 72-hours intervals for the validation of IL-1 β production from 5 donor MDM experiments.

2.2.3 MDM cells respond to HIV-1 infection/LPS activation

As HIV-1 infection triggered TNF- α , IL-10 and IL-1 β production to different levels, I sought to determine if any differences on the MDM activation levels were observable between the virus mutants. To determine the activation status of infected MDM cells the activation markers CD69, CD80, CD83 and CD86 were measured by flow cytometry. The cell surface molecules are expressed on the cell surface to trigger immune activation in neighbouring cells[266]. While MDMs infected with the WT and S173A plus R264K plus L268M viruses decreased the expression of CD69 and CD80 at 48 and 72 hours post-infection, the escape mutants R264K and R264K plus L268M increased the expression of these two molecules on the cell surface of MDM cells in the 5 donors used in these experiments (figure 25 & 26). The escape mutant R264K plus L268M increased CD69 at 48 hours and then recovered at 72 hours. The R264K and R264K plus L268M mutant both increased CD69 expression at 48 hours, which recovered at 72 hours. The capsid escape mutants were less infectious compared to the WT and the S173A plus R264K plus L268M compensatory mutant determined by percentage of infected MDM cells by flow cytometry.

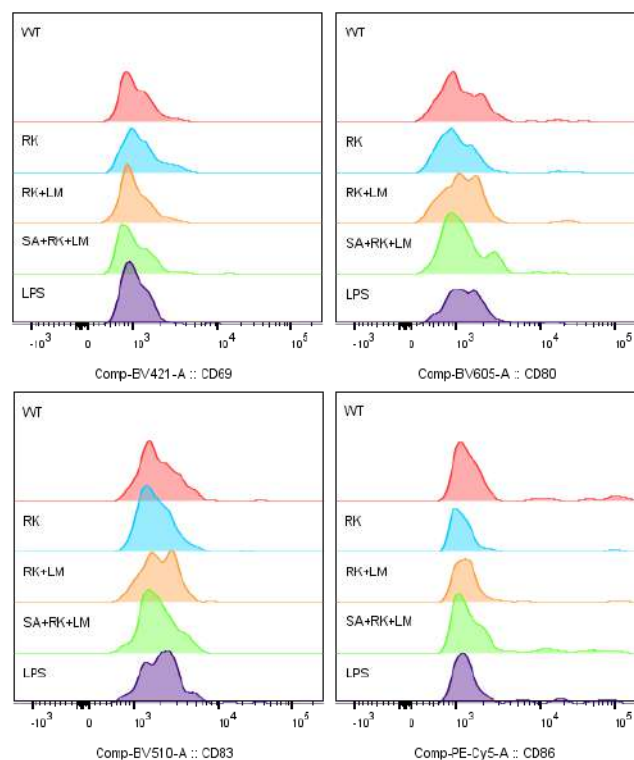


Figure 25 Activation and stimulation of MDM cells overtime.

Flow cytometry plots of cell surface activation markers CD69, CD80, CD83 and CD86 expressed on MDM cells. Shown are WT, escape mutants R264K and R264K plus L268M and the compensatory mutant S173A plus R264K plus L268M. The charts are representative of the 5 donors used in this study.

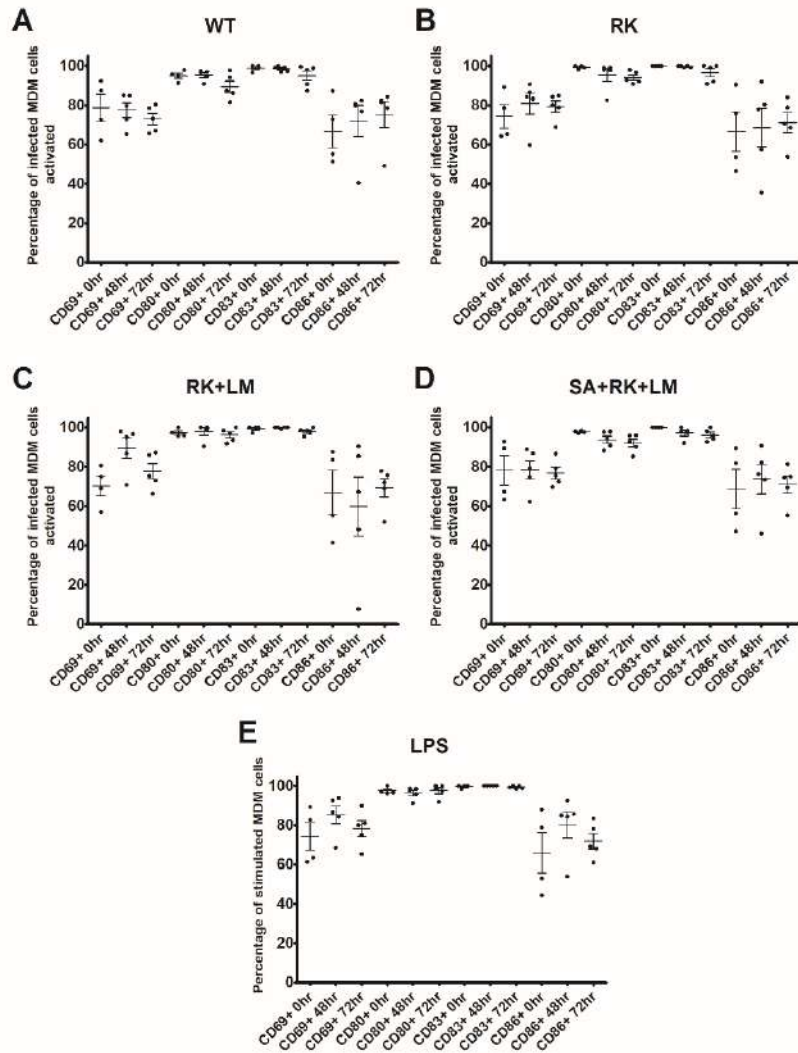


Figure 26 Activation and stimulation of MDM cells overtime.

(A to D) Represents the percentage of infected MDM cells activated against CD69+, CD80+, CD83+, CD86+ expressing MDM cells under infection of (A) WT, (B+C) escape mutants R264K and R264K plus L268M and (D) the compensatory S173A plus R264K plus L268M capsid mutant viruses. (E) Represents the percentage of LPS stimulated MDM cells against CD69+, CD80+, CD83+, CD86+ cell surface expression markers. Number of donors plotted are between 4 to 5 from these experiments.

Altogether, the data suggested that donor variation impacted the level of infection in the MDM cells and their activation status.

2.2.4 Mutations in HIV-1 are dependent on CypA

Human CypA is encoded by peptidyl prolyl isomerase A gene (*PPIA*) and enhances HIV-1 replication by aiding capsid uncoating[267]. The association of genetic variations in the *PPIA* regulatory region with susceptibility to HIV-1 infection, disease progression, and gene expression among individuals at risk for infection or infected with HIV-1 is yet still unknown.

As CypA has shown to be involved in HIV-1 replication and capsid uncoating, I analysed if CypA competitively antagonises innate sensors of the HIV-1 capsid such as MX2 and TRIM5 α . MX2 is an interferon-induced post-entry inhibitor of HIV-1 and TRIM5 α is an interferon-stimulated gene (ISG) that restricts capsid. This would cause HIV-1 virus infection to be abolished upon increasing concentrations of IFN α 2a stimulation. In order to reject the Null hypothesis that CypA protects the HIV-1 capsid allowing infection, several knock out (KOs) mutants were generated using Crispr/Cas9 constructs targeting exon regions of CypA, MX2 and TRIM5 α . Successful KO of CypA, MX2 and the CypA/MX2 were confirmed by western blotting (figure 27). However, unexpectedly, knock down of TRIM5 α increased protein expression instead of depleting it and therefore, this cell line was eliminated from the IFN α 2a sensitivity assay. This may be caused by off-target mutations introduced by the single guide RNA enhancing the expression of TRIM5 α . The IFN α 2a sensitivity assay revealed upon increasing IFN α 2a concentration the extent to which HIV-1 harbouring point mutations in p24 capsid would be sensitive to restriction by IFN α 2a-mediated innate sensors.

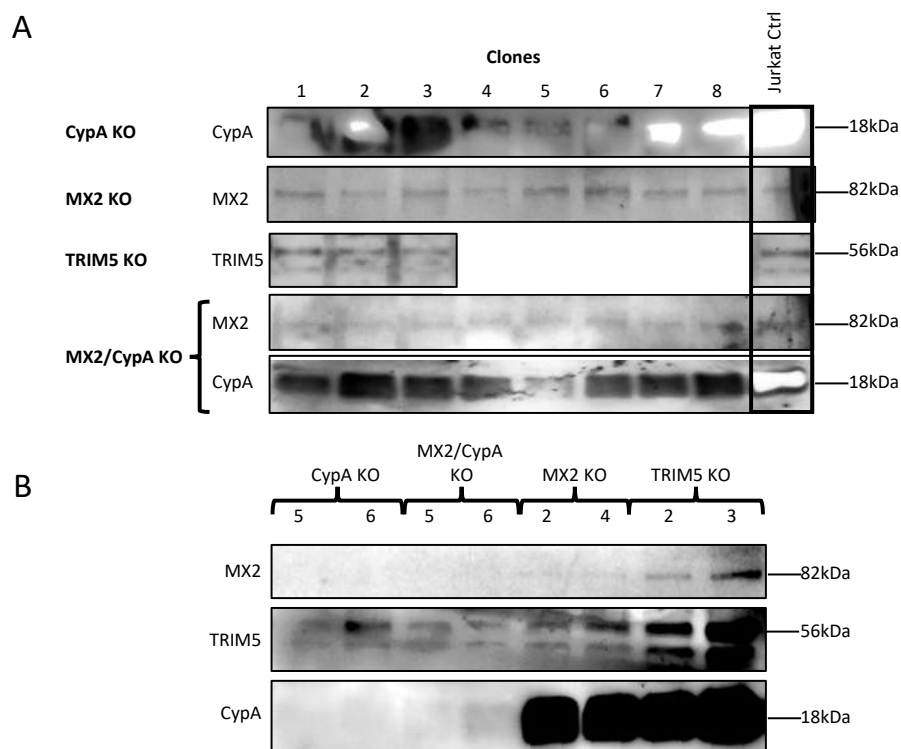


Figure 27 Immunoblot analysis of CypA, MX2, TRIM5 and MX2 plus CypA CRISPR targeted Jurkat T cells.

Human Jurkat T cells were transfected with gRNA constructs targeting exon 1 of *Ppia*, *mx2*, *trim5* and *mx2* plus *Ppia*. (A) After 8 passages of puromycin selection, cell lysates were prepared. (B) After 10 passages of puromycin selection, cell lysates were prepared from clones that showed the strongest knock down. Lysates were run on a 10 % SDS-PAGE. Proteins were transferred to nitrocellulose and identified using antibodies against CypA, MX2, TRIM5 respectively to detect immunosignals.

Capsid mutants were assessed for their IFN α 2a sensitivity by plotting best-fit inhibition curves of respectively mutated HIV-1 versus WT in Jurkat cells and Jurkat CypA $^{-/-}$ or Jurkat MX2 $^{-/-}$ or Jurkat CypA/Mx2 $^{-/-}$ cells at 48h post infection (figure 28). This experiment represents an n. of 1. In IFN α 2a-stimulated Jurkat cells, WT virus infection rates were reduced to 14%. In contrast, increasing concentrations of IFN- α reduced the HIV-1 WT virus infection rates to 59% in Jurkat Mx2 $^{-/-}$ cells and abrogated infection in Jurkat CypA $^{-/-}$ cells and Jurkat CypA/Mx2 $^{-/-}$ cells (0% and 1% respectively) (figure 28). In contrast, the virus capsid mutants and the compensatory mutant were inhibited by IFN α 2a-exposure to different extents (RK: 42%; R264K plus L268M: 30%, S173A R264K plus L268M: 66%) in Jurkat WT cells. Addition of the compensatory S173A mutation (S173A plus R264K plus L268M) reconstituted IFN α 2a sensitivity (figure 28. A). However, the HIV-1 S173A plus R264K plus L268M virus was completely restricted by IFN α 2a-mediated inhibition in Jurkats CypA $^{-/-}$ cells to undetectable levels (figure 28. D).

HIV-1 harbouring escape mutations were in general less CypA- dependent in the Jurkat cell model (figure 28 A). IFN- α -sensitivity of HIV-1 WT in Jurkat Mx2 $^{-/-}$ was reconstituted when compared to Jurkat WT cells and Jurkat CypA/Mx2 $^{-/-}$ cells (figure 28 B & C). Altogether, these data suggested that MX2 and CypA competitively antagonise the HIV-1 WT virus. CypA and MX2 capsid interactions might enable HIV-1 WT and HIV-1 S173A plus R264K plus L268M viruses to evade IFN α 2a-induced restriction factors. However, additional experiments are needed to confirm these observations.

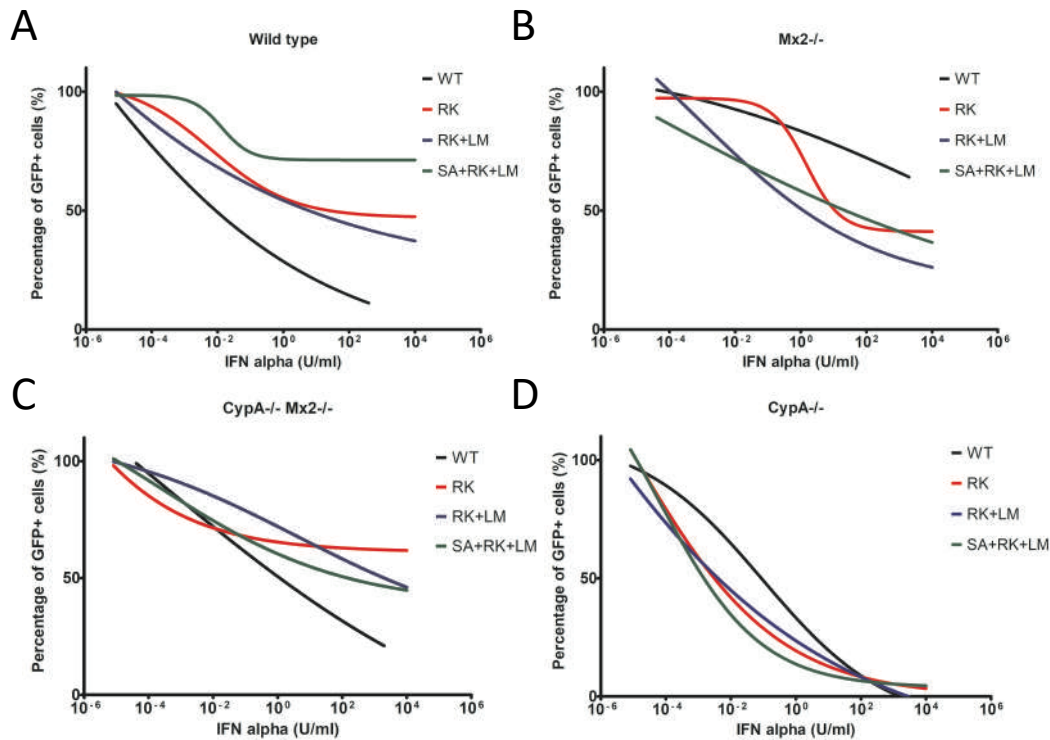


Figure 28 CTL escape mutations render HIV to be more sensitive to $IFN\alpha$ mediated.

WT Jurkat cells vs NL4-3 (14%) and escape mutants (RK: 42%; R264K plus L268M: 31%) and compensatory mutant (S173A plus R264K plus L268M: 66%). $MX2^{-/-}$ Jurkat cells vs NL4-3 (59%) and escape mutants (RK: 33%; R264K plus L268M: 23%) and compensatory mutant (S173A plus R264K plus L268M: 37%). $CypA^{-/-}$ plus $MX2^{-/-}$ Jurkat cells vs NL4-3 (19%) and escape mutants (RK: 61%; R264K plus L268M: 46%) and compensatory mutant (S173A plus R264K plus L268M: 46%). $CypA^{-/-}$ Jurkat cells vs NL4-3 (0%) and escape mutants (RK: 0%; R264K plus L268M: 0%) and compensatory mutant (S173A plus R264K plus L268M: 0%). Infection rates were determined 48 hours post infection.

2.2.5 Jurkat cells respond to $IFN\alpha_2a$ –stimulation and regulate a stronger transcriptional upregulation of $IFN\alpha_2a$ –regulated genes compared to Jurkat $CypA^{-/-}$

Due to the observed differences in $IFN\alpha_2a$ sensitivity exhibited by the WT and capsid mutants, the next experiments were conducted to study the role of CypA in transcriptional regulation. The transcriptomic profile of Jurkat WT (wild type) and Jurkat $CypA^{-/-}$ cells was compared. Both the Jurkat cells and the Jurkat $CypA^{-/-}$ cells responded to $IFN\alpha_2a$ stimulation at an increasing concentration of $IFN\alpha_2a$, as determined by immunoblotting of MX2 (figure 29. A). The protein level of the 82 kDa MX2 protein had a stronger signal in the WT Jurkat cell line than in the Jurkat $CypA^{-/-}$ cell line. By having confirmed at the protein level a clear response to $IFN\alpha_2a$ stimulation, both cell lines were then assessed at the transcriptional level by real-time PCR of interferon–stimulated genes IFITN13, Ly6E, ISG15, OAS3, EPSTI1, MX2 and capsid restriction factors CypA and TRIM5 α . A differential fold induction was observed

between the two cells lines indicating altered transcriptionally regulation: MX2 and EPSTI1 were strongly induced by IFN α 2a-stimulation, however, to a lesser extent in Jurkat CypA $^{-/-}$ cells (figure 29. B). On the contrary, ISG15 is induced by IFN α 2a-stimulation to a greater extent in CypA $^{-/-}$ cells (figure 29. B). Taken together, these data suggest that global gene expression is differentially regulated in the CypA $^{-/-}$ Jurkat cells upon IFN α 2a stimulation.

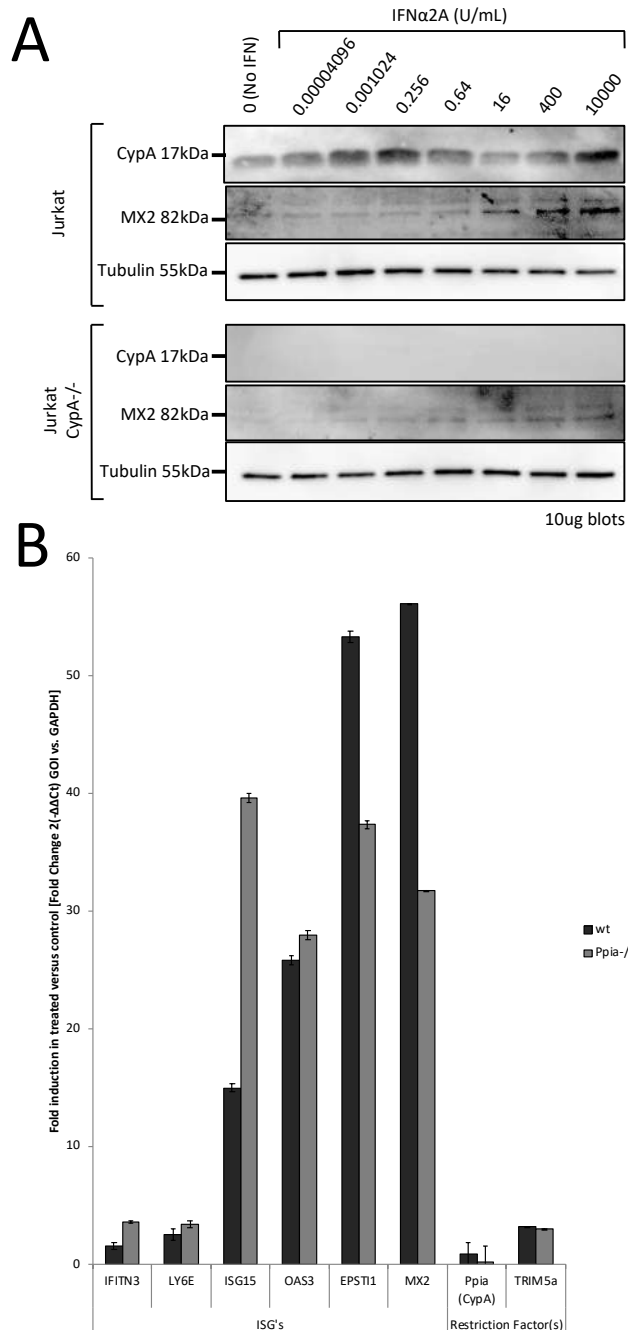


Figure 29 Immunoblots of CypA and MX2 and real-time PCR of ISG's.

Human Jurkat T cells were stimulated with IFN α 2a for immunoblotting and real-time PCR analysis (A) Lysates of Jurkat cells and Jurkat CypA $^{-/-}$ cells were run on a 10 % SDS-PAGE. Proteins were transferred to nitrocellulose and identified using antibodies against CypA, MX2, Tubulin. (B) RNA preparation from TRIzol of Jurkat and Jurkat CypA $^{-/-}$ cells was performed for real-time PCR analysis. Error bars represent SD ($n=3$).

2.2.6 Transcriptional analysis of Jurkat and Jurkat CypA^{-/-} reveals differential regulation

As the Jurkat CypA^{-/-} cells elicited a lower IFN α 2a –mediated response compared to Jurkat cells, I aimed to investigate if CypA was involved in the maintenance of the cellular transcriptional control and homeostasis. To that end, Fluidigm single cell analysis was performed. A total of 96 primer pairs targeting a panel of T cell genes were run on amplified cDNA prepared from single Jurkat and Jurkat CypA^{-/-} cells. Under unstimulated conditions, the expression of CD40LG was not existent in the Jurkat CypA^{-/-} cells and two populations of Jurkat were detected (figure 30. A). CD40LG co-stimulates T-cell proliferation and enhances the production of IL-4 and IL-10 in conjunction with the TCR/CD3 ligation and CD28 co-stimulation. Similarly, the chemokine receptor CCR8 and the transcription factor Bcl-6 were not detectable in Jurkat CypA^{-/-} cells and a mixture of two populations was present in Jurkat cells (figure 30. A). Bcl6 is the master transcription factor for Tfh cell development and CCR8 regulates Th2 responses to drive immune suppression. Loss of these molecules resulted in an altered phenotype of these Jurkat CypA^{-/-} cells. In conclusion, the results showed that Jurkat CypA^{-/-} cells suppressed the mRNA transcription of certain immunomodulatory genes, while on the contrary the Jurkat cell line had a greater dynamic range in gene expression represented by the change in colour intensity (figure 30. B).

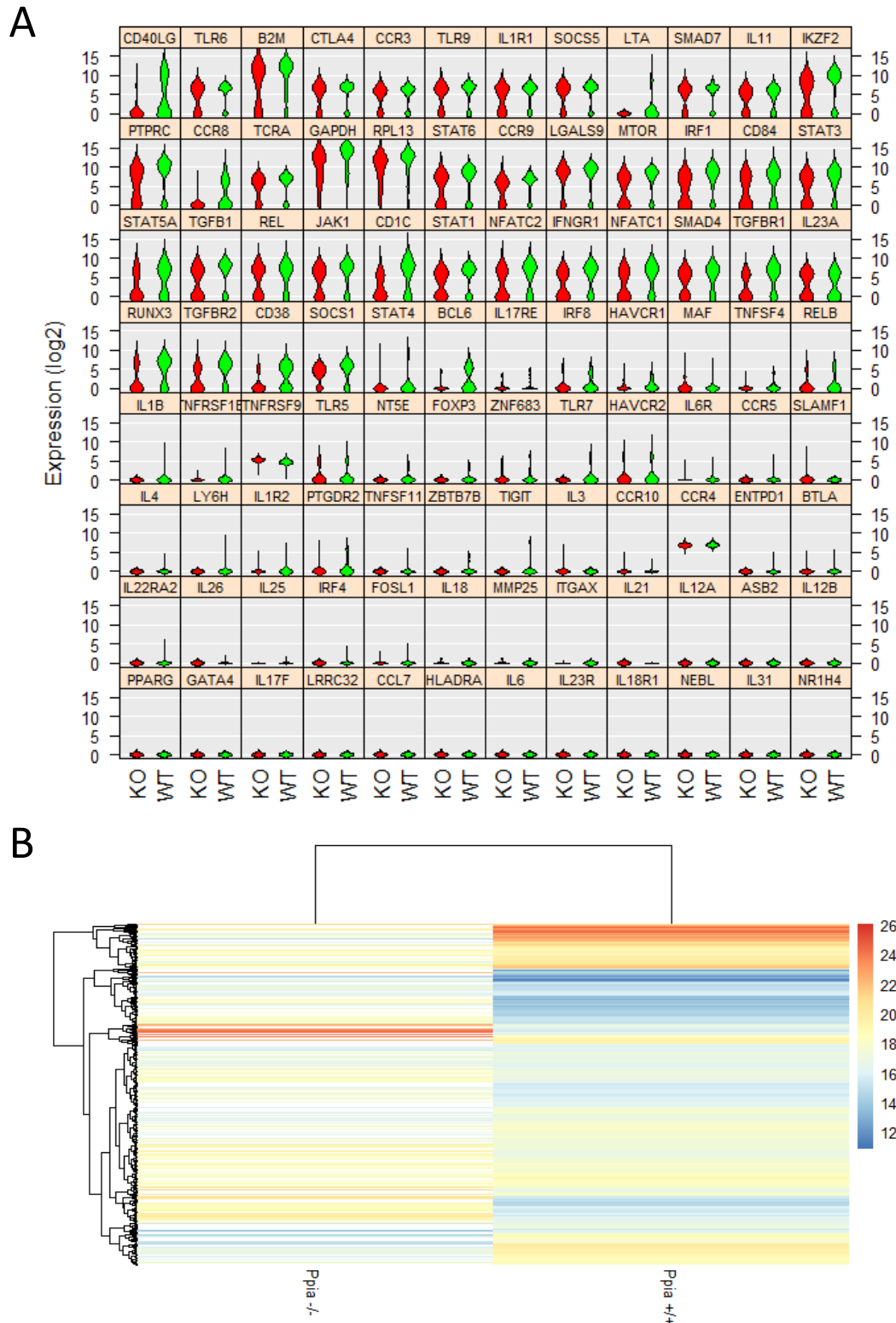


Figure 30 Violin plots and hierarchical clustering of a T cell gene panel comparing Jurkat cells and Jurkat CypA cells.

(A) Violin plots of WT (Jurkat) vs KO (Jurkat CypA^{-/-}) differentially expressed genes. the fold change in gene expression to the log₂ is represented for each gene of interest for all 96 targeted genes in the T cell panel. (B) Unbiased hierarchical clustering of all the genes and single cells in the CypA expressing cells (Jurkats) and *Ppia*^{-/-} cells (Jurkat CypA^{-/-}). Colour bar indicates cycling thresholds for the genes upregulated in blue and the genes downregulated in red. The cycling thresholds were from 12 to 26 representing the Ct score. White bars indicate samples that were not included for analysis due to double cells present in the capture site of the C1 IFC chip.

2.2.7 Proteins are specifically affected upon IFN α 2a stimulation and PBAP may provide a mechanism for the observed CypA $^{-/-}$ (*Ppia* $^{-/-}$) phenotype

As gene transcription was differentially regulated in the Jurkat CypA $^{-/-}$ cells, the proteomic regulation was analysed to confirm if the observed pattern was still maintained at the proteomic level. SILAC-labelled Jurkat cells and Jurkat CypA $^{-/-}$ cells were subjected to LC-MS/MS. The SILAC labelling of Jurkat cells and Jurkat CypA $^{-/-}$ cells would result in the incorporation of heavy lysine and arginine, which, in combination with trypsin digestion, would produce the labelling of every peptide in the mixture, except for the C-terminal peptide of the protein being labelled. SILAC technique relies on the complete incorporation of heavy amino acids during protein turnover. These experiments were supplemented with dialysed serum in order that the added (heavy and light) amino acids are the exclusive source. SILAC labelling of these two Jurkat cell lines was performed by culturing the natural amino acids with two cocktails: $^2\text{H}_4$ -lysine and $^{13}\text{C}_6$ -arginine (light) and with $^{15}\text{N}_2^{13}\text{C}_6$ -lysine and $^{15}\text{N}_4^{13}\text{C}_6$ -arginine (heavy). Labelling was confirmed after 10 passages in labelled and unlabelled media by LC-MS/MS (figure 31). A mass over charge (m/z) shift of the observed peaks of the labelled peptide fragment was observed. (figure 31). A set of proteins were then observed to be fully labelled (table 32).

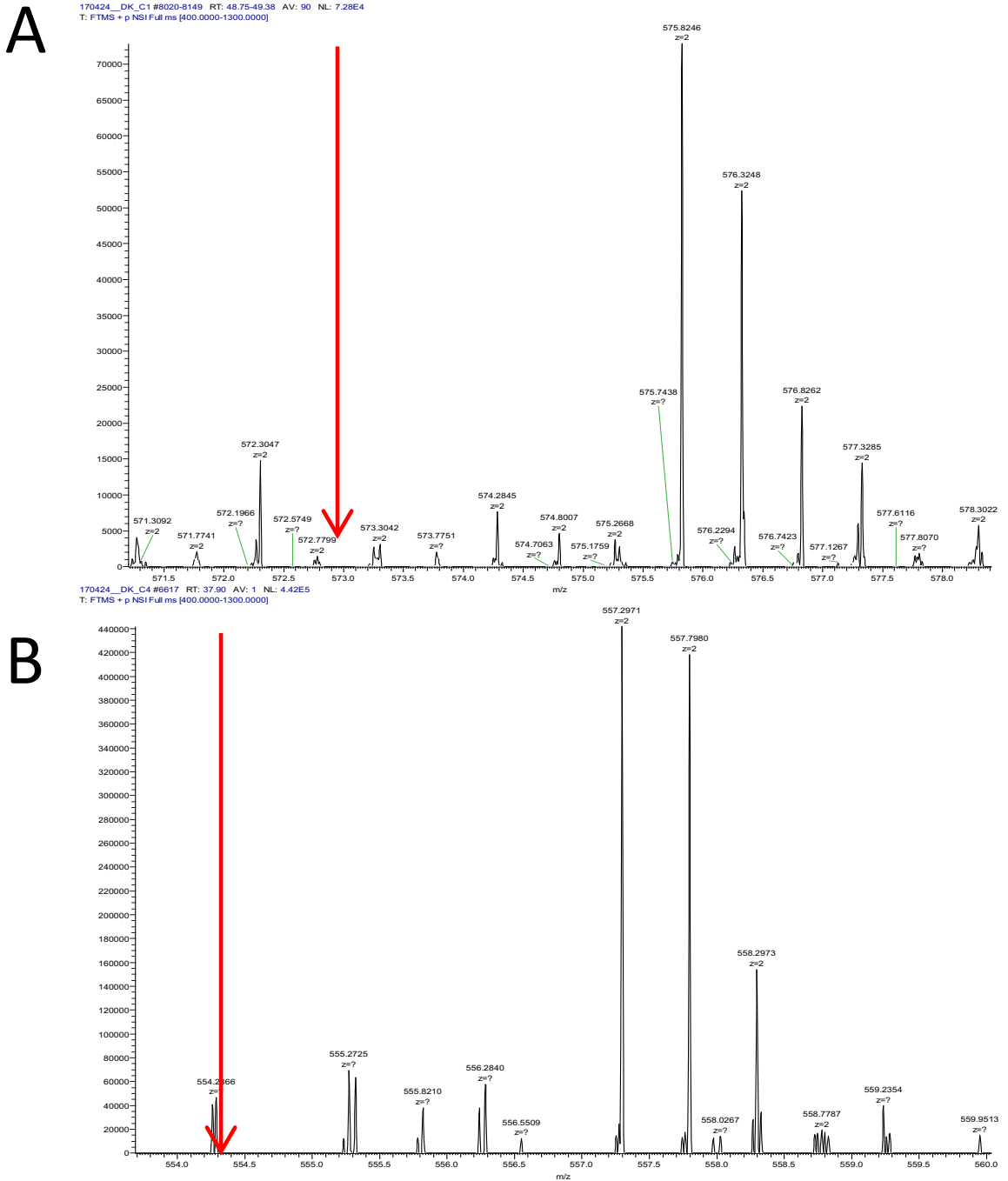


Figure 31 Confirming the incorporation of stable isotope labelling in Jurkat wt and Jurkat CypA-/- (*Ppia*^{-/-}) cells.

Cells were cultured in double labelled $^{15}\text{N}_2^{13}\text{C}_6$ -lysine and $^{15}\text{N}_4^{13}\text{C}_6$ -arginine RPMI1640 media. Jurkat cell lines were pelleted, lysed in lysis buffer supplemented with protease inhibitors and loaded onto a 4 – 10% gradient pre-cast gel. The gel was stained for 1 hour with SimplyBlue solution and washed three times with milli-Q water. Gel pieces were excised, in gel alkylated and digested using endoprotease Lys C to cleave proteins at lysine residues producing peptide fragments. The dried extract was then analysed with LC-MS/MS technique. (A) Jurkat peptide ASGVAVSDGVK. (B) Jurkat CypA-/- peptide ALAAAGYDVEK. Red arrows are positioned to indicate peaks were a non-labelled peptide fragment would be expected. An m/z shift of the observed peaks of the labelled peptide fragment implies a fully labelled peptide fragment.

Poly(A) RNA binding (figure 33). Proteins involved in this process were mainly down-regulated for Jurkat CypA^{-/-} cells from these analyses. An interesting hit was the family of Poly(A)-binding proteins (PABP). PABP has been described to bind the poly(A) tail of mRNA and to mediate mRNA circularisation through binding of the eIF4F translation initiation complex, which is associated with the mRNA 5' cap structure[268]. PABP are ubiquitous and abundant cytosolic proteins and were detected under unstimulated conditions as up-regulated proteins in the Jurkat CypA^{-/-} vs Jurkat WT cells (figure 36 & 37). Specifically, PABPC1;PABPC3;PABPC1L;PABPC4 were upregulated in the unstimulated Jurkat CypA^{-/-}. Conversely, PABPC1;PABPC4 were specifically down-regulated under IFN α 2a stimulation in Jurkat CypA^{-/-} cells. In summary, proteins involved in cellular regulation with respect to PABP proteins were specifically affected in the Jurkat CypA^{-/-} indicating an important role of PABP in maintaining cellular homeostasis.

Independently of the stimuli, 18 proteins were stably expressed Jurkat WT cells and down-regulated in Jurkat CypA^{-/-} cells, one of them being CypA itself, confirming the KO clone (figure 34). Down-regulated proteins in Jurkat CypA^{-/-} were specifically found to be involved in poly (A) RNA binding, mRNA splicing, protein kinase binding and T cell receptor binding pathways. Downregulation of tubulin, actin and protein phosphatases implicated negative control of cell growth and division in the Jurkat CypA^{-/-} cells. Regulatory proteins, specifically affected upon IFN α 2a stimulation, included nuclear elongation and cytosolic ribosomal proteins, thereby, indicating transcription and translation was altered in the Jurkat CypA^{-/-} cells (figure 35). Interestingly, upon high stimulation, the Rab proteins RAB11A and RAB11B were upregulated in the Jurkat CypA^{-/-} (figure 36). The different Rab GTPases are localised to the cytosolic face of specific intracellular membranes[269]. They function as regulators of discrete steps in membrane traffic pathways. Persisting in the GTP-bound form, the Rab GTPases recruit specific sets of effector proteins onto membranes. Rab GTPases regulate vesicle formation, actin- and tubulin-dependent vesicle movement, and membrane fusion. Rab proteins interact with multiple factors that both control the nucleotide cycle and mediate downstream functions (effectors). Taken together, these data showed differential regulation of the Jurkat CypA^{-/-} cells when compared to the Jurkat cell line indicating a phenotypically distinct T cell with altered activation and effector function.

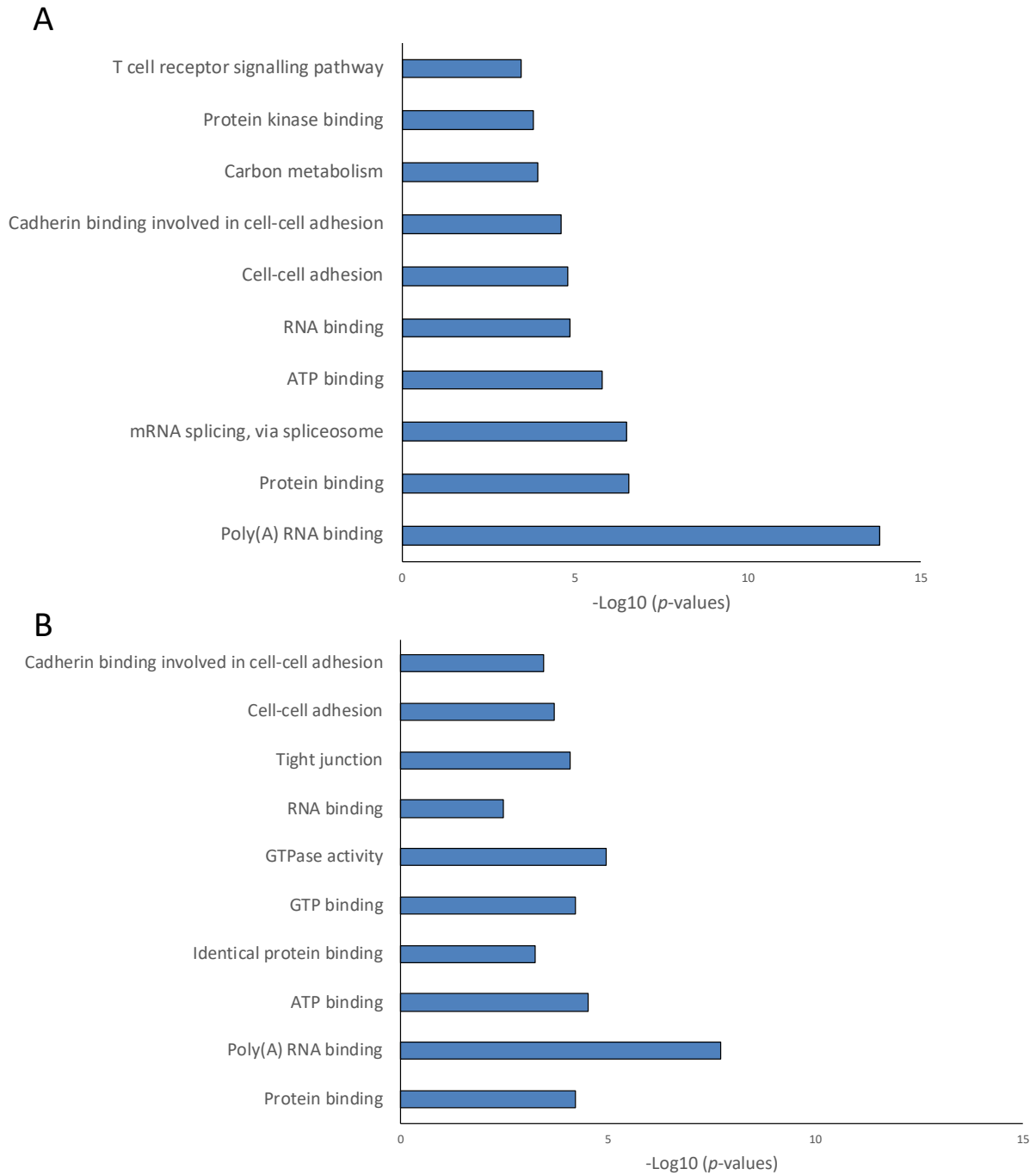


Figure 33 Gene ontology analysis.

Significantly enriched gene ontology (GO) terms in downregulated (A) and upregulated (B) differentially expressed genes in Jurkat CypA^{-/-} cells versus Jurkat WT cells under IFN α 2a stimulation. After GO analysis, every significantly enriched GO term has a p-value. The smaller p-value, the more reliable GO result is.

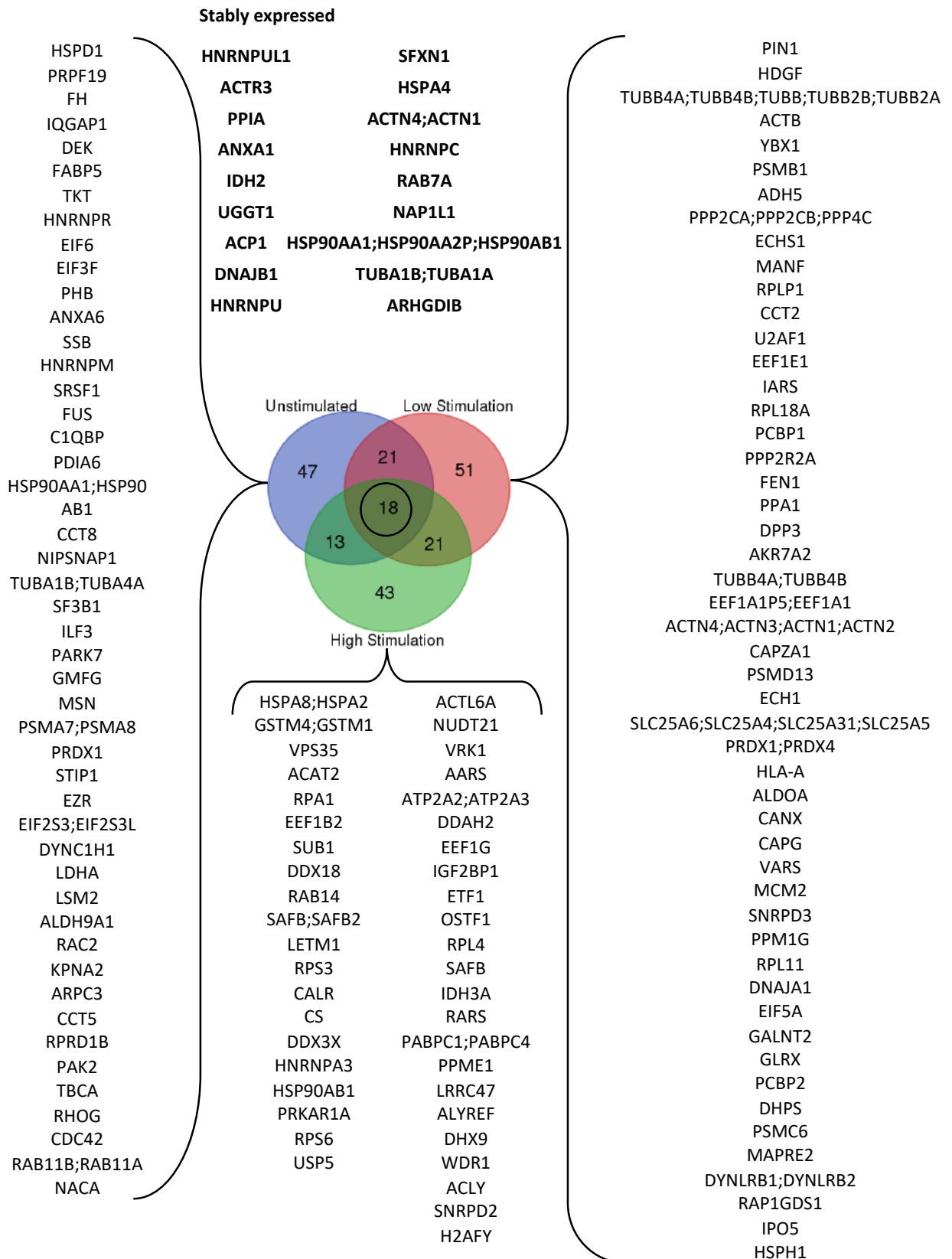


Figure 34 Down Regulated proteins in Jurkat CypA vs WT.

Venn- Diagram of the overlap of the identified peptides in each sample group. Colour code: Unstimulated (blue), Low stimulation (red), High stimulation (green).

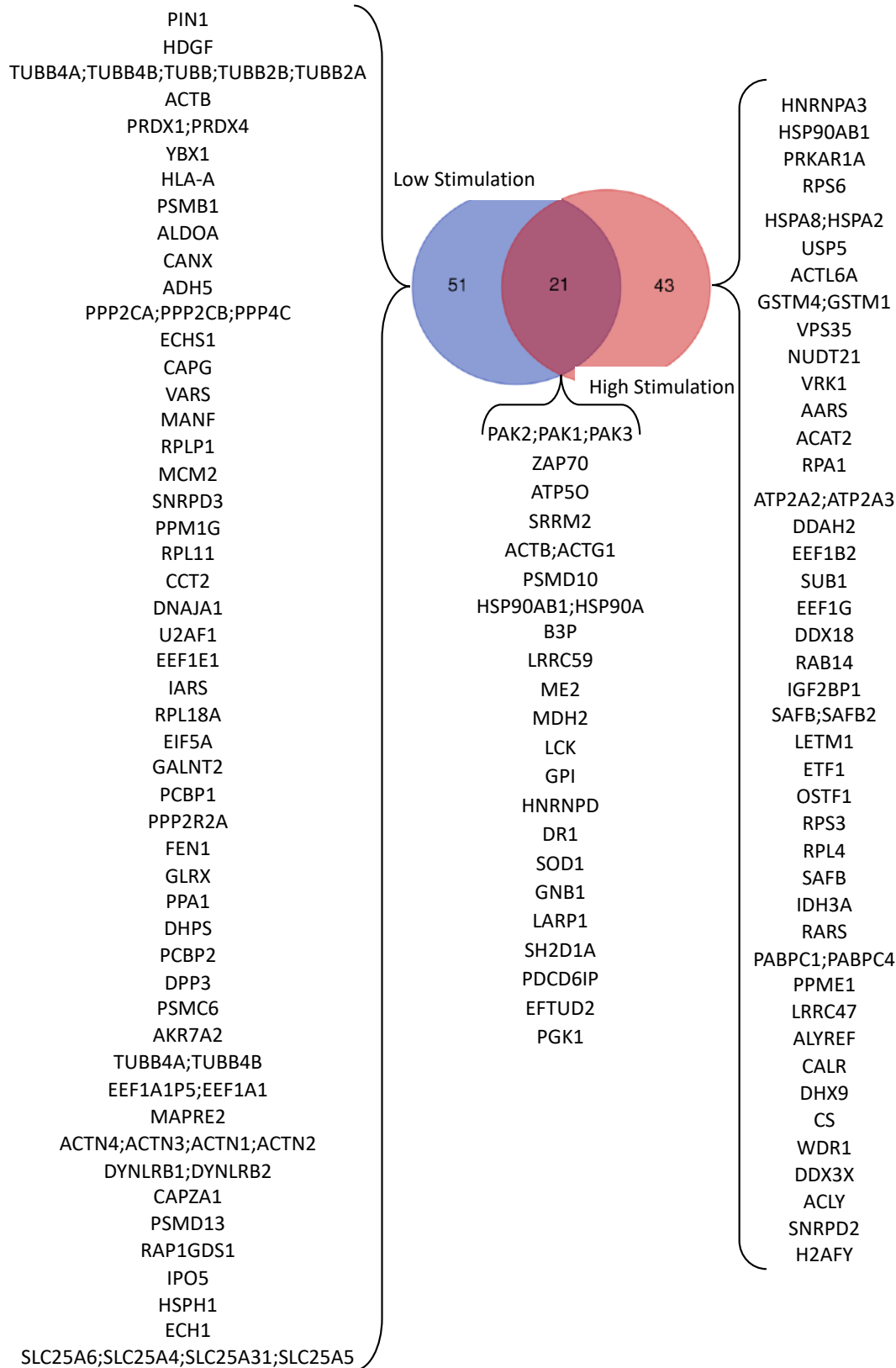


Figure 35 After stimulation differential expression (down-regulated genes).

Venn- Diagram of the overlap of the identified peptides in each sample group. Colour code: Low stimulation (blue), High stimulation (red), overlap (purple).

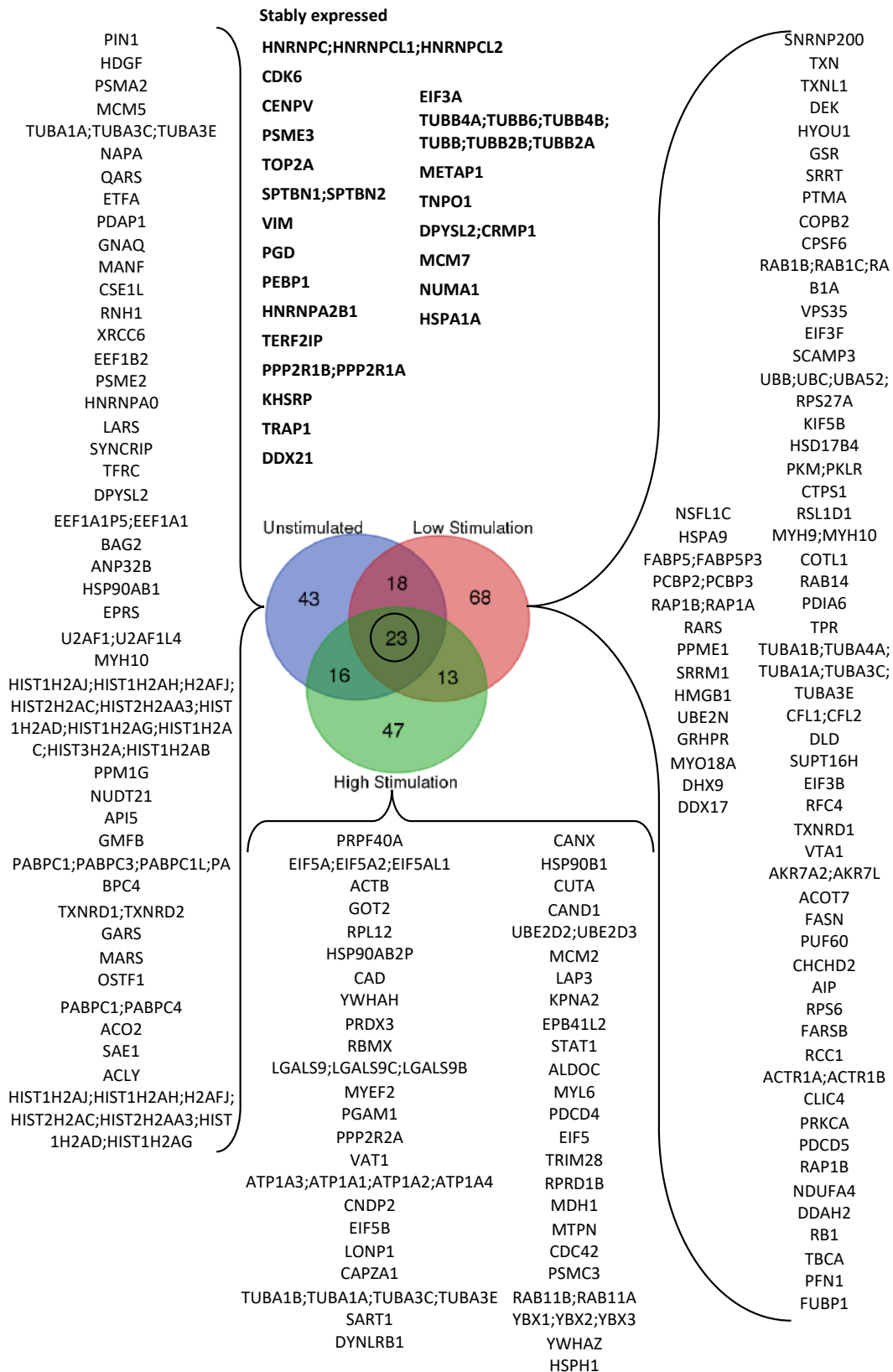


Figure 36 Up-Regulated proteins in Jurkat CypA vs WT.

Venn- Diagram of the overlap of the identified peptides in each sample group. Colour code: Unstimulated (blue), Low stimulation (red), High stimulation (green).

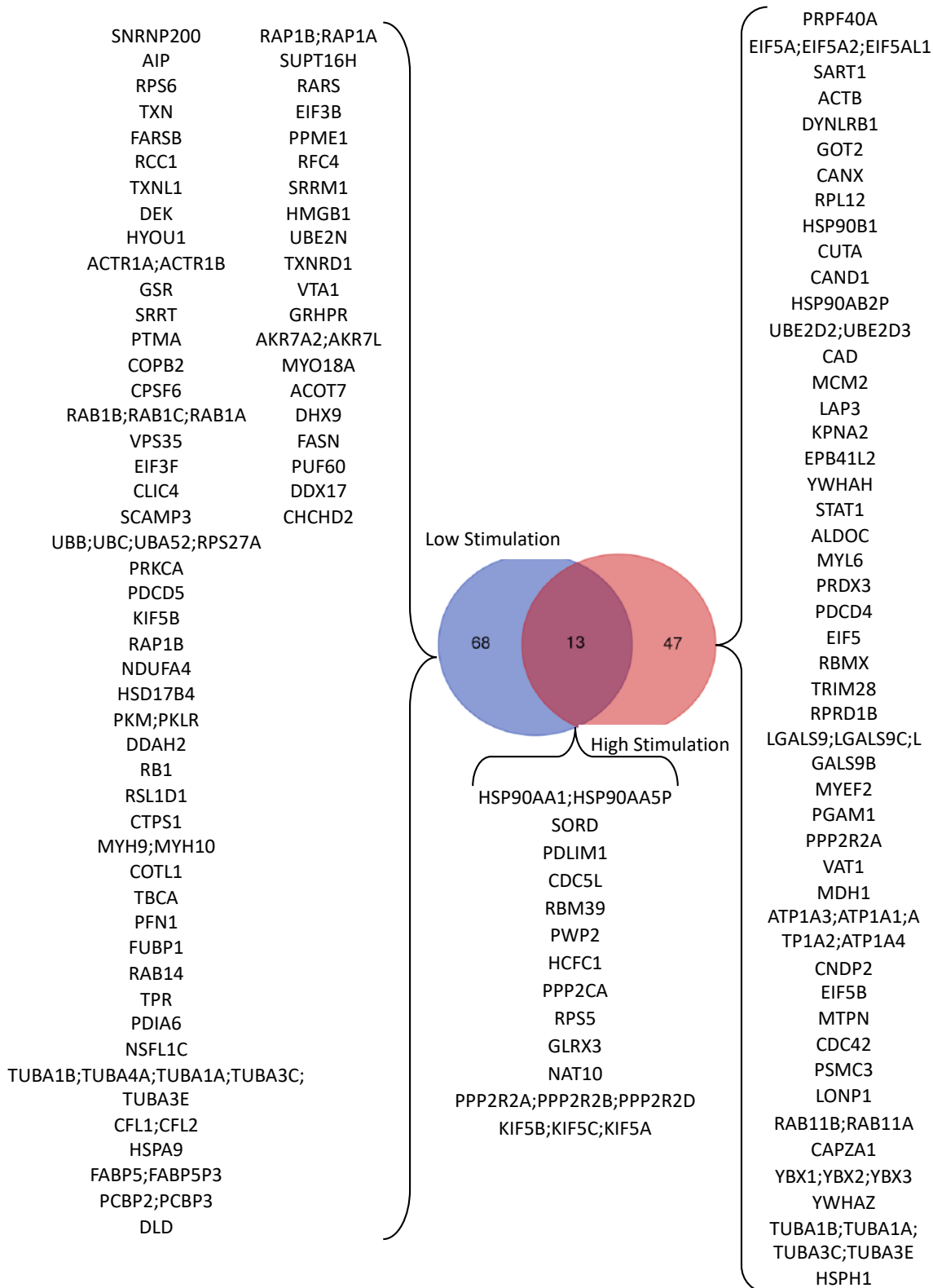


Figure 37 After stimulation differential expression (up-regulated genes).

Venn- Diagram of the overlap of the identified peptides in each sample group. Colour code: Low stimulation (blue), High stimulation (red), overlap (purple).

These results indicated a variation of the proteomic profile of the Jurkat CypA^{-/-} cell line upon IFN α 2a stimulation. Taken together, these results suggest that CypA has a role in cellular function and in maintaining transcriptional regulation of IFN α 2a stimulated genes. However, further experiments are needed to validate these observations.

3. Research Materials and Methods

3.1 Material

3.1.1 Reagents

All reagents are listed here in tables with their respective manufacturer and reference to all reagents and their use is described within the methodologies employed.

Reagent	Manufacturer
10-17 micron Fluidigm C1 single cell auto prep IFC	Fluidigm
13C6 15N4 L-Arginine-HCL isotope	Thermo Fisher Scientific
20x DNA binding dye sample loading reagent	Fluidigm
20x Evagreen DNA binding dye	Biotum
2x assay loading reagent	Fluidigm
2x Phusion Master Mix	Thermo Fisher Scientific
96.96 Dynamic Array IFC	Fluidigm
Acid-Phenol:Chloroform, pH 4.5 (with IAA, 125:24:1)	Sigma
Agarose	Sigma Aldrich
Ampicillin	Sigma Aldrich
Aqua ad iniectabilia	Braun
Biocoll	Merk Millipore
<i>BstEII</i> Restriction enzyme	New England Biolabs
Compensation beads	Thermo Fisher Scientific
Cyclosporin A	Thermo Fisher Scientific
Dialysed FBS	Thermo Fisher Scientific
DNaseI	Thermo Fisher Scientific
<i>DpnI</i>	New England Biolabs
<i>EcoRV-HF</i> ® Restriction enzyme	NEB
<i>EcoRV-HF</i> Restriction enzyme	New England Biolabs
EDTA	Thermo Fisher Scientific
Ethanol	Thermo Fisher Scientific
Ethanol 100%	ROTH
Fetal Bovine Serum	Thermo Fisher Scientific
Gel Loading Dye Purple (6x)	NEB
gM-CSF	Stem cell
Human AB serum	Thermo Fisher Scientific
IFN2a	Peptotech
Isopropanol 100%	ROTH
Kanamycin	Sigma Aldrich
KC57-FITC	Beckman Coulter
LB agar	Thermo Fisher Scientific
LB media	Thermo Fisher Scientific

LB-Agar	Invitrogen
Lenti-X-Concentrator	TaKaRa
Lipofectamine 3000	Thermo Fisher Scientific
Mass Ruler High Range DNA Ladder	Thermo Fisher Scientific
P3000 reagent	Thermo Fisher Scientific
PageRuler Prestained Protein Ladder Plus	Thermo Fisher Scientific
Penicillin-Streptomycin	Sigma Aldrich
PFA	Sigma Aldrich
Phusion HF Master mix	Thermo Fisher Scientific
Polybrene	Sigma Aldrich
Polybrene	Thermo Fisher Scientific
Protease Inhibitor Cocktail	Thermo Fisher Scientific
Puromycin	Thermo Fisher Scientific
RNaseI	Thermo Fisher Scientific
SDS sample buffer	Thermo Fisher Scientific
Syber Safe	Invitrogen
Taqman gene expression master mix	Applied Biosystems
Taqman pre-amp master mix	Applied Biosystems
TEAB buffer	Thermo Fisher Scientific
Trizol	Invitrogen
Trypsin	Thermo Fisher Scientific
<i>XhoI</i> Restriction enzyme	New England Biolabs
<i>XmaI</i> Restriction enzyme	New England Biolabs
β -mercaptoethanol	Agilent

Table 3 General laboratory consumables of reagents used.

3.1.2 Buffers and Solutions

Buffers and Solution	Manufacturer
Ambion buffer	Ambion
CutSmart Buffer	New England Biolabs
Hanks Media	Thermo Fisher Scientific
KLD reaction buffer	New England Biolabs
PBS	Thermo Fisher Scientific
RIPA buffer	Thermo Fisher Scientific
TAE Buffer (1x)	Thermo Fisher Scientific
TBS	Thermo Fisher Scientific

Table 4 Buffer and solutions.

3.1.3 Equipment

Equipment	Manufacturer
14-mL BD Falcon polypropylene round-bottom tube	Corning
Biomark HD	Fluidigm
Cell incubator	Thermo Fischer Scientific

Centrifuge 5415 R	Eppendorf
Centrifuge 5810 R	Eppendorf
Fluidigm C1	Fluidigm
Gel chamber	Thermo Fisher Scientific
Innova 4230 Refrigerated Incubator Shaker	New Brunswick Scientific
NanoDrop 1000	Thermo Fisher Scientific
Nanodrop 1000 Spectrometer	PEQLAB
PowerPac™ Basic Power Supply (Gel electrophoresis)	Bio-Rad
Qubit 2.0	Invitrogen by Life Technologies
Tecan Safire2™ Microplate Reader	TECAN
Thermomixer compact	Eppendorf
UV- Transilluminator 312	Decon Science Tec
Vac-Man® Laboratory Vacuum Manifold	Promega
Vortex CERTOMAT ® MV	B.Braun Biotech International
Water bath 1002	GFL

Table 5 Equipment

3.1.4 Kits

Kit	Manufacturer
2x Quanti FAST SYBR green	VWR
Biorad Protein Assay	Biorad
DNA Ligation Kit	TaKaRa
FIX & PERM Cell Fixation & Cell Permeabilization Kit	Thermo Fisher Scientific
Gensreen™ ULTRA HIV Ag-Ab	Bio-rad
Human IL-1 beta/IL-1F2 Quantikine ELISA Kit	R&D Systems
Human IL-10 Quantikine ELISA Kit	R&D Systems
Mini-PROTEAN® TGX™ Precast Gels	Biorad
One Shot Stb13 Chemically Competent <i>E. coli</i>	Invitrogen
PureLink HiPure Plasmid Maxiprep Kit	Qiagen
Q5® Site-Directed Mutagenesis Kit	NEB
QIAprep Miniprep Kit	Qiagen
QIAquick Gel Extraction Kit	Qiagen
QIAquick PCR Purification Kit	Qiagen
Quanta Qscript cDNA supermix	VWR
Qubit dsDNA HS assay kit	Thermo Fisher Scientific
RNeasy Mini kit Qiagen Kit	Qiagen
SILAC Protein Quantitation Kit	Thermo Fisher Scientific
Silica Bead DNA Gel Extraction Kit	Thermo Fisher Scientific
SuperSignal West Pico Chemiluminescent Substrate	Thermo Fisher Scientific
TNF alpha Human ELISA Kit	Invitrogen
Trans-Blot® Turbo™ Mini Nitrocellulose Transfer Packs	Biorad
Wizard® Plus Midipreps DNA Purification System	Promega

Zombie NIR™ Fixable Viability Kit	Biolgend
-----------------------------------	----------

Table 6 Commercial kits

3.1.5 Bacterial cell lines

Cells line	Genotype	Manufacturer
NEB® 5-alpha Competent <i>E. coli</i> (High Efficiency)	<i>fhuA2 Δ(argF-lacZ)U169 phoA glnV44 Φ80 Δ(lacZ)M15 gyrA96 recA1 relA1 endA1 thi-1 hsdR17</i>	New England Biolabs
One Shot Stb13 cells	<i>F⁻ mcrB mrr hsdS20(r_B⁻, m_B⁻) recA13 supE44 ara-14 galK2 lacY1 proA2 rpsL20(Str^R) xyl-5 λ⁻ leu mtl-1</i>	Invitrogen
XL2-Blue Ultracompetent Cells	<i>endA1 supE44 thi-1 hsdR17 recA1 gyrA96 relA1 lac [F['] proAB lacIqZAM15 Tn10 (Tet^r) Amy Cam^r]</i> .	Agilent Technologies
XL2-Blue-MRF-Ultracompetent Cells	<i>Δ(mcrA)183 Δ(mcrCB-hsdSMR-mrr)173 endA1 supE44 thi-1 recA1 gyrA96 relA1 lac [F['] proAB lacI^rZAM15 Tn10 (Tet^r) AmyCam^r]</i>	Agilent Technologies

Table 7 Bacterial cell lines provided within the commercial kits

3.1.6 Cell lines

Cells line	Description	Species	reference number
HEK 293 Antigen T cells	Human embryonic kidney cells expressing antigen T	<i>Homo sapiens</i>	CRL-3216™ (ATCC)
Jurkat, Clone E6-1	Peripheral blood T cell	<i>Homo sapiens</i>	TIB-152™ (ATCC)
MT4 cells	Human T cell leukaemia	<i>Homo sapiens</i>	120 (NIH AIDS Reagent Program)
Owl Monkey Kidney cells	Owl Monkey Kidney primary cells	<i>Aotus trivirgatus</i>	CRL-1556™ (ATCC)
THP-1 cells	Monocyte leukemic cells	<i>Homo sapiens</i>	TIB-202™ (ATCC)

Table 8 Commercially available cell lines

OMK cells obtained from Prof. Dr. Adam Grundhoff, Heinrich Pette Institute Leibniz Institute for Experimental Virology, Hamburg.

3.1.7 Reporter cell lines

Cell lines	Genotype	Species	Generated by
Jurkat, Clone E6-1 Mx2 knockout	<i>mx2^{-/-}</i>	<i>Homo sapiens</i>	Christopher T. Ford
Jurkat, Clone E6-1 CypA and Mx2 knockout	<i>ppia^{-/-}, mx2^{-/-}</i>	<i>Homo sapiens</i>	Christopher T. Ford
Jurkat, Clone E6-1 CypA knockout	<i>ppia^{-/-}</i>	<i>Homo sapiens</i>	Christopher T. Ford

Table 9 Reporter cell lines generated to address the aim 2 of this dissertation.

3.1.8 Media

Medium	Manufacturer
DMEM- GlutaMAX Medium	Gibco, Thermo Fisher Scientific
LB-Medium	Sigma
NZY+ broth Medium	Sigma
Opti-MEM I Reduced Serum Media	Gibco, Thermo Fisher Scientific
RPMI1640 Medium	Gibco, Thermo Fisher Scientific

Table 10 Commercially available media.

3.1.9 Antibodies

Antibody + Fluorophore	Manufacturer
CD69 BV421	Biolegend
CD83 BV510	Biolegend
CD80 BV605	Biolegend
CD86 PE Cy5	Biolegend

Table 11 Flow cytometry antibodies

Antibody + Fluorophore	Manufacturer
Anti-MX2 rabbit polyclonal	Abcam
Anti TRIM5 alpha rabbit polyclonal	Abcam
Anti Cyclophilin A rabbit polyclonal	Thermo Fisher Scientific
Anti rabbit IgG HRP-linked Antibody	Cell Signaling Technology

Table 12 Immunoblotting antibodies

3.1.10 Plasmids

Provirus	Virus Category	Subtype	Sexual Transmission	VRC	VRC category	Antibiotic Resistance
pNL4-3-EGFPΔEnv	lab adapted strain	B	n/a	n/a	n/a	Ampicillin
pMJ4_CH84_ZM1515M_gag_chimera [†]	infectious molecular clone	C	n/a	2,51	High	Ampicillin
pMJ4_CH55_ZM1008M_gag_chimera [†]	infectious molecular clone	C	n/a	0,35	Low	Ampicillin
pMJ4_CH177_ZM3863F_gag_chimera [†]	infectious molecular clone	C	n/a	2,63	High	Ampicillin
pMJ4_CH167_ZM3681F_gag_chimera [†]	infectious molecular clone	C	n/a	3,09	High	Ampicillin
pMJ4_CH166_ZM3576F_gag_chimera [†]	infectious molecular clone	C	n/a	1,19	Low	Ampicillin
pMJ4_CH160_ZM2003M_gag_chimera [†]	infectious molecular clone	C	n/a	0,38	Low	Ampicillin
pMJ4_CH156_ZM2063M_gag_chimera [†]	infectious molecular clone	C	n/a	2,71	High	Ampicillin
pMJ4_CH155_ZM1123M_gag_chimera [†]	infectious molecular clone	C	n/a	2,80	High	Ampicillin
pMJ4_CH154_ZM2013F_gag_chimera [†]	infectious molecular clone	C	n/a	0,45	Low	Ampicillin
pMJ4_CH152_ZM1781M_gag_chimera [†]	infectious molecular clone	C	n/a	0,85	Low	Ampicillin
CH850_TF*	infectious molecular clone (founder)	C	HSX-female	n/a	n/a	Ampicillin
CH850_6mo*	infectious molecular clone (chronic)	C	HSX-female	n/a	n/a	Ampicillin
CH569_TF*	infectious molecular clone (founder)	C	n/a	n/a	n/a	Ampicillin

CH569_6mo*	infectious molecular clone (chronic)	C	n/a	n/a	n/a	Ampicillin
CH470_TF*	infectious molecular clone (founder)	B	MSM	n/a	n/a	Ampicillin
CH470_6mo*	infectious molecular clone (chronic)	B	MSM	n/a	n/a	Ampicillin
CH264_TF*	infectious molecular clone (founder)	C	HSX-female	n/a	n/a	Ampicillin
CH264_6mo*	infectious molecular clone (chronic)	C	HSX-female	n/a	n/a	Ampicillin
CH236_TF*	infectious molecular clone (founder)	C	HSX-female	n/a	n/a	Ampicillin
CH236_6mo*	infectious molecular clone (chronic)	C	HSX-female	n/a	n/a	Ampicillin
CH185_TF*	infectious molecular clone (founder)	C	HSX-female	n/a	n/a	Kanamycin
CH185_6mo*	infectious molecular clone (chronic)	C	HSX-female	n/a	n/a	Ampicillin
CH164_TF*	infectious molecular clone (founder)	C	MSM	n/a	n/a	Kanamycin
CH164_6mo*	infectious molecular clone (chronic)	C	MSM	n/a	n/a	Kanamycin
CH162_TF*	infectious molecular clone (founder)	C	HSX-male	n/a	n/a	Kanamycin
CH162_6mo*	infectious molecular clone (chronic)	C	HSX-male	n/a	n/a	Ampicillin
CH107_TF*	infectious molecular clone (founder)	B	n/a	n/a	n/a	Ampicillin
CH107_6mo*	infectious molecular clone (founder)	B	n/a	n/a	n/a	Ampicillin
CH077_TF*	infectious molecular clone (founder)	B	MSM	n/a	n/a	Kanamycin
CH077_6mo*	infectious molecular clone (chronic)	B	MSM	n/a	n/a	Kanamycin
CH058_TF*	infectious molecular clone (founder)	B	MSM	n/a	n/a	Kanamycin
CH058_6mo*	infectious molecular clone (chronic)	B	MSM	n/a	n/a	Kanamycin
CH042_TF*	infectious molecular clone (founder)	C	HSX-male	n/a	n/a	Kanamycin
CH042_6mo*	infectious molecular clone (chronic)	C	HSX-male	n/a	n/a	Kanamycin
CH040_TF*	infectious molecular clone (founder)	B	MSM	n/a	n/a	Kanamycin
CH040_6mo*	infectious molecular clone (chronic)	B	MSM	n/a	n/a	Kanamycin

Table 13 Lab adapted and proviral constructs.

Provided from Prof. Dr. Beatrice Han (*) and Prof. Dr. Eric Hunter (†). VRC: viral Replicative Capacity.

Vector	Function	Antibiotic resistance	Additional modification
pMDLg/pRRE_CH152_ZM1781M_gagpol_chimera	packaging plasmid	Ampicillin	<i>XhoI</i> and <i>XmaI</i> restriction sites
pMDLg/pRRE_CH154_ZM2013F_gagpol_chimera	packaging plasmid	Ampicillin	<i>XhoI</i> and <i>XmaI</i> restriction sites
pMDLg/pRRE_CH155_ZM1123M_gagpol_chimera	packaging plasmid	Ampicillin	<i>XhoI</i> and <i>XmaI</i> restriction sites
pMDLg/pRRE_CH156_ZM2063M_gagpol_chimera	packaging plasmid	Ampicillin	<i>XhoI</i> and <i>XmaI</i> restriction sites
pMDLg/pRRE_CH160_ZM2003M_gagpol_chimera	packaging plasmid	Ampicillin	<i>XhoI</i> and <i>XmaI</i> restriction sites
pMDLg/pRRE_CH166_ZM3576F_gagpol_chimera	packaging plasmid	Ampicillin	<i>XhoI</i> and <i>XmaI</i> restriction sites
pMDLg/pRRE_CH167_ZM3681F_gagpol_chimera	packaging plasmid	Ampicillin	<i>XhoI</i> and <i>XmaI</i> restriction sites
pMDLg/pRRE_CH177_ZM3863F_gagpol_chimera	packaging plasmid	Ampicillin	<i>XhoI</i> and <i>XmaI</i> restriction sites
pMDLg/pRRE_CH55_ZM1008M_gagpol_chimera	packaging plasmid	Ampicillin	<i>XhoI</i> and <i>XmaI</i> restriction sites
pMDLg/pRRE_CH84_ZM1515M_gagpol_chimera	packaging plasmid	Ampicillin	<i>XhoI</i> and <i>XmaI</i> restriction sites
pNL4-3-EGFPΔEnv_CH040_TF_gagpol	lab adapted strain	Ampicillin	Kozak sequence and <i>XhoI</i> & <i>XmaI</i> restriction sites
pNL4-3-EGFPΔEnv_CH042_6mo_gagpol	lab adapted strain	Ampicillin	Kozak sequence and <i>XhoI</i> & <i>XmaI</i> restriction sites

pNL4-3-EGFPΔEnv_CH042_TF_gagpol	lab adapted strain	Ampicillin	Kozak sequence and <i>XhoI</i> & <i>XmaI</i> restriction sites
pNL4-3-EGFPΔEnv_CH058_TF_gagpol	lab adapted strain	Ampicillin	Kozak sequence and <i>XhoI</i> & <i>XmaI</i> restriction sites
pNL4-3-EGFPΔEnv_CH077_6mo_gagpol	lab adapted strain	Ampicillin	Kozak sequence and <i>XhoI</i> & <i>XmaI</i> restriction sites
pNL4-3-EGFPΔEnv_CH077_TF_gagpol	lab adapted strain	Ampicillin	Kozak sequence and <i>XhoI</i> & <i>XmaI</i> restriction sites
pNL4-3-EGFPΔEnv_CH107_TF_gagpol	lab adapted strain	Ampicillin	Kozak sequence and <i>XhoI</i> & <i>XmaI</i> restriction sites
pNL4-3-EGFPΔEnv_CH162_6mo_gagpol	lab adapted strain	Ampicillin	Kozak sequence and <i>XhoI</i> & <i>XmaI</i> restriction sites
pNL4-3-EGFPΔEnv_CH162_TF_gagpol	lab adapted strain	Ampicillin	Kozak sequence and <i>XhoI</i> & <i>XmaI</i> restriction sites
pNL4-3-EGFPΔEnv_CH164_6mo_gagpol	lab adapted strain	Ampicillin	Kozak sequence and <i>XhoI</i> & <i>XmaI</i> restriction sites
pNL4-3-EGFPΔEnv_CH164_TF_gagpol	lab adapted strain	Ampicillin	Kozak sequence and <i>XhoI</i> & <i>XmaI</i> restriction sites
pNL4-3-EGFPΔEnv_CH185_6mo_gagpol	lab adapted strain	Ampicillin	Kozak sequence and <i>XhoI</i> & <i>XmaI</i> restriction sites
pNL4-3-EGFPΔEnv_CH185_TF_gagpol	lab adapted strain	Ampicillin	Kozak sequence and <i>XhoI</i> & <i>XmaI</i> restriction sites
pNL4-3-EGFPΔEnv_CH236_6mo_gagpol	lab adapted strain	Ampicillin	Kozak sequence and <i>XhoI</i> & <i>XmaI</i> restriction sites
pNL4-3-EGFPΔEnv_CH236_TF_gagpol	lab adapted strain	Ampicillin	Kozak sequence and <i>XhoI</i> & <i>XmaI</i> restriction sites
pNL4-3-EGFPΔEnv_CH264_6mo_gagpol	lab adapted strain	Ampicillin	Kozak sequence and <i>XhoI</i> & <i>XmaI</i> restriction sites
pNL4-3-EGFPΔEnv_CH264_TF_gagpol	lab adapted strain	Ampicillin	Kozak sequence and <i>XhoI</i> & <i>XmaI</i> restriction sites
pNL4-3-EGFPΔEnv_CH470_6mo_gagpol	lab adapted strain	Ampicillin	Kozak sequence and <i>XhoI</i> & <i>XmaI</i> restriction sites
pNL4-3-EGFPΔEnv_CH470_TF_gagpol	lab adapted strain	Ampicillin	Kozak sequence and <i>XhoI</i> & <i>XmaI</i> restriction sites
pNL4-3-EGFPΔEnv_CH569_6mo_gagpol	lab adapted strain	Ampicillin	Kozak sequence and <i>XhoI</i> & <i>XmaI</i> restriction sites
pNL4-3-EGFPΔEnv_CH569_TF_gagpol	lab adapted strain	Ampicillin	Kozak sequence and <i>XhoI</i> & <i>XmaI</i> restriction sites
pNL4-3-EGFPΔEnv_CH850_6mo_gagpol	lab adapted strain	Ampicillin	Kozak sequence and <i>XhoI</i> & <i>XmaI</i> restriction sites
pNL4-3-EGFPΔEnv_CH850_TF_gagpol	lab adapted strain	Ampicillin	Kozak sequence and <i>XhoI</i> & <i>XmaI</i> restriction sites
pNL4-3-EGFPΔEnv_RK*	lab adapted strain	Ampicillin	No modifications
pNL4-3-EGFPΔEnv_RK_LM*	lab adapted strain	Ampicillin	No modifications
pNL4-3-EGFPΔEnv_SA_RK_LM*	lab adapted strain	Ampicillin	No modifications
pNL4-3-EGFPΔEnv_AP†	lab adapted strain	Ampicillin	No modifications
pNL4-3-EGFPΔEnv_AS†	lab adapted strain	Ampicillin	No modifications
pNL4-3-EGFPΔEnv_IL†	lab adapted strain	Ampicillin	No modifications
pNL4-3-EGFPΔEnv_AG†	lab adapted strain	Ampicillin	No modifications
pNL4-3-EGFPΔEnv_SN†	lab adapted strain	Ampicillin	No modifications
pNL4-3-EGFPΔEnv_ST†	lab adapted strain	Ampicillin	No modifications
pNL4-3-EGFPΔEnv_AG_SN†	lab adapted strain	Ampicillin	No modifications
pNL4-3-EGFPΔEnv_AG_SN_ST†	lab adapted strain	Ampicillin	No modifications

Table 14 Lab adapted constructs.

(*) Provided by Dr Philipp Schommers. (†) In silico designs constructed by C.Ford and mutations introduced by Genscript.

Vector	Antibiotic	Purpose
pRSV-Rev*	Ampicillin	3rd generation lentiviral packaging plasmid; Contains Rev; also requires pMDLg/pRRE (Addgene#12251) and envelope expressing plasmid (Addgene#12259)
pCMV-VSV-G	Ampicillin	(Empty Backbone) Envelope protein for producing lentiviral retroviral particles. Use in conjunction with a packaging vector or proviral vector with deletion/frameshift in env.
pSH0-GFP*	Ampicillin	Production of GFP protein as read-out for flow cytometry
pLentiCRISPR v2	Ampicillin	Replaces original lentiCRISPRv1 and produces approximately 10 fold higher titre virus. 3rd generation lentiviral backbone. Carries Cas9 gRNA sequence. Puromycin resistance in cell culture.
psPAX2**	Ampicillin	(Empty Backbone) 2nd generation lentiviral packaging plasmid. Can be used with 2nd or 3rd generation lentiviral vectors and envelope expressing plasmid

Table 15 Constructs required for Lenti-viral vector systems.

(*) Provided by Dr Niklas Beschoner. (**) Provided by Dr Glòria Martrus Zapater.

Vector	Antibiotic	gRNA sequence
pLentiCRISPR v2_MX2_1	Ampicillin	AAATTGACTTCTCCTCCGGT
pLentiCRISPR v2_MX2_2	Ampicillin	GGACGCTGCTTTCCTCGCCA
pLentiCRISPR v2_MX2_3	Ampicillin	AATTGACTTCTCCTCCGGTA
pLentiCRISPR v2_TRIM5_1	Ampicillin	ATGTTGGCTACATGCCGATT
pLentiCRISPR v2_TRIM5_2	Ampicillin	GTTGATCATTGTGCACGCCA
pLentiCRISPR v2_TRIM5_3	Ampicillin	TGGTAACTGATCCGGCACAC
pLentiCRISPR v2_PPIA_1	Ampicillin	TGCCAGGACCCGTATGCTTT
pLentiCRISPR v2_PPIA_2	Ampicillin	ATCCTAAAGCATACGGGTCC
pLentiCRISPR v2_PPIA_3	Ampicillin	GGTGACTTCACAGCCATAA

Table 16 CRISPR/Cas9 gRNA constructs generated to establish reporter cell lines.

Produced by Genscript.

3.1.11 Primer Oligonucleotides

Primer	Primer Oligo 5' to 3'
gag_s	ATTTA <u>ctc</u> gagccgcccATGGGTGCGAGAGCGT
pol Hunter_as	TAAATcccgggCTAATCTTCATCCTGTCTACTTGCCA
pol Hahn_CH040_as	TAAATcccgggCTTTCCATGCTCTAATCCTCATCCT
pol Hahn_CH077_as	TAAATcccgggTTAATCCTCATCCTGTCTACTTGC
pol Hahn_CH107_as	TAAATcccgggCTAATCCTCATCCTGTCTACTTGC
pol Hahn_CH162_as	TAAATcccgggCTATTCCATGTTCTGATCCTCATCCT
pol Hahn_CH164_as	TAAATcccgggCTAATCTTCATCCTGTCTACTTGC
pol Hahn_CH185_as	TAAATcccgggCTATTCCATGTTCTAATCCTCATCCT
pol Hahn_CH236_as	TAAATcccgggCTATTCCATGTTCTAATCCTCATCCT
pol Hahn_CH264_as	TAAATcccgggCTGATCTTCATCCTGTCTACTTGC
pol Hahn_CH42_as	TAAATcccgggCTGATCCTCATCCTGTCTACTTGC
pol Hahn_CH569_as	TAAATcccgggTTAATCTTCATCCTGTCTACTTGC
pol Hahn_CH58_470_as	TAAATcccgggCTGATCCTCATCCTGTCTACTTGC
pol Hahn_CH850_as	TAAATcccgggCTAAACTATTCCATGTTCTAATCCT

Table 17 Oligonucleotides for cloning gag-pol.

Kozak (underlined). XhoI (highlighted in blue) and XmaI (highlighted in yellow) modifications.

Primer	Primer Oligo 5' to 3'
HXB2ncs623to649_s	AAATCTCTAGCAGTGGCGCCCGAACAG
HXB2ncs2849to2826_as	TAACCCTGCGGGATGTGGTATTCC
695to794_s	GACTCGGCTTGCTGAAGCGCGCACGGCAAGAGGGCGAGGGGCGGCGAC TGGTGAGTACGCCAAAAATTTTGACTAGCGGAGGCTAGAAGGAGAGAGATGGG
2646to2547_as	ATGCTTTTATTTTTCTTCTGTCAATGGCCATTGTTTAACTTTTGGGCCATCCATTCC TGGCTTAAATTTTACTGGTACAGTCTCAATAGGACTAATGGG

Table 18 Oligonucleotides for 2-step cloning of gag-protease.

Primer	Primer Oligo 5' to 3'
CH058_TF_6mo_mut_s	CAAGGGGAGGCCAGGAAATTTTCTTC
CH058_TF_6mo_mut_as	TTGGAAGGCCAGATTTTC
CH166_ZM3576F_mut_s	GCCGCCATGGGTGCGAGAGCGTCA
CH166_ZM3576F_mut_as	CTCGAGGGCAGATCTCGAATTC
Q5Mut_seq_s	AAGAAACCATCAATGAGGAAGC
Mutagenesis Control Primer_s	AACCCTGGCGttAcCcAACTTAATCG
Mutagenesis Control Primer_as	TTCCCAGTCACGACGTTGTAAAA

Table 19 Oligonucleotides for removal of XhoI restriction site in CH058 transmitted founder and 6 month chronic pro-virus and removal in CH166_ZM3576F pro-virus.

Primer	Primer Oligo 5' to 3'
HIV_LTR_s	CGAGCCCTCAGATGCTACATATAA
gag(Vector)_s	AAATCTCTAGCAGTGGCGCCCGAACAG
G00_s	GACTAGCGGAGGCTAGAAG
gag_839bp_s	GCATTTTGGACATAAGACAAGGGCC
pol_1900bp_s	GGAGGTTTTATCAAAGTAAGAC
pol_2529bp_s	GATATACAGAAGTTAGTGG
pol_3369bp_s	GCACACAAAGGAATTGGAG
pol_3958bp_s	CAGCAGTACAAATGGCAGTATTC
CH185_pol_2529bp_s	GACATACAGAAGCTAGTGG
CH850_pol_2529bp_s	GATATACAAAAGTTAGTGG
CH162_pol_1900bp_s	GGAGGTTTTATTAAAGTCAGAC
Consensus_1_gag_as	AAATCTTTCCAGCTCCCTGCTTG

Table 20 Oligonucleotides for sequencing gag-pol cloned into vector backbones.

Primer	Primer Oligo 5' to 3'
CypA_s	GCTGGACCCAACACAAATGG
CypA_as	GCTCCATGGCCTCCACAATA
TRIM5 α _s	CCAGGATAGTTCCTTCCATAC
TRIM5 α _as	AGAGCTTGGTGAGCACAGAGTC
MX2_s	AAGCAGTATCGAGGCAAGGA
MX2_as	TCGTGCTCTGAACAGTTTGG
EPSTI1_s	CCAGAAGCTGGGCTTACAGA
EPSTI1_as	CCTGTGTTTTCAGTCTGGTGGA
OAS3_s	GACCTAAGGGATGGCTGTGA
OAS3_as	CAGGAAACTGAAGGCTCAGG
ISG15_s	GAGAGGCAGCGAACTCATCT
ISG15_as	CTTCAGCTCTGACACCGACA
LY6E_s	TGATGTGCTTCTCCTGCTTG
LY6E_as	ACAGGTCTTGCTCAGGCTGT
Hu_RT_GAPDH_s	CGGAGTCAACGGATTGG
Hu_RT_GAPDH_as	TGATGACAAGCTTCCCGTTC

Table 21 Oligonucleotides used for real-time PCR.

Target	Sense Primer Oligo (5' to 3')	Antisense Primer Oligo (5' to 3')	Design RefSeq	Gene Full Name
CD40LG	GAGGCCAGCAGTAAAACA AC	AGTTGTTGCTCATGGGTAGT A	NM_000074.N	CD40 ligand
TLR6	CCACAGAACAGCATTCCCA AC	TCCTTGGGCCACTGCAAATA	NM_006068.N	toll like receptor 6
B2M	TTAGCTGTGCTCGCGCTAC	CTCTGCTGGATGACGTGAGT AA	NM_004048.N	beta-2-microglobulin
CTLA4	CATGGACACGGGACTCTAC A	AATCTGGGTCCGTTGCCTA	NM_005214.N	cytotoxic T-lymphocyte associated protein 4
CCR3	GGACACCTACAATGTGGC TA	TCCGCTCACAGTCATTCCA	NM_001837.N	C-C motif chemokine receptor 3
TLR9	TGCAACTGGCTGTTCTGA A	ACAAGGAAAGGCTGGTGACA	NM_017442.N	toll like receptor 9
IL1R1	AGAACAAGCCTCCAGGATT CA	CCTGAATCCTCCACCTTAGCA	NM_00132098 0.N	interleukin 1 receptor type 1
SOCS5	TGTGCCACAGAAATCCCTC A	AGTCTTGTCTCTGGGGTAAAC AC	NM_144949.N	suppressor of cytokine signaling 5
LTA	CTCAAACCTGTGCTCACC T	ACGGTCCGTGTTTGCTCTC	NM_00115974 0.N	lymphotoxin alpha
SMAD7	CTTCATCAAGTCCGCCACA C	TTGATGGAGAAACCGGGAA	NM_005904.N	SMAD family member 7
IL11	GCTGCACCTGACACTTGAC	GGTCACAGCCGAGTCTTCA	NM_000641.N	interleukin 11
IKZF2	AGGAAAGTCCAGGAGCTTC AA	AGAAGCTCCACACTGGTTAC A	NM_00107952 6.N	IKAROS family zinc finger 2
PTPRC	GTGGCTTAAACTCTTGCCA TTT	GGGAAGGTGTTGGGCTTT	NM_002838.N	protein tyrosine phosphatase, receptor type C
CCR8	GCAACACTGAAACCTCCAG AAC	ACTGTTGTCCACTGAGGTC AA	NM_005201.N	C-C motif chemokine receptor 8
TCRA	TGGCTGAATCTTTGCAGTC C	CATGGACACACACCCTCAC	FLDM- 061106.1	T cell receptor alpha
GAPDH	GAACGGGAAGCTTGTCATC AA	ATCGCCCACTTGATTTGG	NM_00128974 5.N	glyceraldehyde-3-phosphate dehydrogenase
RPL13A	GAGGCCCTACCACTTCC	GCCGTCAAACACCTTGAGAC	NM_012423.N	ribosomal protein L13a
STAT6	TGCTCTGGTCGAGTTCA	TCCAGGACACCATCAAACCA	NM_00117807 8.N	signal transducer and activator of transcription 6

CCR9	TGTTGGTGCAGACCATTGAC	TGACCTGGAAGCAGATGTCA	NM_00125636 9.N	C-C motif chemokine receptor 9
LGALS9	GTACCCATCCAAGTCCATCCT	TTCCCAGAGCACAGGTTGAT	NM_009587.N	galectin 9
MTOR	CCAAACCCAGGTGTGATCAA	TCCTCATTCCAGGCCACTA	NM_004958.N	mechanistic target of rapamycin
IRF1	AACAAGGATGCCTGTTTGTTC	TGGGATCTGGCTCCTTTTCC	NM_002198.N	interferon regulatory factor 1
CD84	TCCAAGGAAGAGCCAGTGAAC	GCTTGAAGTCCCAGGAGGTTA	NM_00118487 9.N	CD84 molecule
STAT3	AGCATCGAGCAGCTGACTAC	CCATGTGATCTGACACCCTGAA	NM_139276.N	signal transducer and activator of transcription 3
STAT5A	CCCAGGCTCCCTATAACATGTA	ATGGTCTCATCCAGGTCGAA	NM_00128871 8.N	signal transducer and activator of transcription 5A
TGFB1	CTACTACCCAAGGAGGTCAAC	GCTGTGTGACTCTGCTTGAAAC	NM_000660.N	transforming growth factor beta 1
REL	TTCTCCTGTGTCTCGAACCTC	TCCACAATTCTGTTTACACGACAAA	NM_002908.N	REL proto-oncogene, NF-kB subunit
JAK1	CCCACAAACACATCGTGTGTA	CCCCTTCCACAAACTCTTCCA	NM_00132185 3.N	Janus kinase 1
CD1C	AGGCCAGGACATCATCCTCTA	CCAAGGGCACTATCACTACCAA	NM_001765.N	CD1c molecule
STAT1	ATGCTGGCACCAGAACGAA	GCTGGCACAATTGGGTTTCAA	NM_007315.N	signal transducer and activator of transcription 1
NFATC2	TGGAAGCCACGGTGGATAA	TGTGCGGATATGCTTGTTC	NM_012340.N	nuclear factor of activated T-cells 2
IFNGR1	AAGCCAGGTTGGACAAAA	GATATCCAGTTTAGTGGTCCAA	NM_000416.N	interferon gamma receptor 1
SMAD4	CACCAAAACGGCCATCTTCA	GGAATGCAAGCTCATTGTGAAAC	NM_005359.N	SMAD family member 4
TGFBR1	ACAGAAGTTAAGCCAAATATCCC	GCTCCATTGGCATACCAACA	NM_00130621 0.N	transforming growth factor beta receptor 1
IL23A	TCACAGAAGCTCTGCACAC	TCCCACTGGATATGGGGAA	NM_016584.N	interleukin 23 subunit alpha
RUNX3	AGCACCACAAGCCACTTCA	TCGGAGAATGGGTTCAAGTTC	NM_00103168 0.N	runt related transcription factor 3
TGFBR2	TTCCCAGTTCTGGCTCAAC	GGTCCCAGCACTCAGTCAAC	NM_00102484 7.N	transforming growth factor beta receptor 2
CD38	ACCTCACATGGTGTGGTGAAC	GTTGCTGCAGTCCTTTCTCC	NM_001775.N	CD38 molecule
SOCS1	CATCCGCGTGCACCTTCA	GCTCGAAGAGGCAGTCGAA	NM_003745.N	suppressor of cytokine signaling 1
STAT4	GCAAGACGAATTTGACTACAGGTA	TCCTGATTCACCATGGCACTA	NM_003151.N	signal transducer and activator of transcription 4
BCL6	GATGGAGCATGTTGTGGACAC	AGGAGGCTTGATGGCAGAAA	NM_00113084 5.N	B-cell CLL/lymphoma 6
IL17RE	TTCCAGAGCTGGCCAGAA	ATCTGAGTGTGCTGGCTGTA	NR_104198.N	interleukin 17 receptor E
IRF8	GGAGTCAGCTCCTCCAGACCT	CGCGTCGTAGGTGGTGA	NM_002163.N	interferon regulatory factor 8
HAVCR1	GTGGTCATCTTAAGCCTCACTCC	TGCCTCTCCACCAACCTTTA	NM_012206.N	hepatitis A virus cellular receptor 1
MAF	TCGACGACCGCTTCTCC	ATCACCTCCTCTTGCTGAC	NM_00103180 4.N	MAF bZIP transcription factor
TNFSF4	CACATCGGTATCCTCGAATCTCA	TGATTTTCATCCTCCTTTTGGGAA	NM_003326.N	tumor necrosis factor superfamily member 4
RELB	TGCTTTCCGAGCCCGTCTA	CGGCCCGCTTTCCTTGTTAA	NM_006509.N	RELB proto-oncogene, NF-kB subunit
IL1B	GACCTGAGCACCTCTTTCC	CGTGACATAAGCCTCGTTA	NM_000576.N	interleukin 1 beta
TNFRSF1B	ACATACACCCAGCTCTGGAAC	AGTGCAGGCTTGAGTTCCA	NM_001066.N	TNF receptor superfamily member 1B
TNFRSF9	GGGGCAGAAAGAAACTCCTGTA	TCTGGAAATCGGCAGCTACA	NM_001561.N	TNF receptor superfamily member 9

TLR5	GGACCTCTGCCCTAGAA TAA	AGAAGGTCCAGGTGGTCTCC	NM_003268.N	toll like receptor 5
NT5E	ATGAACGCCCTGCGCTAC	GTGGCTCGATCAGTCTTCC	NM_002526.N	5'-nucleotidase ecto
FOXP3	TGTGGGGTAGCCATGGAAA	GGGTCGCATGTTGTGGAA	NM_014009.N	forkhead box P3
ZNF683	GAGCTTGGGCAGCTCTCC	TCTTCTGGCACAAGGCACAC	NM_00130792 5.N	zinc finger protein 683
TLR7	TCTTCAACCAGACCTCTAC ATTCC	AGCCCCAAGGAGTTTGAAA	NM_016562.N	toll like receptor 7
HAVCR 2	GGATCCAAATCCCAGGCAT AA	CTTGAAAGGCTGCAGTGAA	NM_032782.N	hepatitis A virus cellular receptor 2
IL6R	GTAGTGTGGGAGCAAGTT CA	ATGTTGGCAGGCGGATCA	NM_000565.N	interleukin 6 receptor
CCR5	TGAGACATCCGTTCCCTCA CA	TGGCAGGGCTCCGATGTATA	NM_000579.N	C-C motif chemokine receptor 5 (gene/pseudogene)
SLAMF1	TCAGCAACAATCCCAGAC C	CCTAACAGCCAGCATAACAC	NM_003037.N	signaling lymphocyte activation molecule family member 1
IL4	CAGCTGATCCGATTCTGA AA	GTTGGCTTCTTCACAGGAC	NM_000589.N	interleukin 4
LY6H	AGTGTCCGAATCACCGATC C	AGGAGGCACACATCTTGTT CA	NM_00113047 8.N	lymphocyte antigen 6 family member H
IL1R2	GTTTCTGCCTTCACCTTCA	CTTGTAATGCCTCCACGAA	NM_004633.N	interleukin 1 receptor type 2
PTGDR2	TCCAGGGCTGGAATCCTGT	GGCAGAGTGGCTTCAGTGT	NM_004778.N	prostaglandin D2 receptor 2
TNFSF1 1	CTCAGCCTTTTGCTCATCTC AC	GGTACCAAGAGGACAGACTC AC	NM_033012.N	tumor necrosis factor superfamily member 11
ZBTB7B	GGTCTGCGGTGTTGATTC A	ATGAGTAGGGGCGCTCTCC	NM_00125240 6.N	zinc finger and BTB domain containing 7B
TIGIT	GTGGTGGTCGCGTTGACTA	TCCTGTCCAGCTGATTTTCTC C	NM_173799.N	T-cell immunoreceptor with Ig and ITIM domains
IL3	CAATGGGGAAGACCAAGA CA	CTCTTGACAGCCCTGTTGAA	NM_000588.N	interleukin 3
CCR10	GGACGGAGGCCACAGA	AGTGGCTCAGCCGAGTAT	NM_016602.N	C-C motif chemokine receptor 10
CCR4	CCTGGCATTGCCTCACAGA	GCTCCTCAAGGCAGGTCTG	NM_005508.N	C-C motif chemokine receptor 4
ENTPD1	AGGTGCCTATGGCTGGATT AC	GTCCAAAGCTCCAAAGGTTT CC	NM_001776.N	Ectonucleoside triphosphate diphosphohydrolase 1
BTLA	TCCCATATCTGGACATCTG GAAC	CTCCTGCTAAGATGGAGTGT TCA	NM_181780.N	B and T lymphocyte associated
IL22RA2	TTGCAACCATGATGCCTAA AC	TCGGGACTGAAATTGTACCC	NM_052962.N	interleukin 22 receptor subunit alpha 2
IL26	AAAATACGCTTTGTGGAGG AC	TAGCTGATGAAGCACAGGAA	NM_018402.N	interleukin 26
IL25	CAGTGAAGATGGACCCCTC A	AGCCTGTCTGTAGGCTGAC	NM_022789.N	interleukin 25
IRF4	CGGGCAAGCAGGACTACAA	TGTCGATGCCTTCTCGGAAC	NR_046000.N	interferon regulatory factor 4
FOSL1	CGACCCATCTGCAAAATCC C	CCTGGGAAAGGGAGATACA A	NM_005438.N	FOS like 1, AP-1 transcription factor subunit
IL18	ACCAAGGAAATCGGCCTCT A	ACCTCTAGGCTGGCTATCTTT A	NM_001562.N	interleukin 18
MMP25	ACGATGTCACCGTCAGCAA	CTTGGGGAAGGCCAGTA	NM_022468.N	matrix metalloproteinase 25
ITGAX	AGGACAATCTCGGCATCTC C	ACTTCTGCGTTCAGCTCCA	NM_000887.N	integrin subunit alpha X
IL21	CTGAATTTCTGCCAGTCC A	TTGTTTCTGTATTTGCTGAC TTTA	NM_00120700 6.N	interleukin 21
IL12A	ATGCCTTACCACCTCCAA A	TCTCTTCAGAAGTGCAAGGG TAAA	NM_000882.N	interleukin 12A
ASB2	CTCCAACAATCCCGAGAG ACA	GTGCTGCACCAAGATCTTCA C	NM_00120242 9.N	ankyrin repeat and SOCS box containing 2
IL12B	TCCCTGACATCTGCGTTCA	GGTCTTGTCGTAAGACTCT A	NM_002187.N	interleukin 12B

PPARG	TAGATGACAGCGACTTGGC AATA	TGGGCTTCACATTCAGCAA C	NM_138711.N	peroxisome proliferator activated receptor gamma
GATA4	AAAACGGAAGCCCAAGAA CC	AAGGCTCTCACTGCCTGAA	NM_002052.N	GATA binding protein 4
IL17F	CGCGTTTCCATGTCACGTA	CTGTACAACCTCCGAGGGGT A	NM_052872.N	interleukin 17F
LRRC32	CTAGGCCTGGCTGCACAA	CCAGAACCTGGCAGGAGAC	NM_005512.N	leucine rich repeat containing 32
CCL7	CCTCACCTCCAACATGAA A	CTGTAGCAGCAGGTAGTTGA A	NM_006273.N	C-C motif chemokine ligand 7
HLA- DRA	CGCTCAGGAATCATGGGCT A	CGCCTGATTGGTCAGGATTC A	NM_019111.N	major histocompatibility complex, class II, DR alpha
IL6	AGAGCTGTGCAGATGAGTA CAA	GTTGGGTCAGGGGTGGTTA	NM_000600.N	interleukin 6
IL23R	GCACTAGGCATGGAAGAGT CAA	TGGAAATGACGGCTGCAGAA	NM_144701.N	interleukin 23 receptor
IL18R1	GGGAGGCACAGACACCAA AA	TGAAGACGTGGCCTGGGATA	NM_003855.N	interleukin 18 receptor 1
NEBL	CCAGACCAGTGTGTCATCC A	TCCTGGGCACTGTAATCGTA C	NM_006393.N	nebulette
IL31	CCGTCCGTTTACTACGACC AA	AGACACGGCAGCGTGTA	NM_00101433 6.N	interleukin 31
NR1H4	AGGTCGTGACTTGCGACAA	CTGTTGATCTGGGGTGAGTTC A	NM_00120697 7.N	nuclear receptor subfamily 1 group H member 4

Table 22 Oligonucleotides use for the amplification of cDNA transcripts using Fluidigm technology. T cell panel primers listed.

3.1.12 Software

Name	Manufacturer
FACSDiva	BD Biosciences
FlowJo	Tree Star Inc.
GraphPad/ Prism7	Graphpad Software, Inc.
Microsoft Office 365 version 16.24	Microsoft Corporation
NanoDrop 1000	Thermo Fisher Scientific
Qubit 2.0	Invitrogen by Life Technologies
Snappgene Viewer	GSL Biotech LLC

Table 23 Software packages

3.2 Methods

3.2.1 Transformation of bacteria

3.2.1.1 Transformation of lab adapted constructs

Production of lab-adapted constructs (see table 13 & 14) was performed through transformation using One Shot Stb13 Chemically Competent *E. coli* cells. 50 μL of One Shot Stb13 Competent *E. coli* cells were thawed on ice and 1 μL plasmid DNA with a concentration $<100\text{ ng}/\mu\text{L}$ was added. After 30 minutes of incubation on ice, the cells were heat-shocked for 45 seconds at 42°C and placed on ice for 3 mins. Next, 250 μL of pre-warmed SOC medium was added to the vial and was shaken at 37°C at 225 rpm for 1h. 50 μL of each vial were then spread on pre-warmed LB section plates containing ampicillin. The plates were incubated at 37°C overnight. The next day one colony of each plate was picked and incubated in 150 mL of LB medium with 150 μL ampicillin overnight.

3.2.1.2 Transformation of proviral HIV-1 constructs

HIV-1 proviral constructs (see table 13) were transformed using XL2-Blue ultracompetent Cells and XL2-Blue MRF-ultracompetent Cells. Cells were thawed on ice and 100 μL of XL2-Blue ultracompetent Cells or 20 μL of XL2-Blue MRF' ultracompetent Cells were placed into a 14-mL BD falcon polypropylene round-bottom tube. 1 μL of plasmid DNA (25 ng) was added to an aliquot of cells and incubated on ice for 30 mins. The tubes were heat-shocked in a 42°C water bath for 30 secs and incubated on ice for 3 mins. 200 mL of NZY+ medium was added to each tube and incubated at 37°C at 225 rpm for 1 hour. For each transformation reaction, 50 μL of the transformed cells were plated on LB agar plates containing ampicillin or kanamycin, depending on the plasmid. All LB plates were incubated at 37°C overnight. The next day, one colony of each plate was picked and inoculated in 150 mL of LB medium with 150 μL ampicillin or kanamycin and incubated overnight at 37°C at 225 rpm. Midipreps and Maxipreps of proviral constructs were performed.

3.2.1.3 Transformation of ligated gag/pol into pMDLg pRRE Δgag/pol

10 μL of XL2-Blue MRF⁺ ultracompetent cells were added to each ligation reaction and the tubes were incubated on ice for 30 mins. Cells were heat-shocked at 42°C for 45 seconds and chilled on ice for 3 mins. 200 μL SOC medium was added to each tube and the reactions were shaken at 37°C for one hour. 200 μL of each transformation reactions were plated on agar-plates with 0.1 % ampicillin. Plates were incubated on agar plates overnight at 37°C. Colonies were obtained and a master plate was prepared. The master plate is a LB agar plate divided into sections where all bacterial samples are dotted and serves as a back-up. The picked colonies were incubated in 5 mL of LB medium with 5 μL ampicillin overnight to perform a Miniprep previous to confirm the insert gag/pol sequence was correct.

3.2.1.4 Transformation of mutagenesis products

NEB 5-alpha Competent *E. coli* cells were thawed on ice. 50 μL of NEB cells was mixed with 5 μL of the KDL mix or 2μL of the provided control DNA were added. The tube was mixed by flicking and placed on ice for 30 mins. Cells were heat-shocked at 42 °C for 30 secs and placed back on ice for 5 min. 500 μL or 950 μL for the control plasmid of SOC medium were pipetted into the mixture. The tubes were incubated at 37°C for 60 mins with shaking (225 rpm). Lastly 200 μL and 300 μL of cells were plated. For the puc19 DNA prior to plating a 1:10 dilution was performed and 100μL of the dilution were plate. Antibiotic selection plates were incubated overnight at 37 °C. The next day colonies were picked, a master plate was set up and a miniprep was performed. Positive clones were sequenced using the Q5Mut_seq_s primer (5'-AAGAAACCATCAATGAGGAAGC-3') and maxi preps were performed for the desired clones.

3.2.2 DNA preparations

3.2.2.1 Minipreparation

Minipreps were performed using buffers of the QIAprep Miniprep Kit and 100% isopropanol and 70% ethanol. 5 mL LB media inoculated with transformed bacteria was centrifuged at 4000 rpm for 10 minutes. 300 μL of resuspension buffer (P1) was added to each bacteria pellet.

Following re-suspension of the bacterial pellet, 300 μL of lysis buffer (P2) was added. The suspension was incubated for 5 mins, 300 μL of neutralisation buffer (N3) was added and the bacterial lysate was transferred to eppendorf tubes and were centrifuged at 14,000 rpm for 10 mins. The supernatants were transferred into new tubes containing 500 μL 100 % isopropanol and centrifuged at 14,000 rpm for 15 mins. Discarding the supernatant, tubes were tap dried on tissue paper. 500 μL 70% ethanol was added to each elution. Tubes were centrifuged at 14,000 rpm for 5 minutes and the supernatants were discarded. Tubes were dried at 80°C on a heat block. 50 μL of water were added to the tubes to bring into solution the plasmid DNA. Quantification and purity measurements were performed using the nanodrop and 1 μL of the plasmid was run on an 0.8% agarose gel. The preparations underwent quantification and quality control.

3.2.2.2 Midi preparation of constructs

Midipreps were performed using the Wizard® Plus Midipreps DNA Purification System. 150 mL bacteria cultures were centrifuged at 4,000 rpm for 10 minutes. 3 mL of resuspension buffer was added to each bacteria pellet and vortexed until pellet was re-suspended. 3 mL of lysis buffer was then added until suspension appeared translucent. 3 mL of neutralisation buffer was added and centrifuged at 4,000 rpm for 15 minutes. The supernatants were mixed with 10 mL purification resin, filled into columns and placed on a vacuum manifold. The samples were run through the columns completely, 30 mL of washing buffer was then filled into the columns twice. When all the liquid had passed through under vacuum, the filters of each column were placed into eppendorf tubes and centrifuged at 14,000 rpm for 3 minutes. Subsequently, the filters were transferred into new eppendorf tubes and 300 μL of water pre-warmed at 80°C were added to each tube and incubated for 5 minutes. Following centrifugation, the filters were discarded, and the eluent collected. The preparations underwent quantification and quality control.

3.2.2.3 Maxi preparation

To obtain high amounts of purified plasmid DNA, plasmids were amplified in *E. coli* and isolated with the QIAGEN plasmid Maxi Kit (QIAGEN) according to the manufacturer's manual. A 5 mL preculture was inoculated with the respective plasmid transformed *E. coli*

clone and propagated overnight. Approximately 500 μL of the preculture was transferred to 250 mL of sterile LB medium supplemented with 100 $\mu\text{g}/\text{mL}$ ampicillin and/or 25 $\mu\text{g}/\text{mL}$ kanamycin for selection. After overnight cultivation (16-20 h), the bacteria were pelleted (10 min; 4°C; 6,300 $\times g$) and plasmids were isolated and purified following the principle of alkaline lysis: In three consecutive steps, cells were resuspended in resuspension buffer, lysed in NaOH-solution, neutralised in sodium acetate solution and the released plasmid DNA was purified using an anion exchange column. After elution, the DNA was precipitated with 100 % isopropanol (v/v) and washed in 75% ethanol (v/v). The DNA precipitate was finally dissolved in 500 μL water.

3.2.3 Mutagenesis

3.2.3.1 Mutagenesis – Deletion of internal restriction sites

Proviral constructs CH058 TF and CH058 6mo carried an internal *XmaI* restriction site in the *gag-pol* sequence preventing the subsequent digestion and ligation step. Therefore, the sequence *cccggg* was mutagenised to *ccagga*, prior to cloning. Mutagenesis using the midipreps of the proviral templates and the Q5-site directed Mutagenesis kit was performed. The PCR reaction mixture was composed of 12.5 μL Q5 Hot Start High Fidelity 2X Master Mix, 1.25 μL of mutagenesis sense primer and 1.25 μL mutagenesis anti-sense primer (listed in table xxx) and 1-20 ng template DNA to a final volume of 25 μL with water. A control reaction supplied in the kit was performed following manufacturer's instructions. An extra positive internal mutagenesis control, using pUC19 DNA (100pg) was added. PCR conditions were as followed: initial denaturation at 98°C, 24 cycles of denaturation at 98°C for 10 secs; annealing at 60°C for 10 secs; extension at 72°C for 4 mins; followed by a final extension at 72°C for 2 mins after the cycling conditions. To digest the non-mutated parental DNA, amplified plasmid DNA containing the modified target sequence was DpnI (KDL)-treated using 1 μL of PCR product; 5 μL of 2x KDL reaction buffer and 1 μL 10x KDL enzyme mix to a final volume of 10 μL with water. The reaction was briefly vortexed and incubated for 5 mins at room temperature and the mutated plasmid DNA was transformed following the previously described method.

3.2.4 Cloning

3.2.4.1 gag-pol gene segment PCR-out

Production of lentiviral constructs as shown in table 14 containing the proviral derived gag and pol gene segment were cloned by High-Fidelity PCR using overhang primers. The forward primer overhang contained the Kozak and XhoI restriction site complementary to the plasmid sequence. The reverse primer overhang contained the XmaI restriction sequence complementary to the vector sequence. Primer sequences are found in table 17, 1:10 diluted midi prep prepared template were added to the PCR master mix. The PCR reaction mixture contained 25 μ L 2x Phusion-HF Master Mix; 2.5 μ L of sense primer and 2.5 μ L of antisense primer; 10 μ L of template DNA to a total volume of 50 μ L using water. PCR thermocycler conditions were performed; initial denaturation at 98°C for 30 secs, 34 cycles of denaturation at 98°C for 10 secs; annealing at 63°C for 30 secs; extension at 72°C for 3 mins 30 secs; followed by a final extension at 72°C for 5 mins after the cycling conditions were met.

3.2.4.2 Digestion of XhoI and XmaI containing constructs

Production of single-stranded PCR product overhangs for sticky-end ligation was performed using 20 μ L of template incubated with 2 μ L CutSmart Buffer and 1 μ L of the enzyme *XhoI* and *XmaI* for two hours at 37°C.

3.2.4.3 Agarose gel electrophoresis

Agarose gels were used for DNA purification of restriction-enzyme digested DNA for cloning. Agarose was dissolved in 1x TAE buffer to a final concentration of 0.8 % (w/v) and melted in a microwave. For the detection of DNA, SYBR Safe was added according to manufacturer's instructions. The DNA fragments were separated by continuous current using a voltage of 5-10 V/cm. The results were documented with a transilluminator system using UV light at 312 nm. DNA from was isolated with the QIAquick Gel Extraction Kit or the Gene Clean protocol.

3.2.4.4 QIAquick Gel Extraction Kit

The gene fragments were excised with a clean scalpel and transferred into a 1.5 mL eppendorf tube. Afterwards, DNA was isolated with the QIAquick Gel Extraction Kit, according the manufacturer's instructions. Briefly, the gel was dissolved, and the DNA was bound to a column and samples were eluted in 50 μ L water for further processing.

3.2.4.5 Gel dissolution and Gene Clean

The gene fragments of the correct size containing the insert DNA were cut out from the gel, placed in eppendorf tubes and cleaned with the Silica Bead DNA Gel Extraction Kit. 300 μ L binding buffer was added to the gel pieces and the tubes were shaken at 500 rpm at 55°C for 5 minutes. 5 μ L of the Silica powder was then added to each tube and incubated for 5 minutes with shaking at 55°C. Tubes were centrifuged for 20 seconds at 14,000 rpm and the supernatants were discarded. Pellets were washed and resuspended with 500 μ L of washing buffer. The centrifugation and washing step were repeated twice. After the third washing step, the silica pellets were dried at 55°C. Pellets were dissolved with 10 μ L of water and incubated for 5 minutes at 55°C. The tubes were centrifuged at 14,000 rpm for 5 minutes and the supernatant was then used for the ligation step.

3.2.4.6 Digestion of the pMDLg pRRE vector

The pMDLg pRRE vector containing an XhoI restriction site flanking the 5' end of the gag gene and an XmaI restriction site flanking the 3' end of the pol gene was linearised by restriction digestion. 2 μ g of the vector DNA, 2 μ L of the enzymes *XhoI*, *XmaI* and *EcoRV-HF*, 8 μ L of CutSmart Buffer and 64 μ L H₂O were mixed and incubated at 37°C overnight. 1 μ L was ran on an 0.8 % agarose gel at 140 mV in 1x TAE Buffer for approximatively 1 hr to confirm that the vector fragment pMDLg pRRE Δ gag/pol was excised. The pMDLg pRRE Δ gag/pol fragment was cleaned as described previous and eluted in 30 μ L of water.

3.2.4.7 Ligation

Ligation was performed by combining 2 μL of the cloned gag/pol insert, 0.5 μL of the pMDLg-pRRE $\Delta\text{gag-pol}$ vector and 2.5 μL of solution I of the Takara DNA Ligation Kit incubated for 1 hour at 16°C.

3.2.4.8 Digestion of ligated cloned gag/pol into pMDLg pRRE $\Delta\text{gag-pol}$

The digestion of the miniprep products was performed to confirm the incorporation of gag/pol insert. 5 μL DNA, 0.5 μL of the restriction enzymes *EcoRV-HF* and *XhoI*, 2 μL CutSmart Buffer and 12 μL H₂O were incubated for 1 hr at 37°C. The digested product was run on a 0.8% agarose gel at 140 mV in 1x TAE Buffer for 25 minutes. Positive clones were identified by two visible fragments on the gel while negative clones contained only one fragment.

3.2.4.9 DNA sequencing of clones

Confirmation by sequencing of positive clones was performed using 2 μL of DNA containing 720-1200 ng mixed with 3 μL of the primer (30pmol) to a final volume of 15 μL with water. DNA samples were sent for commercial sequencing (Seqlab, Göttingen).

3.2.4.10 Quantitative determination of nucleic acid concentrations

The concentration of DNA/RNA was measured with a NanoDrop ND1000 (PEQLAB) spectrophotometer at a wavelength of 260 nm. The quality of DNA/RNA was assessed by the ratio of OD₂₆₀/OD₂₈₀, which is theoretically optimal at 1.8 (DNA) and 2.0 (RNA) for highly purified nucleic acids. The Qubit fluorometer was used to quantify the amount of plasmid DNA. Using the Qubit dsDNA HS assay kit (HS = high sensitivity) plasmid concentration was determined in the range of 10 pg/ μL to 100 ng/ μL . The Qubit working solution was prepared using HS reagent diluted 1:200 in HS buffer. The two DNA standards (components A and B) as well as the plasmids were mixed 1:10 and 1:100 to a final volume of 200 μL in the working solution and incubated at room temperature for 5 minutes. The fluorescence of the dye was measured using the Qubit fluorometer and the DNA concentration was determined.

3.2.4.11 nested PCR amplification of gag-protease from proviral vectors

To amplify the *gag-protease* region from the proviral vectors obtained from Beatrice Hahn and Eric Hunter, the first-round PCR was performed using Phusion HF DNA polymerase, Hot Start version. 50 μ L of reaction mixture was composed of 25 μ L of 2 \times Phusion Master Mix, 2 μ L of 10 μ M forward and reverse, and 1 μ L of 1:10 diluted template DNA (<250ng) and water. Second-round PCR was performed using 100-mer primers that completely matched the pNL4-3 sequence using Phusion HF DNA polymerase, Hot Start version. 100 μ L of reaction mixture was composed of 25 μ L of 2 \times Phusion Master Mix, 6 μ L of 10 μ M forward primer and reverse primer, and 2 μ L of first-round PCR product and water. The forward primer overlapped the gag coding sequence by five bases (underlined), and the reverse primer ended just one base downstream of the protease gene. Thermal cycler conditions were as follows: 95°C for 2 min, followed by 40 cycles of 94°C for 30 s, 65°C for 30 s, and 72°C for 2 min and then followed by 7 min of 72°C. PCR products were purified with the QIAquick PCR Purification Kit and eluted in 50 μ L of DNase-RNase-free water.

3.2.5 Cell Culture

3.2.5.1 Cell lines

Cell line	Medium used	Passage frequency	Maximal density
HEK293 T cells	DMEM-GlutaMAX, 10% heat-inactivated FBS and 1% Penicillin-Streptomycin (10 units/mL penicillin and 1mg/mL streptomycin)	3 days	2 \times 10 ⁶ cells/mL
Jurkat cell lines	RPMI-1640, 10% heat-inactivated FBS and 1% Penicillin-Streptomycin (10 units/mL penicillin and 1mg/mL streptomycin)	2-3 days	5 \times 10 ⁵ cells/mL

OMK cell line	DMEM-GlutaMAX, 10% heat-inactivated FBS and 1% Penicillin-Streptomycin (10 units/mL penicillin and 1mg/mL streptomycin)	7 days	1×10^6 cells/mL
MT4 cell line	RPMI-1640, 10% heat-inactivated FBS and 1% Penicillin-Streptomycin (10 units/mL penicillin and 1mg/mL streptomycin)	2-3 days	5×10^5 cells/mL
THP-1 cell line	RPMI-1640, 10% heat-inactivated FBS and 1% Penicillin-Streptomycin (10 units/mL penicillin and 1mg/mL streptomycin)	2-3 days	5×10^5 cells/mL

3.2.5.2 Cryopreservation of cell lines

Cryopreservation was performed to store the cells lines at long-term. Cells were counted using a TC20 automated cell counter. The volume of a cell suspension was calculated for 10 to maximal 50×10^6 cells per mL, transferred into a 15 mL falcon and adjusted to 10 mL with DPBS. The cells were then centrifuged at room temperature for 5 min at 500 xg at maximum acceleration and deceleration. The cell pellet was resuspended in 1mL freezing solution (FBS supplemented with 10% DMSO) and transferred into a cryotube that was subsequently placed in a pre-cooled stratacooler held at 4°C. The stratacooler was stored at -80 °C overnight. The following day, the samples were transferred into the liquid nitrogen (LN) tank and maintained at -160 °C.

3.2.5.3 Cell thawing

Frozen vials were thawed in a water bath at 37 °C and cell suspension was transferred into a 15 mL falcon tube containing 9 mL cell culture medium, immediately centrifuged at room temperature for 5 mins at 500 xg at maximum acceleration and deceleration. After the

centrifugation step, the supernatant was discarded, and the pellet was resuspended in the corresponding cell culture medium at a concentration of 5×10^5 cells/mL and transferred to a T75 cell culture flask. The cells were maintained in the incubator at 37°C and 5% CO₂ in a humidified atmosphere.

3.2.6 Methods for the production of virus particles and reporter cell lines

3.2.6.1 Lipofectamine Transfection of Plasmid DNA

The following given numbers refer to a transfection done in a T75 flask. On the day before transfection, 2×10^6 cells were plated in 10 mL of growth medium (DMEM GlutaMAX +10% FBS) to ensure that the cells are 80-90% confluent on the day of transfection. On the day of transfection 60 µL of Lipofectamine 3000 was diluted in 750 µL of OptiMem and incubated for 5 min. 24 µg of plasmid DNA were diluted with 750 µL of OptiMem in a FACS tube. 750 µL of the diluted Lipofectamine were added dropwise to the FACS tube with the diluted DNA (1:1 ratio) and incubated at room temperature for 20 mins. The DNA-lipid complexes were added dropwise to the media overlaying the HEK 293T cells. The cells were incubated again at 37°C 48h, when the lentiviruses were harvested from the supernatant. The supernatant was centrifuged at 200 *xg* for 5 min and filtered through a 0.45 µm syringe filter. Aliquots of the lentiviruses (LV) were frozen down at -80°C.

3.2.6.2 Production of gag-prot chimeric HIV-1 by gene electrotransfer in MT4 cells

pSH0_GFP (transfer and selection plasmid), pRSV-Rev (helper plasmid) and pVSV-G (expression plasmid) constructs were transfected together with the pMDLg-pRRE gag-pol packaging plasmid for the production of the lentiviral particle containing gag-pol derived capsid from clinical isolates in addition to the pNL4-3-EGFPΔEnv mutated constructs.

In order to generate *gag-prot* chimeric viruses, a the pNL4-3ΔenvΔgagprot-eGFP was constructed by inserting the unique restriction enzyme site BstEII at the 5' end of *gag* and then 45 bases downstream from the 3' end of *protease*. This vector was then linearized by BstEII digestion at 60°C for 2 h and purified. MT4 cells, cultured until confluent in RPMI+10 media, were prepared at a concentration of 20×10^6 cells/mL in a 50 mL falcon. The cells were pelleted

at 500 g for 5 mins. Following centrifugation, the supernatant was discarded, and the pellet was resuspended in 1 mL of RPMI+10 media to a final concentration of 20×10^6 cells/mL. Electroporation cuvettes were labelled and the corresponding T25 flasks required for virus production. To the cuvettes, 500 ng *gag protease* was added with 100 ng of *BstEII* digested pNL4-3 $\Delta env \Delta gag prot$ -eGFP and 750 ng pCMV-VSVg along with 250 μ L of cells to a concentration of 5×10^6 cells/mL. The mixture of cells and DNA was rested for 10 mins to allow the DNA to stick to the lipid bilayer. Electroporation was performed at 250 V with a resistance of 975 μ F to allow the DNA to enter the cells. Following gene electrotransfer, the cells were resuspended in 10 mL of RPMI+10 with 25 μ L of fresh MT4 cells at a concentration of 5×10^5 cells/mL in a T25 flasks. At time points 24, 48, 72 hrs up to 5 days supernatant was collected and virus production was confirmed by p24 ELISA.

3.2.6.3 Production of CRISPR/Cas9 reporter Jurkat cells

HEK293T cells were transduced with 12 μ g pLentiCRISPR v2 containing the respective guide RNA (table 16), 9 μ g psPAX2 and 3 μ g pCMV-VSVg as previously described. Lenti-virus supernatant was harvested and stored at -80°C . Jurkat E.6.1 cells were transduced following the spinoculation described in the next section of titration of viral stocks. Targeted knock-down was performed by the transduction of 3 lentiviral particles targeting exonic regions of the gene of interest. Selection of successfully transduced clones was performed by adding 0.5 – 1 μ g/mL puromycin to the media. Confirmation of an efficient knockdown was confirmed by immunoblotting.

3.2.6.4 Concentration of viral stocks

48hrs post-transfection the lentiviruses were harvested from the supernatant and were centrifuged at 200 *xg* for 5 mins, but instead of the filter step the clarified supernatant was transferred to a new tube and was 30x concentrated through the Lenti-X reagent. Therefore, 3 mL of lentiviral supernatant was mixed with 1 mL of Lenti-X Concentrator and was incubated overnight at 4°C . The mixture was then centrifuged at 1,500 *xg* for 45 min at 4°C . The supernatant was carefully removed, and the pellet was resuspended in 100 μ L DMEM. Finally, the pellets were frozen down to -80°C .

3.2.6.5 Titration of Viral Stocks

Virus is titrated under the same conditions as the CsA washout assay using a 1/2 dilution series in the presence of CsA or EtOH. OMK cells are used for this assay due to their endogenous expression of TRIM-CypA. OMK cells were seeded out in a 96 well tissue flat bottom culture plate at a concentration of 10,000 cells/well 20-24h hours prior to the planned spinoculation step on the next day, to achieve 90% confluency on the next day. For each virus that was tested at least 12 wells of a 96 well plate was used with an additional 3 wells of uninfected cells in cell culture media as a negative control for flow cytometry. The medium with cells was around 200 μ L final volume.

On the next day, the medium was brought to room temperature and the centrifuge was cooled to 16°C. The prepared 10 cm round plates (LB plates) were taken out of the incubator before the next step so that they can get close to room temperature already. Next, the specific media's were prepared; 2X CsA media was prepared by adding 1 μ L of 5mM CsA and 1 μ L of 10 mg/mL polybrene to 1mL cell culture media. 1X CsA media was prepared by adding 0.5 μ L 5mM CsA and 0.5 μ L 10 mg/mL polybrene to 1 mL cell culture media. The 2X and 1X EtOH media was prepared the same way. Media was used at room temperature for the following steps until the spinoculation step. Media was aspirated from one row of the 96 well plate. 100 μ L 2X CsA media was added to the first well of a row. 100 μ L 1X CsA media was added to the next 5 wells. 100 μ L 2X EtOH media was added to the next well and 100 μ L 1X EtOH media was added to the next 5 wells. 100 μ L of virus was added to the first well of the row and pipette several times to mix with the media (1/2 dilution). 100 μ L was transferred to the next well of the row and pipetted to mix (1/4 dilution). The serial dilution was continued across the next 4 wells and the last 100 μ L was discarded into bleach solution waste container. The same serial dilution was performed with the EtOH test wells (second half of the row). The plate was placed in the centrifuge and spinoculated at 1,200 xg at 16°C for 1.5 hours. The CsA and EtOH media were prepared and stored at 4°C until the plate was removed from the centrifuge. The plate was removed from the centrifuge and incubated at 37°C for 30 minutes. The CsA and EtOH medium were placed in the water bath at 37°C. Inoculation media was aspirated from all wells and replaced with 200 μ L warmed CsA or EtOH media. The transduced cells were then incubated 2 days.

After 2 days the media was aspirated, and the cells were washed twice with 100 μ L PBS and

100 μ L of trypsin was added to each well. The LB plates were then incubated at 37°C for 10 min until the cells appeared small and round on the bottom of the plate. 100 μ L of 4% PFA was added to each well and pipette several times so that the cells detach from the surface. The edges of the plate were wrapped in parafilm, the entire plate was wrapped in foil and stored at 4°C for about 1 hour to allow any residual virus to fix. The fixed samples were analysed on a flow cytometer for GFP/FITC to determine the percentage of infected cells.

To determine the correct viral dilution to use the CsA and EtOH reactions were compared. A dilution where the percentage of infected cells in the CsA reaction is below 50% was chosen so that only one virus is infecting a cell. The percentage of GFP positive cells in the corresponding EtOH reaction should be 0–0.1% indicating that TRIM-CypA restriction is not saturated at that dilution. Viral dilutions that yield 30–40% GFP positive cells were chosen in order to observe changes in infectivity over a broad range. When comparing two or more viruses' dilutions were chosen for each virus that yield similar infectivity.

3.2.7 Preparation of RNA and Real-time PCR

3.2.7.1 RNA Extraction

Cell pellets were resuspended in 800 μ L-1000 μ L Trizol and vortexed for 1 min, incubated at RT for 5 mins and directly stored at -80°C. TRIzol samples were thawed on ice, vortexed briefly and placed on ice. 200 μ L of phenol-chloroform was added to each sample and was immediately shaken by hand for 15 sec and incubated at RT for 2-3 mins. Next, samples were centrifuged at >12,000 $\times g$ for 15 minutes at 4°C to obtain three phases: a lower, pinkish phenol-chloroform phase, an interphase and the upper colourless, aqueous phase containing the RNA. The upper colourless phase was transferred to a new RNase-free 1.5 mL Microcentrifuge tube where an equal volume of 70% Ethanol (~500 μ L) was added and vortexed briefly. All subsequent steps used the RNeasy Mini kit Qiagen Kit following manufacturer's instructions. RNA samples were eluted in 25 μ L-50 μ L of RNase-free water (dependent on amount of starting material) directly to the centre of the column membrane, incubated from 2 - 30 mins at RT and were centrifuged for 5 min at 10,000 rpm. The RNA concentration and purity were determined by nanodrop measurements. All samples were stored at -80°C.

3.2.7.2 DNase treatment

RNA concentrations >200 µg/mL were diluted to 0.2 µg/µL. 1µL of Dnase I (2U) removes genomic DNA for 10 µg RNA in a 50µL reaction. A DNase master mix was prepared using 1 µL RNase out, 3.33 µL ambion buffer, 3.33 µL DNase I (2U/µL). 8.3 µL/tube of DNase Master mix was added to 25µL of RNA extract and flicked and centrifuged briefly. Samples were incubated for 15 mins at 37°C before 3.3 µL/tube of EDTA 25mM was added, flicked and centrifuged briefly. Tubes were placed at 65°C for 10 mins and were briefly centrifuged. The preparations were split in two (2*25 µL), if enough RNA was extracted from the TRIzol step. Samples were stored at -80°C or were used directly in the cDNA step.

3.2.7.3 cDNA transcription

RNA was reverse-transcribed to cDNA serving as template for PCR detection. The Quanta Qscript cDNA supermix (Cat. No. QUNT95048-100) was used following manufacturer's instructions. After completion of cDNA synthesis, $1/5^{\text{th}}$ to $1/10^{\text{th}}$ of the first-strand reaction for was used for PCR amplification. Preparations were stored short term at 4°C or for longer at -20°C.

3.2.7.4 RT-PCR

For each primer set, a well with RNase-free water in place of sample was used as a control for master mix contamination. A housekeeping gene (HKG) primer set for normalisation was included and all samples were pipetted in duplicate. A RT-master mix was prepared using 5 µL 2X QuantiFast SYBR Green Master Mix, 2 µL RNase/DNase-free water, 0.5 µL sense primer (10uM) and 0.5 µL anti-sense primer (10uM) to a total volume of 8 µL. 8 µL of the master mix was pipetted into each well of a 200 µL PCR tube containing 2 µL of sample/RNase-free water. The RT-PCR cycling conditions are shown in the table 24.

	Temperature	Time	Number of cycles
RT	50 °C	10:00	1
Reactivation	95 °C	05:00	1
Cycling		95 °C	40
	(fluorescence acquisition step)	60 °C	
Melting curve	95 °C	00:15	1
	60 °C	00:15	1
	Ramp to 95 °C (continuous fluorescence acquisition)		
Cooling	40 °C	00:30	1

Table 24 PCR conditions for Real-time PCR

Controls:

- Ct values above **35** were excluded from analysis due to mis-priming and amplification of target DNA.
- Standard deviations of greater than 1 resulted in samples were not included for analysis.

Each sample was measured in duplicates and the average threshold cycle (CT) value served to calculate ΔCT for normalisation. Subsequently, $\Delta\Delta CT$ was calculated to determine the fold induction of the DNA of interest.

$$\text{Log}_2(\Delta Ct) = \text{mean}(Ct_{ref}) - \text{mean}(Ct_{sample})$$

$$\text{Log}_2(\Delta\Delta Ct) = \text{Log}_2(\Delta Ct_{Inf}) - \text{Log}_2(\Delta Ct_{uninfected})$$

$$\text{Fold expression} = 2^{-(\Delta\Delta Ct)}$$

1. Calculation of the ΔCt (correction to control): (gene in sample (Ct)) = (gene in control sample (Ct)) This correction was performed for each gene individually.
2. Calculation of the $\Delta\Delta Ct$ (internal correction to a housekeeping gene): (ΔCt of gene) = (ΔCt of GAPDH)
This was done for each gene accordingly.
3. Calculation of the relative expression level in the sample vs. the control: $2^{-(\Delta\Delta Ct \text{ of a gene})}$

3.2.8 Proteomic techniques

3.2.8.1 SILAC labelling of Jurkat and Jurkat CypA^{-/-} cells

Stable Isotope Labelling with Amino Acids in Cell Culture (SILAC) is a metabolic labelling technique for mass spectrometric (MS)-based quantitative proteomics. In SILAC, differentially labelled samples are mixed early in the experimental process, and analysed together by LC-MS/MS. To increase peptide coverage for MS analysis for double labelling, L-arginine-HCl was substituted for $^{13}\text{C}_6$ $^{15}\text{N}_4$ L-Arginine-HCl. 50 mg of labelled amino acids were dissolved independently in 1 mL of media and subsequently used to prepare 500 mL of RPMI+10 labelled as either the “Heavy” media, containing $^{13}\text{C}_6$ L-Lysine-2HCl (heavy), and the “Light” media, containing $^{13}\text{C}_6$ $^{15}\text{N}_4$ L-Arginine-HCl and L-Lysine-2HCL. Cells were cultured in heavy or light SILAC media until passage 8, where label incorporation efficiency is determined before subsequent experimentation.

3.2.8.2 Preparation of whole cell lysates for MS analysis

Isotopically labelled and unlabelled Jurkat E.6.1 cells IFN-stimulated and -unstimulated were lysed in 500 μL 1% w/v SDS (Sodium Deoxycholate) + 0.1 M TEAB buffer (SDS buffer) for 5 min at 98° C for protein denaturation. The samples were subsequently cooled on ice and centrifuged at 14,000 rpm for 10 mins. The supernatant was transferred to a new clean-ependorf tube, 1 μL of DNase was added and the vortexed briefly. This protein fraction was incubated for 30 min at room temperature to digest the genomic DNA and the protein concentration was determined by Bradford assay[270]. To determine if proteins are up or downregulated between the Jurkat CypA^{-/-} and the Jurkats upon IFN treatment the samples were mixed as follows:

Jurkat light label no stimulation with JurkatCypA^{-/-} heavy label no stimulation

Jurkat light label low stimulation with JurkatCypA^{-/-} heavy label low stimulation

Jurkat light label high stimulation with JurkatCypA^{-/-} heavy label high stimulation

Jurkat heavy label no stimulation with JurkatCypA^{-/-} light label no stimulation

Jurkat heavy label low stimulation with JurkatCypA^{-/-} light label low stimulation

Jurkat heavy label high stimulation with JurkatCypA^{-/-} light label high stimulation

Samples were flash frozen in liquid nitrogen and provided on dry ice to Prof. Dr.rer.nat Hartmut Schlüter at the Institute for Clinical Chemistry and Laboratory Medicine at the University Medical Centre Hamburg Eppendorf (UKE). The 6 samples from Mass spectrometry under the three conditions (no IFN stimulation, low and high stimulation) were compared. First, within each sample, the values of high and low intensity for each protein were taken and presented as a ratio: Ratio=High. Intensity/Low Intensity, where all zero values were preliminary replaced by 0.001. 0.25 and 0.75 quantiles among all the ratios per sample were calculated. All the proteins with ratios lower than 0.25 quantile were considered as down-regulated within the sample while proteins with ratios higher than 0.75 quantile were selected as up-regulated for this particular sample. Differently expressed proteins, which overlapped between two samples for each condition, were taken into further consideration. Only proteins, which were uniquely up- or down-regulated under the specific condition (low or high stimulation), were extracted and analysed as being involved in the response to the stimulation. GO-terms analysis and clustering of differently expressed proteins were performed using DAVID tool[271].

3.2.8.3 Preparation of whole cell lysates

Whole cell lysates were prepared with highly stringent RIPA lysis buffer containing protease inhibitors and EDTA. Briefly, cell lysates were cooled on ice and lysed in 500 µl RIPA buffer. To ensure efficient cell lysis, samples were incubated on ice for 30 mins and vortexed every 10 min. Afterwards, the cell debris as well as the insoluble fraction were pelleted (5 mins; 4 °C; 20,000 xg) and the supernatant was transferred to a new 1.5 mL reaction tube (Eppendorf). Protein concentrations were determined using the Bradford assay and adjusted to a total protein concentration of 1.5 - 4 mg/mL. For the reduction of disulphide bonds, 5x SDS sample buffer, containing 200 mM β-mercaptoethanol, was added before heat denaturation for 10 mins at 95 °C.

3.2.8.4 SDS – Polyacrylamide gel electrophoresis

Protein samples were separated on sodium dodecyl sulphate (SDS) polyacrylamide pre-cast gels according their molecular weight. PageRuler Prestained Protein Ladder Plus served as molecular weight marker, to estimate the size of the proteins of interest.

3.2.8.5 Western blotting

Following separation by SDS-PAGE, proteins were blotted onto nitrocellulose membranes using the Trans Blot Electrophoretic Transfer Cell System (Biorad). A “Gel Sandwich” was assembled on a gel holder cassette. The sandwich is made up of several layers, composed of the SDS acrylamide gel, placed on a nitrocellulose membrane and then two layers of TBS buffer-soaked blotting paper on each side. Electrophoretic transfer was performed in TBE buffer for 3 mins at continuous current per blotting chamber. Non-specific antibody binding sites were blocked with PBS containing 5 % non-fat dry milk powder for 1 hr at RT. All antibodies used are listed in table x. To ensure that all membranes are equally immersed in the wash buffer and anti-body suspensions, all incubation steps were carried out on an orbital shaker. After blocking, the solution was discarded, and the membranes were washed three times for 5 min in TBS. For the detection of proteins, specific primary antibodies were incubated for at least 2 h (or overnight) at 4 °C. The primary antibody was removed, by washing three times for 15 min with TBS at RT. Afterwards the secondary HRP-conjugated antibodies were diluted 1:10.000 in 5 % non-fat dry milk powder PBS solution and incubated for 2 h at RT. Finally, the secondary antibody was also removed in three 10 min washing steps and protein bands were visualised by enhanced chemiluminescence using SuperSignal West Pico Chemiluminescent Substrate according the manufacturer’s instructions. The protein signals were detected using a transilluminator connected to a camera.

3.2.9 PBMC Acquisition

3.2.9.1 Peripheral blood sample acquisition

Peripheral blood samples were obtained from selected healthy blood donors recruited at the Research Department for Virus Immunology, Heinrich Pette Institute Leibniz Institute for Experimental Virology, Hamburg. All blood donors gave were consented in compliance with the ethics committee of the Ärztekammer Hamburg (German Medical Association). EDTA-blood was fractionated through density gradient centrifugation using Biocoll to obtain peripheral blood mononuclear cells (PBMCs).

3.2.9.2 PBMC isolation through density gradient centrifugation

The isolation of the PBMCs was performed in order to separate blood components according to their differences in size, density and aggregation behaviour. The separation takes place by layering blood on a separation solution (biocoll) following centrifugation. Full blood liquid biopsy donations are enriched in thrombocytes, monocytes, lymphocytes and granulocytes. The donation was equally distributed into two 50 mL falcon tubes (20 mL blood per falcon) and each tube was mixed with 15 mL HBSS (Hanks' balanced salt solution). Afterwards, each of the blood-HBSS mixtures were carefully layered on room-tempered 15 mL biocoll separation solution in a new 50 mL falcon tube. The samples were then centrifuged at room temperature for 30 min at 500 *xg*, with the lowest level of acceleration and with the brake turned off. Following centrifugation, the samples were separated into three compartmental layers. The upper yellow layer consisted of fresh plasma, the lower dark red layer contains the erythrocytes and the middle layer, which separated the plasma from the erythrocytes was composed of the PBMCs. The PBMC compartment contains thrombocytes, monocytes, lymphocytes and granulocytes. This layer was carefully removed from the other layers and transferred into a new 15 mL falcon tube. The samples were centrifuged at room temperature for 15 min at 500 *xg* and maximum acceleration and deceleration, to wash the cells and separate them from the biocoll-containing surrounding solution. Following centrifugation, the supernatant was discarded, equal pellets were pooled and re-suspended in 10 mL HBSS. The samples were centrifuged at room temperature for 13 min at 300 *xg* at maximum acceleration and deceleration, to separate the lymphocytes from thrombocytes. Subsequently, the supernatant was discarded, and the pellet was re-suspended in 50 mL cell RPMI+10. The cells were counted and transferred into cell culture flasks in a concentration of $2-4 \times 10^6$ cells/mL cell culture medium supplemented with 100 ng/mL gM-CSF and stored in the incubator at 37°C and 5% CO₂ for infection assays.

3.2.10 Functional Experiments

3.2.10.1 The IFN sensitivity assay

To determine the sensitivity of Jurkat and Jurkat reporter cells to IFN and HIV-1 infection, the IFN sensitivity assay was established based on the measurement of the cellular effect of increasing concentrations of IFN (figure 38). In the setting of viral infection, a standardised

titre of virus was added as determined from titration of viral stocks in OMK cells. On day 1, a serial 1:5 dilution of IFN media was prepared at twice the final concentration as this was diluted 1:2. 75,000 U of IFN alpha (Peprotec #300-02A, according to the cytotoxicity assay using TF-1 cells was written in the spec sheet) (75µL of 1000U/µL Stock solutions) was added to 3,75 mL of RPMI+10 to a concentration of 10,000 U/mL. 14 tubes were then prepared with 3 mL of RPMI10+1 with 750 µL (20,000 U/mL) added to the first tube and then was further diluted. 350µL of IFN-Media was pipetted into wells of a flat shaped-well. 100µL of this “Media-plate” was transferred into a new U-well-96 well plate maintaining the same plate format 3 U-well shaped plates were prepared. The cells are prepared at a concentration of 1×10^6 /mL and 100µL of cells were added to each of the prepared wells with 100µL of respective IFN media using a multipipette. 200 µL of R10 plus pen/strep as then added to the edge wells of the plate and the plates containing cell were incubates in IFN-Media for 4 hours.

For experimental determination of the effect of virus restriction under IFN conditions, a determined amount of virus stocks can be added to the dilutions. The IFN-titrations from the morning were removed out of the fridge and a new “Media-Plate” was prepared according to the previous plate layout (table 25) and placed it at room temperature. Plates were incubated for 30 mins and the plates were then centrifuged at 500 *xg* for 5 mins. The supernatant was removed, and the cells were resuspended in fresh IFN-titration media. Cells were spinoculated at 1200 *xg* for 90 mins at 22°C and incubated at 37°C for 30 mins with the virus added. The plates were then incubated for 24 hours. On day 3, the cell plates were centrifuged at 500 *xg* for 5 mins and the supernatant was removed. The cells were washed by resuspending the pellet in 200 µL of FACS-Buffer (2% FBS in PBS) and centrifuged at 500 *xg* for 5 mins. The supernatant was removed, and the cells were resuspended in 120 µL PBS + 100 µL 4% PFA and were fixed for 30 mins in the fridge at 4°C. Flow cytometry was performed to determine the amount of GFP+ cells. For experiments were no virus was added and the effect of IFN was determined, qPCR, Immunoblotting and mass spectrometry studies were performed. Reporter cells were kept under puromycin selection at a concentration of 0.5 µg/mL.

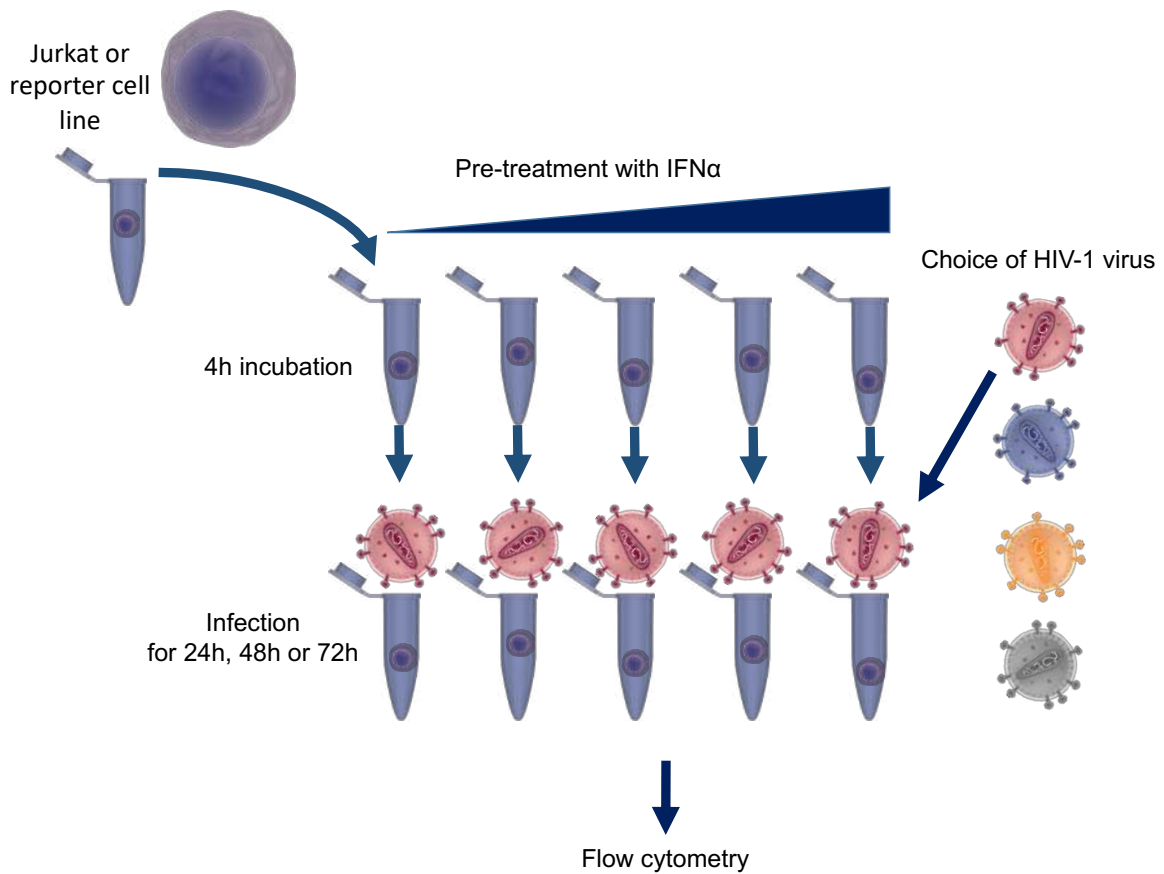


Figure 38 Cartoon of pre-treated cells under increasing IFN α 2a concentrations with the addition of viral suspension.

	1	2	3	4	5	6	7	8	9	10	11	12
A	Medium	Medium	Medium	Medium	Medium	Medium	Medium	Medium	Medium	Medium	Medium	Medium
B	Medium	10000	2000	400	80	16	3.2	0.64	0.128	0.0256	0.00512	Medium
C	Medium	0.001024	0.0002	0.00004	0.000008	No IFN	10000	2000	400	80	16	Medium
D	Medium	3.2	0.64	0.128	0.0256	0.00512	0.001024	0.0002	0.00004	0.000008	No IFN	Medium
E	Medium	10000	2000	400	80	16	3.2	0.64	0.128	0.0256	0.00512	Medium
F	Medium	0.001024	0.0002	0.00004	0.000008	No IFN	10000	2000	400	80	16	Medium
G	Medium	3.2	0.64	0.128	0.0256	0.00512	0.001024	0.0002	0.00004	0.000008	No IFN	Medium
H	Medium	Medium	Medium	Medium	Medium	Medium	Medium	Medium	Medium	Medium	Medium	Medium

Table 25 Plate layout used for the correct pipetting strategy.

Tabulated pipetting schematic for IFN α 2a. Numbers are represented in U/mL of IFN α 2a.

3.2.10.2 The MDM infection assay

3.2.10.2.1 Isolation of monocyte-derived macrophages (MDM) from EDTA tubes

Superseding PBMC isolation by density gradient centrifugation, the pellet was resuspended in 10 mL RPMI supplemented with 10% (v/v) heat-inactivated FBS, L-glutamine (2 mM), streptomycin (100 μ g/mL), penicillin (100 U/mL) and cells were counted using an automated haemocytometer following manufacturer's instructions. Cells were then resuspended with RPMI1640, 10% heat-inactivated human AB serum, 100 ng/mL gM-CSF to a final concentration of 6×10^6 cells/mL. On day 3 (72 h after isolation), MDMs were re-plated at a

concentration of 100,000 cells per well in 1 mL MDM medium (DMEM + 10% heat-inactivated human AB serum + 100 ng/mL gM-CSF). 5 days after isolation, the MDMs were ready HIV-1 infection (figures 39 & 40).

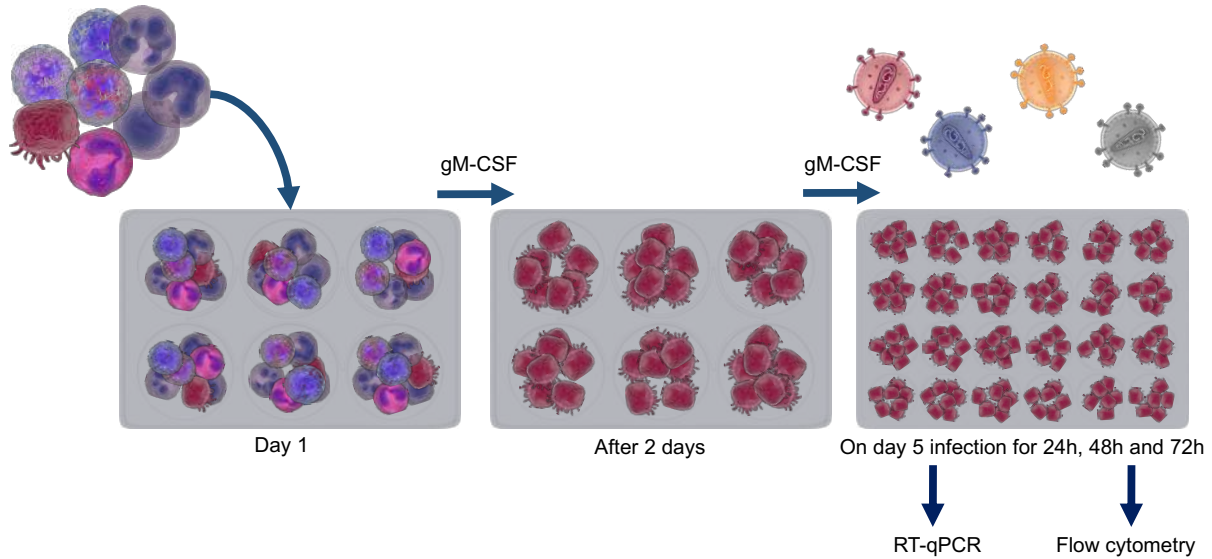


Figure 39 Representative workflow of the MDM assay.

		Infected Cells				LPS	
		0	24	48	72	LOW	HIGH
WT	A	0	24	48	72	0	0
RK	B	0	24	48	72	24	24
RKLM	C	0	24	48	72	48	48
SARKLM	D	0	24	48	72	72	72

Figure 40 Plate set-up for the infection of MDMs.

3.2.10.2.2 Preparation of MDMs for RNA extraction, antibody staining and supernatant ELISA

Following infection, at the appropriate time point, the 24 well plate was removed from the incubator and the media supernatant was collected and frozen at -80 °C for subsequent ELISA assays. The cells were washed with PBS before adding 200 µL of trypsin and incubated until the detachment of the MDMs. Then, 200 µL of DMEM+10 media was added and 100 µL was removed to a new tube for RNA extraction. Cells were pelleted, 800 µL of TRIzol were added

to the pellet and the sample was vortexed for 1 – 2 minutes and transferred for storage at -80C. The remaining 300 µL volume of cells was transferred to a FACs tube for cell surface staining and intracellular p24 staining.

3.2.10.2.3 MDM staining for flow cytometry analysis

Compensation beads were prepared by adding 1µL of antibody to 1 drop of beads in 100 µL PBS. Beads were stained with an APC-Cy7 antibody to compensate for the Zombie Nir stain for the detection of live/dead cells. Stained MDMs were used as a positive control. Negative controls used were unstained MDMs, unstained J89Cas9Δ*vpv* (which constitutively express GFP) cells and unstained beads. 100 µL of the following master mix was added to the pellet of MDMs and incubated for 20 mins at room temperature in the dark:

Antibodies	V for 1 sample (µl)
CD69 BV421	1
CD83 BV510	1
CD80 BV605	1
CD86 PE Cy5	1
LD Zombie Nir	1 (1/10)
PBS	95

Table 26 Antibody master mix.

100 µL of fixation reagent (Medium A) was added and the cells were incubated for 20 min at room temperature. The cells were washed with 200 µL PBS/2% FBS. Supernatant was discarded and cell pellet was resuspended in 1 µL of p24 PE stain (KC57-FITC) and 99 µL of permeabilisation reagent (Medium B) and incubated for 20 mins at room temperature in the dark. Cells were washed in 200 µL PBS/2% FBS and resuspended in 200 µL PBS/FBS. Fixed and stained cells plus controls were then analysed by flow cytometry.

3.2.10.3 ELISA assays

3.2.10.3.1 Determination of cytokine and HIV-1 production by ELISA

For the validation of cytokine production, the ELISA Kit's for Human TNF-α, Human IL-10 and Human IL1B were used following the manufacturers protocol (table x). Cytokine

quantification was determined by fitting to standard curves. ELISA's were performed using cell culture media supernatant from MDM infection assays.

For the validation of virus production, the ELISA Kit for Human p24 antigen, was used following the manufacturer's protocol. HIV-1 quantification was determined by fitting to standard curves. ELISA plates were subsequently measured in a TECAN photospectrometer at 595nm.

3.2.10.4 Fluidigm

Fluidigm is a microfluidic-based technology that enables single cell preparation, RNA extraction, reverse transcription and PCR amplification. The Fluidigm C1 system was used for targeted gene expression analysis on single cells to reveal the differences between Jurkat cells and Jurkat CypA KO cells in a T cell gene panel of 96 primers (table 22).

3.2.10.4.1 Single cell capture and cDNA synthesis

For each culture condition, 4,000 cells were loaded on to a 10-17 micron Fluidigm C1 Single-Cell Auto Prep IFC, and cell capture was performed according to the manufacturer's instructions. The capture efficiency was determined using a microscope to exclude samples from the analysis with no or more than one cell captured or samples were in addition to cell there was cellular debris visible. Upon capture, reverse transcription and cDNA preamplification were performed in the 10-17 microns Fluidigm C1 Single-Cell Auto Prep IFC according to the manufacturers protocol.

3.2.10.4.2 Quantitative PCR (qPCR) using 96.96 Dynamic Array Integrated Fluidic Circuits

The BioMark System 96.96 Dynamic Array is a high-throughput platform allowing the user to combine 96 samples with 96 primer pairs into 9,216 qPCRs in one integrated fluidic circuit (IFC). The system includes optical, thermal cycling and software modules to perform quantitative PCR. The Dynamic Array IFC is a nanofluidic network permitting 24-fold more reactions compared to 384-well plate format. Advantageously the liquid handling steps, number of pipetting steps and reaction volumes are all significantly reduced. The high-resolution CCD

camera that detects the whole chip area collecting images of all the reactions simultaneously allows for fast data collection and reduces waiting times. The quantification cycle (C_q) values from each reaction chamber in the chip are visualised as an easy to view heat map.

3.2.10.4.3 Preamplification

Preamplification was performed using TaqMan PreAmp Master Mix. 200 nM primer mix was prepared from stock concentration and were combined in equal concentration of all primers used in the following qPCR. TaqMan PreAmp Master Mix (10 µL) was mixed with 5 µL of 200 nM stock primer mix and 5 µL of cDNA in concentration of approximately 185 ng/µL. Reaction tubes were vortexed and centrifuged before PCR. All samples were incubated at 95°C for 10 min and amplified through 14 cycles of 95°C for 15 secs and 60°C for 4 min. Pre-amplified cDNA was then processed in the next step for qPCR amplification and detection.

3.2.10.4.4 Quantitative PCR assay and sample master mix preparation

The quantitative PCR assay mix was prepared by mixing 2.5 µL 2X Assay Loading Reagent, 2.3 µL of primer pair mix and 0.2 µL low EDTA TE buffer to a reaction volume of 5 µL per assay mix. The sample mix was prepared by mixing 2.5 µL TaqMan Gene Expression Master Mix (Applied Biosystems; PN 4369016), 0.25 µL 20X DNA Binding Dye Sample Loading Reagent, 20X EvaGreen DNA binding dye and 2 µL of pre-amplified cDNA to a reaction volume of 5 µL per sample mix.

3.2.10.4.5 Chip priming

96.96 Dynamic Array IFC was primed by injecting 150 µL of control line fluid into each accumulator on the chip followed by placing the chip into the Integrated Fluidic Circuit (IFC) controller and running the Chip Prime (138x) script.

3.2.10.4.6 Chip loading

The assay mix and sample mix solutions (5 μ L) were pipetted into the inlets on the chip after priming. Using IFC controller software, Load Mix (138x) script was applied. After loading finished, the chip was removed from IFC controller.

3.2.10.4.7 qPCR and data analysis

Quantitative PCR was performed in the BioMark HD instrument using the Data Collection Software. The loaded chip was placed into the reader. After barcode verification, application was set as Gene Expression (GE), passive reference as ROX, probe as single probe and probe type as EvaGreen. Thermal cycling protocol was chosen for 96.96 chip: GE 96x96 PCR+Melt v1.pcl. Auto Exposure was confirmed, and the program was verified. Thermal conditions for GE 96x96 qPCR: Thermal mix: 50°C for 2 min 70°C for 30 min 25°C for 10 min; Hot start: 50°C for 2 min 95°C for 10 min; PCR cycle (x30): 95°C for 15 sec 60°C for 60 sec; Melting: 60°C for 3 sec to 95°C. Real-Time PCR Analysis software was used to visualise results. Analysis of Fluidigm Data and creation of Violin plots was done using the Singular Analysis Toolset Software (Fluidigm) in R Studio (Version 3.4.0) according to the instructions provided by Fluidigm.

3.2.10.5 The Cyclosporine washout assay

The CsA washout assay (shown in figure 41) was performed to determine the uncoating kinetics of capsid dissociation and was assessed by the number of GFP⁺ single cells after gating. OMK cells were plated in a 96-wellplate 1 day prior to starting the CsA washout assay. On day 2, wild-type HIV-GFP or HIV-GFP containing the point mutations or lenti-viral particles, together with CsA and Polybrene, was added to OMK cells following spinoculation for 90 min at 1,200 xg cooled to 16°C. After spinoculation, medium containing HIV-GFP, CsA, and Polybrene was removed and replaced by pre-warmed DMEM10 with CsA. At time points 0, 1, 2,3, 4, and 5 h, the medium was replaced by DMEM lacking CsA, and therefore, CsA was washed out of the cell culture. Additionally, an aliquot of medium with HIV-GFP, CsA, and Polybrene was left after spinoculation as a positive control. Two days after infection, cells were harvested with trypsin, and the percentage of GFP⁺ cells was determined by FACS analysis. As an increasing

number of capsids uncoated over time and uncoated particles were not inhibited any longer by the endogenous Trim-CypA of OMK cells, increasing amounts of GFP⁺ OMK cells were observed over time when cells were harvested and analysed after 2 days. At each time point, the CsA washout assay was performed in triplicate for each virus, and two viruses were directly compared on a single plate, resulting in 60 wells used per plate. To determine the half-life of capsid uncoating, the best-fit line was drawn between the 2 time points within which 50% of the cells were infected.

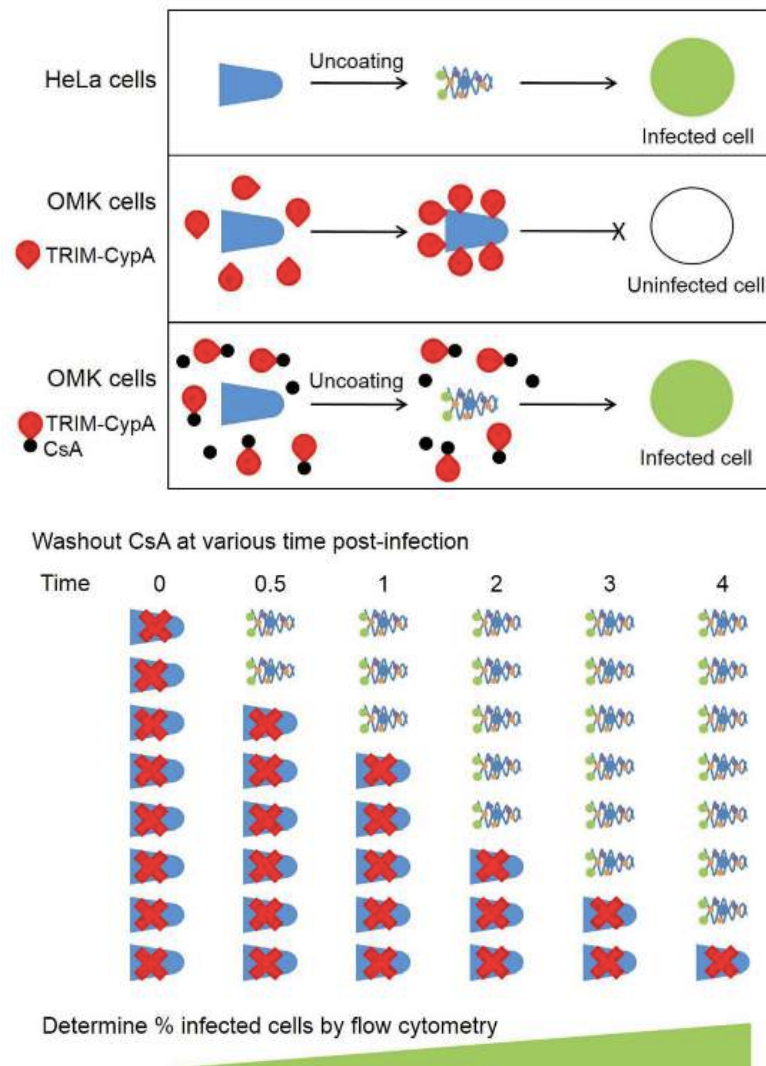


Figure 41 Mechanism of the CsA washout assay

HIV GFP reporter virus infection of OMK cells in the presence of CsA determined by flow cytometry. HIV uncoats and infects HeLa cells and OMK cells that can be assayed using flow cytometry. In OMK cells TRIM-CypA binds to the capsid to restricts HIV infection. HIV can infect OMK cells in the presence of cyclosporine A (CsA) that binds to TRIM-CypA, thereby, preventing its binding to the HIV capsid (taken from [272]).

4. Discussion

4.1 HLA and Capsid mutants

Well reported is the role that HLA class I molecules play in equipping the immune system against HIV-1 infection and disease progression. The anti-retroviral response mediated by the different HLA molecules are discrete and reflect the heterogeneity of polymorphisms within the human population[190]. Particular HLA molecules have associations between the signature of the immune response and the differential HIV-1 disease outcomes and progression towards AIDS[273]. Widely described is the observed HLA-mediated CTL response in suppressing HIV-1 infection and in the maintenance of immune control in the early phase and later phases during an individual's disease progression [183, 188, 202, 251]. Nevertheless, HIV-1-specific CD8⁺ T cell mediated immunity is unable to eliminate the virus completely and viral reservoirs can persist over many decades in latently infected cells[274]. There is, however, a rare faction of individuals (<1% in the population) expressing protective HLA-B alleles that are able to provide long term control in the setting of antiretroviral therapy, whereby, their immune system are actively suppressing viral load to undetectable levels[275]. Over many years, a focus of HIV-1 research has been on elucidating the anti-viral mechanism in these elite controllers in order to develop a vaccine or achieve functional cure[276]. A major factor that impairs CTL immune control are viral escape mutations from the epitopes targeted by T cells. Escape mutations are disingenuous acting to help the virus evade host immune surveillance at the potential cost of reducing the viral replicative capacity. Compensatory mutations can re-instate the fitness cost caused by escape mutations. It was shown that CTL-driven escape mutations within p24 Gag restricted by protective HLA class I alleles have a significant impact on capsid stability [3]. Differences in capsid stability might contribute to the persistent control of viral replication observed despite viral escape from CTL orchestrated responses[248].

One of the defining characteristics of HIV-1 is the disparity in the time between initial infection to the progression towards AIDS. Few infected individuals experience a very rapid progression of the disease and the development of AIDS within one year of infection[277]. Opposingly other infected individuals have not developed AIDS after more than 25 years following infection[278]. The mechanisms leading to this heterogeneity in the speed of HIV-1 disease progression remain incompletely understood, but several studies have now demonstrated that host genetic factors, and in particular the expression of specific HLA class I alleles, are

responsible for these differences in HIV-1 disease outcome. It has also been shown that the expression of HLA-B57 and HLA-B27 is significantly associated with slower HIV-1 disease progression[279-281]. A large genome-wide association study (GWAS) performed in individuals that were able to control virus replication at low levels in the absence of antiretroviral therapy demonstrated that single nucleotide polymorphisms (SNPs) associated with viral control were all located in HLA class I genes[183]. These studies revealed HLA-B57, and to a lesser extent HLA-B27, as those HLA class I alleles most strongly associated with viral control. Functional studies have also demonstrated that virus-specific CD8⁺ T cell responses in HIV-1-infected individuals encoding for protective HLA class I alleles developed early during primary infection[282, 283] and contributed over-proportionally to the total HIV-1-specific immune directed response[279]. Taken together, protective HLA class I alleles HLA-B27 and –B57 displayed better control of viral replication and slower HIV-1- disease progression and developed strong virus-specific immune responses restricted by these HLA class I molecules.

In this dissertation, I have examined the impact of cytotoxic T-lymphocyte (CTL)-driven viral escape mutations within HIV-1 capsids on capsid stability and innate immune sensing. Using a VSV-G-pseudotyped HIV-1 NL4-3ΔEnv strain expressing GFP (enabling flow cytometric quantification of infected cells producing viral proteins by measuring GFP⁺ cells), viral infection of cells was standardised. Changes in GFP⁺ cells were a result of post-fusion differences, including capsid uncoating, reverse transcription, formation of the PIC, integration of cDNA into the host genome, and GFP transcription and translation. VSV-G pseudotyping was used for all the viruses that were used in this dissertation. Infection assays and the CsA washout assay is based on the use of MDM's and OMK cells, respectively. In order to begin to correlate capsid uncoating and infectivity, VSV-G-pseudotyped viral strains were used in all the assays applied, even though VSV-G pseudotyping has been reported to modify entry pathways compared to viruses with the native HIV-1 envelope[284, 285]. Viruses containing HLA-B27-associated mutations were generated by cloning clinical isolate derived *gag/pol* into the expression vector pMDLg-pRRE and the NL4-3 vector, respectively. Given that HLA-B27- and HLA-B57-associated sequence mutations used in this study were all located in HIV-1 p24 Gag, which encodes capsid, the impact of these mutations on infectivity would have been affected by the process of capsid uncoating following infection. The difference between the percentage of GFP⁺ cells as measured using the CsA washout assay would have been due to differences in capsid stability and can be attributed to the different mutations. However, due to

premature uncoating these experiments were discontinued using the 3rd generation lenti-viral packaging system approach. This was due to the percentage of GFP⁺ cells being above an acceptable threshold of 10% to accurately determine the uncoating time. Unfortunately, the newer approach of generating NL4-3 *gag/pol* chimera's failed and the latter approach adapted from Bruce Walker and colleagues methodology did not yield detectable p24[189, 260]. HIV employs a sophisticated system of differential RNA splicing to obtain capsid packaging its RNA genome. It is likely the *gag/pol* and *gag protease* gene segments do not package the RNA genome correctly using the NL4-3 backbone or that the level of transcription is too low to yield particles without the aid of a strong CMV promoter. In order to continue to study capsid stability, selection of mutations in Gag epitope ISPRTLNAW (IW9; Gag 147 to 155) and Gag epitope KAFSPEVIPMF (KF11; Gag 162 to 172) can be introduced into the NL4-3 lab adapted strain. These two peptide-binding motifs in the Gag protein are recognised by HLA-B*27/B*57, as these epitopes may be crucial for the control of viral replication. Our lab previously reported differences in capsid stability of point mutations introduced into the Gag epitope KRWIILGLNK (KK10; Gag 263–272)[3].

It has been reported that better HIV-1 disease outcome in individuals encoding for HLA-B57 and -B27 is associated with the selection of viruses containing immune escape mutations within capsid[286]. HIV-1-specific CD8⁺ T cell responses restricted by HLA-B alleles are directed against HIV-1 Gag, but not HIV-1 Env, were associated with better control of viremia[188, 193]. A number of subsequent studies showed that including those conducted within our department [287], reported that the virus can escape from these virus-specific T cell responses by the selection of point mutations either within targeted cytotoxic T lymphocytes (CTL) epitopes impairing their recognition by epitope-specific CTLs or flanking these epitopes and impairing their processing and presentation[224, 288]. Even those CTL responses restricted by protective HLA class I alleles, such as HLA-B27 and –B57, resulted in viral escape from CTL mediated immune pressure. Curiously, however, these escape mutations were frequently located within areas of low viral entropy[213], and in particular within HIV-1 p24 capsid, suggesting functional restraints and consequences of these viral immune escape mutations (reviewed in [289]). I hypothesised that p24 escape mutations may increase immune sensing and activation. However, increased TNF- α production was not observed upon viral infection of the capsid escape mutants p24 Gag R254K and p24 Gag R264K plus p24 Gag L268M or by the compensatory mutant p24 Gag S173A plus p24 Gag R264K plus p24 Gag L268M compared to WT. On the contrary I observed that viral fitness was highly affected by p24 escape

mutations. In conclusion I report that p24 escape mutations p24 Gag R264K and p24 Gag R264K plus p24 Gag LM do not increase viral sensitivity of HIV-1. This I hypothesise is due to host restriction factors being unable to fully interact with the binding caused by steric hindrance induced by these mutations. The second hypothesis is that the capsid structure is more rigid and uncoats at the nuclear pore complex through interaction with nucleoporins. Taken together, these studies demonstrated that, in the context of protective HIV-1-specific CD8⁺ T cell responses, restriction by HLA-B27 and –B57 target very conserved regions of the virus, and in particular p24 capsid structures, and resulted in sequence mutations within capsid as a result of the virus attempting to evade these strong antiviral immune responses.

Mutations within the Gag epitope KAFSPEVIPMF (KF11; Gag 162 to 172), and to a lesser extent the Gag epitope ISPRTLNAW (IW9; Gag 147 to 155), might strongly affect capsid stability due to their location close to the pore structure. The escape mutations within Gag epitope KAFSPEVIPMF (KF11; Gag 162 to 172), e.g. p24 Gag A163X (principally p24 Gag A163G), have been shown to be strongly associated with the presence of HLA-B*5703 genotype, and have a high fitness cost for the virus[290-292]. The viral replication capacity of p24 Gag A163G was demonstrated to be restored by the additional compensatory p24 Gag S165N mutation[292]. This could explain the persistence of the p24 Gag A163G plus p24 Gag S165N mutant in HLA- B*5703-negative persons and the rapid reversion of p24 Gag A163G when it occurs alone. It can be hypothesised that the introduction of either p24 Gag A163G or p24 Gag S165N into the NL43 backbone in combination with p24 Gag S173T also significantly reduces viral spread, but substantially more than in the absence of p24 Gag S173T due to differences in capsid uncoating. The effect of combining the p24 Gag S173T and both of the KF11 mutations, p24 Gag A163G and p24 Gag S165N, upon capsid stability might result in a significant cost to viral fitness of this combination of viral mutations in a B clade virus. Gag epitope KAFSPEVIPMF (KF11; Gag 162 to 172) escape mutant p24 Gag S173T is more commonly selected in B clade virus-infected subjects expressing HLA-B*57:03. Subsequent mutations in addition to p24 Gag S173T may result in altered capsid stability.

Immune escape mutations within capsid associated with slower disease progression are located within structurally conserved areas. To further elucidate the role of viral immune escape mutations for capsid structure, our department and others investigated the precise location of these mutations, and initial results demonstrated that viral escape mutations from CD8⁺ T cell responses restricted by HLA-B27 and –B57 were located in very conserved area of p24

Gag[248, 293, 294]. A more comprehensive study revealed that individuals whom robustly controlled HIV-1 without therapy favourably targeted regions within capsid with higher order evolutionary constraints, indicating previously unrecognised multidimensional constraints on viral evolution within HIV-1 capsid[213]. The results obtained in this thesis indicated that mutations in HIV-1 might depend upon CypA-mediated restriction. Cyclophilin A might then act to stabilise the capsid through a novel non-canonical binding site. CTL escape mutations rendered HIV-1 to be more sensitive to IFN α mediated restriction. Moreover, upon an IFN α 2a stimulation in Jurkat CypA $^{-/-}$, cells, we observed a complete viral replication abrogation of WT and p24 escape mutants p24 Gag R264K and p24 Gag R264K plus p24 Gag L268M and the compensatory mutant p24 Gag S173A plus p24 Gag R264K plus p24 Gag L268M. These results suggested that CypA competitively bounded capsid for timely uncoating and protected against complete restriction, by an unknown innate sensor. Taken together, these studies support previous findings that immune responses restricted by protective HLA class I molecules targeted highly conserved regions within HIV-1 capsid and might have functional consequences for viral structure and function.

HLA-B57- and HLA-B27-associated mutations within HIV-1 capsid have been linked to reduced viral fitness[46, 248, 293]. Investigations of HIV-1 transmission and evolution in the setting of mother-to-child transmission have demonstrated that viral escape mutations within HIV-1 capsid that developed in an infected mother encoding for HLA-B57 rapidly reverted back to wild type following transmission to a child that did not encode for HLA-B57, but persisted in children that also encoded for HLA-B57[280]. Reversion of CTL escape mutations was also reported in a cohort of sexually infected individuals following primary infection and in humanised mouse models infected with HIV-1[295, 296]. These observations led to further studies to assess the consequences of CTL escape mutations on viral replication fitness, which revealed that HLA-B57- and HLA-B27-driven mutations within HIV-1 capsid resulted in reduced viral fitness[248, 293]. By using immortalised cell lines and PBMCs, further studies were able to measure viral replication capacity, and reproduce previous results. Furthermore, it demonstrated that mutations within capsid that emerge as a consequence of HLA-B27-restricted CD8 $^{+}$ T cell responses directed against an immunodominant epitope within p24 Gag resulted in a significant reduction of viral replicative fitness that was reconstituted through the selection of compensatory mutations, as previously described[248]. These studies demonstrated that CTL escape mutations within p24 capsid could result in a significant reduction in VRC.

4.2 Oligonucleotide Innate sensing

Mammalian cells are exposed to various encounters from exogenous pathogens such as retroviruses and endogenous parasitic nucleic acids such as retrotransposons. Consequently, cells have evolved various host-defence mechanisms in order to guard themselves and their genome against foreign nucleotide incorporation. Innate immunity utilises pathogen recognition receptors (PRRs) to identify danger-associated (DAMPs) or pathogen-associated molecular patterns (PAMPs) that upon stimulation initiate an intracellular signalling cascade to stop the incoming insult as reviewed in [297]. The human CypA protein is encoded by peptidyl prolyl isomerase A gene (*PPIA*) and enhances HIV-1 replication by aiding capsid uncoating to protect viral DNA being sensed upon infection [267]. I was able to show that CypA competitively antagonises innate sensors of the HIV-1 capsid such as MX2 and TRIM5 α . The IFN α 2a sensitivity assay revealed upon increasing IFN α 2a concentration the extent to which HIV-1 harbouring point mutations in p24 capsid would be sensitive to restriction by IFN α 2a-mediated innate sensors. Furthermore, sensing of foreign nucleic acids induces an immune response under various conditions reviewed in [298, 299] and I was able to show that mutations p24 Gag are dependent on CypA. Triggering of signalling pathways resulting in sensing and restriction of incoming oligonucleotides is performed by cytosolic DNA sensors to regulate and activate transcription factors IFN regulatory factor 3 (IRF3) and nuclear factor kappa B (NF- κ B). These factors trigger the production of IFN type I and pro-inflammatory cytokines resulting in inflammation due to the activation of the central adaptor molecule stimulator of interferon genes (STING). Innate sensing of DNA accumulating within the cytoplasm from exogenous viral or bacterial infection or alternatively from endogenous sources such as DNA damage or cell stress results in a pro-inflammatory state. The cytosolic DNA sensor cyclic GMP-AMO (cGAMP) synthase (cGAS) involved in the clearance of infection is intensively investigated. Recognised DNA for example, RT products of HIV-1 reverse transcription are bound by cGAS catalysing the synthesis of the second messenger cGAMP resulting in STING activation [300]. Antiviral immunity mediated by restriction factors are the foot soldiers and first line of defence against retroviral infection to limit infection and shielding the viral DNA during uncoating is pivotal to reducing cellular activation.

Intensive efforts in HIV-1 research have identified several proteins that not only inhibit HIV-1 viral replication, but also restrict endogenous transposable elements [301, 302]. To date five potent restriction factors have been shown to effectively block HIV-1 replication. These are

TRIM5 proteins, SAMHD-1, members of the APOBEC3 (A3) family, MX2 and Tetherin/BST-2 [303]. SAMHD-1 specifically depletes the intracellular pool of deoxyribonucleotides (dNTPs), thereby, inhibiting reverse transcription [304]. Herein, I was able to show that HIV-1 harbouring escape mutations were in general less CypA- dependent in the Jurkat cell model and IFN- α -sensitivity of HIV-1 WT in Jurkat Mx2^{-/-} was reconstituted when compared to Jurkat WT cells and Jurkat CypA/Mx2^{-/-} cells. I was also able to show that MX2 and CypA competitively antagonise the HIV-1 WT virus, and that CypA and MX2 capsid interactions might enable HIV-1 WT and HIV-1 S173A plus R264K plus L268M viruses to evade IFN α 2 α -induced restriction factors. However, further experiments are needed to confirm and validate this finding. I was also able to show that Jurkat cells respond to IFN α 2 α -stimulation and regulate a stronger transcriptional upregulation of IFN α 2 α -regulated genes compared to Jurkat CypA^{-/-} and that global gene expression is differentially regulated in the CypA^{-/-} Jurkat cells upon IFN α 2 α stimulation. In Jurkat CypA^{-/-} cells I found that mRNA transcription of certain immunomodulatory genes was suppressed, while the Jurkat cell line had a greater dynamic range in gene expression. This was reflected at the protein level as revealed by proteomic analysis I found that proteins are specifically affected upon IFN α 2 α stimulation and SILAC MS/MS analysis revealed that PBAP may provide a mechanism for the observed CypA^{-/-} (*Ppia*^{-/-}) phenotype. Specifically, PABPC1; PABPC3; PABPC1L; PABPC4 proteins was found to be upregulated in the unstimulated Jurkat CypA^{-/-}. Conversely, PABPC1;PABPC4 was specifically down-regulated under IFN α 2 α stimulation in Jurkat CypA^{-/-} cells. Taken together I was able to show that proteins involved in cellular regulation with respect to PABP proteins was specifically affected in the Jurkat CypA^{-/-} indicating an important role of PABP in maintaining cellular homeostasis. In summary, differential regulation of the Jurkat CypA^{-/-} cells when compared to the Jurkat cell line indicated a phenotypically distinct T cell with altered activation and effector function. In conclusion these experiments in this thesis reveal that although limited information is available, the possibility that recently discovered restriction factors may play a role in anti-viral cellular immunity beyond viral restriction should not be excluded and be worth exploring. The work further supports published data showing that HIV-1 induces an IFN-1 response that in itself is not sufficient to clear infection [305, 306].

5. Outlook

Future prospects would be to assess the consequences of immune-modulated capsid stability for sensing of viral oligonucleotides by cytoplasmatic receptors. Identification of CTL-driven sequence mutations within capsid that reduce capsid stability enabling better sensing of the viral oligonucleotides by cytoplasmatic innate immune receptors, resulting in the production of antiviral cytokines, and the upregulation of ISGs and host restriction genes would be of significant interest in the field. The capsid of HIV-1 plays a central role in shuttling the viral RNA and cDNA following reverse transcription to the nucleus, shielding viral oligonucleotides from recognition through cytoplasmatic sensors [136]. Impairment of capsid stability, as a result of immune-induced sequence variations, can reduce this shuttling and shielding function of the capsid, exposing viral oligonucleotides to sensing by innate immune receptors. Sensing of viral oligonucleotides results in the activation of cellular antiviral mechanisms, including the production of antiviral cytokines and the upregulation of ISGs, which include host restriction factors, such as tetherin (BST2), TRIM5 α or APOBEC3G 35 previously mentioned. The selection of viral escape mutations from CTL-mediated immune pressure within HIV-1 capsid, while allowing evasion from recognition by cytotoxic CD8⁺ T cells, might therefore render these viruses more susceptible to cellular host restriction factors. In the context of capsid mutations selected by CTL responses restricted by protective HLA class I alleles, such as HLA-B27 and HLA-57, this enhanced sensing by cytoplasmatic innate receptors might contribute to the observed control of viral replication and reduced replicative capacity, and thereby, to the delayed HIV-1 disease progression observed in these individuals. In this I would propose to assess the impact of reduced capsid stability resulting from CTL-driven viral escape mutations on innate sensing of HIV-1 and the induction of antiviral effector mechanisms. The exact mechanism by which cellular immune pressure exerts heightens the sensing of infection remains elusive, and therefore, requires in depth investigation. Altogether, HLA-B27 restricted CTL-escape mutations might increase sensitivity of HIV-1 to IFN α and this dissertation forms the basis for further exploration of the mechanisms of HIV-1 capsid sensing and restriction.

6. Conclusions

My data suggested that HIV-1 containing the p24 Gag R264K and p24 Gag R264K plus p24 Gag L268M mutations were less dependent on CypA than WT. However, weak CypA/capsid interactions might expose these mutated strains to IFN α 2a-induced restriction factors that compete with CypA for their binding site. Therefore, p24 Gag R264K and p24 Gag R264K plus p24 Gag L268M might have been more sensitive to IFN α 2a-restriction compared to WT in Jurkat cell model. Therefore, p24 Gag escape mutations might be dependent on a CypA-independent mechanism, whereby, an undescribed restriction factor was mediating restriction.

This work highlights the role of CypA/capsid interactions in protecting HIV-1 from antiviral restriction factors and provides a mechanism by which HLA-B27-restricted CTL escape mutations in capsid can result in a loss of viral fitness.

7. References

1. Faria, N.R., et al., *HIV epidemiology. The early spread and epidemic ignition of HIV-1 in human populations*. Science (New York), 2014. **346**(6205): p. 56-61.
2. D'arc, M., et al., *Origin of the HIV-1 group O epidemic in western lowland gorillas*. Proceedings of the National Academy of Sciences, 2015. **112**(11): p. E1343.
3. Schommers, P., et al., *Changes in HIV-1 Capsid Stability Induced by Common Cytotoxic-T-Lymphocyte-Driven Viral Sequence Mutations*. J Virol, 2016. **90**(16): p. 7579-7586.
4. Korber, B., et al., *Timing the ancestor of the HIV-1 pandemic strains*. Science, 2000. **288**(5472): p. 1789-96.
5. WHO-UNAIDS., *Global AIDS update 2018*. 2018.
6. Sharp, P.M. and B.H. Hahn, *Origins of HIV and the AIDS Pandemic*. Cold Spring Harbor Perspectives in Medicine, 2011. **1**(1).
7. Gao, F., et al., *Origin of HIV-1 in the chimpanzee *Pan troglodytes troglodytes**. Nature, 1999. **397**(6718): p. 436-41.
8. Shaw, G.M. and E. Hunter, *HIV Transmission*. Cold Spring Harbor Perspectives in Medicine, 2012. **2**(11).
9. Gaschen, B., et al., *Diversity considerations in HIV-1 vaccine selection*. Science, 2002. **296**(5577): p. 2354-60.
10. Buonaguro, L., M.L. Tornesello, and F.M. Buonaguro, *Human immunodeficiency virus type 1 subtype distribution in the worldwide epidemic: pathogenetic and therapeutic implications*. Journal of virology, 2007. **81**(19): p. 10209-10219.
11. De Cock, K.M., H.W. Jaffe, and J.W. Curran, *The evolving epidemiology of HIV/AIDS*. Aids, 2012. **26**(10): p. 1205-13.
12. Hladik, F. and M.J. McElrath, *Setting the stage: host invasion by HIV*. Nat Rev Immunol, 2008. **8**(6): p. 447-57.
13. Powers, K.A., et al., *Rethinking the heterosexual infectivity of HIV-1: a systematic review and meta-analysis*. Lancet Infect Dis, 2008. **8**(9): p. 553-63.
14. Boily, M.C., et al., *Heterosexual risk of HIV-1 infection per sexual act: systematic review and meta-analysis of observational studies*. Lancet Infect Dis, 2009. **9**(2): p. 118-29.
15. Baggaley, R.F., R.G. White, and M.-C. Boily, *HIV transmission risk through anal intercourse: systematic review, meta-analysis and implications for HIV prevention*. International journal of epidemiology, 2010. **39**(4): p. 1048-1063.
16. Wawer, M.J., et al., *Rates of HIV-1 transmission per coital act, by stage of HIV-1 infection, in Rakai, Uganda*. J Infect Dis, 2005. **191**(9): p. 1403-9.
17. Shaw, G.M. and E. Hunter, *HIV transmission*. Cold Spring Harb Perspect Med, 2012. **2**(11).
18. Pilcher, C.D., et al., *Brief but efficient: acute HIV infection and the sexual transmission of HIV*. J Infect Dis, 2004. **189**(10): p. 1785-92.
19. Pilcher, C.D., et al., *Frequent detection of acute primary HIV infection in men in Malawi*. Aids, 2004. **18**(3): p. 517-24.
20. Vernazza, P.L., et al., *Sexual transmission of HIV: infectiousness and prevention*. Aids, 1999. **13**(2): p. 155-66.
21. Baeten, J.M., et al., *Genital HIV-1 RNA predicts risk of heterosexual HIV-1 transmission*. Sci Transl Med, 2011. **3**(77): p. 77ra29.

22. Butler, D.M., et al., *Herpes simplex virus 2 serostatus and viral loads of HIV-1 in blood and semen as risk factors for HIV transmission among men who have sex with men.* AIDS (London, England), 2008. **22**(13): p. 1667-1671.
23. Moss, W.J., et al., *Suppression of human immunodeficiency virus replication during acute measles.* J Infect Dis, 2002. **185**(8): p. 1035-42.
24. Watt, G., P. Kantipong, and K. Jongsakul, *Decrease in human immunodeficiency virus type 1 load during acute dengue fever.* Clin Infect Dis, 2003. **36**(8): p. 1067-9.
25. Anzala, A.O., et al., *Acute sexually transmitted infections increase human immunodeficiency virus type 1 plasma viremia, increase plasma type 2 cytokines, and decrease CD4 cell counts.* J Infect Dis, 2000. **182**(2): p. 459-66.
26. Malott, R.J., et al., *Neisseria gonorrhoeae-derived heptose elicits an innate immune response and drives HIV-1 expression.* Proc Natl Acad Sci U S A, 2013. **110**(25): p. 10234-9.
27. Nagot, N., et al., *Reduction of HIV-1 RNA Levels with Therapy to Suppress Herpes Simplex Virus.* New England Journal of Medicine, 2007. **356**(8): p. 790-799.
28. Haaland, R.E., et al., *Inflammatory Genital Infections Mitigate a Severe Genetic Bottleneck in Heterosexual Transmission of Subtype A and C HIV-1.* PLOS Pathogens, 2009. **5**(1): p. e1000274.
29. Carlson, J.M., et al., *Selection bias at the heterosexual HIV-1 transmission bottleneck.* Science, 2014. **345**(6193): p. 1254031.
30. Cohen, M.S., et al., *Acute HIV-1 Infection.* New England Journal of Medicine, 2011. **364**(20): p. 1943-1954.
31. Fideli, U.S., et al., *Virologic and immunologic determinants of heterosexual transmission of human immunodeficiency virus type 1 in Africa.* AIDS Res Hum Retroviruses, 2001. **17**(10): p. 901-10.
32. Burgener, A., I. McGowan, and N.R. Klatt, *HIV and mucosal barrier interactions: consequences for transmission and pathogenesis.* Curr Opin Immunol, 2015. **36**: p. 22-30.
33. Quinn, T.C., et al., *Viral load and heterosexual transmission of human immunodeficiency virus type 1. Rakai Project Study Group.* N Engl J Med, 2000. **342**(13): p. 921-9.
34. El-Sadr, W.M., K.H. Mayer, and S.L. Hodder, *AIDS in America--forgotten but not gone.* The New England journal of medicine, 2010. **362**(11): p. 967-970.
35. Klatzmann, D., et al., *Selective tropism of lymphadenopathy associated virus (LAV) for helper-inducer T lymphocytes.* Science, 1984. **225**(4657): p. 59-63.
36. Masur, H., et al., *An Outbreak of Community-Acquired Pneumocystis carinii Pneumonia.* New England Journal of Medicine, 1981. **305**(24): p. 1431-1438.
37. Small, C.B., et al., *Community-acquired opportunistic infections and defective cellular immunity in heterosexual drug abusers and homosexual men.* Am J Med, 1983. **74**(3): p. 433-41.
38. Masur, H., et al., *CD4 counts as predictors of opportunistic pneumonias in human immunodeficiency virus (HIV) infection.* Ann Intern Med, 1989. **111**(3): p. 223-31.
39. Accola, M.A., S. Hoglund, and H.G. Gottlinger, *A putative alpha-helical structure which overlaps the capsid-p2 boundary in the human immunodeficiency virus type 1 Gag precursor is crucial for viral particle assembly.* J Virol, 1998. **72**(3): p. 2072-8.
40. Greene, W.C. and B.M. Peterlin, *Charting HIV's remarkable voyage through the cell: Basic science as a passport to future therapy.* Nat Med, 2002. **8**(7): p. 673-80.
41. Jacks, T., et al., *Characterization of ribosomal frameshifting in HIV-1 gag-pol expression.* Nature, 1988. **331**(6153): p. 280-3.

42. Wilson, W., et al., *HIV expression strategies: Ribosomal frameshifting is directed by a short sequence in both mammalian and yeast systems*. Cell, 1988. **55**(6): p. 1159-1169.
43. Könnnyü, B., et al., *Gag-Pol Processing during HIV-1 Virion Maturation: A Systems Biology Approach*. PLOS Computational Biology, 2013. **9**(6): p. e1003103.
44. Los Alamos. *HIV database*.
45. Burton, D.R., *What Are the Most Powerful Immunogen Design Vaccine Strategies? Reverse Vaccinology 2.0 Shows Great Promise*. Cold Spring Harbor perspectives in biology. **9**(11): p. a030262.
46. Schneidewind, A., et al., *Structural and Functional Constraints Limit Options for Cytotoxic T-Lymphocyte Escape in the Immunodominant HLA-B27-Restricted Epitope in Human Immunodeficiency Virus Type 1 Capsid*. Journal of Virology, 2008. **82**(11): p. 5594.
47. R, G.A.a.W., *Encyclopedia of Virology, Three Volume Set, 2nd Edition*. 1999: p. 763-774.
48. Lu, K., X. Heng, and M.F. Summers, *Structural determinants and mechanism of HIV-1 genome packaging*. J Mol Biol, 2011. **410**(4): p. 609-33.
49. Murphy, K., et al., *Janeway's Immunobiology*. Vol. 7th Edition. 2007, New York: Garland Science. 196-199, 536.
50. Foley, B., *An overview of the molecular phylogeny of lentiviruses*. , in *HIV sequence compendium*. 2000. p. 35-43.
51. Campbell, E.M. and T.J. Hope, *HIV-1 capsid: the multifaceted key player in HIV-1 infection*. Nature Reviews Microbiology, 2015. **13**: p. 471.
52. Ganser, B.K., et al., *Assembly and analysis of conical models for the HIV-1 core*. Science, 1999. **283**(5398): p. 80-3.
53. Li, S., et al., *Image reconstructions of helical assemblies of the HIV-1 CA protein*. Nature, 2000. **407**(6802): p. 409-13.
54. Gamble, T.R., et al., *Structure of the carboxyl-terminal dimerization domain of the HIV-1 capsid protein*. Science, 1997. **278**(5339): p. 849-53.
55. Towers, G.J., et al., *Cyclophilin A modulates the sensitivity of HIV-1 to host restriction factors*. Nat Med, 2003. **9**(9): p. 1138-43.
56. Sokolskaja, E., D.M. Sayah, and J. Luban, *Target cell cyclophilin A modulates human immunodeficiency virus type 1 infectivity*. J Virol, 2004. **78**(23): p. 12800-8.
57. Ganser-Pornillos, B.K., M. Yeager, and W.I. Sundquist, *The structural biology of HIV assembly*. Curr Opin Struct Biol, 2008. **18**(2): p. 203-17.
58. Patarca, R. and W.A. Haseltine, *A major retroviral core protein related to EPA and TIMP*. Nature, 1985. **318**(6044): p. 390-390.
59. Wills, J.W. and R.C. Craven, *Form, function, and use of retroviral gag proteins*. Aids, 1991. **5**(6): p. 639-54.
60. Strambio-de-Castillia, C. and E. Hunter, *Mutational analysis of the major homology region of Mason-Pfizer monkey virus by use of saturation mutagenesis*. Journal of virology, 1992. **66**(12): p. 7021-7032.
61. Mammano, F., et al., *Role of the major homology region of human immunodeficiency virus type 1 in virion morphogenesis*. Journal of virology, 1994. **68**(8): p. 4927-4936.
62. Craven, R.C., et al., *Genetic analysis of the major homology region of the Rous sarcoma virus Gag protein*. J Virol, 1995. **69**(7): p. 4213-27.
63. Byeon, I.-J.L., et al., *Structural convergence between Cryo-EM and NMR reveals intersubunit interactions critical for HIV-1 capsid function*. Cell, 2009. **139**(4): p. 780-790.
64. Zhao, G., et al., *Mature HIV-1 capsid structure by cryo-electron microscopy and all-atom molecular dynamics*. Nature, 2013. **497**: p. 643.

65. Takemura, T. and T. Murakami, *Functional constraints on HIV-1 capsid: their impacts on the viral immune escape potency*. *Frontiers in Microbiology*, 2012. **3**(369).
66. Wilen, C.B., J.C. Tilton, and R.W. Doms, *HIV: cell binding and entry*. Cold Spring Harb Perspect Med, 2012. **2**(8).
67. Connor, R.I., et al., *Change in coreceptor use correlates with disease progression in HIV-1--infected individuals*. *J Exp Med*, 1997. **185**(4): p. 621-8.
68. Scarlatti, G., et al., *In vivo evolution of HIV-1 co-receptor usage and sensitivity to chemokine-mediated suppression*. *Nat Med*, 1997. **3**(11): p. 1259-65.
69. Keele, B.F., et al., *Identification and characterization of transmitted and early founder virus envelopes in primary HIV-1 infection*. *Proc Natl Acad Sci U S A*, 2008. **105**(21): p. 7552-7.
70. Salazar-Gonzalez, J.F., et al., *Genetic identity, biological phenotype, and evolutionary pathways of transmitted/founder viruses in acute and early HIV-1 infection*. *J Exp Med*, 2009. **206**(6): p. 1273-89.
71. Parrish, N.F., et al., *Phenotypic properties of transmitted founder HIV-1*. *Proceedings of the National Academy of Sciences*, 2013. **110**(17): p. 6626.
72. Gartner, S., et al., *The role of mononuclear phagocytes in HTLV-III/LAV infection*. *Science*, 1986. **233**(4760): p. 215-9.
73. Koenig, S., et al., *Detection of AIDS virus in macrophages in brain tissue from AIDS patients with encephalopathy*. *Science*, 1986. **233**(4768): p. 1089-93.
74. Patterson, S. and S.C. Knight, *Susceptibility of human peripheral blood dendritic cells to infection by human immunodeficiency virus*. *J Gen Virol*, 1987. **68** (Pt 4): p. 1177-81.
75. Tschachler, E., et al., *Epidermal Langerhans cells--a target for HTLV-III/LAV infection*. *J Invest Dermatol*, 1987. **88**(2): p. 233-7.
76. Chan, D.C. and P.S. Kim, *HIV Entry and Its Inhibition*. *Cell*, 1998. **93**(5): p. 681-684.
77. Vanhamel, J., A. Bruggemans, and Z. Debyser, *Establishment of latent HIV-1 reservoirs: what do we really know?* *Journal of virus eradication*, 2019. **5**(1): p. 3-9.
78. Nabel, G. and D. Baltimore, *An inducible transcription factor activates expression of human immunodeficiency virus in T cells*. *Nature*, 1987. **326**(6114): p. 711-3.
79. Siekevitz, M., et al., *Activation of the HIV-1 LTR by T cell mitogens and the trans-activator protein of HTLV-I*. *Science*, 1987. **238**(4833): p. 1575-8.
80. Duh, E.J., et al., *Tumor necrosis factor alpha activates human immunodeficiency virus type 1 through induction of nuclear factor binding to the NF-kappa B sites in the long terminal repeat*. *Proc Natl Acad Sci U S A*, 1989. **86**(15): p. 5974-8.
81. Ott, M., M. Geyer, and Q. Zhou, *The control of HIV transcription: keeping RNA polymerase II on track*. *Cell Host Microbe*, 2011. **10**(5): p. 426-35.
82. Kao, S.Y., et al., *Anti-termination of transcription within the long terminal repeat of HIV-1 by tat gene product*. *Nature*, 1987. **330**(6147): p. 489-93.
83. Wei, P., et al., *A novel CDK9-associated C-type cyclin interacts directly with HIV-1 Tat and mediates its high-affinity, loop-specific binding to TAR RNA*. *Cell*, 1998. **92**(4): p. 451-62.
84. Price, D.H., *P-TEFb, a cyclin-dependent kinase controlling elongation by RNA polymerase II*. *Mol Cell Biol*, 2000. **20**(8): p. 2629-34.
85. Feinberg, M.B. and W.C. Greene, *Molecular insights into human immunodeficiency virus type 1 pathogenesis*. *Curr Opin Immunol*, 1992. **4**(4): p. 466-74.
86. Langer, S. and D. Sauter, *Unusual Fusion Proteins of HIV-1*. *Frontiers in Microbiology*, 2017. **7**(2152).
87. Cullen, B.R., *Retroviruses as model systems for the study of nuclear RNA export pathways*. *Virology*, 1998. **249**(2): p. 203-10.

88. Rausch, J.W. and S.F. Le Grice, *HIV Rev Assembly on the Rev Response Element (RRE): A Structural Perspective*. *Viruses*, 2015. **7**(6): p. 3053-75.
89. Kuzembayeva, M., et al., *Life of psi: how full-length HIV-1 RNAs become packaged genomes in the viral particles*. *Virology*, 2014. **454-455**: p. 362-70.
90. Sundquist, W.I. and H.-G. Kräusslich, *HIV-1 Assembly, Budding, and Maturation*. Cold Spring Harbor Perspectives in Medicine, 2012. **2**(8): p. a015420.
91. Strack, B., et al., *A role for ubiquitin ligase recruitment in retrovirus release*. *Proceedings of the National Academy of Sciences of the United States of America*, 2000. **97**(24): p. 13063-13068.
92. Peterlin, B.M. and D. Trono, *Hide, shield and strike back: how HIV-infected cells avoid immune eradication*. *Nat Rev Immunol*, 2003. **3**(2): p. 97-107.
93. Bioinformatics, S.S.I.o., *HIV replication cycle* <https://viralzone.expasy.org/5096>. ExPASy Bioinformatics Resource Portal, 2019.
94. Haase, A.T., *Early events in sexual transmission of HIV and SIV and opportunities for interventions*. *Annu Rev Med*, 2011. **62**: p. 127-39.
95. Hladik, F. and T.J. Hope, *HIV infection of the genital mucosa in women*. *Curr HIV/AIDS Rep*, 2009. **6**(1): p. 20-8.
96. Eid, S.G., et al., *Blocking HIV-1 transmission in the female reproductive tract: from microbicide development to exploring local antiviral responses*. *Clin Transl Immunology*, 2015. **4**(10): p. e43.
97. Keele, B.F. and J.D. Estes, *Barriers to mucosal transmission of immunodeficiency viruses*. *Blood*, 2011. **118**(4): p. 839-846.
98. Miller, C.J., et al., *Propagation and dissemination of infection after vaginal transmission of simian immunodeficiency virus*. *J Virol*, 2005. **79**(14): p. 9217-27.
99. Maher, D., et al., *HIV binding, penetration, and primary infection in human cervicovaginal tissue*. *Proc Natl Acad Sci U S A*, 2005. **102**(32): p. 11504-9.
100. Hladik, F., et al., *Initial events in establishing vaginal entry and infection by human immunodeficiency virus type-1*. *Immunity*, 2007. **26**(2): p. 257-70.
101. Li, Q., et al., *Glycerol monolaurate prevents mucosal SIV transmission*. *Nature*, 2009. **458**(7241): p. 1034-8.
102. Miller, C.J., J.R. McGhee, and M.B. Gardner, *Mucosal immunity, HIV transmission, and AIDS*. *Lab Invest*, 1993. **68**(2): p. 129-45.
103. Auvert, B., et al., *Randomized, controlled intervention trial of male circumcision for reduction of HIV infection risk: the ANRS 1265 Trial*. *PLoS Med*, 2005. **2**(11): p. e298.
104. Bailey, R.C., et al., *Male circumcision for HIV prevention in young men in Kisumu, Kenya: a randomised controlled trial*. *Lancet*, 2007. **369**(9562): p. 643-56.
105. Gray, R.H., et al., *Male circumcision for HIV prevention in men in Rakai, Uganda: a randomised trial*. *Lancet*, 2007. **369**(9562): p. 657-66.
106. Fischetti, L., et al., *HIV-1 infection of human penile explant tissue and protection by candidate microbicides*. *Aids*, 2009. **23**(3): p. 319-28.
107. Patterson, B.K., et al., *Susceptibility to human immunodeficiency virus-1 infection of human foreskin and cervical tissue grown in explant culture*. *The American journal of pathology*, 2002. **161**(3): p. 867-873.
108. Fiebig, E.W., et al., *Dynamics of HIV viremia and antibody seroconversion in plasma donors: implications for diagnosis and staging of primary HIV infection*. *Aids*, 2003. **17**(13): p. 1871-9.
109. Zhu, T., et al., *Genetic characterization of human immunodeficiency virus type 1 in blood and genital secretions: evidence for viral compartmentalization and selection during sexual transmission*. *J Virol*, 1996. **70**(5): p. 3098-107.

110. Ribeiro, R.M., et al., *Estimation of the Initial Viral Growth Rate and Basic Reproductive Number during Acute HIV-1 Infection*. Journal of Virology, 2010. **84**(12): p. 6096.
111. Heffernan, J.M., R.J. Smith, and L.M. Wahl, *Perspectives on the basic reproductive ratio*. Journal of the Royal Society, Interface, 2005. **2**(4): p. 281-293.
112. Schacker, T.W., et al., *Biological and virologic characteristics of primary HIV infection*. Ann Intern Med, 1998. **128**(8): p. 613-20.
113. Wei, X., et al., *Viral dynamics in human immunodeficiency virus type 1 infection*. Nature, 1995. **373**(6510): p. 117-22.
114. Mellors, J.W., et al., *Prognosis in HIV-1 infection predicted by the quantity of virus in plasma*. Science, 1996. **272**(5265): p. 1167-70.
115. Lyles, R.H., et al., *Natural history of human immunodeficiency virus type 1 viremia after seroconversion and proximal to AIDS in a large cohort of homosexual men. Multicenter AIDS Cohort Study*. J Infect Dis, 2000. **181**(3): p. 872-80.
116. Pantaleo, G. and A.S. Fauci, *IMMUNOPATHOGENESIS OF HIV INFECTION*. Annual Review of Microbiology, 1996. **50**(1): p. 825-854.
117. Payne, R., et al., *Impact of HLA-driven HIV adaptation on virulence in populations of high HIV seroprevalence*. Proc Natl Acad Sci U S A, 2014. **111**(50): p. E5393-400.
118. Poropatich, K. and D.J. Sullivan, Jr., *Human immunodeficiency virus type 1 long-term non-progressors: the viral, genetic and immunological basis for disease non-progression*. J Gen Virol, 2011. **92**(Pt 2): p. 247-68.
119. Gaardbo, J.C., et al., *Thirty Years with HIV Infection-Nonprogression Is Still Puzzling: Lessons to Be Learned from Controllers and Long-Term Nonprogressors*. AIDS Res Treat, 2012. **2012**: p. 161584.
120. Okulicz, J.F., et al., *Clinical outcomes of elite controllers, viremic controllers, and long-term nonprogressors in the US Department of Defense HIV natural history study*. J Infect Dis, 2009. **200**(11): p. 1714-23.
121. Deeks, S.G. and B.D. Walker, *Human immunodeficiency virus controllers: mechanisms of durable virus control in the absence of antiretroviral therapy*. Immunity, 2007. **27**(3): p. 406-16.
122. Hubert, J.B., et al., *Natural history of serum HIV-1 RNA levels in 330 patients with a known date of infection. The SEROCO Study Group*. Aids, 2000. **14**(2): p. 123-31.
123. Osmond, D., et al., *Changes in AIDS Survival Time in Two San Francisco Cohorts of Homosexual Men, 1983 to 1993*. JAMA, 1994. **271**(14): p. 1083-1087.
124. Gail, M.H., et al., *Survival after AIDS diagnosis in a cohort of hemophilia patients. Multicenter Hemophilia Cohort Study*. J Acquir Immune Defic Syndr Hum Retrovirol, 1997. **15**(5): p. 363-9.
125. Tough, R.H. and P.J. McLaren, *Interaction of the Host and Viral Genome and Their Influence on HIV Disease*. Frontiers in Genetics, 2019. **9**(720).
126. Aiken, C., *Cell-free assays for HIV-1 uncoating*. Methods Mol Biol, 2009. **485**: p. 41-53.
127. Matreyek, K.A. and A. Engelman, *The Requirement for Nucleoporin NUP153 during Human Immunodeficiency Virus Type 1 Infection Is Determined by the Viral Capsid*. Journal of Virology, 2011. **85**(15): p. 7818.
128. Sowd, G.A., et al., *A critical role for alternative polyadenylation factor CPSF6 in targeting HIV-1 integration to transcriptionally active chromatin*. Proc Natl Acad Sci U S A, 2016. **113**(8): p. E1054-63.
129. Chin, C.R., et al., *Direct Visualization of HIV-1 Replication Intermediates Shows that Capsid and CPSF6 Modulate HIV-1 Intra-nuclear Invasion and Integration*. Cell Rep, 2015. **13**(8): p. 1717-31.

130. Di Nunzio, F., et al., *Nup153 and Nup98 bind the HIV-1 core and contribute to the early steps of HIV-1 replication*. *Virology*, 2013. **440**(1): p. 8-18.
131. Ocwieja, K.E., et al., *HIV Integration Targeting: A Pathway Involving Transportin-3 and the Nuclear Pore Protein RanBP2*. *PLOS Pathogens*, 2011. **7**(3): p. e1001313.
132. Koh, Y., et al., *Differential Effects of Human Immunodeficiency Virus Type 1 Capsid and Cellular Factors Nucleoporin 153 and LEDGF/p75 on the Efficiency and Specificity of Viral DNA Integration*. *Journal of Virology*, 2013. **87**(1): p. 648.
133. Matreyek, K.A., et al., *Nucleoporin NUP153 Phenylalanine-Glycine Motifs Engage a Common Binding Pocket within the HIV-1 Capsid Protein to Mediate Lentiviral Infectivity*. *PLOS Pathogens*, 2013. **9**(10): p. e1003693.
134. Hulme, A.E., et al., *Complementary Assays Reveal a Low Level of CA Associated with Viral Complexes in the Nuclei of HIV-1-Infected Cells*. *J Virol*, 2015. **89**(10): p. 5350-61.
135. Peng, K., et al., *Quantitative microscopy of functional HIV post-entry complexes reveals association of replication with the viral capsid*. *Elife*, 2014. **3**: p. e04114.
136. Campbell, E.M. and T.J. Hope, *HIV-1 capsid: the multifaceted key player in HIV-1 infection*. *Nat Rev Microbiol*, 2015. **13**(8): p. 471-83.
137. Yamashita, M. and M. Emerman, *Capsid is a dominant determinant of retrovirus infectivity in nondividing cells*. *J Virol*, 2004. **78**(11): p. 5670-8.
138. Ganser-Pornillos, B.K., A. Cheng, and M. Yeager, *Structure of full-length HIV-1 CA: a model for the mature capsid lattice*. *Cell*, 2007. **131**(1): p. 70-9.
139. Lowe, A.R., et al., *Selectivity mechanism of the nuclear pore complex characterized by single cargo tracking*. *Nature*, 2010. **467**(7315): p. 600-3.
140. Panté, N. and M. Kann, *Nuclear pore complex is able to transport macromolecules with diameters of about 39 nm*. *Molecular biology of the cell*, 2002. **13**(2): p. 425-434.
141. Suzuki, Y. and R. Craigie, *The road to chromatin - nuclear entry of retroviruses*. *Nat Rev Microbiol*, 2007. **5**(3): p. 187-96.
142. Bukrinsky, M., *A hard way to the nucleus*. *Mol Med*, 2004. **10**(1-6): p. 1-5.
143. Lehmann-Che, J. and A. Saib, *Early stages of HIV replication: how to hijack cellular functions for a successful infection*. *AIDS Rev*, 2004. **6**(4): p. 199-207.
144. Dvorin, J.D. and M.H. Malim, *Intracellular trafficking of HIV-1 cores: journey to the center of the cell*. *Curr Top Microbiol Immunol*, 2003. **281**: p. 179-208.
145. Miller, M.D., C.M. Farnet, and F.D. Bushman, *Human immunodeficiency virus type 1 preintegration complexes: studies of organization and composition*. *J Virol*, 1997. **71**(7): p. 5382-90.
146. Fassati, A. and S.P. Goff, *Characterization of intracellular reverse transcription complexes of human immunodeficiency virus type 1*. *J Virol*, 2001. **75**(8): p. 3626-35.
147. Rasaiyaah, J., et al., *HIV-1 evades innate immune recognition through specific cofactor recruitment*. *Nature*, 2013. **503**(7476): p. 402-405.
148. Gao, D., et al., *Cyclic GMP-AMP synthase is an innate immune sensor of HIV and other retroviruses*. *Science*, 2013. **341**(6148): p. 903-6.
149. Lahaye, X., et al., *The capsids of HIV-1 and HIV-2 determine immune detection of the viral cDNA by the innate sensor cGAS in dendritic cells*. *Immunity*, 2013. **39**(6): p. 1132-42.
150. Hulme, A.E., O. Perez, and T.J. Hope, *Complementary assays reveal a relationship between HIV-1 uncoating and reverse transcription*. *Proceedings of the National Academy of Sciences of the United States of America*, 2011. **108**(24): p. 9975-9980.
151. Warrilow, D., G. Tachedjian, and D. Harrich, *Maturation of the HIV reverse transcription complex: putting the jigsaw together*. *Rev Med Virol*, 2009. **19**(6): p. 324-37.

152. McDonald, D., et al., *Visualization of the intracellular behavior of HIV in living cells*. J Cell Biol, 2002. **159**(3): p. 441-52.
153. Hilditch, L. and G.J. Towers, *A model for cofactor use during HIV-1 reverse transcription and nuclear entry*. Curr Opin Virol, 2014. **4**: p. 32-6.
154. Towers, G.J. and M. Noursadeghi, *Interactions between HIV-1 and the cell-autonomous innate immune system*. Cell host & microbe, 2014. **16**(1): p. 10-18.
155. Sumner, R.P., et al., *Are Evolution and the Intracellular Innate Immune System Key Determinants in HIV Transmission?* Front Immunol, 2017. **8**: p. 1246.
156. Yamashita, M. and A.N. Engelman, *Capsid-Dependent Host Factors in HIV-1 Infection*. Trends Microbiol, 2017. **25**(9): p. 741-755.
157. Sayah, D.M., et al., *Cyclophilin A retrotransposition into TRIM5 explains owl monkey resistance to HIV-1*. Nature, 2004. **430**(6999): p. 569-73.
158. Forshey, B.M., J. Shi, and C. Aiken, *Structural Requirements for Recognition of the Human Immunodeficiency Virus Type 1 Core during Host Restriction in Owl Monkey Cells*. Journal of Virology, 2005. **79**(2): p. 869.
159. Sastri, J. and E.M. Campbell, *Recent insights into the mechanism and consequences of TRIM5alpha retroviral restriction*. AIDS Res Hum Retroviruses, 2011. **27**(3): p. 231-8.
160. Ambrose, Z. and C. Aiken, *HIV-1 uncoating: connection to nuclear entry and regulation by host proteins*. Virology, 2014. **454-455**: p. 371-379.
161. Shah, V.B. and C. Aiken, *In vitro uncoating of HIV-1 cores*. J Vis Exp, 2011(57).
162. Stremlau, M., et al., *Specific recognition and accelerated uncoating of retroviral capsids by the TRIM5a restriction factor*. Proceedings of the National Academy of Sciences, 2006. **103**(14): p. 5514.
163. Yang, Y., J. Luban, and F. Diaz-Griffero, *The Fate of HIV-1 Capsid: A Biochemical Assay for HIV-1 Uncoating*, in *Human Retroviruses: Methods and Protocols*, E. Vicenzi and G. Poli, Editors. 2014, Humana Press: Totowa, NJ. p. 29-36.
164. Robinson, J., et al., *The IMGT/HLA database*. 2011: Nucleic Acids Research.
165. Horton, R., et al., *Gene map of the extended human MHC*. Nature Reviews Genetics, 2004. **5**(12): p. 889-899.
166. Rock, K.L., et al., *Inhibitors of the proteasome block the degradation of most cell proteins and the generation of peptides presented on MHC class I molecules*. Cell, 1994. **78**(5): p. 761-71.
167. Neefjes, J.J., F. Momburg, and G.J. Hammerling, *Selective and ATP-dependent translocation of peptides by the MHC-encoded transporter*. Science, 1993. **261**(5122): p. 769-71.
168. van Endert, P.M., et al., *Powering the peptide pump: TAP crosstalk with energetic nucleotides*. Trends Biochem Sci, 2002. **27**(9): p. 454-61.
169. Ortman, B., et al., *A Critical Role for Tapasin in the Assembly and Function of Multimeric MHC Class I-TAP Complexes*. Science, 1997. **277**(5330): p. 1306.
170. Garbi, N., et al., *Impaired immune responses and altered peptide repertoire in tapasin-deficient mice*. Nat Immunol, 2000. **1**(3): p. 234-8.
171. Dick, T.P., et al., *Disulfide bond isomerization and the assembly of MHC class I-peptide complexes*. Immunity, 2002. **16**(1): p. 87-98.
172. Serwold, T., et al., *ERAAP customizes peptides for MHC class I molecules in the endoplasmic reticulum*. Nature, 2002. **419**(6906): p. 480-3.
173. Reits, E., et al., *Peptide diffusion, protection, and degradation in nuclear and cytoplasmic compartments before antigen presentation by MHC class I*. Immunity, 2003. **18**(1): p. 97-108.

174. Hang, I., et al., *Analysis of site-specific N-glycan remodeling in the endoplasmic reticulum and the Golgi*. *Glycobiology*, 2015. **25**(12): p. 1335-49.
175. Bjorkman, P.J., et al., *The foreign antigen binding site and T cell recognition regions of class I histocompatibility antigens*. *Nature*, 1987. **329**(6139): p. 512-8.
176. Bjorkman, P.J., et al., *Structure of the human class I histocompatibility antigen, HLA-A2*. *Nature*, 1987. **329**(6139): p. 506-12.
177. Marsch, S., P. Parham, and L. Barber, *The HLA factsbook*. 2000, Academic Press. p. 52-56, 218-219.
178. Sidney, J., et al., *HLA class I supertypes: a revised and updated classification*. *BMC Immunology*, 2008. **9**(1): p. 1.
179. Altfeld, M. and P. Goulder, *'Unleashed' natural killers hinder HIV*. *Nature Genetics*, 2007. **39**: p. 708.
180. Martin, M.P., et al., *Innate partnership of HLA-B and KIR3DL1 subtypes against HIV-1*. *Nat Genet*, 2007. **39**(6): p. 733-40.
181. Goulder, P.J. and B.D. Walker, *HIV and HLA class I: an evolving relationship*. *Immunity*, 2012. **37**(3): p. 426-40.
182. Limou, S., et al., *Genomewide association study of an AIDS-nonprogression cohort emphasizes the role played by HLA genes (ANRS Genomewide Association Study 02)*. *J Infect Dis*, 2009. **199**(3): p. 419-26.
183. Pereyra, F., et al., *The major genetic determinants of HIV-1 control affect HLA class I peptide presentation*. *Science*, 2010. **330**(6010): p. 1551-7.
184. Emu, B., et al., *HLA class I-restricted T-cell responses may contribute to the control of human immunodeficiency virus infection, but such responses are not always necessary for long-term virus control*. *J Virol*, 2008. **82**(11): p. 5398-407.
185. Kaslow, R.A., et al., *Influence of combinations of human major histocompatibility complex genes on the course of HIV-1 infection*. *Nature Medicine*, 1996. **2**(4): p. 405-411.
186. Fellay, J., et al., *A whole-genome association study of major determinants for host control of HIV-1*. *Science (New YoR264K N.Y.)*, 2007. **317**(5840): p. 944-947.
187. Migueles, S.A., et al., *HLA B*5701 is highly associated with restriction of virus replication in a subgroup of HIV-infected long term nonprogressors*. *Proc Natl Acad Sci U S A*, 2000. **97**(6): p. 2709-14.
188. Kiepiela, P., et al., *Dominant influence of HLA-B in mediating the potential co-evolution of HIV and HLA*. *Nature*, 2004. **432**(7018): p. 769-75.
189. Wright, J.K., et al., *Gag-protease-mediated replication capacity in HIV-1 subtype C chronic infection: associations with HLA type and clinical parameters*. *J Virol*, 2010. **84**(20): p. 10820-31.
190. Carlson, J.M., et al., *Widespread Impact of HLA Restriction on Immune Control and Escape Pathways of HIV-1*. *Journal of Virology*, 2012. **86**(9): p. 5230.
191. Carrington, M., et al., *HLA and HIV-1: Heterozygote Advantage and B*35-Cw*04 Disadvantage*. *Science*, 1999. **283**(5408): p. 1748-1752.
192. Almeida, J.R., et al., *Antigen sensitivity is a major determinant of CD8+ T-cell polyfunctionality and HIV-suppressive activity*. *Blood*, 2009. **113**(25): p. 6351-60.
193. Kiepiela, P., et al., *CD8+ T-cell responses to different HIV proteins have discordant associations with viral load*. *Nat Med*, 2007. **13**(1): p. 46-53.
194. Sacha, J.B., et al., *Pol-specific CD8+ T cells recognize simian immunodeficiency virus-infected cells prior to Nef-mediated major histocompatibility complex class I downregulation*. *J Virol*, 2007. **81**(21): p. 11703-12.
195. Kawashima, Y., et al., *Adaptation of HIV-1 to human leukocyte antigen class I*. *Nature*, 2009. **458**(7238): p. 641-5.

196. Payne, R.P., et al., *Efficacious early antiviral activity of HIV Gag- and Pol-specific HLA-B 2705-restricted CD8+ T cells*. J Virol, 2010. **84**(20): p. 10543-57.
197. Chen, H., et al., *TCR clonotypes modulate the protective effect of HLA class I molecules in HIV-1 infection*. Nature Immunology, 2012. **13**: p. 691.
198. Bevan, M.J., *Helping the CD8(+) T-cell response*. Nat Rev Immunol, 2004. **4**(8): p. 595-602.
199. Trapani, J.A. and M.J. Smyth, *Functional significance of the perforin/granzyme cell death pathway*. Nat Rev Immunol, 2002. **2**(10): p. 735-47.
200. Schmitz, J.E., et al., *Control of viremia in simian immunodeficiency virus infection by CD8+ lymphocytes*. Science, 1999. **283**(5403): p. 857-60.
201. Saez-Cirion, A., et al., *HIV controllers exhibit potent CD8 T cell capacity to suppress HIV infection ex vivo and peculiar cytotoxic T lymphocyte activation phenotype*. Proc Natl Acad Sci U S A, 2007. **104**(16): p. 6776-81.
202. Ndhlovu, Z.M., et al., *Magnitude and Kinetics of CD8+ T Cell Activation during Hyperacute HIV Infection Impact Viral Set Point*. Immunity, 2015. **43**(3): p. 591-604.
203. Quigley, M., et al., *Transcriptional analysis of HIV-specific CD8+ T cells shows that PD-1 inhibits T cell function by upregulating BATF*. Nat Med, 2010. **16**(10): p. 1147-51.
204. Migueles, S.A., et al., *HIV-specific CD8+ T cell proliferation is coupled to perforin expression and is maintained in nonprogressors*. Nat Immunol, 2002. **3**(11): p. 1061-8.
205. Zimmerli, S.C., et al., *HIV-1-specific IFN-gamma/IL-2-secreting CD8 T cells support CD4-independent proliferation of HIV-1-specific CD8 T cells*. Proc Natl Acad Sci U S A, 2005. **102**(20): p. 7239-44.
206. Migueles, S.A., et al., *Lytic granule loading of CD8+ T cells is required for HIV-infected cell elimination associated with immune control*. Immunity, 2008. **29**(6): p. 1009-21.
207. Elahi, S., et al., *Protective HIV-specific CD8+ T cells evade Treg cell suppression*. Nat Med, 2011. **17**(8): p. 989-95.
208. Betts, M.R., et al., *HIV nonprogressors preferentially maintain highly functional HIV-specific CD8+ T cells*. Blood, 2006. **107**(12): p. 4781-9.
209. Almeida, J.R., et al., *Superior control of HIV-1 replication by CD8+ T cells is reflected by their avidity, polyfunctionality, and clonal turnover*. J Exp Med, 2007. **204**(10): p. 2473-85.
210. Zuniga, R., et al., *Relative dominance of Gag p24-specific cytotoxic T lymphocytes is associated with human immunodeficiency virus control*. J Virol, 2006. **80**(6): p. 3122-5.
211. Sacha, J.B., et al., *Gag-specific CD8+ T lymphocytes recognize infected cells before AIDS-virus integration and viral protein expression*. J Immunol, 2007. **178**(5): p. 2746-54.
212. Miura, T., et al., *HLA-B57/B*5801 human immunodeficiency virus type 1 elite controllers select for rare gag variants associated with reduced viral replication capacity and strong cytotoxic T-lymphocyte [corrected] recognition*. J Virol, 2009. **83**(6): p. 2743-55.
213. Dahiriel, V., et al., *Coordinate linkage of HIV evolution reveals regions of immunological vulnerability*. Proceedings of the National Academy of Sciences, 2011. **108**(28): p. 11530.
214. Maness, N.J., et al., *Comprehensive immunological evaluation reveals surprisingly few differences between elite controller and progressor Mamu-B*17-positive simian immunodeficiency virus-infected rhesus macaques*. J Virol, 2008. **82**(11): p. 5245-54.

215. Valentine, L.E. and D.I. Watkins, *Relevance of studying T cell responses in SIV-infected rhesus macaques*. Trends Microbiol, 2008. **16**(12): p. 605-11.
216. Takemura, T. and T. Murakami, *Functional constraints on HIV-1 capsid: their impacts on the viral immune escape potency*. Frontiers in microbiology, 2012. **3**: p. 369-369.
217. Phillips, R.E., et al., *Human immunodeficiency virus genetic variation that can escape cytotoxic T cell recognition*. Nature, 1991. **354**(6353): p. 453-459.
218. Price, D.A., et al., *Positive selection of HIV-1 cytotoxic T lymphocyte escape variants during primary infection*. Proceedings of the National Academy of Sciences of the United States of America, 1997. **94**(5): p. 1890-1895.
219. Jones, N.A., et al., *Determinants of human immunodeficiency virus type 1 escape from the primary CD8+ cytotoxic T lymphocyte response*. J Exp Med, 2004. **200**(10): p. 1243-56.
220. Goonetilleke, N., et al., *The first T cell response to transmitted/founder virus contributes to the control of acute viremia in HIV-1 infection*. The Journal of Experimental Medicine, 2009. **206**(6): p. 1253.
221. Liu, M.K.P., et al., *Vertical T cell immunodominance and epitope entropy determine HIV-1 escape*. The Journal of Clinical Investigation, 2013. **123**(1): p. 380-393.
222. Matthews, P.C., et al., *Central Role of Reverting Mutations in HLA Associations with Human Immunodeficiency Virus Set Point*. Journal of Virology, 2008. **82**(17): p. 8548.
223. Roberts, H.E., et al., *Structured Observations Reveal Slow HIV-1 CTL Escape*. PLOS Genetics, 2015. **11**(2): p. e1004914.
224. Allen, T.M., et al., *Selection, transmission, and reversion of an antigen-processing cytotoxic T-lymphocyte escape mutation in human immunodeficiency virus type 1 infection*. J Virol, 2004. **78**(13): p. 7069-78.
225. Milicic, A., et al., *CD8+ T cell epitope-flanking mutations disrupt proteasomal processing of HIV-1 Nef*. J Immunol, 2005. **175**(7): p. 4618-26.
226. Schmid, B.V., C. Keşmir, and R.J. de Boer, *The Specificity and Polymorphism of the MHC Class I Prevents the Global Adaptation of HIV-1 to the Monomorphic Proteasome and TAP*. PLOS ONE, 2008. **3**(10): p. e3525.
227. Draenert, R., et al., *Immune selection for altered antigen processing leads to cytotoxic T lymphocyte escape in chronic HIV-1 infection*. J Exp Med, 2004. **199**(7): p. 905-15.
228. Yokomaku, Y., et al., *Impaired processing and presentation of cytotoxic-T-lymphocyte (CTL) epitopes are major escape mechanisms from CTL immune pressure in human immunodeficiency virus type 1 infection*. J Virol, 2004. **78**(3): p. 1324-32.
229. Reid, S.W., et al., *Antagonist HIV-1 Gag Peptides Induce Structural Changes in HLA B8*. The Journal of Experimental Medicine, 1996. **184**(6): p. 2279.
230. Carlson, J.M., et al., *Correlates of Protective Cellular Immunity Revealed by Analysis of Population-Level Immune Escape Pathways in HIV-1*. Journal of Virology, 2012. **86**(24): p. 13202.
231. Bronke, C., et al., *HIV escape mutations occur preferentially at HLA-binding sites of CD8 T-cell epitopes*. AIDS (London, England), 2013. **27**(6): p. 899-905.
232. Kelleher, A.D., et al., *Clustered mutations in HIV-1 gag are consistently required for escape from HLA-B27-restricted cytotoxic T lymphocyte responses*. The Journal of experimental medicine, 2001. **193**(3): p. 375-386.
233. Yu, X.G., et al., *Mutually exclusive T-cell receptor induction and differential susceptibility to human immunodeficiency virus type 1 mutational escape associated with a two-amino-acid difference between HLA class I subtypes*. J Virol, 2007. **81**(4): p. 1619-31.

234. Goulder, P.J.R., et al., *Late escape from an immunodominant cytotoxic T-lymphocyte response associated with progression to AIDS*. Nature Medicine, 1997. **3**(2): p. 212-217.
235. Geels, M.J., et al., *Identification of Sequential Viral Escape Mutants Associated with Altered T-Cell Responses in a Human Immunodeficiency Virus Type 1-Infected Individual*. Journal of Virology, 2003. **77**(23): p. 12430.
236. Jamieson, B.D., et al., *Epitope escape mutation and decay of human immunodeficiency virus type 1-specific CTL responses*. J Immunol, 2003. **171**(10): p. 5372-9.
237. Furutsuki, T., et al., *Frequent transmission of cytotoxic-T-lymphocyte escape mutants of human immunodeficiency virus type 1 in the highly HLA-A24-positive Japanese population*. J Virol, 2004. **78**(16): p. 8437-45.
238. Leslie, A., et al., *Transmission and accumulation of CTL escape variants drive negative associations between HIV polymorphisms and HLA*. The Journal of experimental medicine, 2005. **201**(6): p. 891-902.
239. Oxenius, A., et al., *Loss of viral control in early HIV-1 infection is temporally associated with sequential escape from CD8+ T cell responses and decrease in HIV-1-specific CD4+ and CD8+ T cell frequencies*. J Infect Dis, 2004. **190**(4): p. 713-21.
240. Allen, T.M., et al., *De novo generation of escape variant-specific CD8+ T-cell responses following cytotoxic T-lymphocyte escape in chronic human immunodeficiency virus type 1 infection*. J Virol, 2005. **79**(20): p. 12952-60.
241. Feeney, M.E., et al., *HIV-1 viral escape in infancy followed by emergence of a variant-specific CTL response*. J Immunol, 2005. **174**(12): p. 7524-30.
242. Leslie, A.J., et al., *HIV evolution: CTL escape mutation and reversion after transmission*. Nature Medicine, 2004. **10**: p. 282.
243. Duda, A., et al., *HLA-associated clinical progression correlates with epitope reversion rates in early human immunodeficiency virus infection*. J Virol, 2009. **83**(3): p. 1228-39.
244. Brener, J., et al., *Disease progression despite protective HLA expression in an HIV-infected transmission pair*. Retrovirology, 2015. **12**: p. 55.
245. Quinones-Mateu, M.E. and E.J. Arts. *HIV-1 Fitness : Implications for Drug Resistance , Disease Progression , and Global Epidemic Evolution*. 2002.
246. Perez, C.L., et al., *Targeting of conserved gag-epitopes in early HIV infection is associated with lower plasma viral load and slower CD4(+) T cell depletion*. AIDS research and human retroviruses, 2013. **29**(3): p. 602-612.
247. Martinez-Picado, J., et al., *Fitness cost of escape mutations in p24 Gag in association with control of human immunodeficiency virus type 1*. J Virol, 2006. **80**(7): p. 3617-23.
248. Schneidewind, A., et al., *Escape from the Dominant HLA-B27-Restricted Cytotoxic T-Lymphocyte Response in Gag Is Associated with a Dramatic Reduction in Human Immunodeficiency Virus Type 1 Replication*. Journal of Virology, 2007. **81**(22): p. 12382.
249. Crawford, H., et al., *The hypervariable HIV-1 capsid protein residues comprise HLA-driven CD8+ T-cell escape mutations and covarying HLA-independent polymorphisms*. Journal of virology, 2011. **85**(3): p. 1384-1390.
250. Bailey, J.R., et al., *Evidence of CD8+ T-cell-mediated selective pressure on human immunodeficiency virus type 1 nef in HLA-B*57+ elite suppressors*. J Virol, 2009. **83**(1): p. 88-97.
251. Miura, T., et al., *HLA-associated viral mutations are common in human immunodeficiency virus type 1 elite controllers*. J Virol, 2009. **83**(7): p. 3407-12.
252. Crawford, H., et al., *Compensatory Mutation Partially Restores Fitness and Delays Reversion of Escape Mutation within the Immunodominant HLA-B*5703-Restricted*

- Gag Epitope in Chronic Human Immunodeficiency Virus Type 1 Infection*. Journal of Virology, 2008. **82**(6): p. 3161.
253. Gijssbers, E.F., et al., *HIV-1 replication fitness of HLA-B*57/58:01 CTL escape variants is restored by the accumulation of compensatory mutations in gag*. PLoS One, 2013. **8**(12): p. e81235.
 254. Noviello, C.M., et al., *Second-site compensatory mutations of HIV-1 capsid mutations*. Journal of virology, 2011. **85**(10): p. 4730-4738.
 255. Wright, J.K., et al., *Impact of HLA-B*81-associated mutations in HIV-1 Gag on viral replication capacity*. J Virol, 2012. **86**(6): p. 3193-9.
 256. Hinkley, T., et al., *A systems analysis of mutational effects in HIV-1 protease and reverse transcriptase*. Nat Genet, 2011. **43**(5): p. 487-9.
 257. Brockman, M.A., et al., *Early selection in Gag by protective HLA alleles contributes to reduced HIV-1 replication capacity that may be largely compensated for in chronic infection*. Journal of virology, 2010. **84**(22): p. 11937-11949.
 258. Chopera, D.R., et al., *Virological and Immunological Factors Associated with HIV-1 Differential Disease Progression in HLA-B*58:01-Positive Individuals*. Journal of Virology, 2011. **85**(14): p. 7070.
 259. Claiborne, D.T., et al., *Replicative fitness of transmitted HIV-1 drives acute immune activation, proviral load in memory CD4+ T cells, and disease progression*. Proc Natl Acad Sci U S A, 2015. **112**(12): p. E1480-9.
 260. Miura, T., et al., *HLA-associated alterations in replication capacity of chimeric NL4-3 viruses carrying gag-protease from elite controllers of human immunodeficiency virus type 1*. J Virol, 2009. **83**(1): p. 140-9.
 261. Miura, T., et al., *HLA-B57/B*5801 Human Immunodeficiency Virus Type 1 Elite Controllers Select for Rare Gag Variants Associated with Reduced Viral Replication Capacity and Strong Cytotoxic T-Lymphocyte Recognition*. Journal of Virology, 2009. **83**(6): p. 2743.
 262. Blanco-Melo, D., S. Venkatesh, and P.D. Bieniasz, *Intrinsic cellular defenses against human immunodeficiency viruses*. Immunity, 2012. **37**(3): p. 399-411.
 263. Fenton-May, A.E., et al., *Relative resistance of HIV-1 founder viruses to control by interferon-alpha*. Retrovirology, 2013. **10**: p. 146-146.
 264. Yamashita, M. and A.N. Engelman, *Capsid-Dependent Host Factors in HIV-1 Infection*. Trends in microbiology, 2017. **25**(9): p. 741-755.
 265. Song, H., et al., *Impact of immune escape mutations on HIV-1 fitness in the context of the cognate transmitted/founder genome*. Retrovirology, 2012. **9**: p. 89-89.
 266. Martrus, G., et al., *CD49a Expression Identifies a Subset of Intrahepatic Macrophages in Humans*. Frontiers in immunology, 2019. **10**: p. 1247-1247.
 267. Madlala, P., et al., *Association of Polymorphisms in the Regulatory Region of the Cyclophilin a Gene (PPIA) with Gene Expression and HIV/AIDS Disease Progression*. Journal of acquired immune deficiency syndromes (1999), 2016. **72**(5): p. 465-473.
 268. Gallie, D.R., *The role of the poly(A) binding protein in the assembly of the Cap-binding complex during translation initiation in plants*. Translation (Austin, Tex.), 2014. **2**(2): p. e959378-e959378.
 269. StenmaR264K H. and V.M. Olkkonen, *The Rab GTPase family*. Genome biology, 2001. **2**(5): p. REVIEWS3007-REVIEWS3007.
 270. Harlow, E. and D. Lane, *Bradford assay*. CSH Protoc, 2006. **2006**(6).
 271. Huang da, W., B.T. Sherman, and R.A. Lempicki, *Systematic and integrative analysis of large gene lists using DAVID bioinformatics resources*. Nat Protoc, 2009. **4**(1): p. 44-57.

272. Hulme, A.E. and T.J. Hope, *The cyclosporin A washout assay to detect HIV-1 uncoating in infected cells*. *Methods Mol Biol*, 2014. **1087**: p. 37-46.
273. Kløverpris, H.N., A. Leslie, and P. Goulder, *Role of HLA Adaptation in HIV Evolution*. *Frontiers in immunology*, 2016. **6**: p. 665-665.
274. Jones, R.B. and B.D. Walker, *HIV-specific CD8⁺ T cells and HIV eradication*. *The Journal of clinical investigation*, 2016. **126**(2): p. 455-463.
275. Tebit, D.M., et al., *Analysis of the diversity of the HIV-1 pol gene and drug resistance associated changes among drug-naïve patients in Burkina Faso*. *Journal of Medical Virology*, 2009. **81**(10): p. 1691-1701.
276. Hernandez-Vargas, E.A., *Modeling Kick-Kill Strategies toward HIV Cure*. *Frontiers in Immunology*, 2017. **8**(995).
277. Olson, A.D., et al., *Evaluation of rapid progressors in HIV infection as an extreme phenotype*. *J Acquir Immune Defic Syndr*, 2014. **67**(1): p. 15-21.
278. Olson, A.D., et al., *An evaluation of HIV elite controller definitions within a large seroconverter cohort collaboration*. *PLoS One*, 2014. **9**(1): p. e86719.
279. Altfeld, M., et al., *Influence of HLA-B57 on clinical presentation and viral control during acute HIV-1 infection*. *Aids*, 2003. **17**(18): p. 2581-91.
280. Leslie, A.J., et al., *HIV evolution: CTL escape mutation and reversion after transmission*. *Nature Medicine*, 2004. **10**(3): p. 282-289.
281. Goulder, P.J., et al., *Evolution and transmission of stable CTL escape mutations in HIV infection*. *Nature*, 2001. **412**(6844): p. 334-8.
282. Altfeld, M., et al., *Cellular immune responses and viral diversity in individuals treated during acute and early HIV-1 infection*. *J Exp Med*, 2001. **193**(2): p. 169-80.
283. Altfeld, M., et al., *HLA Alleles Associated with Delayed Progression to AIDS Contribute Strongly to the Initial CD8(+) T Cell Response against HIV-1*. *PLoS Med*, 2006. **3**(10): p. e403.
284. Aiken, C., *Pseudotyping human immunodeficiency virus type 1 (HIV-1) by the glycoprotein of vesicular stomatitis virus targets HIV-1 entry to an endocytic pathway and suppresses both the requirement for Nef and the sensitivity to cyclosporin A*. *J Virol*, 1997. **71**(8): p. 5871-7.
285. Melikyan, G.B., *HIV entry: a game of hide-and-fuse?* *Curr Opin Virol*, 2014. **4**: p. 1-7.
286. Merindol, N., et al., *HIV-1 capsids from B27/B57+ elite controllers escape Mx2 but are targeted by TRIM5a, leading to the induction of an antiviral state*. *PLOS Pathogens*, 2018. **14**(11): p. e1007398.
287. Yu, X.G., et al., *Consistent patterns in the development and immunodominance of human immunodeficiency virus type 1 (HIV-1)-specific CD8⁺ T-cell responses following acute HIV-1 infection*. *J Virol*, 2002. **76**(17): p. 8690-701.
288. Altfeld, M., et al., *Enhanced detection of human immunodeficiency virus type 1-specific T-cell responses to highly variable regions by using peptides based on autologous virus sequences*. *J Virol*, 2003. **77**(13): p. 7330-40.
289. Altfeld, M. and T.M. Allen, *Hitting HIV where it hurts: an alternative approach to HIV vaccine design*. *Trends Immunol*, 2006. **27**(11): p. 504-10.
290. Boutwell, C.L., C.F. Rowley, and M. Essex, *Reduced viral replication capacity of human immunodeficiency virus type 1 subtype C caused by cytotoxic-T-lymphocyte escape mutations in HLA-B57 epitopes of capsid protein*. *Journal of virology*, 2009. **83**(6): p. 2460-2468.
291. Boutwell, C.L., et al., *Frequent and variable cytotoxic-T-lymphocyte escape-associated fitness costs in the human immunodeficiency virus type 1 subtype B Gag proteins*. *Journal of virology*, 2013. **87**(7): p. 3952-3965.

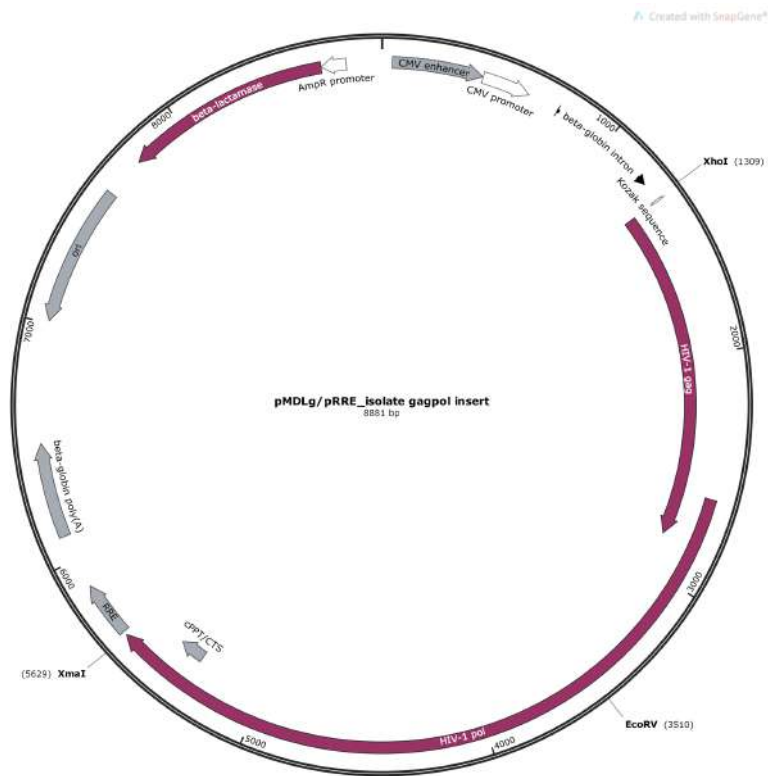
292. Crawford, H., et al., *Evolution of HLA-B*5703 HIV-1 escape mutations in HLA-B*5703-positive individuals and their transmission recipients*. The Journal of experimental medicine, 2009. **206**(4): p. 909-921.
293. Brockman, M.A., et al., *Escape and Compensation from Early HLA-B57-Mediated Cytotoxic T-Lymphocyte Pressure on Human Immunodeficiency Virus Type 1 Gag Alter Capsid Interactions with Cyclophilin A*. Journal of Virology, 2007. **81**(22): p. 12608.
294. Gaiha, G.D., et al., *Structural topology defines protective CD8+ T cell epitopes in the HIV proteome*. Science, 2019. **364**(6439): p. 480.
295. Li, B., et al., *Rapid reversion of sequence polymorphisms dominates early human immunodeficiency virus type 1 evolution*. J Virol, 2007. **81**(1): p. 193-201.
296. Dudek, T.E., et al., *Rapid evolution of HIV-1 to functional CD8(+) T cell responses in humanized BLT mice*. Sci Transl Med, 2012. **4**(143): p. 143ra98.
297. Dempsey, P.W., S.A. Vaidya, and G. Cheng, *The art of war: Innate and adaptive immune responses*. Cell Mol Life Sci, 2003. **60**(12): p. 2604-21.
298. Ahlers, L.R. and A.G. Goodman, *Nucleic acid sensing and innate immunity: signaling pathways controlling viral pathogenesis and autoimmunity*. Curr Clin Microbiol Rep, 2016. **3**(3): p. 132-141.
299. Radoshevich, L. and O. Dussurget, *Cytosolic Innate Immune Sensing and Signaling upon Infection*. Front Microbiol, 2016. **7**: p. 313.
300. Chen, Q., L. Sun, and Z.J. Chen, *Regulation and function of the cGAS-STING pathway of cytosolic DNA sensing*. Nat Immunol, 2016. **17**(10): p. 1142-9.
301. Colomer-Lluch, M., L.S. Gollahon, and R. Serra-Moreno, *Anti-HIV Factors: Targeting Each Step of HIV's Replication Cycle*. Curr HIV Res, 2016. **14**(3): p. 175-82.
302. Goodier, J.L., *Restricting retrotransposons: a review*. Mob DNA, 2016. **7**: p. 16.
303. Colomer-Lluch, M., et al., *Restriction Factors: From Intrinsic Viral Restriction to Shaping Cellular Immunity Against HIV-1*. Frontiers in immunology, 2018. **9**: p. 2876-2876.
304. Baldauf, H.-M., et al., *Vpx overcomes a SAMHD1-independent block to HIV reverse transcription that is specific to resting CD4 T cells*. Proceedings of the National Academy of Sciences of the United States of America, 2017. **114**(10): p. 2729-2734.
305. Altfeld, M. and M. Gale, Jr., *Innate immunity against HIV-1 infection*. Nat Immunol, 2015. **16**(6): p. 554-62.
306. Jakobsen, M.R., D. OLAGNIER, and J. HISCOTT, *Innate immune sensing of HIV-1 infection*. Curr Opin HIV AIDS, 2015. **10**(2): p. 96-102.

8. Appendix

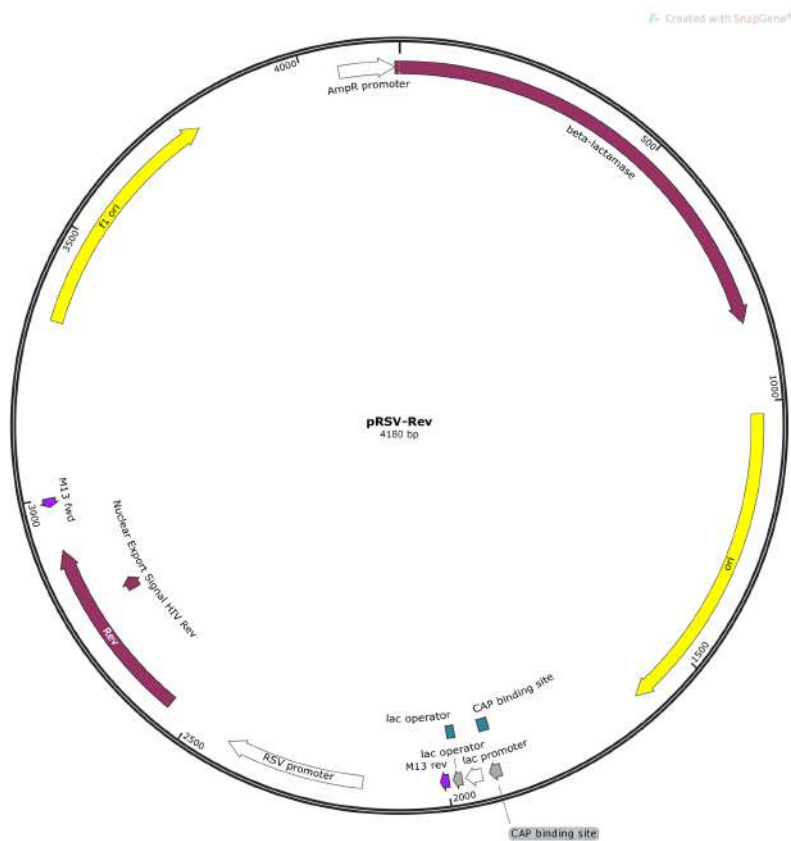
8.1 Risk and safety statements/List of hazards substances utilised according to GSH

Chemical name	GHS symbol	Hazard statements	Precautionary statements
Trypsin		H319, H335, H315, H334	P285, P261, P305, P351, P338, P321, P405, P501
Hydrogen peroxide		H302, H318, H412	P280, P301, P312, P330, P305, P351, P338, P310
Acid-Phenol: Chloroform pH4.5		H301, H311, H331 H314, H372, H361, H351, H341, H411	P264, P280, P261
Dithiothreitol		H302, H315, H319, H335	P302, P352, P305, P351, P338
Ethanol		H225-H319	P210-P280-P305, P351, P338-P337, P313-P403, P235
Isopropanol		H225-H319-H336	P210-P305, P351, P338-P370, P378-P403, P235
Methanol		H225, H301, H311, H331, H370	P210, P280, P233, P302, P352, P309, P310
Trifluoroacetic acid		H332, H314, H412	P271, P273, P301, P330, P331, P305, P351, P338, P309, P310
Tris		H315, H319, H335	P261, P305, P351, P338
TRIZOL		H301 + H311, H331-H314-H341-H373-H411	P201-P261-P280-P301, P310, P330-P303, P361, P353-P305, P351, P338
β -mercaptoethanol		H301, H331-H310-H315-H317-H318-H373-H410	P261-P273-P280-P301, P310-P302, P350-P305, P351 + P338

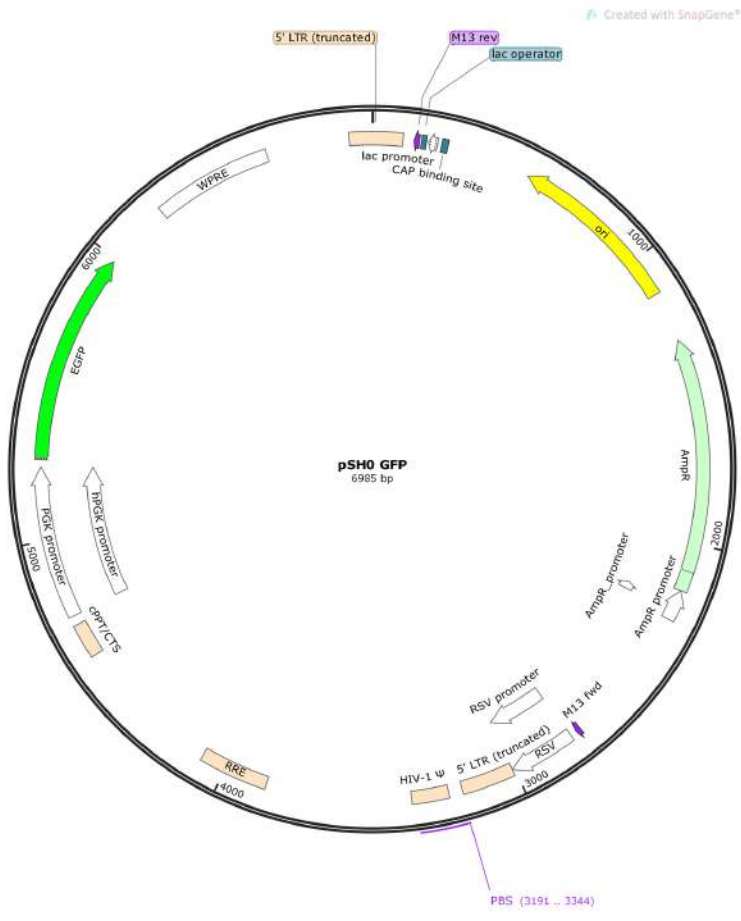
8.2 Plasmid Maps



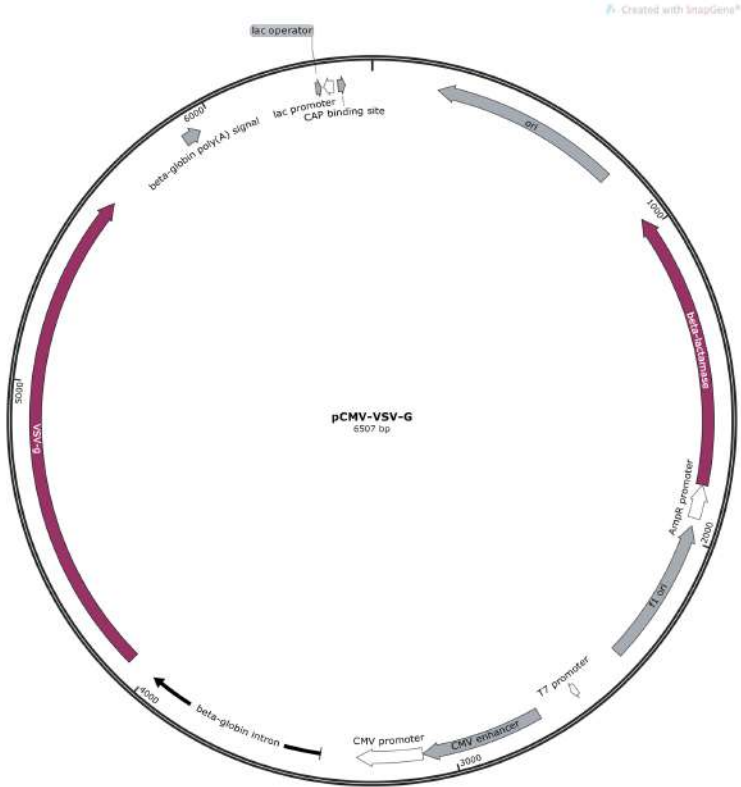
Map of pMDLg/pRRE_isolate gag-pol insert. Construct includes Kozak sequence upstream of gag/pol and *XhoI* and *XmaI* modifications.



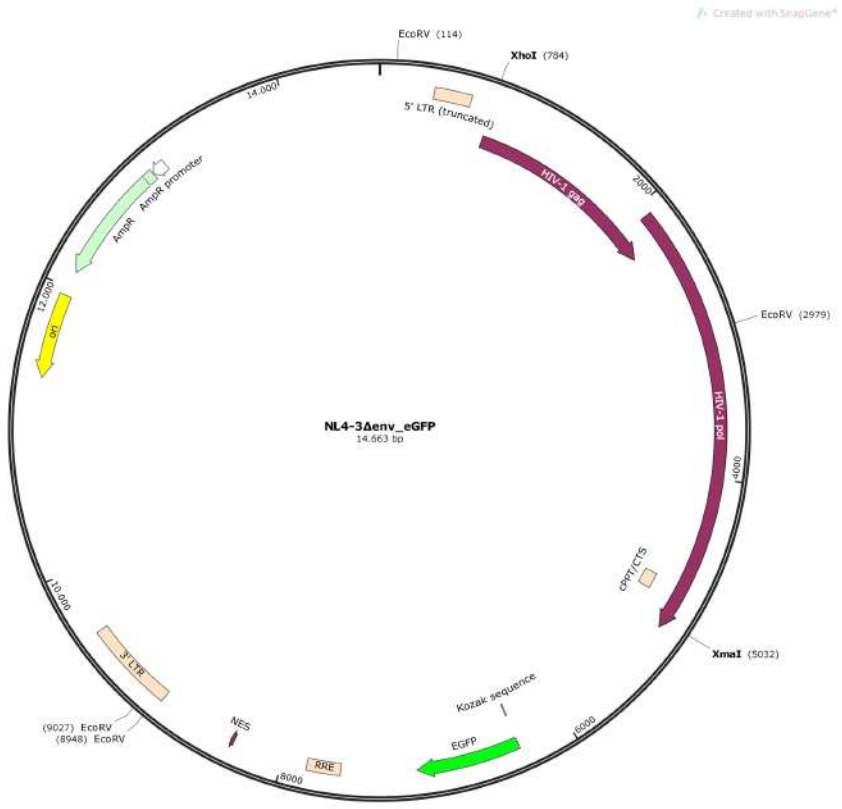
Map of pRSV-rev.



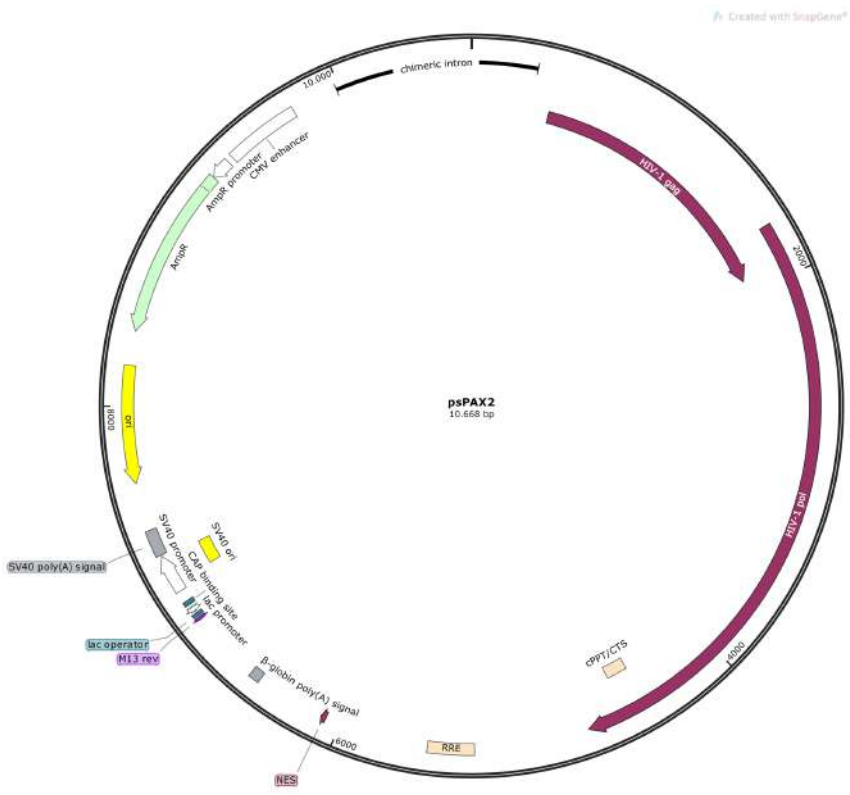
Map of pSH0-GFP.



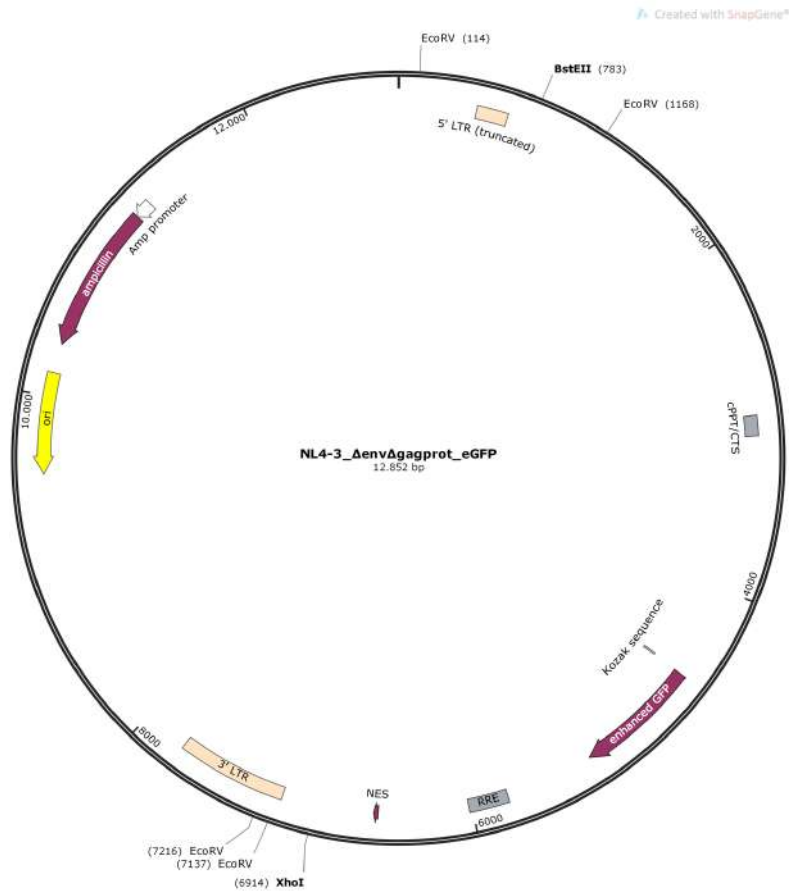
Map of pSH0-GFP.



Map of NL4-3Δenv_eGFP. Plasmid map is representative of constructs generated from gag-pol derived pro-viral sequences.



Map of psPAX2.



Map of NL4-3 Δ env Δ gagprot-eGFP

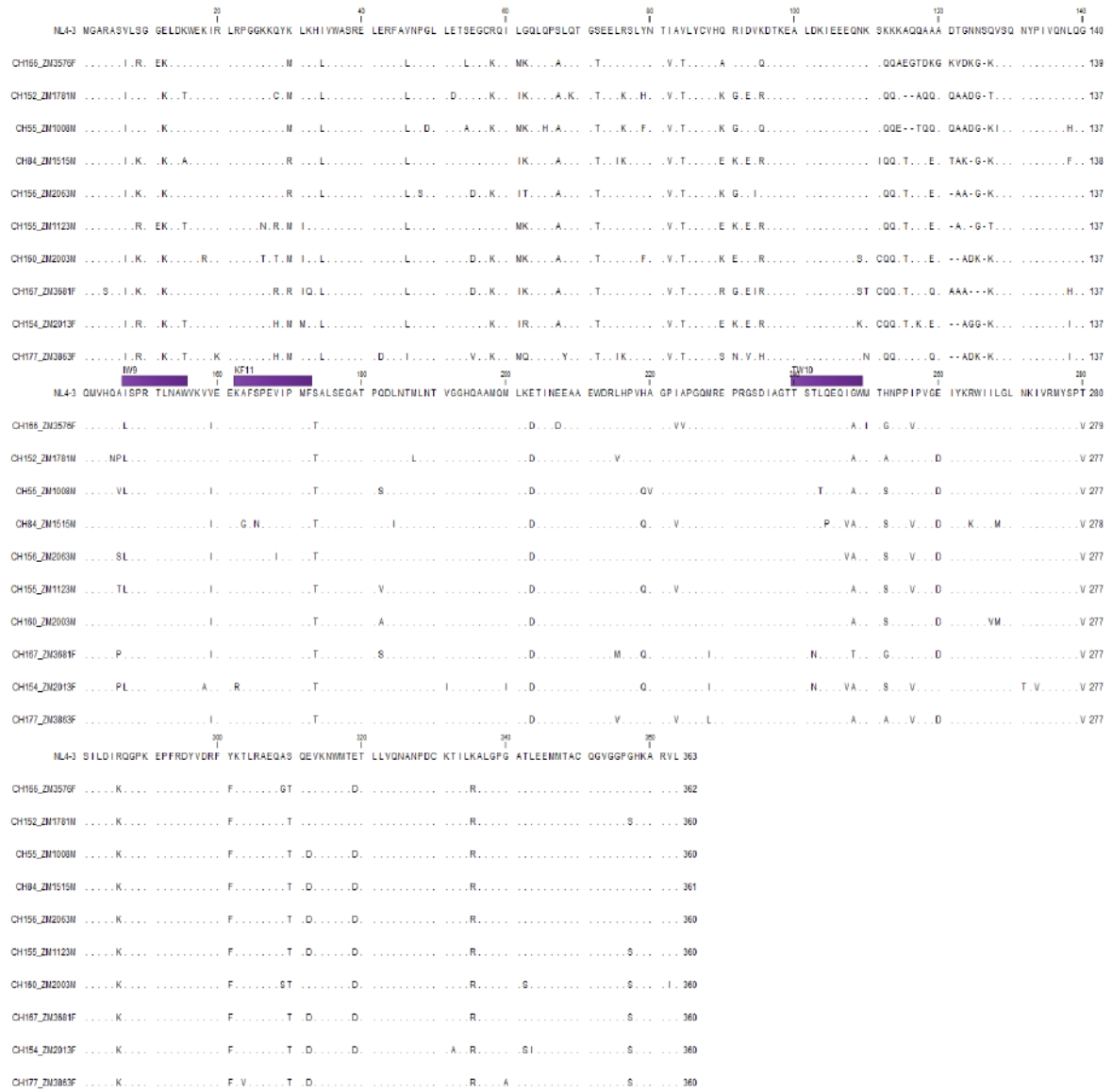


Figure 43 Gag chronic virus sequences

Aligned gag amino acid sequences of the chronic viruses gifted by Professor Eric Hunter.

9. Curriculum Vitae

Lebenslauf entfällt aus datenschutzrechtlichen Gründen.

Resume is omitted due to data protection reasons.

10. Acknowledgements

I would like to thank **Professor Marcus Altfeld** for his support and providing the environment for my doctoral studies. My thanks also goes to my supervisors **Professor Zoya Ignatova** and **Dr Philipp Schommers** (University Medical Center Cologne, Cologne) for their support and guidance. I thank my second reviewer **Professor Kay Grünewald**.

I also wish to acknowledge **Professor Frank Kirchhoff**, **Dr Christina Stürzel** and **Dr Dominik Hotter** for their expertise (Ulm University Medical Center, Institute of Molecular Virology, Ulm). I also thank **Professor Eric Hunter** (Emory University School of Medicine, Atlanta, GA) and **Professor Beatrice Hahn** (Perelman School of Medicine University of Pennsylvania, Philadelphia, PA) for gifting proviral constructs for generating patient isolate *gag/pol* constructs. I thank **Esther Jiménez Moyano** for advice given on generating MDM cells (IrsiCaixa AIDs Research Institute, Barcelona). Special thanks to **Dr Niklas Beschoner** for helping to develop cloning strategies and helpful discussions.

I wish to specifically acknowledge **Dr Glòria Martrus Zapater** for adopting me under her wing. She has been a real pillar of support helping me to see “the light” in tough times. I wish to thank **Heike Hildebrandt** for her patience with me when I have been particularly “demanding” and for the fun we have had in the lab together.

I wish to thank my parents **Paula and Thomas** and to my sisters **Louisa and Ellie** for supporting me through to the end! My friends have had to put up with many evenings in the pub spent talking about PhD projects, HIV and world domination – **James Garrett**, **Antje Wessler**, **Hao Yan**, **Shelddon Phaguda**, **Alex Miles**, **Clara Weger** – thank you to you guys and to the **Pulverteich WG** and **Zoe Bar** “Sofa Bar” for accommodating these discussions. Special thanks goes to **Pia Fittje** for our coffee sessions and for being a rock of support!

I wish to acknowledge the **Department for Virus Immunology** and the **healthy donors** who donated blood for my experiments, without which would have not been possible – thank you!

I wish to thank the **German AIDS Society (Deutsche AIDS-gesellschaft)** for the award I received at the German Austrian AIDS conference (DAIG 2019).

This work is supported by the **German Research Foundation DFG SPP1923**. I also wish to thank the **Heinrich Pette Institute**, **Leibniz Institute for Experimental Virology** and the **Free and Hanseatic City of Hamburg** and the **Federal Ministry of Health** for supporting my PhD and providing the facilities

11. Declaration on oath

Eidesstattliche Versicherung

I, Christopher Thomas Ford, hereby declare, on oath, that I have written the present dissertation by my own and have not used other than the acknowledged resources and aids.

Hiermit versichere ich an Eides statt, die vorliegende Dissertation selbst verfasst und keine anderen als die angegebenen Hilfsmittel benutzt zu haben. Die eingereichte schriftliche Fassung entspricht der auf dem elektronischen Speichermedium. Ich versichere, dass diese Dissertation nicht in einem früheren Promotionsverfahren eingereicht wurde.

Hamburg, August the 14th, 2019

Christopher T Ford

city and date

signature

Ort und Datum

Unterschrift